Coherence
in
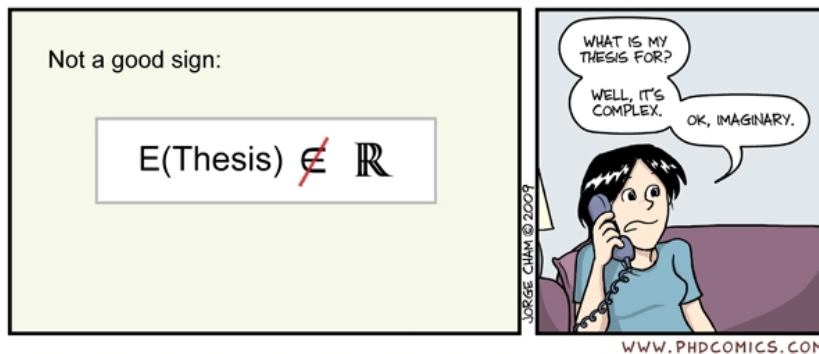# Classical Electromagnetism
and
Quantum Optics

Hanne-Torill Mevik

Thesis submitted for the degree of
Master in Physics
(Master of Science)

Department of Physics
University of Oslo
June 2009

Acknowledgements

It sure hasn't been easy to explain to friends, family or even fellow students what my thesis is about. To be honest, most of the time I myself had no clue. Although, I guess there is nothing unique about neither me nor this thesis in that regard. But now the day finally has arrived. The day when the final Ctrl-z's and Ctrl-s's has been typed and it's time for Ctrl-p. This is also the last day that I can rightly call myself a student, at least as far as Lånekassen is concerned. Four years, 10 months and a few days later after first setting foot on Blindern Campus, with the contours of my posterior firmly imprinted on the seat of my chair, the credit is not mine alone. My heartfelt thanks goes to...

... My mother whom I owe everything. Thank you for always being proud of me even though I didn't become a lawyer or a surgeon. Her unwavering faith in me made sure I never for one second hesitated in enrolling at the Physics Department, where I was greeted by...

... The 4 o'clock Dinner Gang (you know who you are!). An infinite well of brain dead topics for discussion over any type of beverages and/or edibles. Without you I would never have met...

... Lars S. Løvlie, balm for my soul. His invaluable moral support and last minute proof reading ensured that I could present this thesis in its never-to-be-edited-again form to...

... My supervisor, Jon Magne Leinaas. Infinite patience incarnate, thank you for the interesting topic which has been thoroughly enjoyable to delve into and for the gentle nudges to put me back on track when I diverged. I frequently say that there is no fun in easy achievements (a meagre comfort at most), and when the MDD[1] set in...

... Joar Bølstad was there to listen to my whining over a steaming cup of Earl Grey. We made it to graduation day! :)

You all put the "fun" in "student loan"! (Hey, wait a minute...)

Blindern, Oslo   .htm
2nd of June 2009

---

[1]Master student's Depression Disorder: a mental disorder characterized by an all-encompassing low mood accompanied by low self-esteem, and loss of interest or pleasure in normally enjoyable activities.

iii

Abstract

This thesis is a study of coherence theory in light in classical electromagnetism and quantum optics. Specifically two quantities are studied: The degree of first-order temporal coherence, which quantifies the field-field coherence, and the degree of second-order coherence, quantifying the intensity-intensity coherence. In the first part of the thesis these concepts are applied to classical electric fields; to both the ideal plane wave and to chaotic light. We then study how they can be measured using two interferometer technologies from optical astronomy, specifically with the Michelson stellar interferometer and the intensity interferometer.

In the second part we define the quantum degrees of first- and second-order coherence. These are calculated for light in a quantum coherent state, in a Fock state and for light in a mixed thermal state. The results for the coherent state and the thermal state are found to be analogous to those obtained for the ideal plane wave and chaotic light, respectively, from the classical coherence theory seen in the first part.

We proceed to investigate the properties of the three-level laser with the aim of showing that far above threshold it develops similar photon statistics and values for the degrees of first- and second-order coherence, to light in a coherent state. The mechanism of phase-drift in the laser is also looked into. Subsequently the Mølmer-model is discussed, where it is demonstrated that the coherent state is not a necessary construct, but merely a convenient one, in describing phenomena in quantum optics.

Contents

Introduction

Optics may very well be the oldest field in physics, with evidence of systematic (if not scientific by modern standards) writings dating back to antiquity and the Greek philosophers and mathematicians. Two millennia later the field is still in full vigour, especially these last six decades, where new discoveries keep pushing the frontiers. In 1704 Sir Isaac Newton gave out *Opticks*, which is considered one of the greatest works in the history of science. The geometrical optics of this time treated the light as rays travelling in straight lines until bending through refraction, and white light rays could be split into colours by a prism. James Clerk Maxwell (1873) succeeded in combining the then separate theories of electricity and magnetism, which by conjecture led to light waves being electromagnetic waves. Since then and up until today the very successful language of optics has been the theory of electromagnetism, or the more contemporary, semi-classical theory in which the fields are treated as electromagnetic waves and matter is treated with quantum mechanics.

However, the validity of the electromagnetic theory of light is limited. While it is capable of explaining the phenomena dealing with propagation of light, it fails when it comes to the finer features of the interaction between light and matter, such as the processes of emission and absorption. Here the theory must be replaced by quantum mechanics. The advent of quantum mechanics also brought with it the view that light is quantised as *photons*. Experiment after experiment confirmed both the particle and the wave description of light, leading to the "middle-ground" concept of the wave-particle-duality. The wave-particle duality says that all matter and energy exhibits both wave-like and particle-like properties and it has since it was first uttered been imprinted in the minds of (at least three) generations of physicists. Apparently the particle aspect of light, the photon view, became so deeply entrenched that it excluded the wave aspect almost entirely, at least for the visible part of the electromagnetic spectrum. These inflexible mindsets only grudgingly bent to include the wave view when the intensity interferometer for optical wavelengths was invented by R. Hanbury Brown and R. Twiss in 1956.

The problem was that the intensity interferometer was designed to measure *coherence*, but coherence was thought to be a property related to the classical electromagnetic wave, leading to interference. And this was accepted for radio waves, but not for the optical wavelengths as the light was believed to be so energetic as to be quantised in a relative small number of photons. Even so, Hanbury Brown and Twiss made successful measurements; Evidently a better understanding of the coherence properties of light

and their effect on the interaction between light and matter was required. The classical coherence theory has been around since classical electromagnetism was formulated, and it accounts well for phenomena like interference. But the quantum coherence theory was not fully formulated until Roy J. Glauber in 1963 presented the "coherent state" as particularly appropriate for the quantum treatment of optical coherence. Incidentally, the intensity interferometer could now be fully described by both the classical and the quantum theory. But it was mainly the development of the laser in the 1960s that led to the emergence of quantum optics as a new discipline. The laser was a completely new type of light source that provided very intense, coherent and highly directional beams which very closely resembled ideal plane waves. Recent "quantum leaps" in experimental techniques the last half of the 21st century has enabled measurements of single photons, and while the semi-classical theory of light is in good agreement with experiments on high frequency light, it yields incorrect results for experiments relying on photon statistics.

The central theme to this work is *coherence in light*. What is coherence and how is it quantified, calculated, measured? What is the difference between coherent light and incoherent light? Can light be something in between? Can coherence be explained by both classical electromagnetism and quantum mechanics? Are the explanations equivalent? Does it matter which statistical properties the light has?

The attempt to answer these questions is divided into two parts; First we take on coherence in classical terms where the mathematical description is developed in chapter 1, before applying the coherence theory to concrete cases. We have chosen two examples from optical astronomy for this purpose, where coherence is used to measure the angular diameter of a binary star, namely the Michaelson stellar interferometer and the intensity interferometer is explained in chapter 2. From the historical overview above it should be apparent why the intensity interferometer is interesting. The Michelson stellar interferometer then serves as a good contrast as it employs the less "controversial" classical coherence-effect of electric field interference.

In the second part we tackle the coherence problem on the quantum side of the ballpark. This requires the quantised electric field and the density operator, both of which are derived in chapter 3, to subsequently be put to use in the quantum coherence theory. In chapter 4 coherence is calculated for light in the coherent state, the Fock number state and the mixed thermal state. Chapter 5 is devoted to the principles of the laser. There we investigate its photon statistics and its coherence properties in order to see why the laser under certain conditions is a good approximation to the classical ideal plane wave. Finally, in chapter 6 we look into the Mølmer-model to see whether it is really necessary to use the coherent state to explain the occurrence of coherence in light.

For this work to be intelligible for students in their late bachelor's or early master's stage, some introductory material has been included in detail. For example, the derivation of the free classical electric field (which clarifies what is meant by a *mode* of the field) and the quantisation of the electric field (for the explicit relation between the complex classical field amplitude and the quantum harmonic oscillator operators).

Part I

Coherence in classical electromagnetism

Chapter 1

Classical electromagnetism and coherence

First on the agenda is to recapitulate the basics of the electromagnetic theory that pertains to the goal of this thesis: examining the concept of coherence in light, using both classical electric field theory and the quantum mechanical photon description. In the present chapter we will use Maxwell's equations to derive a form of the electric field which will be used in the discussion of coherence in section 1.2. It will also come in handy when we move on to the quantum theory in chapter 3 and need to work with the quantised electric field.

The goal of section 1.2 is to develop an understanding of coherence and of the two correlation functions famously known as the degree of first-order temporal coherence and the degree of second-order temporal coherence. The former tells us how the electric field measured at two points in time is correlated, and the latter quantifies the correlation of the electric field intensity in a similar way. We will also look into how these two functions are related to each other, and how the Wiener-Khinchin theorem relates the degree of first-order temporal coherence to the power spectrum of the radiation field.

This will all culminate in chapter 2 with the application of the degree of first- and second-order temporal coherence on two seemingly similar, but as we will see, fundamentally different, stellar interferometers.

1.1   Classical description of light

In this part we will take the semi-classical approach, in the sense that particles are described by quantum mechanical wave functions while the electromagnetic field is treated as classical waves. To find the required expressions for the electromagnetic field we start with Maxwell's equations.

1.1.1   Maxwell's equations

In the presence of a charge density $\rho(\mathbf{r}, t)$ and a current density $\mathbf{j}(\mathbf{r}, t)$, the electric and magnetic vector fields $\mathbf{E}$ and $\mathbf{B}$ satisfy Maxwell's equations [1]

$$\boldsymbol{\nabla} \cdot \mathbf{E} = \rho/\epsilon_0 \tag{1.1a}$$

$$\boldsymbol{\nabla} \cdot \mathbf{B} = 0 \tag{1.1b}$$

$$\boldsymbol{\nabla} \times \mathbf{E} = -\frac{\partial \mathbf{B}}{\partial t} \tag{1.1c}$$

$$\boldsymbol{\nabla} \times \mathbf{B} = \frac{1}{c^2}\frac{\partial \mathbf{E}}{\partial t} + \mu_0 \mathbf{J} \tag{1.1d}$$

where we have used SI units, and μ_0 is the magnetic constant and ϵ_0 the electric constant such that $\mu_0 \epsilon_0 = c^{-2}$. As usual c denotes the speed of light in vacuum[2]. We will consider the case of the free field, i.e., in absence of charges and currents, equivalent to setting $\rho = 0$ and $\mathbf{J} = 0$.

Gauss' law Eq. (1.1a) describes how the electric field will behave in the vicinity of an electric charge: the field lines points towards a negative charge and away from a positive charge. Gauss' law for magnetism Eq. (1.1b) tells us that unlike electricity, there is no "positive" or "negative" particles that can make the magnetic field tend to point towards or away from them. Instead these particles must come in pairs of both negative and positive. Faraday's law of induction Eq. (1.1c) says that a change in the magnetic field can induce an electric field, and Ampere's law Eq. (1.1d) shows how a change in the electric field or an electric current can induce a magnetic field.

From Gauss' law for magnetism and Faraday's law of induction one can define the scalar and the vector potentials $\phi(\mathbf{r}, t)$ and $\mathbf{A}(\mathbf{r}, t)$ as follows

$$\mathbf{B} = \boldsymbol{\nabla} \times \mathbf{A}, \qquad \mathbf{E} = -\boldsymbol{\nabla}\phi - \frac{\partial \mathbf{A}}{\partial t}. \tag{1.2}$$

This does not determine the potentials uniquely, however, since there are many different choices of ϕ and $\mathbf{A}$ that will yield the same $\mathbf{E}$ and $\mathbf{B}$. To cope with the redundant degrees of freedom in the field variables we can choose the typical gauge

$$\boldsymbol{\nabla} \cdot \mathbf{A} = 0. \tag{1.3}$$

This constraint on the vector potential is known as the *Coulomb gauge* and it has the advantage that it decouples the equations for $\phi(\mathbf{r}, t)$ and $\mathbf{A}(\mathbf{r}, t)$. Eq. (1.3) is also called a *transverse gauge*, since a vector field satisfying it is a transverse wave. If at point $\mathbf{r}$ in space, at time t, the vector potential is

$$\mathbf{A}(\mathbf{r}, t) = \sum_{\mathbf{k}} \mathbf{A}_{\mathbf{k}} e^{i(\mathbf{k} \cdot \mathbf{r} - \omega_k t)}$$

---

[1] In this work all vectors are in boldface. Also the del operator is

$$\boldsymbol{\nabla} \equiv \mathbf{e}_x \frac{\mathrm{d}}{\mathrm{d}x} + \mathbf{e}_y \frac{\mathrm{d}}{\mathrm{d}y} + \mathbf{e}_z \frac{\mathrm{d}}{\mathrm{d}z}$$

where $(\mathbf{e}_x, \mathbf{e}_y, \mathbf{e}_z)$ are unit vectors in the respective coordinate directions.

[2] The speed of light in vacuum is $c = 3.0 \cdot 10^8$ m/s.

where $\mathbf{A}_0$ is the field amplitude, $\mathbf{k}$ is the wave vector and $\omega_k = |\mathbf{k}|c$ is the angular frequency, then

$$\boldsymbol{\nabla} \cdot \mathbf{A} \propto \sum_{\mathbf{k}} \mathbf{k} \cdot \mathbf{A_k} = 0, \tag{1.4}$$

which means that $\mathbf{A}$ is perpendicular to the direction of the propagation $\mathbf{k}$ of the wave. The electric and magnetic fields $\mathbf{E}$ and $\mathbf{B}$ can be expressed in terms of the transverse field $\mathbf{A}$, and are therefore themselves transverse fields. $\mathbf{A}$ is often referred to as the radiation field and we will frequently use the term "radiation field". However, as the majority of the calculations in this work involves the electric field, it is implied that we are interested in just the electric part of the radiation field. After all, even if technically the radiation field is composed of both an electric and a magnetic component, we can always choose a reference frame where we only perceive the electric field.

1.1.2 The free classical electric field

At any given instant in time the electric field $\mathbf{E}$ must be specified at every point $\mathbf{x}$ in space. But this implies that the electric field has an infinite number of degrees of freedom. To work around this problem we consider the radiation to be confined in a cubic *cavity* with sides of length L and periodic boundary conditions imposed at the walls of the cavity. We can then represent the electric field as a Fourier series, with an infinite, but countable, number of Fourier coefficients.

From Maxwell's equations we can take the curl of Eq.(1.1c) and then use Eq.(1.1a) while inserting Eq.(1.1d). A key ingredient is the relation

$$\boldsymbol{\nabla} \times (\boldsymbol{\nabla} \times \mathbf{E}) = \boldsymbol{\nabla}(\boldsymbol{\nabla} \cdot \mathbf{E}) - \boldsymbol{\nabla}^2 \mathbf{E}.$$

The end result shows that $\mathbf{E}(\mathbf{r}, t)$ satisfies the wave equation

$$\boldsymbol{\nabla}^2 \mathbf{E} - \frac{1}{c^2} \frac{\partial^2 \mathbf{E}}{\partial t^2} = 0. \tag{1.5}$$

The electric vector field can be split up in a scalar and a vector part like

$$\mathbf{E} = \sum_{\mathbf{k}} \sum_{\lambda} \boldsymbol{\epsilon}_{\mathbf{k}\lambda} E_{\mathbf{k}\lambda} \tag{1.6}$$

where $E_{\mathbf{k}\lambda}$ is the scalar electric field of mode $\mathbf{k}$, the meaning of which will soon be apparent, and $\boldsymbol{\epsilon}_{\mathbf{k}\lambda}$ is the unit polarisation vector of mode $\mathbf{k}$ in direction λ. It is pretty straight forward to solve the partial differential equation, especially since the boundary conditions on the cavity should be independent of time. One can then do a separation of the variables $\mathbf{r}$ and t, e.g.,

$$E_{\mathbf{k}\lambda}(\mathbf{r}, t) = X_{\mathbf{k}\lambda}(\mathbf{r}) a_{\mathbf{k}\lambda}(t). \tag{1.7}$$

which leads to two ordinary differential equations for each mode $\mathbf{k}$

$$\frac{1}{X_{\mathbf{k}\lambda}} \boldsymbol{\nabla}^2 X_{\mathbf{k}\lambda} = \frac{1}{c^2 a_{\mathbf{k}\lambda}} \frac{\partial^2 a_{\mathbf{k}\lambda}}{\partial t^2} = -|\mathbf{k}|^2. \tag{1.8}$$

We can assume a running-wave solution, in which case the boundary conditions will give

$$X_{\mathbf{k}\lambda}(\mathbf{r}) = \boldsymbol{\epsilon}_{\mathbf{k}\lambda} e^{i\mathbf{k}\cdot\mathbf{r}} \tag{1.9}$$

Then the scalar electric field can be written on the form

$$E_{\mathbf{k}\lambda}(\mathbf{r},t) = a_{\mathbf{k}\lambda}(t)e^{i\mathbf{k}\cdot\mathbf{r}} + a^*_{\mathbf{k}\lambda}(t)e^{-i\mathbf{k}\cdot\mathbf{r}}. \tag{1.10}$$

This form ensures that the electric field is real: $E = E^*$. The periodic boundary conditions are ensured by

$$\mathbf{k} = (k_x, k_y, k_z) = \frac{2\pi}{L}(n_x, n_y, n_z), \qquad n_x, n_y, n_z = 0, \pm1, \pm2, \ldots \tag{1.11}$$

$\sum_{\mathbf{k}}$ is understood to be the sum over the integers n_x, n_y, n_z and the set of numbers (n_x, n_y, n_z) defines a *mode* of the electromagnetic field. So later when we talk about one *mode of the electric field*, we mean one of the possible solutions to the electric field wave equation.

With $\boldsymbol{\epsilon}_{\mathbf{k}\lambda}$ as the unit polarization vector we see from Eq. (1.1a) that the electric field is purely transverse since

$$\left[\boldsymbol{\nabla} E_{\mathbf{k}\lambda}(\mathbf{r},t)\right] \cdot \boldsymbol{\epsilon}_{\mathbf{k}\lambda} = 0 \qquad \Rightarrow \qquad \mathbf{k} \cdot \boldsymbol{\epsilon}_{\mathbf{k}\lambda} = 0. \tag{1.12}$$

This means that there are only two independent polarization directions of $\hat{\epsilon}_{\mathbf{k}}$ for each $\mathbf{k}$. These two unit vectors are mutually perpendicular:

$$\boldsymbol{\epsilon}_{\mathbf{k}\lambda} \cdot \boldsymbol{\epsilon}_{\mathbf{k}\lambda'} = \delta_{\lambda\lambda'}, \qquad \lambda, \lambda' = 1, 2. \tag{1.13}$$

The electric field is now essentially expanded as a Fourier series

$$\mathbf{E}(\mathbf{r},t) = \sum_{\mathbf{k}} \sum_{\lambda} \left(\frac{\hbar\omega_k}{2\epsilon_0 L^3}\right)^{1/2} \boldsymbol{\epsilon}_{\mathbf{k}\lambda}\left[a_{\mathbf{k}\lambda}(t)e^{i\mathbf{k}\cdot\mathbf{r}} + a^*_{\mathbf{k}\lambda}(t)e^{-i\mathbf{k}\cdot\mathbf{r}}\right] \tag{1.14}$$

The factor $(\hbar\omega_k/2\epsilon_0 L^3)^{1/2}$ is a convenient choice[3]. The modal components of $\mathbf{E}$ must satisfy the wave equation Eq. (1.5), so we insert Eq. (1.14) into it with the result that each mode $\mathbf{k}$ must fulfill

$$\left(\boldsymbol{\nabla}^2 - \frac{1}{c^2}\frac{\partial^2}{\partial t^2}\right)\left(\frac{\hbar\omega_k}{2\epsilon_0 L^3}\right)^{1/2} \boldsymbol{\epsilon}_{\mathbf{k}\lambda} a_{\mathbf{k}\lambda}(t)e^{i\mathbf{k}\cdot\mathbf{r}} = 0 \tag{1.15}$$

giving

$$\frac{\partial^2}{\partial t^2}a_{\mathbf{k}\lambda}(t) + \omega_k^2 a_{\mathbf{k}\lambda}(t) = 0. \tag{1.16}$$

This is the equation for the harmonic oscillator for the normal mode $\mathbf{k}$ of the radiation field. A convenient solution is

$$a_{\mathbf{k}\lambda}(t) = a_{\mathbf{k}\lambda}e^{-i\omega_k t}, \tag{1.17}$$

---

[3] The Planck constant is defined as $h = 2\pi\hbar = 6.626 \cdot 10^{-34}$ Js.

where $\omega_k = c|\mathbf{k}|$ and $a_{\mathbf{k}\lambda}$ is the initial amplitude at time $t = 0$. The electric field then becomes

$$\mathbf{E}(\mathbf{r}, t) = \sum_{\mathbf{k}} \sum_{\lambda} \left(\frac{\hbar\omega_k}{2\epsilon_0 L^3} \right)^{1/2} \boldsymbol{\epsilon}_{\mathbf{k}\lambda} \left[a_{\mathbf{k}\lambda} e^{i(\mathbf{k}\cdot\mathbf{r} - \omega_k t)} + a_{\mathbf{k}\lambda}^* e^{-i(\mathbf{k}\cdot\mathbf{r} - \omega_k t)} \right]. \quad (1.18)$$

Now that we have an expression for the free electric field we can use Eq. (1.1c) to find the magnetic field. The fairly straight forward calculation gives

$$\mathbf{B}(\mathbf{r}, t) = \sum_{\mathbf{k}} \sum_{\lambda} \left(\frac{\hbar\omega_k}{2\epsilon_0 L^3} \right)^{1/2} \frac{\mathbf{k} \times \boldsymbol{\epsilon}_{\mathbf{k}\lambda}}{\omega_k} \left[a_{\mathbf{k}\lambda} e^{i(\mathbf{k}\cdot\mathbf{r} - \omega_k t)} + a_{\mathbf{k}\lambda}^* e^{-i(\mathbf{k}\cdot\mathbf{r} - \omega_k t)} \right]. \quad (1.19)$$

With the expressions for $\mathbf{E}$ and $\mathbf{B}$ in place, we have the solution for the transverse electromagnetic waves in free space. The total energy of the radiation field in the cavity with volume $V = L^3$ is

$$H_R = \frac{1}{2} \epsilon_0 \int_V (\mathbf{E}^2 + c^2 \mathbf{B}^2) \mathrm{d}\mathbf{r}. \quad (1.20)$$

This calculation is carried out in Appendix B.1 and the resulting total radiative energy is

$$H_R = \sum_{\mathbf{k}} \sum_{\lambda} \frac{1}{2} \hbar\omega_k (a_{\mathbf{k}\lambda} a_{\mathbf{k}\lambda}^* + a_{\mathbf{k}\lambda}^* a_{\mathbf{k}\lambda}) = \sum_{\mathbf{k}} \sum_{\lambda} \hbar\omega_k a_{\mathbf{k}\lambda} a_{\mathbf{k}\lambda}^* \quad (1.21)$$

i.e., a sum of the time-independent contributions from field amplitudes of the individual modes $\mathbf{k}$. The field amplitudes $a_{\mathbf{k}\lambda}$ and $a_{\mathbf{k}\lambda}^*$ are classical coefficients which commute, so the two terms can be added to form one single term. This form for the radiative energy suggests an analogy between the mode amplitudes $a_{\mathbf{k}\lambda}, a_{\mathbf{k}\lambda}^*$ and an ensemble of the individual one-dimensional harmonic oscillators. From chapter 3 and on, we need the quantised radiation field, which will be found by replacing the classical harmonic oscillator with the corresponding quantum mechanical harmonic oscillator, and converting the classical field variables into field operators. Eq. (1.21) will show the conversion from the classical electric amplitudes to the quantum mechanical mode operators.

1.1.3 The Poynting vector

The electric field comes in many shapes and forms depending on what will be most suitable for the pending calculation. In the above we have found a form of the electric field which will be very convenient when we later move on to the quantum part of quantum optics, but in the immediate future we do not need such a complicated form of the field and we can stick to just the positive frequency part

$$\mathbf{E}(\mathbf{r}, t) = \sum_{\mathbf{k}} \sum_{\lambda} \left(\frac{\hbar\omega_k}{2L^3} \right)^{1/2} \boldsymbol{\epsilon}_{\mathbf{k}\lambda} a_{\mathbf{k}\lambda} e^{i(\mathbf{k}\cdot\mathbf{r} - \omega_k t)} \quad (1.22)$$

This is justified by the fact that $\mathbf{E}(\mathbf{r}, t)$ is real and that the negative frequency part does not contain any new information that is not already provided by the positive frequency part since they are the complex conjugated of each other. While we know that the electric field is *real*; our eyes detect it, the nerve endings in our skin prickles from the intensity of it; it is a matter of mathematical convenience to do calculations with a *complex* electric wave function. However, when we in the end need the real field, it is only a question of adding the negative frequency part back into Eq. (1.22).

The intensity of the complex electromagnetic field is given by the Poynting vector

$$\mathbf{S} = \frac{1}{2}\epsilon_0 c^2 (\mathbf{E} \times \mathbf{B}). \tag{1.23}$$

From Eqs. (1.14) and (1.19) we have for a selected mode

$$\mathbf{B_k} = \frac{\mathbf{k}}{kc} \times \mathbf{E_k} \tag{1.24}$$

giving

$$\mathbf{S_k} = \frac{1}{2}\epsilon c^2 \mathbf{E_k} \times \left(\frac{\mathbf{k}}{kc} \times \mathbf{E_k}\right) = \frac{1}{2}\epsilon_0 c \left[\frac{\mathbf{k}}{k}(\mathbf{E_k} \cdot \mathbf{E_k}) - \mathbf{E_k}\left(\frac{\mathbf{k}}{k} \cdot \mathbf{E_k}\right)\right]$$

$$= \frac{1}{2}\epsilon_0 c |\mathbf{E_k}|^2 \frac{\mathbf{k}}{k}, \tag{1.25}$$

where the rightmost term on the second line is zero due to Eq. (1.12).

It is impractical, or even impossible, to resolve the oscillations in the electric field in Eq. (1.22) that occur at the frequency ω_k. According to [1], a good experimental resolving time is of the order of 10^{-9} s, which is far too long to detect oscillations at visible frequencies (e.g. $\omega_k \sim 10^{15}$Hz). It is therefore more meaningful to instead use $\bar{I}(t)$ in the calculations. The overbar denotes the cycle-averaged intensity, which means that the theoretical expression for the intensity has been averaged over one period of the wave,

$$\bar{I}(t) = |\bar{\mathbf{S}}| = \frac{1}{T}\int_T \frac{1}{2}\epsilon_0 c |E(\mathbf{r}, t)|^2 \mathrm{d}t = \frac{1}{2}\epsilon_0 c |\bar{E}(\mathbf{r}, t)|^2. \tag{1.26}$$

1.2   Coherence

This section is devoted to explaining what *coherence* is and what it means for light to be coherent. This will pave the way for chapter 2 where we will investigate how one can utilise the coherence of light to determine the diameter of a binary star with stellar interferometers.

Interferometers have their name from the effect they exploit to study the properties of light, namely *interference*. As we are taught early on in undergrad-hood, interference creates a new wave pattern when two or more waves are superposed on each other.

The interference effect is due to the relative difference in the phases of the superposed waves. Depending of the relative phase, two waves will either interfere constructively (difference of $2m\pi$, m is an integer) or destructively (difference of $2(m+1)\pi$). If the waves have the same frequency with a constant relative phase difference, they are said to be *coherent*.

The classical description of the electric part of an ideal plane light wave is

$$E(\mathbf{r}, t) = E_0 e^{i(\mathbf{k} \cdot \mathbf{r} - \omega t)}. \tag{1.27}$$

From now on for the rest of this work, we for simplicity assume that the field is linearly polarized in one direction and is thus scalar. The ideal plane wave is perfectly coherent, which means that if we know the amplitude and phase at one time, we can deduce if for all times. To create interference we could for instance split the ideal wave in two, and let each part follow two different paths until they are brought back together again. If the paths have different lengths, the path difference $\Delta d = c\tau$ (where τ can be called the time delay) will introduce a relative phase difference of $\Delta\phi = \omega\tau$ between the two fields when they are superposed. Changes in the path difference, i.e., in τ, will reveal itself in transitions between constructive and destructive interference.

In practice, however, a single free atom does not at all radiate ideal monochromatic light, but rather the generalised field

$$E(\mathbf{r}, t) = |E(\mathbf{r}, t)| e^{i\phi(\mathbf{r}, t)}. \tag{1.28}$$

where $\phi(\mathbf{r}, t)$ contains some range of angular frequencies $\Delta\omega$. So if the relative phase of the superposed fields is not constant overall, but only approximately constant within a time interval τ_c, the fields are *partially coherent*. The frequency spread in the source leads to the possibility that intensity maxima for one frequency coincides with the minima of another. In effect this washes out the interference pattern and imposes practical limits on the maximum time delay τ that will give an observable interference pattern. So in a sense coherence is a measure of the frequency stability of the light, and it is quantified by the *coherence time* τ_c. From this we obtain the *coherence length* $d_c = c\tau_c$. If we know the phase of the wave at some position z at time t, then we will know the phase at the same position at $t + \tau$ with high certainty if $\tau \ll \tau_c$, or with very low certainty if $\tau \gg \tau_c$.

To quantify coherence we can calculate the *correlation*. We will focus on two types of correlations of the electric field, the first of which is the first-order correlation of one field at two points in space that are separated by a distance $d = c\tau$. The equivalent would be one field at the same point in space, measured at two times t and $t + \tau$. In both cases τ can be seen as a delay in the measurements. Secondly we will look at the second-order correlation of the field *intensity* at two points in space, also separated by $d = c\tau$. Much of this chapter follows the discussion in [1].

It should be pointed out that there are in general *two types* of coherence: *temporal* and *spatial* coherence. We have made a choice to focus on temporal coherence; it is in principle simpler and more intuitive than spatial coherence and the examples we will look at in chapter 2 will work just fine without the added complications.
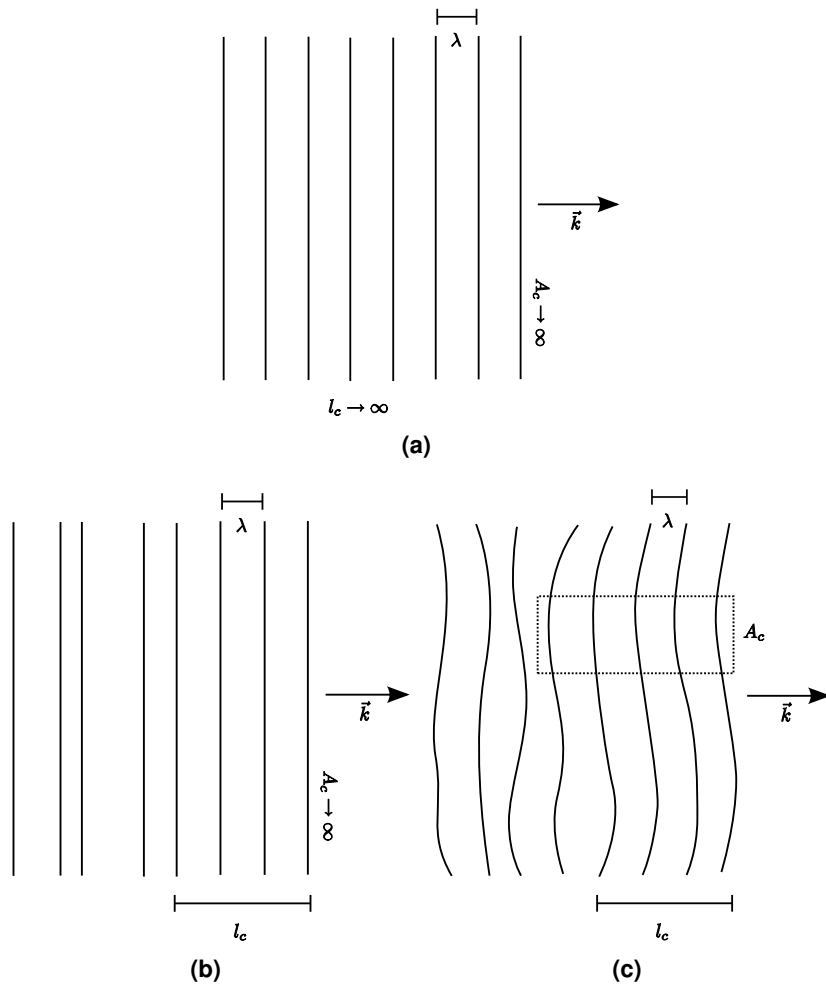
Figure 1.1: Visualisation of different types of coherent light. (a) Light with both infinite coherence length l_c and infinite coherence area A_c. (b) Spatially coherent light with infinite coherence area A_c, but only partially temporal coherence as seen from the finite coherence length l_c. (c) Partially spatial and temporal coherent light, with finite coherence length and area.

Nevertheless, a few words are well spent on explaining what is meant by temporal and spatial coherence. The ideal wave case has an infinite temporal coherence length l_c and an infinite spatial coherence area A_c, as can be seen in Fig. 1.1(a). Temporal coherence is a measure of how well correlated the phases of a light wave are at different points along the direction of propagation. In that sense one could call this a longitudinal coherence. Sampling the field at time t, how well could you then predict the amplitude and phase a time τ later? This prediction would be pretty accurate as long as τ is within the coherence time τ_c of the light, which is infinite for the ideal wave. The more temporally coherent the light is, the more monochromatic it is.

Spatial coherence is in contrast a measure of how well correlated the phases are at different points normal to the direction of propagation. In that respect one could call it transverse coherence. The more spatially coherent the light is, the more uniform

the wave front is. A perfect point source would be perfectly spatially coherent, but in practice of course, a real source must have a finite physical size and as such spatial coherence should only be neglected in gedankenversuche and master's theses.

The *coherence area* A_c is defined as the length of the coherent wave front multiplied with the wavelengths where the profile of the field is unchanged. In order to observe interference when the light passes through two slits, the coherence area A_c must be large enough that the wave front is more or less constant, otherwise the interference pattern is washed out. Light can be temporally and/or spatially coherent; The one does not preclude nor imply the other. Examples can be seen in Fig. 1.1(b), where light is spatially coherent, but have only partial temporal coherence, while in Fig. 1.1(c) the light have partial spatial and temporal coherence[4].

1.2.1   Different types of light

In this work we will deal with mainly two types of light sources: Those that emit coherent light and those that emit chaotic light. The laser[5] is thought to be a coherent light source in that it emits (mostly) monochromatic light with a constant relative phase. To really understand the laser we need to use quantum theory. This is postponed until chapter 5 in the second part, dedicated to the laser and its intriguing properties.

Chaotic sources, like for example the filament lamp or the sun, are so-called *thermal* sources where the radiation is the result of high temperature. They consist of a very large number of atoms which radiates almost independently of each other, leading to the term *chaotic*. The frequency and phase of the emitted light is determined by the unstable energy levels of the atoms, the statistical spread in atomic velocities and random collisions between atoms. Thus the statistical properties of chaotic light are profoundly different from that of coherent light.

We adopt the common convention that chaotic light is ergodic. If a random process is ergodic, any average calculated along a sample function (i.e., a time average of the electric field emitted by a single atom) must equal the same average calculated across the ensemble (i.e., a simultaneous ensemble average over the ν equivalent atoms). A less restrictive demand is that the statistics governing chaotic light is wide-sense stationary, meaning that the following two conditions are met

1. $E[u(t)]$ is independent of t.
2. $E[u(t_1)u(t_2)]$ is independent of $\tau = t_2 - t_1$.

where $E[]$ denotes the expectation value of the random process[6] $u(t)$ [2]. So by wide-sense stationary it is meant that the random fluctuations in the light are governed by influences that does not change with time.

---

[4]Please allow for artistic interpretation!

[5]Light Amplification by Stimulated Emission of Radiation.

[6]The definition of a random process is to assign the real valued function $u(A; t)$, at independent variable t, to an event A. In our case $u(t)$ would be the real electric field produced by a source emission at time t.

1.3   The degree of first-order coherence

The *degree of first-order temporal coherence* of light is useful for quantifying the coherence of either two electric fields simultaneously at two points in space, or of one field at one point in space at two different times. It is defined as

$$g^{(1)}(\tau) = \frac{\langle E^*(t)E(t+\tau)\rangle}{\langle E^*(t)E(t)\rangle} \tag{1.29}$$

which is a normalised version of the *first-order correlation function* for the electric field sampled at times t and $t + \tau$

$$\langle E^*(t)E(t+\tau)\rangle = \frac{1}{T}\int_{t-T/2}^{t+T/2} E^*(t')E(t'+\tau)\mathrm{d}t'. \tag{1.30}$$

The angle brackets denotes time averaging. If the light has wide-sense stationary statistics the correlation only depends on the time delay τ between the two field values. In that case Eq. (1.30) is independent of the starting time t, at least in so far that the interval T is much longer than the characteristic time scale of the fluctuations. The characteristic time is also called the coherence time, denoted by τ_c.

From

$$\langle E^*(t)E(t-\tau)\rangle = \langle E^*(t)E(t+\tau)\rangle^* = \langle E(t)E^*(t+\tau)\rangle$$

it follows that

$$g^{(1)}(-\tau) = g^{(1)}(\tau)^*. \tag{1.31}$$

By the definition in Eq. (1.29) it is obvious that for $\tau = 0$

$$g^{(1)}(0) = 1, \tag{1.32}$$

which means that at zero delay time τ, the light is first-order coherent and for delay times $\tau \ll \tau_c$ it will remain approximately coherent.

For chaotic light   (of any kind) the field correlations vanish for delay times much longer than the coherence time. This is because the coherence time is the average time between random changes to the field, e.g. in amplitude or phase. When the field undergoes random changes there should be no correlation between the field before the change and the field after the change. This will be discussed in more detail in section 1.3.1. Since the electric field has a period much shorter than T, its expectation value vanishes

$$\langle E(t)\rangle = 0,$$

and the degree of first-order coherence[7] has the limiting value

$$g^{(1)}(\tau) \to 0 \quad \text{for} \quad \tau \gg \tau_c. \tag{1.33}$$

---

[7]*Temporal* coherence is implied throughout unless stated otherwise.

So, in terms of the value of $g^{(1)}(\tau)$ the following describes the light at two pairs of space-time points

$$
\text{For} \quad |g^{(1)}(\tau)|
\begin{cases}
= 1 \\
\in (0,1) \\
= 0
\end{cases}
\quad \text{the light is} \quad
\begin{cases}
\text{first-order coherent} \\
\text{partially coherent} \\
\text{incoherent}
\end{cases}
\tag{1.34}
$$

Note that the coherence property Eq. (1.33) strictly refers to chaotic light and does not apply to the classical wave of constant amplitude and phase.

For an ideal plane wave propagating in the z-direction with wave vector $k = \omega_0/c$ and constant phase ϕ,

$$
E(z,t) = E_0 e^{i(kz - \omega_0 t + \phi)},
\tag{1.35}
$$

the electric field correlation is

$$
\langle E^*(t)E(t+\tau)\rangle = \langle E_0^2 e^{-i(kz-\omega_0 t+\phi)} e^{i(k(z+c\tau)-\omega_0 t+\phi)}\rangle = E_0^2 e^{i\omega_0\tau}
\tag{1.36}
$$

where $\tau = t_2 - t_1 - (z_2 - z_1)/c$. Then the degree of first-order coherence is simply

$$
g^{(1)}(\tau) = e^{i\omega_0\tau} \qquad \rightarrow \qquad |g^{(1)}(\tau)| = 1.
\tag{1.37}
$$

Thus the ideal wave is first-order coherent at all pairs of space-time points [1]. In section 5, we will see that the beam from a single-mode laser is a close approximation to such an ideal, stable wave.

It is also interesting for comparison with later calculations, to express the degree of first-order coherence with the electric field on the form of

$$
\mathbf{E}(\mathbf{r},t) = \sum_{\mathbf{k}} \sum_{\lambda} \left(\frac{\hbar\omega_k}{2\epsilon_0 L^3}\right)^{1/2} \hat{\epsilon}_{\mathbf{k}\lambda} a_{\mathbf{k}\lambda} e^{i(\mathbf{k}\cdot\mathbf{r}-\omega_k t)}
\tag{1.22}
$$

but for simplicity we can assume a linear polarisation λ so that we can use the scalar electric field, $E(\mathbf{r},t)$. This gives

$$
\begin{aligned}
g^{(1)}(\tau) &= \frac{\displaystyle\sum_{\mathbf{k}\mathbf{k}'} \left\langle \sqrt{\omega_k} a_{\mathbf{k}}^* e^{-i(\mathbf{k}\cdot\mathbf{r}-\omega_k t)} \sqrt{\omega_{k'}} a_{\mathbf{k}'} e^{i(\mathbf{k}'\cdot\mathbf{r}+k'c\tau-\omega_{k'}t)} \right\rangle}{\displaystyle\sum_{\mathbf{k}\mathbf{k}'} \left\langle \sqrt{\omega_k} a_{\mathbf{k}}^* e^{-i(\mathbf{k}\cdot\mathbf{r}-\omega_k t)} \sqrt{\omega_{k'}} a_{\mathbf{k}'} e^{i(\mathbf{k}'\cdot\mathbf{r}-\omega_{k'}t)} \right\rangle} \\[2em]
&= \frac{\displaystyle\sum_{\mathbf{k}\mathbf{k}'} \sqrt{\omega_k \omega_{k'}} \left\langle a_{\mathbf{k}} a_{\mathbf{k}'}^* e^{-i(\omega_{k'}-\omega_k)t} \right\rangle e^{i(\mathbf{k}'-\mathbf{k})\cdot\mathbf{r}+i\omega_{k'}\tau}}{\displaystyle\sum_{\mathbf{k}\mathbf{k}'} \sqrt{\omega_k \omega_{k'}} \left\langle a_{\mathbf{k}} a_{\mathbf{k}'}^* e^{-i(\omega_{k'}-\omega_k)t} \right\rangle e^{i(\mathbf{k}'-\mathbf{k})\cdot\mathbf{r}}} \\[2em]
&= \frac{\displaystyle\sum_{\mathbf{k}} \sqrt{\omega_k} a_{\mathbf{k}}^* \left\langle e^{-i\omega_k t} \right\rangle e^{i\mathbf{k}\cdot\mathbf{r}+i\omega_k\tau}}{\displaystyle\sum_{\mathbf{k}} \sqrt{\omega_k} a_{\mathbf{k}}^* \left\langle e^{-i\omega_k t} \right\rangle e^{i\mathbf{k}\cdot\mathbf{r}}}.
\end{aligned}
\tag{1.38}
$$

So in contrast to the case with only one field mode $\mathbf{k}$, $g^{(1)}(\tau)$ is now effectively a sinusoidal function weighted by the normalised statistical ensemble of modes. In the following section we will see how this weighting function can be ascribed to primarily two frequency distributions, the Lorentzian and the Gaussian, and how this is related to the nature of excited atoms and their interaction with the environs.

1.3.1   Concrete models of radiation for $g^{(1)}(\tau)$

In Eq. (1.38) we saw that the degree of first-order coherence is a sinusoidal function of the delay between two measurements of the electric field, weighted by a factor which we can interpret as statistical fluctuations of the field-modes. We will now look at three different cases which induces fluctuations in either the relative phase or the angular frequency of the light. These three cases are

- Lifetime (natural) broadening
- Collision (pressure) broadening
- Doppler broadening

and each can be put into two categories. The first two are *homogeneous* broadening mechanisms while the third is an *inhomogeneous* broadening mechanism [3]. In general the electric field is on the form

$$E(\mathbf{r}, t) = |E(\mathbf{r}, t)| e^{i(\mathbf{k}\cdot\mathbf{r} - \omega_k(t)t + \phi(t))} \tag{1.39}$$

By homogeneous it is meant that all the individual atoms in the light source behave in the same way and produce light of the same angular frequency so only their relative phase is different (i.e., $\omega_k(t) \rightarrow \omega_0$ and $\phi(t)$). The latter case is inhomogeneous in the sense that the individual atoms behave differently and produce light with slightly differing angular frequency, while their relative phase remains unchanged (i.e., $\phi(t) \rightarrow \phi$ and $\omega_k(t)$). A detailed derivation of $g^{(1)}(\tau)$ for collision broadened and Doppler broadened light can be found in appendix A.

Light experiencing inhomogeneous broadening mechanisms will have a Lorentzian frequency distribution, yielding the degree of first-order coherence

$$g^{(1)}(\tau) = e^{-i\omega_0\tau - |\tau|/\tau_c}. \tag{1.40}$$

where τ_c can be due to either the natural line width of a spontaneous emission spectrum or the mean free flight time between collisions of source atoms leading to emission. Light with a homogeneous broadening mechanism displays a Gaussian frequency distribution, yielding the degree of first-order coherence

$$g^{(1)}(\tau) = e^{-i\omega_0\tau - \frac{\pi}{2}(\tau/\tau_c)^2}. \tag{1.41}$$

Here τ_c can be related to the temperature of a gas of atomic sources where the emission spectrum is Doppler shifted. Fig. 1.2 shows $|g^{(1)}(\tau)|$ for coherent light and chaotic light with a Lorentzian and Gaussian frequency distribution. We see that near $\tau = 0$ chaotic light is first-order coherent.
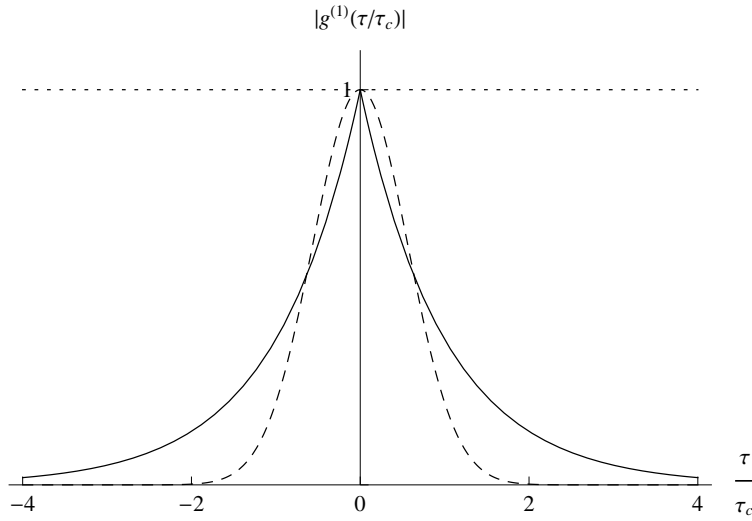
Figure 1.2: The modulus of the degree of first-order coherence of coherent light (dotted lined) and of chaotic light with a Lorentzian (solid line) and Gaussian (dashed line) frequency distribution. Adapted from [1].

1.3.2 The physical interpretation of $g^{(1)}(\tau)$

To understand the physical meaning of $g^{(1)}(\tau)$ we can consider the visibility of the interference pattern that forms when two (or more) light waves are superposed. Visibility is a measure of the contrast between the light and dark patches (also called fringes) and it is defined as

$$V = \frac{\langle I \rangle_{\text{max}} - \langle I \rangle_{\text{min}}}{\langle I \rangle_{\text{max}} + \langle I \rangle_{\text{min}}} \tag{1.42}$$

where $\langle I \rangle_{\text{max}}$ and $\langle I \rangle_{\text{min}}$ represent the maximum and minimum intensity of the fringes, respectively. In fact, the visibility is a measure of the coherence between the two fields (or between the same field at two different times). We will see in chapter 2 that the intensity of two superposed electric fields can be written in terms of the degree of first-order coherence, essentially meaning that

$$V \sim |g^{(1)}(\tau)|, \tag{1.43}$$

i.e., the visibility is proportional to the magnitude of the first degree of coherence. So from Eq. (1.34) the maximum visibility of the fringes is obtained when $|g^{(1)}(\tau)| = 1$ and the two light beams are completely coherent. Maximal contrast means that the dark patches are completely dark due to perfect destructive interference. If the two light beams are incoherent, the contrast of the fringes is zero and there are no discernible darker patches. That is, if the light waves are incoherent there will be no visible interference pattern.

Another important aspect of $g^{(1)}(\tau)$ is its relation to the frequency spectrum of the emitted light through the Fourier transform of an electric field $E(t)$ over the integration range T,

$$E_T(\omega) = \frac{1}{\sqrt{2\pi}} \int_T \mathrm{d}t E(t) e^{i\omega t}. \tag{1.44}$$

The *power spectral density* of an electromagnetic wave is defined as

$$f(\omega) = \frac{|E_T(\omega)|^2}{T} = \frac{1}{2\pi T} \iint_T E^*(t)E(t')e^{-i\omega(t-t')} \mathrm{d}t\mathrm{d}t', \qquad (1.45)$$

i.e., how the average power is distributed over frequency. As stated earlier, the statistics of wide-sense stationary light beams depends only on the time difference $\tau = t' - t$. Changing variables in Eq. (1.45) will put the spectral density on the form of the first-order correlation function,

$$\begin{aligned} f(\omega) &= \frac{1}{2\pi T} \iint_T E^*(t)E(t')\mathrm{d}t e^{i\omega\tau}\mathrm{d}\tau \\ &= \frac{1}{2\pi} \int_{-\infty}^{\infty} \langle E^*(t)E(t+\tau)\rangle e^{i\omega\tau}\mathrm{d}\tau \end{aligned} \qquad (1.46)$$

where we have inserted infinite limits since the correlation time τ_c is much smaller than the integrated time T. If Eq. (1.46) is divided by the term $\langle E^*(t)E(t)\rangle$ we will get $g^{(1)}(\tau)$. This can be achieved by doing a trick involving the delta-function

$$\delta(t_0 - t) = \frac{1}{2\pi} \int_{-\infty}^{\infty} e^{i\omega(t_0-t)}\mathrm{d}\omega \qquad (1.47)$$

which we use to rewrite Eq. (1.46)

$$\begin{aligned} \int_{-\infty}^{\infty} f(\omega)\mathrm{d}\omega &= \frac{1}{2\pi} \iint_{-\infty}^{\infty} \langle E^*(t)E(t+\tau)\rangle e^{i\omega\tau}\mathrm{d}\omega\mathrm{d}\tau \\ &= \int_{-\infty}^{\infty} \langle E^*(t)E(t+\tau)\rangle\delta(\tau)\mathrm{d}\tau = \langle E^*(t)E(t)\rangle. \end{aligned}$$

Division of Eq. (1.46) by this result yields an expression for a normalized spectrum

$$S(\omega) = f(\omega)/\int_{-\infty}^{\infty} f(\omega)\mathrm{d}\omega = \frac{1}{2\pi} \int_{-\infty}^{\infty} g^{(1)}(\tau)e^{i\omega\tau}\mathrm{d}\tau. \qquad (1.48)$$

This relation is known as the *Wiener-Khinchin theorem*, and it gives a direct link between time-dependent fluctuations in light and its power spectral density[8]. To compute the power spectrum we need the degree of first-order correlation at positive τ, so with Eq. (1.31) in mind we rewrite $S(\omega)$ as

$$S(\omega) = \frac{1}{\pi} \operatorname{Re} \int_0^{\infty} g^{(1)}(\tau)e^{i\omega\tau}\mathrm{d}\tau. \qquad (1.49)$$

The shape of the spectral lines can be predicted with the relationship between the normalised power spectral density and the degree of first-order coherence. If the broadening of a spectral line is due to Doppler shifts, the line will have an approximately *Gaussian* shape [4]. This is easy to show by inserting Eq. (1.41) into Eq. (1.48) and performing the Gaussian integral over τ:

$$S_G(\omega) = \frac{1}{2\pi} \int_{-\infty}^{\infty} e^{-[(\pi/2\tau_c^2)\tau^2 - i(\omega-\omega_0)\tau]}\mathrm{d}\tau = \frac{\sqrt{2}\tau_c}{\pi} e^{-(2/\pi)(\omega-\omega_0)^2\tau_c^2}, \quad (1.50)$$

---

[8] Actually, the Wiener-Khinchin theorem does not really shine until one deals with a system where the input/output signal is not square-integrable, meaning its Fourier transform does not exist.
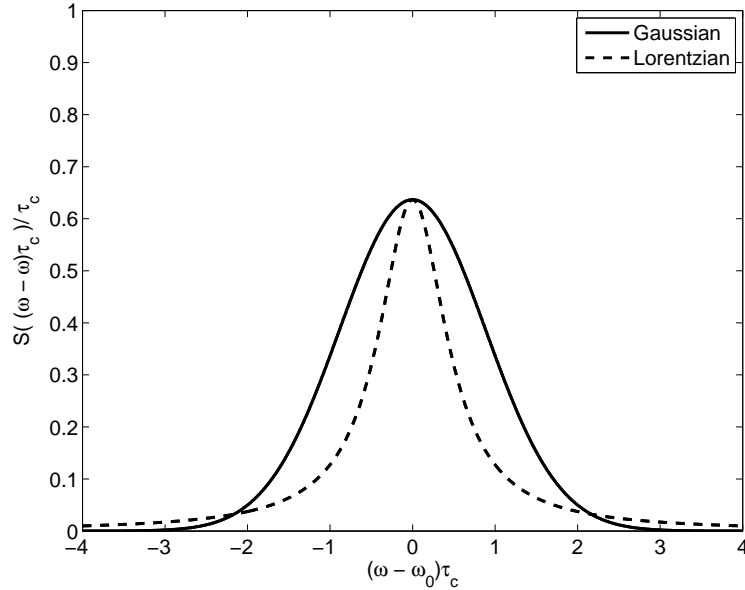
Figure 1.3: The normalised power spectral density $S(\omega)$ with both Gaussian and Lorentzian lineshape.

which has been normalised to satisfy

$$\int_{-\infty}^{\infty} S(\omega)\mathrm{d}\omega = 1,$$

and where ω_0 is the average frequency of the radiated light.

If the radiation is mainly due to collisions between atoms or molecules, the spectral lines will have a *Lorentzian* shape [4],

$$S_L(\omega) = \frac{2\tau_c/\pi}{1 + 4(\omega - \omega_0)^2\tau_c^2}. \tag{1.51}$$

Both the Gaussian and the Lorentzian line shapes are shown in Fig. 1.3. It is then a simple matter of doing an inverse Fourier transformation to go from the power spectral density to the degree of first-order coherence. Often it is easier to measure the coherence of a signal rather than its power density spectrum, which is of particular relevance in for example, Fourier transform spectroscopy and imaging. Of course, in real applications the radiation will likely have a combination of Gaussian and Lorentzian distribution.

The trade off between the width of the frequency band and the coherence time is of vital importance when conducting experiments. In up until around the 1950s pure monochromatic sources were not available for use in experiments and obviously, astronomers have little say in what kind of light their sources emit. In order to measure light from a star emitting thermal light one seriously has to weigh the cost of having a narrow band width, which gives a longer coherence time (at least within the resolution of the experimental setup), and getting as much light as possible on the detection

devices. Starlight is of very low intensity, so filtering out just a small portion $\Delta\omega$ of its total frequency spectrum could have a significant impact on observation time and thus exposure to unavoidable noise.

It is possible to find a simple relation between the width of the frequency spectrum and the coherence time by calculating the Full Width Half Maximum (FWHM). The FWHM is useful to describe the width of profiles that has no sharp edges or any other natural "extent". In the examples above where the power spectral density is either given as a Gaussian distribution or a Lorentzian distribution, the profile of the curve extends to infinity. The FWHM however is a simple and well-defined number which can be used to compare different curves. For instance, in optical astronomy the FWHM can be used to compare the quality of images under differing observation conditions.

For a Gaussian frequency distribution the maximum power density is

$$\max S_G(\omega') = S_G(0) = \frac{\sqrt{2}\tau_c}{\pi}. \tag{1.52}$$

where $\omega' = \omega - \omega_0$. Clearly the half maximum occurs at

$$\frac{1}{2}\max S_G(\omega') = \frac{\sqrt{2}\tau_c}{2\pi} = \frac{\sqrt{2}\tau_c}{\pi}e^{-(2/\pi)\omega'^2\tau_c^2}$$
$$\Rightarrow \qquad \omega' = \pm\frac{\sqrt{\pi/2\ln 2}}{\tau_c}, \tag{1.53}$$

and the full width at half maximum is

$$\text{FWHM}_G \; : \; \Delta\omega = \omega'_+ - \omega'_- = \frac{\sqrt{2\pi\ln 2}}{\tau_c}. \tag{1.54}$$

A similar calculation yields the FHWM for light with a Lorentzian frequency distribution

$$\text{FWHM}_L \; : \; \Delta\omega = \omega'_+ - \omega'_- = \frac{2}{\tau_c} \tag{1.55}$$

So in both cases the width of the frequency band is inversely proportional to the coherence time of the light, meaning that a decrease in $\Delta\omega$ increases the coherence time τ_c. In the next chapter we will discuss applications of coherence theory where this consideration is important for the outcome.

1.4   The degree of second-order coherence

The degree of second-order coherence plays a crucial role in the distinction between light beams that can or cannot be described by classical theory, something which the degree of first-order coherence is not able to do. First some essential ground work must be laid down before returning to this topic in section 3.2.

To derive the intensity-fluctuation properties of chaotic light in a similar way as what was done for the field-fluctuation in the previous section, we consider two-time

measurements in which many pairs of readings of the intensity are taken at a fixed point in space, with a fixed time delay τ. For simplicity light with only a single polarization is measured.

The average of the product of each pair of readings is the intensity correlation function of the light, analogous to the electric-field correlation Eq. (1.30). The normalised form of the correlation function is called the *degree of second-order temporal coherence*,

$$g^{(2)}(\tau) = \frac{\langle \bar{I}(t)\bar{I}(t+\tau)\rangle}{\bar{I}^2} = \frac{\langle E^*(t)E^*(t+\tau)E(t+\tau)E(t)\rangle}{\langle E^*(t)E(t)\rangle^2} \qquad (1.56)$$

where $\bar{I}$ is the long-time average intensity in a plane parallel light beam radiated by ν atoms,

$$\bar{I} \equiv \langle \bar{I}(t)\rangle = \frac{1}{2}\epsilon_0 c\langle E^*(t)E(t)\rangle = \frac{1}{2}\epsilon_0 c\sum_{i=1}^{\nu}\langle E_i^*(t)E_i(t)\rangle$$

$$= \frac{1}{2}\epsilon_0 c\langle |E_1 e^{i\phi_1(t)} + E_2 e^{i\phi_2(t)} + \ldots + E_\nu e^{i\phi_\nu(t)}|^2\rangle$$

$$= \frac{1}{2}\epsilon_0 c\nu E_i^2 \qquad (i = 1, 2, \ldots, \nu) \qquad (1.57)$$

The total electric field is defined as

$$E(t) = E_1(t) + E_2(t) + \ldots + E_\nu(t)$$

$$= E_0 e^{-i\omega_0 t}\left[e^{i\phi_1(t)} + e^{i\phi_2(t)} + \ldots + e^{i\phi_\nu(t)}\right] \qquad (1.58)$$

where the light beam consists of independent contributions from ν equivalent, radiating atoms. The cross-terms between different sources gives a zero average contribution to $\bar{I}$, due to the random phases $\phi_i(t)$.

The limits of $g^{(2)}(0)$ can be derived by considering the variance of the intensity

$$(\Delta \bar{I}(t))^2 = \langle \bar{I}(t)^2\rangle - \langle \bar{I}(t)\rangle^2. \qquad (1.59)$$

By definition the variance must be greater than or equal to zero, so that

$$\langle \bar{I}(t)^2\rangle \geq \langle \bar{I}(t)\rangle^2. \qquad (1.60)$$

Thus

$$\bar{I}^2 \equiv \langle \bar{I}(t)\rangle^2 \leq \langle \bar{I}(t)^2\rangle \qquad (1.61)$$

which implies that for $\tau = 0$

$$g^{(2)}(0) = \frac{\langle \bar{I}(t)^2\rangle}{\bar{I}^2} \geq 1. \qquad (1.62)$$

It is not possible to establish an upper limit so the allowed range of values is [1]

$$1 \leq g^{(2)}(0) \leq \infty. \qquad (1.63)$$

For nonzero time delays the positive nature of the intensity gives only the restriction

$$0 \leq g^{(2)}(\tau) \leq \infty, \quad \tau \neq 0. \tag{1.64}$$

However, there is an additional conclusion to draw by using the Cauchy-Schwarz inequality, where

$$\bar{I}(t)^2 + \bar{I}(t+\tau)^2 \geq 2\bar{I}(t)\bar{I}(t+\tau). \tag{1.65}$$

The derivation involves a trick of writing the intensities as sums over the time variable t_i

$$\frac{1}{2N}\sum_{i=1}^{N}\left(\bar{I}(t_i)^2 + \bar{I}(t_i+\tau)^2\right) \geq \frac{1}{N}\sum_{i=1}^{N}\bar{I}(t_i)\bar{I}(t_i+\tau)$$

$$\frac{1}{N}\sum_{i=1}^{N}\bar{I}(t_i)^2 \geq \frac{1}{N}\sum_{i=1}^{N}\bar{I}(t_i)\bar{I}(t_i+\tau)$$

$$\langle \bar{I}(t)^2 \rangle \geq \langle \bar{I}(t)\bar{I}(t+\tau) \rangle \tag{1.66}$$

where we in the second step have used that the mean intensity of an ergodic light beam is independent on when it is measured. This gives

$$g^{(2)}(\tau) \leq g^{(2)}(0). \tag{1.67}$$

The degree of second-order coherence can therefore never exceed its value for zero time delay. Eq. (1.63) and Eq. (1.67) are valid for all varieties for classical light.

For an ideal plane wave   the degree of second-order coherence is on a particularly simple form. If an ideal plane wave propagates in the z-direction with a constant amplitude E_0 and phase ϕ

$$E(z,t) = E_0 e^{i(kz-\omega_0 t)} \tag{1.68}$$

we find that

$$g^{(2)}(\tau) = \frac{\langle E^*(t)E^*(t+\tau)E(t+\tau)E(t)\rangle}{\langle E^*(t)E(t)\rangle^2} = 1. \tag{1.69}$$

As seen in Eq. (1.37), such a stable wave is first-order coherent at all space-time points and it is said to be second-order coherent if simultaneously

$$|g^{(1)}(\tau)| = 1 \quad \text{and} \quad g^{(2)}(\tau) = 1. \tag{1.70}$$

It can be shown that the classical stable wave is nth-order coherent with $g^{(n)}(\tau) = 1$, hence it is often called just *coherent light*.

For chaotic light a different approach can be taken. If the chaotic lights source consists of ν radiating atoms, each of which is not correlated with any of the others, then the second-order electric-field correlations in Eq. (1.56) can be written in terms of the single atom contributions as

$$\langle E^*(t)E^*(t+\tau)E(t+\tau)E(t)\rangle$$
$$= \sum_{i=1}^{\nu}\langle E_i^*(t)E_i^*(t+\tau)E_i(t+\tau)E_i(t)\rangle + \sum_{i\neq j}\big[\langle E_i^*(t)E_j^*(t+\tau)E_j(t+\tau)E_i(t)\rangle$$
$$+ \langle E_i^*(t)E_j^*(t+\tau)E_i(t+\tau)E_j(t)\rangle\big]. \quad (1.71)$$

All terms where the field from each atom is not multiplied with its complex conjugate will vanish. With equivalent contributions from all atoms we get

$$\langle E^*(t)E^*(t+\tau)E(t+\tau)E(t)\rangle$$
$$= \nu\langle E_i^*(t)E_i^*(t+\tau)E_i(t+\tau)E_i(t)\rangle + \nu(\nu-1)\big[\langle E_i^*(t)E_j^*(t+\tau)E_j(t+\tau)E_i(t)\rangle^2$$
$$+ \big|\langle E_i^*(t)E_j^*(t+\tau)E_i(t+\tau)E_j(t)\rangle\big|^2\big]. \quad (1.72)$$

The factor $\nu(\nu-1)$ in the last term on the right hand side comes from elementary combinatorics, for the number of possible permutations between two different atoms without repetition. If the number of atoms ν is very large, the dominating contribution to the second-order electric-field correlations will involve pairs of atoms. Then to a good approximation

$$\langle E^*(t)E^*(t+\tau)E(t+\tau)E(t)\rangle = \nu^2\big[\langle E_i^*(t)E_i(t)\rangle^2 + |\langle E_i^*(t)E_i(t+\tau)\rangle|^2\big]. \quad (1.73)$$

Note that the rightmost term corresponds to the definition of the first-order correlation function. This implies that the degree of second-order coherence can be related to the degree of first-order coherence Eq. (1.29),

$$g^{(2)}(\tau) = 1 + |g^{(1)}(\tau)|^2, \qquad \nu \gg 1. \quad (1.74)$$

The limits of $g^{(2)}(\tau)$ can be found by using the limiting values of $g^{(1)}(\tau)$ (the Eqs. (1.32) and (1.33)), yielding

$$g^{(2)}(0) = 2 \quad (1.75)$$

and

$$g^{(2)}(\tau) \to 1 \quad \text{for} \quad \tau \gg \tau_c. \quad (1.76)$$

These limits are only valid for chaotic light. The statistical distributions of collision broadened (Eq. (1.40)) and Doppler broadened (Eq. (1.41)) light is inserted into Eq. (1.74),

$$g^{(2)}(\tau) = 1 + e^{-2|\tau|/\tau_c} \quad (1.77)$$

and

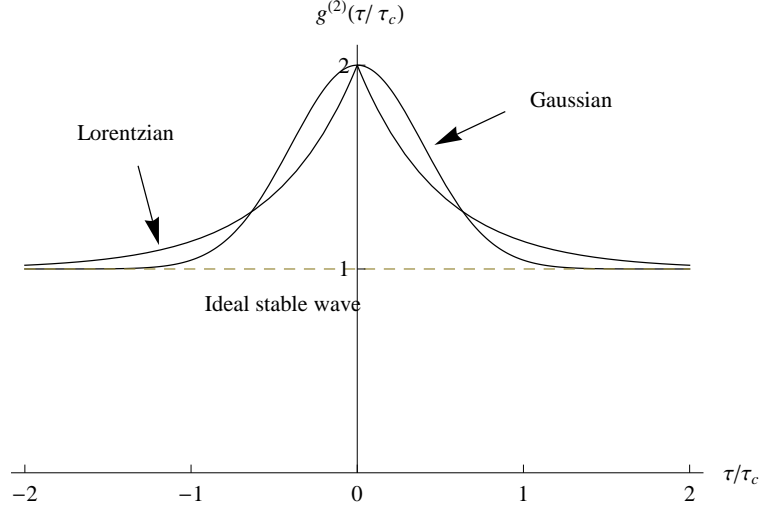$$g^{(2)}(\tau) = 1 + e^{-\pi(\tau/\tau_c)^2}. \quad (1.78)$$

Figure 1.4: A representation of the degrees of second-order coherence of chaotic light having Lorentzian and Gaussian frequency distribution with coherence time τ_c. The dashed line shows the constant unit $g^{(2)}(\tau)$ of coherent light (ideal plane wave). Adapted from [1].

Fig. 1.4 shows the behaviour of $g^{(2)}(\tau)$ for the different distributions, including for the classical stable plane wave. According to the criterion for second-order coherence, Eq. (1.70), chaotic light is not second-order coherent. While Fig. 1.2 shows that chaotic light is first-order coherent for very short values of τ, such short times produces a degree of second-order coherence equal to 2, and criterion Eq. (1.70) cannot be fulfilled. Therefore chaotic light is second-order *in*coherent for *any pairs of space-time points*.

For comparison with later calculations, $g^{(2)}(\tau)$ is expressed in the form of the positive frequency part of the electric field, as was done for $g^{(1)}(\tau)$,

$$
\begin{aligned}
&g^{(2)}(\tau) \\
&= \frac{\displaystyle\sum_{\mathbf{k}_{1,2,3,4}} \sqrt{\omega_{k_1}\omega_{k_2}\omega_{k_3}\omega_{k_4}} \left\langle a_{\mathbf{k}_1}^* a_{\mathbf{k}_2}^* a_{\mathbf{k}_3} a_{\mathbf{k}_4} e^{-i(\omega_{k_4}+\omega_{k_3}-\omega_{k_2}-\omega_{k_1})t} \right\rangle}{\left[\displaystyle\sum_{\mathbf{k}_{1,2}} \sqrt{\omega_{k_1}\omega_{k_2}} \left\langle a_{\mathbf{k}_1}^* a_{\mathbf{k}_2} e^{-i(\omega_{k_2}-\omega_{k_1})t} \right\rangle e^{i(\mathbf{k}_2-\mathbf{k}_1)\cdot\mathbf{r}}\right]^2} \\
&\quad\times e^{i(\mathbf{k}_4+\mathbf{k}_3-\mathbf{k}_2-\mathbf{k}_1)\cdot\mathbf{r}} e^{i(\omega_{k_3}-\omega_{k_2})\tau} \\
&= \frac{\displaystyle\sum_{\mathbf{k}_{1,2}} \sqrt{\omega_{k_1}\omega_{k_2}} a_{\mathbf{k}_1}^* a_{\mathbf{k}_2} \left\langle e^{-i(\omega_{k_2}-\omega_{k_1})t} \right\rangle e^{i(\mathbf{k}_2-\mathbf{k}_1)\cdot\mathbf{r}} e^{i(\omega_{k_2}-\omega_{k_1})\tau}}{\displaystyle\sum_{\mathbf{k}_{1,2}} \sqrt{\omega_{k_1}\omega_{k_2}} a_{\mathbf{k}_1}^* a_{\mathbf{k}_2} \left\langle e^{-i(\omega_{k_2}-\omega_{k_1})t} \right\rangle e^{i(\mathbf{k}_2-\mathbf{k}_1)\cdot\mathbf{r}}}
\end{aligned} \tag{1.79}
$$

where $\sum_{\mathbf{k}_{1,2,3,4}}$ is the four-sum over each mode $\mathbf{k}_i$. The modes are assumed to be isolated harmonic oscillators so that the ith mode is uncorrelated with the other $i \neq j$ modes.

1.5   Summary and discussion

This chapter was spent on reintroducing the reader to the derivation of the electric field from Maxwell's equations. Important tools like the degrees of first- and second-order coherence of light was also introduced and discussed in detail. As promised, the next chapter focusses on two examples of how both $g^{(1)}(\tau)$ and $g^{(2)}(\tau)$ can be measured and used in experiments, specifically in optical stellar interferometry.

To summarise the most important concepts of this chapter; $g^{(1)}(\tau)$ is a measure of the field-field fluctuations where the phase difference from t to $t + \tau$ is preserved. It is also a Fourier pair with the normalised power spectral density of the field. By finding $g^{(1)}(\tau)$ at various time delays τ it is possible to reconstruct the frequency spectrum of the source, a technique which is called Fourier transform spectroscopy.

$g^{(2)}(\tau)$ on the other hand is a measure of the intensity-intensity fluctuations and as such no phase differences are preserved. It then contains *less* information than $g^{(1)}(\tau)$, however, this is not necessarily a bad thing. As can be seen in Eqs. (1.77) and (1.78), $g^{(2)}(\tau)$ is not a sinusoidal function, but instead a much more calculation friendly dampening factor.

Also a key concept to keep in mind is that the wave vector (or *field mode*) $\mathbf{k}$ is related to the boundary conditions used when solving the electric wave equation. Later, specifically in chapter 5, we will say things like "photons are in a *mode*". The energy of the photon is related to $\mathbf{k}$ via its angular frequency, and a *cavity* can be designed such that it will only support fields of a certain $\mathbf{k}$.

The coherence properties of two types of classical light was considered: the ideal plane wave and chaotic light. The former was shown to be both first- and second-order coherent for all pairs of space-time points, supporting the nomenclature *coherent light*. The latter on the other hand, was shown to be only first-order coherent for zero or very short time delays τ and *never* second-order coherent for *any* pairs of space-time points.

The degrees of both first- and second-order coherence calculated above assume a stationary, polarized, plane-parallel beam of light and a common observation point. Their definitions Eqs. (1.29) and (1.56) can be generalised to cover non-stationary optical fields with a three-dimensional spatial dependence, which would be necessary for calculations of spatial coherence. Luckily this work covers only temporal coherence, hence this kind of computational complications are avoided.

Chapter 2

Measuring coherence with interferometers

Optical interferometry has several useful applications, one of which is in the field of observational astronomy, where it can be used to measure the apparent angular diameter of stars. For the naked eye all stars look like dots regardless of how hard you squint, so the problem lies in measuring the angular diameter accurately, where accurately is on the order of a hundredth of an arc second[1].

In this chapter we will see how two types of interferometers can be applied in observational astronomy. These two are the Michelson stellar interferometer, invented by A. A. Michelson (1890), and the intensity interferometer (often referred to as the Hanbury Brown-Twiss interferometer), invented by R. Hanbury Brown and R. Q. Twiss (1954). While these two interferometers achieve the same goal, mainly determining the apparent angular diameter of distant sources, the methods by which they do this are fundamentally different.

Interferometers rely on some type of *interference* effect, which usually is thought to involve electromagnetic waves. The last few decades however, interferometers have found new areas of application, most notably in high-energy physics. Interferometry exploits interference between superposed waves, and since *all* matter exhibits wave-like properties, successful experiments of interferometry with atoms, and even molecules, have been carried out.

But first we will develop the geometric relations between the so-called baseline of the interferometer and the angular diameter. We have chosen to model a binary star, which is a system of two stars orbiting around their common centre of mass, so we will actually find the apparent angular separation of the two stars. This is followed by section 2.2 where the Michelson stellar interferometer is used to determine the diameter of a binary star, after which comes an analogous calculation for the intensity interferometer. In the process light will be shed on what exactly the fundamental difference is.

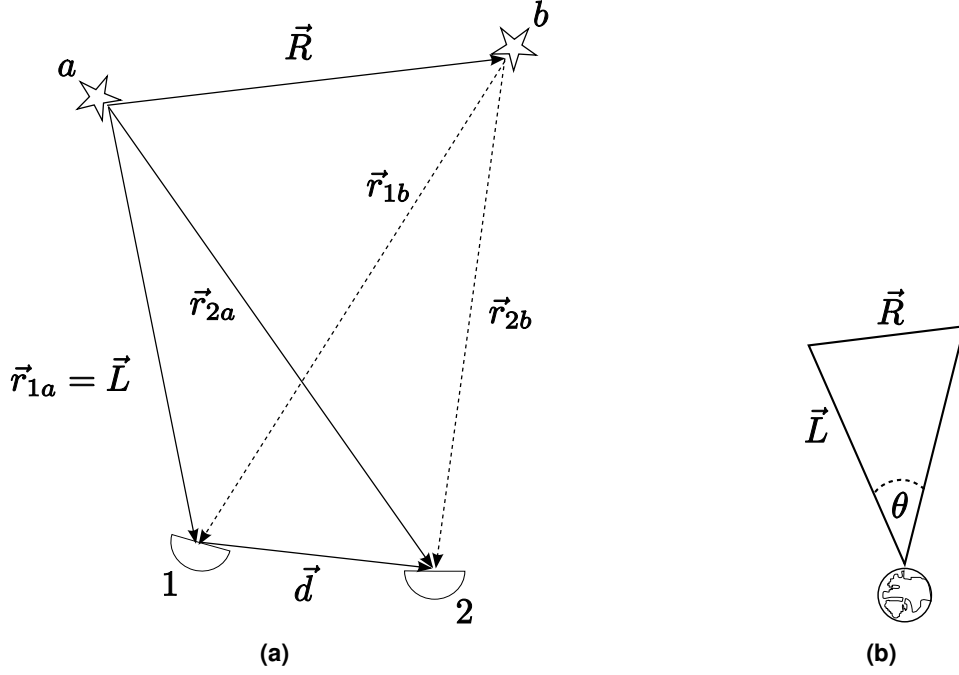[1] An arc second is one sixtieth of one degree, or $4.85 \, \mu$rad.

Figure 2.1: (a) Schematic of the geometry a binary star forms as seen from the Earth. The two stars a and b are separated by a distance $\vec{R}$. The baseline $\vec{d}$ is the separation of the two detectors positioned at 1 and 2 on the Earth's surface. (b) The apparent angular diameter θ of the two sources as seen from the detectors on Earth.

2.1   The apparent angular diameter of a binary star

The model used in this work is that of a binary star, where we dub one star source a, and the other source b, see Fig. 2.1. Light emitted from source a has a longer path to detector 2 than to detector 1, and the difference is denoted $\Delta r_a = c\tau_a$. Equivalently, light emitted from source b must traverse a longer distance to detector 1 than to detector 2, defined as $\Delta r_b = c\tau_b$.

It is apparent that the path length differences Δr_a and Δr_b can be expressed by the distance $\mathbf{L}$ from source a to detector 1, the separation $\mathbf{d}$ of the detectors and by the separation $\mathbf{R}$ of the two sources. From Fig. 2.1(a) we see that the path the light can take from either source a or b can be written as

$$
\begin{aligned}
\mathbf{r}_{1a} &= \mathbf{L} & &\Rightarrow & |\mathbf{r}_{1a}| &= L \\
\mathbf{r}_{2a} &= \mathbf{L} + \mathbf{d} & &\Rightarrow & |\mathbf{r}_{2a}| &= \sqrt{L^2 + d^2 + 2\mathbf{L} \cdot \mathbf{d}} \\
\mathbf{r}_{1b} &= \mathbf{L} - \mathbf{R} & &\Rightarrow & |\mathbf{r}_{1b}| &= \sqrt{L^2 + R^2 - 2\mathbf{L} \cdot \mathbf{R}} \\
\mathbf{r}_{2b} &= \mathbf{L} + \mathbf{\Delta} & &\Rightarrow & |\mathbf{r}_{2a}| &= \sqrt{L^2 + \Delta^2 + 2\mathbf{L} \cdot \mathbf{\Delta}}
\end{aligned}
\tag{2.1}
$$

where $\mathbf{\Delta} \equiv \mathbf{d} - \mathbf{R}$. The absolute difference in path length for the light from source i is then

$$
\Delta r_i = |\mathbf{r}_{2i}| - |\mathbf{r}_{1i}|, \ \ i = a, b.
\tag{2.2}
$$

To calculate this, the square roots in Eq. (2.1) are expanded in a Taylor series. In the case of $|\mathbf{r}_{2a}|$ the vector $\mathbf{x} = \mathbf{d}/L$ is defined, since $|d/L|$ is known to be a small number. Also, to avoid any complications regarding the scalar products the following relation is employed

$$\mathbf{a} \cdot \mathbf{b} = ab \cos \theta$$

where θ is the angle between $\mathbf{a}$ and $\mathbf{b}$.

So, expanding to the second order in x,

$$f(x) \approx f(0) + x f'(0) + \frac{1}{2} x^2 f''(0)$$

where, if α is the angle between $\mathbf{L}$ and $\mathbf{d}$,

$$f(x) = \sqrt{L^2 + d^2 + 2Ld \cos \alpha} = L\sqrt{1 + x^2 + 2x \cos \alpha},$$
$$f(0) = L$$
$$f'(x) = L(1 + x^2 + 2x \cos \alpha)^{-1/2}(x + \cos \alpha),$$
$$f'(0) = L \cos \alpha$$
$$f''(x) = L(1 + x^2 + 2x \cos \alpha)^{-1/2} - L(x + \cos \alpha)^2(1 + x^2 + 2x \cos \alpha)^{-3/2},$$
$$f''(0) = L - L \cos^2 \alpha$$

giving

$$|\mathbf{r}_{2a}| = f(x) \approx L + \frac{\mathbf{L} \cdot \mathbf{d}}{L} + \frac{d^2}{2L} - \frac{(\mathbf{L} \cdot \mathbf{d})^2}{2L^3}. \tag{2.3}$$

This result is then used to approximate the path difference for the light from source a,

$$\Delta r_a = |\mathbf{r}_{2a}| - |\mathbf{r}_{1a}| \approx \frac{\mathbf{L} \cdot \mathbf{d}}{L} + \frac{d^2}{2L} - \frac{(\mathbf{L} \cdot \mathbf{d})^2}{2L^3} \tag{2.4}$$

This procedure is repeated to find the path difference Δr_b, this time, however, there are two square roots that must be series expanded separately. First out is $|\mathbf{r}_{1b}|$, with $\mathbf{y} = \mathbf{R}/L$ as the tiny quantity and β the angle between $\mathbf{L}$ and $\mathbf{R}$,

$$f(y) = \sqrt{L^2 + R^2 - 2LR \cos \beta} = L\sqrt{1 + y^2 - 2y \cos \beta},$$
$$f(0) = L$$
$$f'(y) = L(1 + y^2 - 2y \cos \beta)^{-1/2}(y - \cos \beta),$$
$$f'(0) = -L \cos \beta$$
$$f''(y) = L(1 + y^2 - 2y \cos \beta)^{-1/2} - L(y - \cos \beta)^2(1 + y^2 - 2y \cos \beta)^{-3/2},$$
$$f''(0) = L - L \cos^2 \beta$$

giving

$$|\mathbf{r}_{1b}| = f(y) \approx L - \frac{\mathbf{L} \cdot \mathbf{R}}{L} + \frac{R^2}{2L} - \frac{(\mathbf{L} \cdot \mathbf{R})^2}{2L^3} \tag{2.5}$$

For the second root on the right hand side

$$\mathbf{z} = \boldsymbol{\Delta}/L = (\mathbf{d} - \mathbf{R})/L$$

is defined to be the small quantity and γ is the angle between $\boldsymbol{\Delta}$ and $\mathbf{L}$,

$$f(z) = \sqrt{L^2 + \Delta^2 + 2L\Delta \cos\gamma} = L\sqrt{1 + z^2 + 2z\cos\gamma},$$
$$f(0) = L$$
$$f'(z) = L(1 + z^2 + 2z\cos\gamma)^{-1/2}(z + \cos\gamma),$$
$$f'(0) = L\cos\gamma$$
$$f''(z) = L(1 + z^2 + 2z\cos\gamma)^{-1/2} - L(z + \cos\gamma)^2(1 + z^2 + 2z\cos\gamma)^{-3/2},$$
$$f''(0) = L - L\cos^2\gamma$$

which gives

$$
\begin{aligned}
|\mathbf{r}_{2b}| = f(z) &\approx L + \frac{\mathbf{L} \cdot \boldsymbol{\Delta}}{L} + \frac{\Delta^2}{2L} - \frac{(\mathbf{L} \cdot \boldsymbol{\Delta})^2}{2L^3} \\
&= L + \frac{\mathbf{L} \cdot \mathbf{d}}{L} - \frac{\mathbf{L} \cdot \mathbf{R}}{L} + \frac{d^2}{2L} + \frac{R^2}{2L} - \frac{\mathbf{d} \cdot \mathbf{R}}{L} \\
&\quad - \frac{(\mathbf{L} \cdot \mathbf{d})^2}{2L^3} - \frac{(\mathbf{L} \cdot \mathbf{R})^2}{2L^3} + \frac{(\mathbf{L} \cdot \mathbf{d})(\mathbf{L} \cdot \mathbf{R})}{L^3}.
\end{aligned}
\tag{2.6}
$$

The difference in path length for light from source b to detector 1 is[2]

$$
\begin{aligned}
\Delta r_b = |\mathbf{r_{2b}}| - |\mathbf{r_{1b}}| &= f(z) - f(y) \\
&\approx \frac{\mathbf{L} \cdot \mathbf{d}}{L} + \frac{d^2}{2L} - \frac{\mathbf{d} \cdot \mathbf{R}}{L} - \frac{(\mathbf{L} \cdot \mathbf{d})^2}{2L^3} + \frac{(\mathbf{L} \cdot \mathbf{d})(\mathbf{L} \cdot \mathbf{R})}{L^3}
\end{aligned}
\tag{2.7}
$$

Finally

$$\Delta r_a - \Delta r_b = \frac{\mathbf{d} \cdot \mathbf{R}}{L} - \frac{(\mathbf{L} \cdot \mathbf{d})(\mathbf{L} \cdot \mathbf{R})}{L^3} \tag{2.8}$$

The form of this expression hints at a possible rewriting into cross product form

$$\Delta r_a - \Delta r_b = \frac{(\mathbf{L} \times \mathbf{d}) \cdot (\mathbf{L} \times \mathbf{R})}{L^3}. \tag{2.9}$$

The difference in path lengths can be interpreted as the vector $\mathbf{d}'$ perpendicular to the plane containing $\mathbf{d}$ and $\mathbf{L}$, which is projected onto the vector $\mathbf{R}'$, where $\mathbf{R}'$ is perpendicular to the plane containing $\mathbf{R}$ and $\mathbf{L}$, see Fig. 2.2. The sense to be made out of this is that the "altitude", or position along $\mathbf{L}$, at which the measurement is being done has no impact on the result. The relevant quantities are the absolute length of $\mathbf{d}$ and the relative angle ϕ between the two resultant vectors $\mathbf{d}'$ and $\mathbf{R}'$, indicated to the right in Fig. 2.2.

---

[2] The reader might be nonplussed by the apparent change of signs in Δr_b in comparison with Fig. 2.1(a), where one could be led to believe that the path from b to 1 is longer than that from b to 2. However, the figure is only a rough sketch and it is a convenient choice to make it the other way around. This choice causes bothersome factors to cancel out in the final expression for $\Delta r_a - \Delta r_b$. The important point is that we remain consistent with this choice in the calculations in section 2.2.
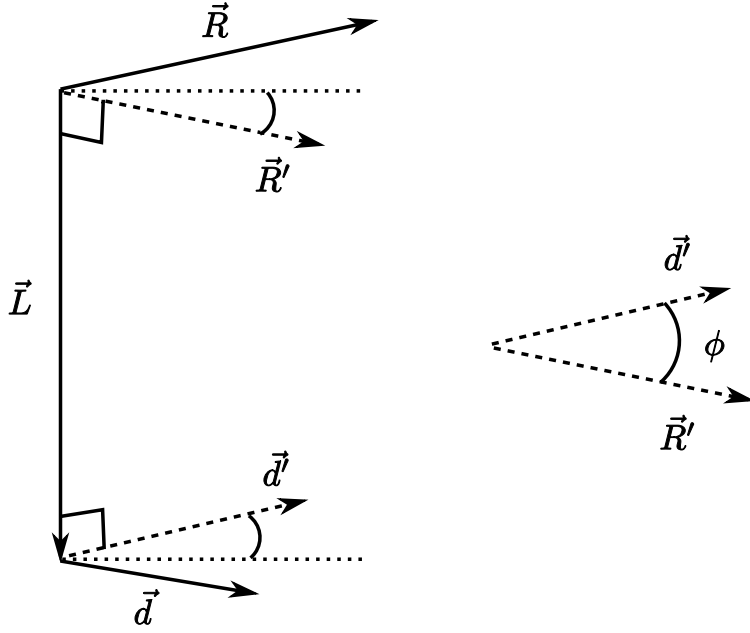
Figure 2.2: A sketch of the geometry in Eq. (2.9) where $\mathbf{L} \times \mathbf{d} = \mathbf{d}'$ and $\mathbf{L} \times \mathbf{R} = \mathbf{R}'$.

We can assume that the incident light is approximately orthogonal to the sighting line between the detectors so that $\mathbf{d} \cdot \mathbf{L} = 0$, and that the angle between $\mathbf{d}$ and $\mathbf{R}$ is very small, $\cos\phi \approx 1^3$, which yields the simplified expression

$$\Delta r_a - \Delta r_b \approx \frac{Rd}{L}. \tag{2.10}$$

The apparent angular separation of the two sources is given as $\theta \approx \tan\theta = R/L$ (see Fig. 2.1(b)), thus the relation between the apparent angular diameter and the separation of the detectors d becomes

$$\omega(\tau_a - \tau_b) = k(\Delta r_a - \Delta r_b) \approx kd\theta = \frac{2\pi d\theta}{\lambda} \tag{2.11}$$

where λ is the wavelength of the incident light. On a side note we can mention that $\mathbf{L}$ need not be an unknown quantity, as decent approximations of the distance to the sources may be obtained by observing the parallax effect. Filters on the detectors can make up for the fact that the two sources in a binary star will emit light of different frequencies, and so it is reasonable to assume that the *detected* light will have a frequency $\omega_a = \omega_b = \omega$. In actual experiments filters will allow some range of frequency $\Delta\omega$ to pass through, since more light means a better detection, but with a trade off in shorter coherence time τ_c. Remember that chaotic light becomes incoherent for a delay $\tau > \tau_c$, which results in no interference, so it is crucial to balance this with the resolution capabilities of the instrument.

---

³ By choosing a very small angle ϕ, we actually turn the problem into one concerning a single star. Binary stars cause problems in interferometry since they bring with them the modulating factor $\cos\left[\frac{2\pi d\theta}{\lambda}\cos\phi\right]$, where $\cos\phi$ varies with time as the position angles of the instrument and the star changes. This will make the measured correlation less than the expected correlation for a single star. The fact that the correlation can vary with time or with baseline in a manner that is inconsistent with a single star is in itself is a way to distinguish a binary star from a single star [5].
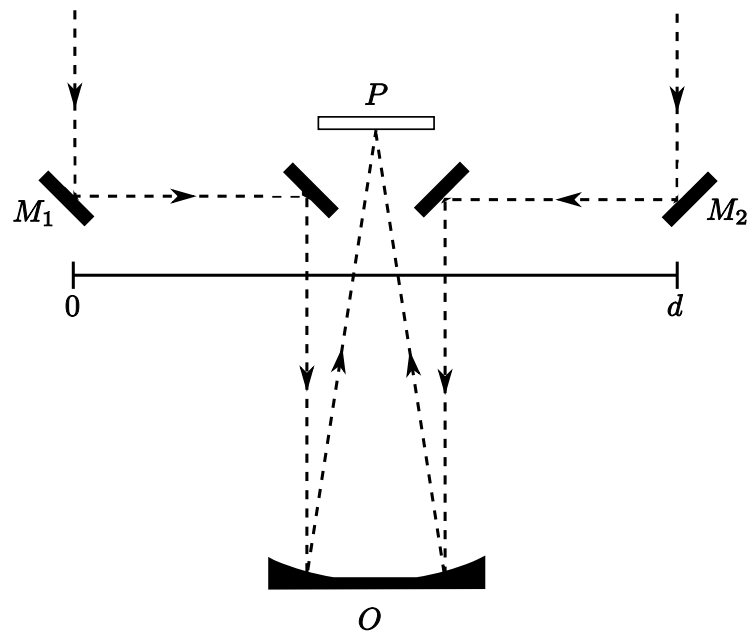
Figure 2.3: Schematic of the Michelson interferometer. Starlight falls on the mirrors M_1 and M_2 and are then sent via O (usually a telescope) to be superposed at a screen in P for the interference pattern to be studied. The length of the baseline d can be altered by moving the mirrors.

2.2   The Michelson stellar interferometer

One of the most common interferometers in astronomy is the *Michelson stellar inter-ferometer*[4]. This is also called an *amplitude* interferometer and it relies on the optical interference of electric fields. Fig. 2.3 shows a simplified schematic for the interfer-ometer. The Michelson interferometer collects light from, in our case, a binary star by two separated mirrors, M_1 and M_2, which is reflected via a primary collector O to be combined on a screen in P where an interference pattern can be observed. In actual, working interferometers there will be a more complicated structure between the mirrors in point O, but we are not very interested in additional effects besides the measurement of correlation, so we will assume that there are no internal path differences from O to P.

On the screen in P an interference pattern of the light from the binary star forms, with alternate bright and dark bands called *fringes*. When the separation of the mirrors increases, the contrast, or visibility of the fringes, decreases until they disappear and what is left is simply a circular uniform spot of light. The disappearance is due to the increased difference in path lengths the light must take to each mirror before they are superposed in P. When the difference is larger than the coherence length ($l = c\tau_c$) the

---

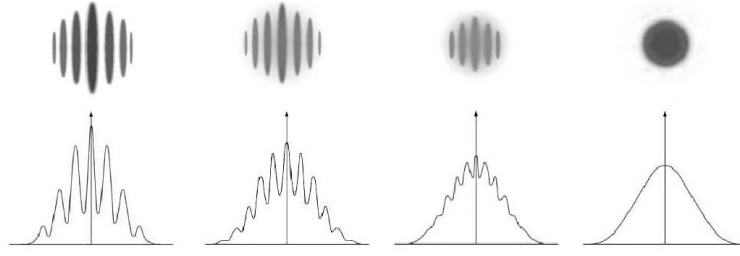[4] From now on referred to as simply the Michelson interferometer.

Figure 2.4: The top part illustrates the fringes as seen on the screen in the Michelson interferometer. When the base line d increases, the contrast of the fringes decreases until they are no longer discernible. Picture adapted from [6].

light waves are incoherent and no interference pattern can be seen. Fig. 2.4 illustrates how the contrast of the fringes degrades with poorer interference. The separation d when the disappearance occurs can be related to the angular diameter of the star in a way which we will now demonstrate.

2.2.1 Calculating the field fluctuations

The intensity of the light beam is determined by the Poynting vector

$$\bar{I}(t) = \frac{1}{2}\epsilon_0 c|E(t)|^2 \propto |E(t)|^2 \tag{1.26}$$

were we "conveniently" neglect the permittivity of free space and speed of light, since they will cancel out in the final result. We also assume that we are working with only one polarisation of the field. So, the intensity of the electric field arriving at the point P on the screen is a superposition of the fields reflected from mirrors 1 and 2,

$$\bar{I}_P = |E_P| = |E_{1a} + E_{2a} + E_{1b} + E_{2b}|^2 \tag{2.12}$$

We switch to writing the explicit time dependence of the field instead of using the indices 1 and 2 to indicate which detector the field is measured at. At the risk of belabouring the obvious, it is the relative difference in *path length* for light from one source to each mirror that is the variable in question, but this delay is *temporal* in the sense that a longer path to traverse means a longer transport time, $l = c\tau$. In order to cut down on the notation, the dependence of the electric field on $\mathbf{r}$ is suppressed and instead the conversion $\mathbf{k} \cdot \Delta\mathbf{r} = \omega_k \tau$ is used. So the notation $E(t + \tau)$ is incorrect in the sense that the electric field $E(t + \tau)$ has *travelled* for a duration τ longer than $E(t)$, but the measurement of the fields at the mirrors are made simultaneously at time t. The translation goes like this [5]:

$$\begin{aligned}
E_{1a} &= E_a(t) = |E_a|e^{i(\mathbf{k}\cdot\mathbf{r}-\omega_k t)} \\
E_{2a} &= E_a(t + \tau_a) = |E_a|e^{i(\mathbf{k}\cdot\mathbf{r}+\omega_k \tau_a-\omega_k t)} \\
E_{1b} &= E_b(t) = |E_b|e^{i(\mathbf{k}\cdot\mathbf{r}-\omega_k t)} \\
E_{2b} &= E_b(t + \tau_b) = |E_b|e^{i(\mathbf{k}\cdot\mathbf{r}+\omega_k \tau_b-\omega_k t)}
\end{aligned} \tag{2.13}$$

---

[5] From the translation it is apparent that a less misleading notation would be $E(t + \tau) \rightarrow E(t - \tau)$, but the former is used in most textbooks and allows for easier cross-referencing.

In other words, the intensity at point P on the screen is

$$
\begin{aligned}
\bar{I}_P &= |E_a(t) + E_a(t + \tau_a) + E_b(t) + E_b(t + \tau_b)|^2 \\
&= |E_a(t)|^2 + |E_a(t + \tau_a)|^2 + |E_b(t)|^2 + |E_b(t + \tau_b)|^2 \\
&\quad + 2\operatorname{Re}\{E_a^*(t)E_a(t + \tau_a)\} + 2\operatorname{Re}\{E_a^*(t)E_b(t)\} \\
&\quad + 2\operatorname{Re}\{E_a^*(t)E_b(t + \tau_b)\} + 2\operatorname{Re}\{E_b^*(t)E_b(t + \tau_b)\} \\
&\quad + 2\operatorname{Re}\{E_a^*(t + \tau_a)E_b(t)\} + 2\operatorname{Re}\{E_a^*(t + \tau_a)E_b(t + \tau_b)\}
\end{aligned} \tag{2.14}
$$

The average electric field intensity over a time T much larger than the coherence time of the field emitted, was defined as

$$
\langle \bar{I} \rangle = \langle E^*(t)E(t + \tau) \rangle = \frac{1}{T} \int_{t-T/2}^{t+T/2} E^*(t')E(t' + \tau)\mathrm{d}t'. \tag{1.30}
$$

Note that according to the discussion in section 1.1.2 we use the cycle averaged intensity denoted by the bar, which should not be confused with the longer time average denoted by the brackets. We assume that the two sources are completely uncorrelated so that $\langle E_a \rangle = \langle E_b \rangle = 0$ and $\langle E_a E_b \rangle = \langle E_a \rangle \langle E_b \rangle = 0$. The averaged intensity incident on point P is of course independent of when it is measured, due to statistically wide-sense stationary fields, and so

$$
\begin{aligned}
\langle \bar{I}_P \rangle &= 2\langle \bar{I}_a \rangle + 2\langle \bar{I}_b \rangle \\
&\quad + 2\operatorname{Re}\{\langle E_a^*(t)E_a(t + \tau_a) \rangle\} + 2\operatorname{Re}\{\langle E_b^*(t)E_b(t + \tau_b) \rangle\}
\end{aligned} \tag{2.15}
$$

Remember the definition of the degree of first-order temporal coherence as Eq. (1.29), where

$$
\langle E_i^*(t)E_i(t + \tau_i) \rangle = \langle I \rangle g_i^{(1)}(\tau_i), \qquad i = a, b
$$

Inserting this into Eq. (2.15) results in

$$
\langle \bar{I}_P \rangle = 2\langle \bar{I}_a \rangle \left[1 + \operatorname{Re}\{g_a^{(1)}(\tau_a)\}\right] + 2\langle \bar{I}_b \rangle \left[1 + \operatorname{Re}\{g_b^{(1)}(\tau_b)\}\right], \tag{2.16}
$$

so the Michelson interferometer actually measures the degree of first-order coherence directly, if only the real part[6]. From the discussion in section 1.3 we know that we can write $g_i^{(1)}(\tau_i)$ as

$$
g_i^{(1)}(\tau_i) = |g_i^{(1)}(\tau_i)|e^{-i\omega\tau_i}, \quad i = a, b \tag{2.17}
$$

for both the Lorentzian and the Gaussian frequency distribution. We then find that the incident intensity can be written as

$$
\langle \bar{I}_P \rangle = 2\langle \bar{I}_a \rangle \left[1 + |g_a^{(1)}(\tau_a)| \cos(\omega_a \tau_a)\right] + 2\langle \bar{I}_b \rangle \left[1 + |g_b^{(1)}(\tau_b)| \cos(\omega_b \tau_b)\right]. \tag{2.18}
$$

It is plain to see that for time delays much longer than the coherence time of the light, $\langle \bar{I}_P \rangle$ will reduce to just the sum of the intensities arriving at point P from one mirror without interfering with the beam reflected by the other mirror, i.e.,

$$
\langle \bar{I}_P \rangle = \langle \bar{I}_1 \rangle + \langle \bar{I}_2 \rangle = 2(\langle \bar{I}_a \rangle + \langle \bar{I}_b \rangle). \tag{2.19}
$$

---

[6] It is *theoretically* possible to extract the argument by measuring the position of the fringes, see for instance [2] and [7], however it is not feasible in practice.

If instead the mirrors are placed on top of each other, so that there is zero time delay, we find that

$$\langle \bar{I}_P \rangle = 4(\langle \bar{I}_a \rangle + \langle \bar{I}_b \rangle), \tag{2.20}$$

in other words that the intensity is twice as large as the sum of the individual contributions. This constructive interference is not unexpected, since any chaotic light can be found to be first-order coherent within a short enough time interval.

Some limitations of the Michelson interferometer are more easily appreciated if we make a few simplifications. Starting from Eq. (2.15) the angular diameter of a binary star with sources a and b is measured and it is assumed that the averaged intensities are equal so that $\langle \bar{I}_a \rangle = \langle \bar{I}_b \rangle = \langle \bar{I}_0 \rangle$, which is somewhat naive. Furthermore it can be assumed that for a time delay $\tau_a, \tau_b \ll \tau_c$

$$|g_a^{(1)}(\tau_a)| \approx 1 \approx |g_b^{(1)}(\tau_b)| \tag{2.21}$$

and that some filtering device in the gedanken experiment ensures that $\omega_a \approx \omega_b = \omega$.

From Eq. (2.18) it is then found that

$$\begin{aligned}
\langle \bar{I}_P \rangle &= 4\langle \bar{I}_0 \rangle \left[1 + \frac{1}{2}\cos(\omega\tau_a) + \frac{1}{2}\cos(\omega\tau_b) \right] \\
&= 4\langle \bar{I}_0 \rangle \left[1 + \cos[\omega(\tau_a + \tau_b)/2]\cos[\omega(\tau_a - \tau_b)/2] \right] \\
&= 4\langle \bar{I}_0 \rangle \left[1 + \cos[\omega(\tau_a + \tau_b)/2]\cos\left(\frac{\pi d\theta}{\lambda} \right) \right]
\end{aligned} \tag{2.22}$$

In the last step we have used the geometrical relations as shown in Fig. 2.1 and we have also made use of Eq. (2.11). The result is a fairly simple relation between the intensity as measured in point P and the baseline d of the collector mirrors. However, along for the ride is the oscillating term $\cos[\omega(\tau_a + \tau_b)]$. The sum $\tau_a + \tau_b$ will in general be much larger than $(\tau_a - \tau_b)$ resulting in a rapid modulation of the otherwise neat expression. Time-dependent changes (e.g., turbulent mixes of air with different temperatures and densities) that affect the light by changing its path length through the atmosphere, is enhanced by this term, causing distortions in the image. Even when viewing a star through a large telescope, the image is usually so blurred by atmospheric conditions, that it is only visible as a shapeless dot several orders of magnitude larger than the true angular size of the star.

2.2.2 From theory to practice

In the most common setup, as illustrated in Fig. 2.3, two movable mirrors are mounted on a rigid cross-arm. The light from these are directed into the primary collector and then merged in the focal plane where a screen is placed. The two images of the star will interfere, forming alternate bright and dark lines across the screen, provided that the separation of the mirrors is not too large. If they are too far apart the contrast of

the bands will go to zero, meaning that the *visibility* of the fringes is zero. The term visibility was coined by A.A. Michelson in 1890, and is defined as

$$V_d = \frac{\bar{I}_{\max} - \bar{I}_{\min}}{\bar{I}_{\max} + \bar{I}_{\min}}, \qquad (2.23)$$

where $\bar{I}_{\max}$ and $\bar{I}_{\min}$ is the maximum and minimum intensity of the fringes. The assumption is that the fringes vary over a length scale that is sufficiently smaller than the envelope [8], so from Eq. (2.22) the maximum and minimum intensity of the fringes is found to be

$$\langle \bar{I}_p \rangle_{\max} = 4\langle \bar{I}_0 \rangle \left[1 + \cos\left(\frac{\pi d\theta}{\lambda} \right) \right],$$

$$\langle \bar{I}_p \rangle_{\min} = 4\langle \bar{I}_0 \rangle \left[1 - \cos\left(\frac{\pi d\theta}{\lambda} \right) \right]. \qquad (2.24)$$

for $\omega(\tau_a + \tau_b)/2 = n\pi$ $(n = 0, \pm 1, \pm 2, \ldots)$. The visibility is then

$$V_d = \cos\left(\frac{\pi d\theta}{\lambda} \right). \qquad (2.25)$$

which vanishes for $d = \pi k/\theta$. Thus, by measuring the visibility of the interference fringes for several baselines d, one can determine the angular diameter of the binary star. The fringe visibility is also a measure of the coherence of the light. When the intensity minima are equal to zero and the intensity maxima are non-zero, the visibility is maximal and equal to unity. At the opposite extreme the visibility is zero when the intensity maxima and minima have the same value. Then no fringes are visible and the image formed on the screen does not show an interference pattern. The former limit corresponds to perfect coherence between the light beams from the two sources, while the latter limit indicates complete incoherence between them. Intermediate states of fringe visibility may then be understood as partial coherence. From this discussion and Eq. (2.18) it is easy to see that the visibility is in fact directly proportional to the degree of first-order coherence

$$V_d \propto |g^{(1)}(\tau)|. \qquad (2.26)$$

It seems like a fairly simple procedure to find the baseline where the visibility vanishes and then use Eq. (2.25) to find the angular diameter of a binary star, but in fact the Michelson interferometer pushed the limits of available technology when it was first proposed. The entire instrument must be carefully aligned to within a fraction of the coherence length of the light for stable fringes to form, since a difference comparable to the wavelength of the light in the path lengths *within* the interferometer will displace the fringes in the focal plane. Also, in order to collect as much light as possible, which is essential for the interference pattern to be at all discernible, a bandwidth of frequencies $\Delta\omega$ as broad as possible must be used. This gives a decreased coherence length l_c, a relation which was discussed earlier in section 1.3.2,

$$\tau_c = 1/\Delta\omega \quad \Rightarrow \quad l_c = \Delta\lambda. \qquad (2.27)$$

As a numerical example, a bandwidth of $\Delta\lambda = 100$nm gives a coherence length of 10^{-8}m. Note that the expression for the visibility in Eq. (2.25) is only valid for

monochrome light and a more complicated form must be used for light of a broader bandwidth. These are some of the drawbacks that explains why the Michelson interferometer was abandoned for the better part of the 21st century.

In resent years, however, modern technology has reduced the critical obstacles of the past to mere mechanical challenges, where video cameras record fringe patterns and laser sensors monitor path differences and internal movement of components. But one still has to overcome the random phase-shifts in the light that is introduced by irregular atmospheric layers. Random temporal variations in the atmosphere gives a time-varying phase difference between the two paths to the collector mirrors, resulting in rapid oscillations in the intensity, as can be seen from Eq. (2.22). This is where the intensity interferometer steps up to the plate.

2.3   The intensity interferometer

The intensity interferometer measures the correlation between the *fluctuations of intensities* at two separate points in a partially coherent field, as opposed to the Michelson interferometer which measures the fluctuations of the field amplitudes at two points. We will again determine the angular diameter of a binary star, but now with the intensity interferometer. The geometry of the problem is the same as shown in Fig. 2.1 and the only difference is what happens to the light *after* it enters the two detectors 1 and 2.

A schematic diagram of the intensity interferometer can be seen in Fig. 2.5. The light is collected by the mirrors A_1 and A_2 and sent to photodetectors P_1 and P_2, respectively. The fluctuating signal goes through the low-pass filters B_1, B_2, which selects a certain band of frequencies, $\Delta\omega$, that is sent into the multiplier M, before entering the correlator C. A variable delay time τ can be put on the signal from one detector to make up for the different path lengths the light has to traverse in order to be incident on the detectors. The correlator multiplies the fluctuating signals together and measures the cross-product averaged over some arbitrary time interval. The result is the correlation as a function of the spacing between the detectors, and from this it is possible to find the angular diameter of the object studied.

The principal advantage of the intensity interferometer is that the correlation is a function of the difference in phase between the currents formed at the two detectors, and *not* a function of the phase differences of light waves at these points. This means that one does not run into the same difficulties regarding the rigidity of the apparatus as with the Michelson interferometer, since the maximum usable base-line d is limited by electronics rather than the optical technique. To achieve a higher resolving power, i.e., a smaller apparent angle, a larger base-line is required. Since it is the electric signal from the detectors that is measured for coherence, the base-line can be extremely long, from hundreds to perhaps thousands of kilometres [7].

A second difficulty with the Michelson interferometer is its sensitivity to atmospheric scintillation and irregularities. In this section we will see that the intensity interferometer can work reliably through the Earth's atmosphere.
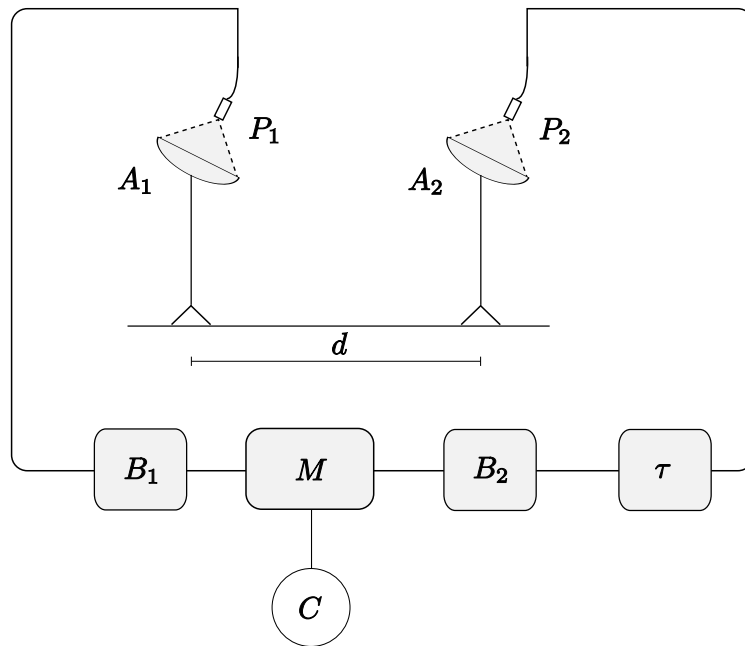
Figure 2.5: Schematic diagram of the intensity interferometer. A_1 and A_2 are the mirrors that collect light in the photodetectors P_1 and P_2, respectively. The signal goes through the low-pass filters B_1, B_2, into the multiplier M, before it enters the correlator C. τ is the delay time which can be put on the signal. Adapted from [9].

2.3.1 Prelude to the intensity interferometer

The first successful measurement of the angular diameter of a star other than the sun was made in 1920 by A.A. Michelson and Francis G. Pease [10], and it was done with the interferometer proposed by Michelson 30 years earlier, the Michelson interferometer [11]. The interferometer was built at the Mount Wilson observatory in Los Angeles, California, and had a baseline of 6.1 metres (20 ft). They measured the diameter of the red super giant Betelgeuse[7] to be 0.047 seconds of an arc ($\sim 2.2 \cdot 10^{-7}$ rad!). In total the diameter of six stars was measured, but attempts at measuring other stars failed. Later Pease built a second interferometer with a larger baseline (15 metres) to improve the optical resolution, but he was unable to produce reliable results and the work was eventually abandoned. Then the whole business of optical stellar interferometry went quiet for a long time.

Robert Hanbury Brown (1916 – 2002), a British astronomer and physicist, was pondering in 1949 on how to design a radio interferometer with a baseline of possibly thousands of kilometres. How could one compare the radio waves received at two points? If one took simultaneous photographs of the detected waves at both points, would the two pictures look the same? This question prompted the invention of the intensity interferometer.

Convinced his idea was worthwhile, Hanbury Brown recruited the mathematician

---

[7]Betelgeuse is possibly the largest star known, with a huge mass of 20 times the mass of the sun.

Richard Q. Twiss (1920 – 2005) to help lay the mathematical foundation for the intensity interferometer. Not long after, in 1952, a complete radio intensity interferometer stood ready to be put to the test at Jodrell Bank Observatory, U.K.. The goal was to measure the angular diameters of the two radio sources Cygnus A and Cassiopeia A. The results agreed with the predicted coherence between the intensities measured at each detector[8] and produced very good estimates for the angular diameter. But it turned out that the test was a success in more than one way.

Hanbury Brown and Twiss initially thought that the sole advantage over the Michelson radio interferometer was that one need not rely on mutually coherent local oscillators at the separated detector stations, something that was difficult to achieve for very long baselines[9]. To their great surprise, Hanbury Brown and Twiss noticed that while the sources were scintillating violently due to irregularities in the atmosphere, the measurement of the correlation proceeded relatively unaffected. In other words, the intensity interferometer could be made to work through a turbulent medium. The Michelson interferometer had been deemed impractical for just the two reasons that 1) it was difficult to extend the baseline long enough to achieve a better resolution (i.e., measuring smaller angular diameters) and 2) its performance was severely hampered by atmospheric turbulence. Two points that the radio intensity interferometer had shown it could overcome. This discovery prompted Hanbury Brown and Twiss to try to build an intensity interferometer for optical wavelengths.

Another boon was soon revealed. The detectors, although in principle telescopes, did not have to be much of a telescope by astronomical standards, as their only function was to collect light "like rain in a bucket and pour it on to the detector" to put it in Hanbury Brown's own words [7]. The telescopes need only be paraboloids clad with light-reflecting material, as it is not necessary to form a conventional image, a fact which implies huge cost savings.

The transition from measuring coherence of radio waves to measuring coherence of light waves was not an entirely smooth one. The radio engineers, brought up on the wave nature of electromagnetic radiation had no problem with accepting the semi-classical model of photoelectric emission presented by Hanbury Brown and Twiss, but the physicists, most with a mindset deeply entrenched in the photon view of light, found this hard to embrace. We will take a closer look on the opposition to the theory in section 3.3.

Early, crude experiments proved that the intensity interferometer did in fact work with visible light, and in particular a successful measurement of Sirius, the brightest star on the sky, showed the angular diameter to be 0.0063 arcseconds [12]. Hanbury-Brown and Twiss then proceeded to raise money to build a large scale interferometer. It was to be a joint project by the Universities of Manchester and Sydney, with the instrument being built in the U.K., but installed and operated near the small town of Narrabri, Australia. The Narrabri interferometer consisted of two large reflectors

---

[8]Antenna is probably a more common name than detector, but oh, bother; it is still a detection device for electromagnetic waves at radio frequencies.

[9] In radio interferometry local oscillators are used as a reference frequency to each detector and also to return the detected signal to the laboratory in order to be correlated with the other detection signals.
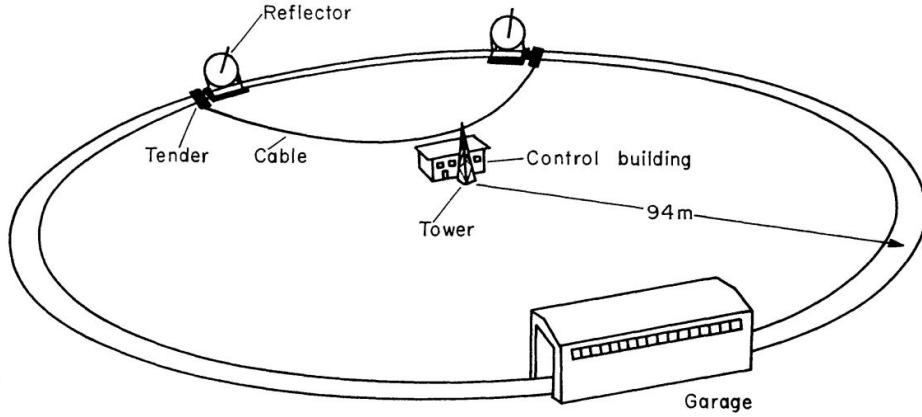
Figure 2.6: The general layout of the Narrabri stellar intensity interferometer, from [5].

mounted on trucks running on a $5.5\,\mathrm{m}$ wide railway track in a circle $188\,\mathrm{m}$ in diameter, with the laboratory in the centre, as illustrated by Fig. 2.6. After the usual financial and technical hurdles the Narrabri stellar intensity interferometer finally made its first successful full-scale measurement on the star Vega in August 1963. Over the next seven years reasonably precise measurements of the angular diameters of 32 single stars was made, thus increasing the number of known diameters from 6 to 38, not a negligible contribution to stellar astronomy.

2.3.2   Calculating the intensity fluctuations

We proceed now to demonstrate how the intensity interferometer differs from the Michelson interferometer. As before, two completely uncorrelated sources a and b emit light which subsequently is measured simultaneously in two detectors, 1 and 2. Detector 1 measures a superposition of the field from a, E_{1a}, and the field from b, E_{1b}, which has travelled a longer distance. Vice versa for detector 2. The complex electric fields incident upon the detectors are

$$E_1 = E_{1a} + E_{1b}$$
$$E_2 = E_{2a} + E_{2b}.$$

$$(2.28)$$

The same procedure as for the Michelson interferometer is followed and the intensities measured in each of the two detectors are

$$\bar{I}_1 = |E_1|^2 = |E_{1a} + E_{1b}|^2 = (E_{1a}^* + E_{1b}^*)(E_{1a} + E_{1b})$$
$$= E_{1a}^* E_{1a} + E_{1a}^* E_{1b} + E_{1b}^* E_{1b} + E_{1b}^* E_{1a}$$

$$(2.29)$$

and

$$\bar{I}_2 = |E_2|^2 = E_{2a}^* E_{2a} + E_{2a}^* E_{2b} + E_{2b}^* E_{2b} + E_{2b}^* E_{2a}$$

$$(2.30)$$

We will also need the product of the intensities,

$$
\begin{aligned}
\bar{I}_1 \bar{I}_2 &= |E_1|^2 |E_2|^2 \\
&= E_{1a}^* E_{1a} E_{2a}^* E_{2a} + E_{1a}^* E_{1a} E_{2b}^* E_{2b} + E_{1a}^* E_{1a} E_{2a}^* E_{2b} + E_{1a}^* E_{1a} E_{2b}^* E_{2a} \\
&\quad + E_{1b}^* E_{1b} E_{2a}^* E_{2a} + E_{1b}^* E_{1b} E_{2b}^* E_{2b} + E_{1b}^* E_{1b} E_{2a}^* E_{2b} + E_{1b}^* E_{1b} E_{2b}^* E_{2a} \\
&\quad + E_{1a}^* E_{1b} E_{2a}^* E_{2a} + E_{1a}^* E_{1b} E_{2b}^* E_{2b} + E_{1a}^* E_{1b} E_{2a}^* E_{2b} + E_{1a}^* E_{1b} E_{2b}^* E_{2a} \\
&\quad + E_{1b}^* E_{1a} E_{2a}^* E_{2a} + E_{1b}^* E_{1a} E_{2b}^* E_{2b} + E_{1b}^* E_{1a} E_{2a}^* E_{2b} + E_{1b}^* E_{1a} E_{2b}^* E_{2a}
\end{aligned}
\tag{2.31}
$$

Now, what is actually measured is the *output current* from the photodetectors. Conveniently, this is proportional to the intensity of the electric field

$$
i(t) = \alpha e I(t)
\tag{2.32}
$$

where α is the quantum efficiency of the detector and e is the electron charge [7], so we can naïvely carry on with our mathematical description of the intensity interferometer in order to easily compare it with the Michelson interferometer[10].

The definition of the time averaged intensity, denoted by angle brackets, is as always

$$
\langle \bar{I} \rangle = \langle E^*(t) E(t+\tau) \rangle = \frac{1}{T} \int_{t-T/2}^{t+T/2} \mathrm{d}t'\, E^*(t') E(t'+\tau)
\tag{1.30}
$$

which, due to the ergodicity of the light, is equivalent to taking the statistical ensemble average. The bar denotes the cycle averaged intensity Eq. (1.26), which is more convenient to work with since no equipment presently is anywhere near the resolution required to measure oscillations at the optical frequency of the electric field.

Because the sources a and b are uncorrelated, cross terms like $\langle E_{1a}^*(t) E_{1b}(t) \rangle$ can be written as $\langle E_{1a}^*(t) \rangle \langle E_{1b}(t) \rangle$. The contribution from such terms will be zero, since the complex field oscillates around a fixed value. So then we find that

$$
\begin{aligned}
\langle \bar{I}_1 \rangle &= \langle E_{1a}^* E_{1a} \rangle + \langle E_{1b}^* E_{1b} \rangle = \langle \bar{I}_a \rangle + \langle \bar{I}_b \rangle \\
\langle \bar{I}_2 \rangle &= \langle E_{2a}^* E_{2a} \rangle + \langle E_{2b}^* E_{2b} \rangle = \langle \bar{I}_a \rangle + \langle \bar{I}_b \rangle
\end{aligned}
\tag{2.33}
$$

Keep in mind that the averaging is over a time much longer than the delay time τ_i, $(i = a, b)$ and that the light obeys stationary statistics. Then the average intensity is time-independent and $\langle \bar{I}_i(t) \rangle = \langle \bar{I}_i(t+\tau_i) \rangle = \langle \bar{I}_i \rangle$; In other words $\langle \bar{I}_{1a} \rangle = \langle \bar{I}_{2a} \rangle$. The measured product of intensities is

$$
\begin{aligned}
\langle \bar{I}_1 \bar{I}_2 \rangle &= 2 \langle \bar{I}_a \rangle \langle \bar{I}_b \rangle + \langle \bar{I}_a(t) \bar{I}_a(t+\tau_a) \rangle + \langle \bar{I}_b(t) \bar{I}_b(t+\tau_b) \rangle \\
&\quad + 2 \,\mathrm{Re}\, \{ \langle E_a^*(t) E_a^*(t+\tau_a) \rangle \langle E_b(t) E_b(t+\tau_b) \rangle \} \\
&\quad + 2 \,\mathrm{Re}\, \{ \langle E_a^*(t) E_a(t+\tau_a) \rangle \langle E_b(t) E_b^*(t+\tau_b) \rangle \}
\end{aligned}
\tag{2.34}
$$

Recall the definitions of the degrees of first- and second-order coherence from the previous chapter

$$
\begin{aligned}
g^{(1)}(\tau) &= \frac{\langle E(t) E^*(t+\tau) \rangle}{\langle E^*(t) E(t) \rangle} = \frac{\langle E(t) E^*(t+\tau) \rangle}{\langle I \rangle} = g^{(1)}(-\tau)^* \\
g^{(2)}(\tau) &= \frac{\langle E^*(t) E^*(t+\tau) E(t+\tau) E(t) \rangle}{\langle E^*(t) E(t) \rangle^2} = \frac{\langle \bar{I}(t) \bar{I}(t+\tau) \rangle}{\langle \bar{I} \rangle^2}
\end{aligned}
$$

---

[10]Technically we should calculate the fluctuations in the *electrical currents*.

Also, the average of two field terms that are not complex conjugate of each other, will give zero contribution, for example,

$$
\begin{aligned}
\langle E(t)E(t+\tau)\rangle &= \frac{1}{T}\int_T \mathrm{d}t E(t)E(t+\tau)\\
&= \frac{1}{T}\int_T E_0(t)E_0(t+\tau)e^{i(kr-\omega t)}e^{i(k(r+c\tau)-\omega t)}\mathrm{d}t\\
&= \frac{1}{T}e^{ikc\tau}\int_T E_0(t)E_0(t+\tau)e^{2i(kr-\omega t)}\mathrm{d}t\\
&= 0 = \langle E^*(t)E^*(t+\tau)\rangle
\end{aligned}
$$

because the integration period is much longer than a cycle of the field, hence the rapid oscillation will give an average value of zero. We then have

$$
\langle \bar{I}_1\bar{I}_2\rangle = 2\langle \bar{I}_a\rangle\langle \bar{I}_b\rangle + \langle \bar{I}_a(t)\bar{I}_a(t+\tau_a)\rangle + \langle \bar{I}_b(t)\bar{I}_b(t+\tau_b)\rangle \\
+ 2\,\mathrm{Re}\left\{\langle E_a^*(t)E_a(t+\tau_a)\rangle\langle E_b(t)E_b^*(t+\tau_b)\rangle\right\} \quad (2.35)
$$

or

$$
\langle \bar{I}_1\bar{I}_2\rangle = \langle \bar{I}_a\rangle^2 g_a^{(2)}(\tau_a) + \langle \bar{I}_b\rangle^2 g_b^{(2)}(\tau_b) \\
+ 2\langle \bar{I}_a\rangle\langle \bar{I}_b\rangle\left[1 + \mathrm{Re}\left\{g_a^{(1)}(\tau_a)g_b^{(1)}(\tau_b)^*\right\}\right] \quad (2.36)
$$

The relative intensity correlation function is found to be

$$
\begin{aligned}
\mathcal{C} &= \frac{\langle \bar{I}_1\bar{I}_2\rangle}{\langle \bar{I}_1\rangle\langle \bar{I}_2\rangle}\\
&= \frac{\langle \bar{I}_a\rangle^2 g_a^{(2)}(\tau_a) + \langle \bar{I}_b\rangle^2 g_b^{(2)}(\tau_b) + 2\langle \bar{I}_a\rangle\langle \bar{I}_b\rangle\left[1 + \mathrm{Re}\left\{g_a^{(1)}(\tau_a)g_b^{(1)}(\tau_b)^*\right\}\right]}{\left[\langle \bar{I}_a\rangle + \langle \bar{I}_b\rangle\right]^2}
\end{aligned}
$$

$$(2.37)$$

The asymptotic behaviour of $g^{(1)}(\tau)$ and consequently $g^{(2)}(\tau)$ for chaotic light, is described in section 1.3 and can be used to test our result. So for $\tau = 0$, i.e., no distance between the detectors 1 and 2, or zero baseline as it is called,

$$
\mathcal{C}(0) = \frac{2\langle \bar{I}_a\rangle^2 + 2\langle \bar{I}_b\rangle^2 + \langle \bar{I}_a\rangle\langle \bar{I}_b\rangle(2+1+1)}{(\langle \bar{I}_a\rangle + \langle \bar{I}_b\rangle)^2} = 2 \quad (2.38)
$$

which is the maximal value of the relative intensity correlation function. When the detectors are moved far away from each other and the baseline grows long so that $\tau_a, \tau_b \gg \tau_c$, we get

$$
\mathcal{C}(\tau_a,\tau_b) = \frac{\langle \bar{I}_a\rangle^2 + \langle \bar{I}_b\rangle^2 + 2\langle \bar{I}_a\rangle\langle \bar{I}_b\rangle}{(\langle \bar{I}_a\rangle + \langle \bar{I}_b\rangle)^2} = 1, \quad \tau_a, \tau_b \gg \tau_c \quad (2.39)
$$

which is then the minimal value of the relative correlation. So then

$$
\mathcal{C}(\tau_a,\tau_b) = \begin{cases} 2 & \text{zero baseline}\\ 1 & \text{large baseline}\\ \in (1,2) & \text{otherwise} \end{cases} \quad (2.40)
$$

If the sources instead had emitted *coherent light* then $g^{(2)}(\tau) = |g^{(1)}(\tau)| = 1$ for all pairs of space-time points, hence $\mathcal{C} = 1$ for all baselines. But this means that the relative intensity correlation for *chaotic light* is a factor 2 larger than for coherent sources at short baselines! This excess intensity is known as the *Hanbury Brown-Twiss effect.*

If each of the two sources consists of a large number ν of uncorrelated atoms radiating chaotic light, the relation

$$g^{(2)}(\tau) = 1 + |g^{(1)}(\tau)|^2, \qquad \nu \gg 1$$

can be used to rewrite the correlation function as

$$\mathcal{C}(\tau_a, \tau_b) = 1 + \frac{\langle \bar{I}_a \rangle^2 |g_a^{(1)}(\tau_a)|^2 + \langle \bar{I}_b \rangle^2 |g_b^{(1)}(\tau_b)|^2 + 2\langle \bar{I}_a \rangle \langle \bar{I}_b \rangle \, \mathrm{Re} \left\{ g_a^{(1)}(\tau_a) g_b^{(1)}(\tau_b)^* \right\}}{\left[\langle \bar{I}_a \rangle + \langle \bar{I}_b \rangle \right]^2}$$

$$(2.41)$$

The correlation is essentially proportional to the square of the degree of first-order coherence. It is therefore also proportional to the square of the fringe visibility (Eq. (2.26)) of the Michelson interferometer

$$\mathcal{C} - 1 = (V_d)^2. \tag{2.42}$$

The relative intensity correlation will decrease with increasing baseline d, and a measurement of this will give the angular diameter of the binary star. But remember that we are measuring the correlation of fluctuations in the *electrical signals* at the linear multiplier, so there will be no interference fringes like in the Michelson interferometer. Also this setup measures the *square of the modulus* of the complex degree of first-order coherence. All information of the phase of the electric field is therefore irretrievably lost. As a consequence one cannot reconstruct the Fourier transform of the frequency distribution across the source[11]. To say it in English; For a system with two unequal sources it is not possible to tell which source is on the "left" and which is to the "right".

The fact that the intensity interferometer did not measure the phase of the electric field created quite a stir, since it is this quantity that leads to interference. How can photocurrents, electrons generated by the photo electric effect, know anything about the phase of the light which kicked it out into the electric current? But think again: Correlation in the intensity means that there is constructive interference. In the particle view the intensity is proportional to the number of photons incident. *One* photon can kick loose *one* photoelectron, so when a higher density of photoelectrons is measured (that is, the correlated electric signal) the question becomes: How can photons know that they should arrive at the detector at the same time as the other photons when the sources are uncorrelated (i.e., all photon emissions are independent, random events) and photons can only interact with themselves? The *Hanbury Brown-Twiss effect* and the quantum interpretation of the intensity interferometer will be discussed in sections 4.5.2 and 3.3, respectively.

---

[11] Recall that in section 1.3.2 we found that $g^{(1)}(\tau)$ forms a Fourier pair with the power spectral density.

2.3.3 From theory to practice

Hints were dropped at the end of section 2.2 that the intensity interferometer would be much less prone to instabilities due to random atmospheric and instrumental variations. The model using two sources emitting light with different wave vectors $\mathbf{k}$ and $\mathbf{k}'$ along two paths $\mathbf{r}$ and $\mathbf{r}'$ is the same as for the Michelson interferometer, so the geometric relations in Fig. 2.1 can be used. A little massaging of Eq. (2.35) gives

$$\langle \bar{I}_1 \bar{I}_2 \rangle = \left[\langle \bar{I}_a \rangle + \langle \bar{I}_b \rangle \right]^2 + \langle \bar{I}_a \rangle^2 |g_a^{(1)}(\tau_a)|^2 + \langle \bar{I}_b \rangle^2 |g_b^{(1)}(\tau_b)|^2$$
$$+ \langle \bar{I}_a \rangle \langle \bar{I}_b \rangle |g_a^{(1)}(\tau_a)||g_b^{(1)}(\tau_b)| \operatorname{Re}\left\{ e^{i\omega_a \tau_a + i\omega_b \tau_b} \right\} \quad (2.43)$$

It is already apparent that this is a much simpler expression than its analogue $\langle \bar{I}_P \rangle$ of the Michelson interferometer (Eq. (2.22)). Nevertheless, to really emphasise the difference we can assume that some filter in the gedanken experiment only admits a certain frequency so that $\omega_a \approx \omega_b \approx \omega$. Then

$$\langle \bar{I}_1 \bar{I}_2 \rangle = \left[\langle \bar{I}_a \rangle + \langle \bar{I}_b \rangle \right]^2 + \langle \bar{I}_a \rangle^2 |g_a^{(1)}(\tau_a)|^2 + \langle \bar{I}_b \rangle^2 |g_b^{(1)}(\tau_b)|^2$$
$$+ \langle \bar{I}_a \rangle \langle \bar{I}_b \rangle |g_a^{(1)}(\tau_a)||g_b^{(1)}(\tau_b)| \cos\left[\omega(\tau_a + \tau_b) \right]$$
$$= \left[\langle \bar{I}_a \rangle + \langle \bar{I}_b \rangle \right]^2 + \langle \bar{I}_a \rangle^2 |g_a^{(1)}(\tau_a)|^2 + \langle \bar{I}_b \rangle^2 |g_b^{(1)}(\tau_b)|^2$$
$$+ \langle \bar{I}_a \rangle \langle \bar{I}_b \rangle |g_a^{(1)}(\tau_a)||g_b^{(1)}(\tau_b)| \cos\left(\frac{2\pi d\theta}{\lambda} \right) \quad (2.44)$$

where the last step has been calculated in the same way as Eq. (2.35). Thus the rapidly oscillating term $\cos[\omega(\tau_a + \tau_b)]$ is not measured by the intensity interferometer. The only oscillating term is the comparatively slow cosine which relates the baseline d and the angular diameter θ. This is the mechanism which makes the intensity interferometer fairly insensitive to atmospheric scintillations and deviations in path lengths within the instrument.

It might be tempting now to hail the intensity interferometer as the saviour of all of stellar astronomy, but it does have its limitations. The most important shortcoming is its rather poor signal-to-noise performance. The incident light waves are translated into a fluctuating electric signal by the photodetectors and this signal will in general consist of three types of noise. While one strives to shield the photodetectors from other light sources in the sky, for instance the Moon[12], other stars and even headlights from passing traffic, it is inevitable that some of this background light appears as noise in the signal regardless. There is also electronic noise in the different components, called *shot noise*. This is related to the discrete nature of the conversion of the light incident on the detectors to current carrying electrons. So as long as the light is of low-intensity, which starlight most definitely is, the (relatively) low number of electrons will show as detectable statistical fluctuations in the current.

These two types of noise are incoherent in the sense that the fluctuation in one photodetector shows no correlation with the fluctuation in the other. The third type

---

[12]Observations with the preliminary intensity interferometer at Jodrell Bank were not possible during the full-moon periods, but could only be conducted during the first and last quarters of the Moon due to the high level of background light [12].

of noise is the *wave noise*, which is smaller than the shot noise [7]. Unfortunately, wave noise is the signal component that corresponds to the intensity fluctuations of the light wave. This noise *is* correlated with the wave noise in the other photodetector. One can think of the wave noise as the envelope of the light wave demodulated by the photodetectors. It can be shown that the signal-to-noise ratio is directly proportional to the light-collecting area of the detectors (i.e., the size of the paraboloid mirrors) [13], including the quantum efficiency of the photodetectors, the electrical bandwidth of the filters and the time interval that the correlator integrates over. So the most serious disadvantage of the intensity interferometer is that it requires very large light collectors, much larger than the Michelson stellar interferometer needs, even for the bright stars.

2.4 Comparison of the Michelson interferometer and the intensity interferometer

To see how the correlation of the incident light on the two interferometers behaves as a function of the baseline d, we plot the relative correlation functions, starting with the Michelson interferometer

$$\langle \bar{I}_P \rangle = 2\langle \bar{I}_a \rangle \big[1 + |g_a^{(1)}(\tau_a)| \cos(\omega_a \tau_a)\big] + 2\langle \bar{I}_b \rangle \big[1 + |g_b^{(1)}(\tau_b)| \cos(\omega_b \tau_b)\big]. \quad (2.18)$$

Regardless of which frequency distribution is chosen, either Lorentzian or Gaussian (Eq. (1.40) or Eq. (1.41)), only the factor $|g_i^{(1)}(\tau_i)|$, $(i = a, b)$, will differ. We know from Eq. (2.11) that we can replace all occurrences of τ_b with $\tau_a - d\theta/c$. We also have the simple relation

$$\tau_a = d/c \cos\alpha \approx d\alpha'/c \quad (2.45)$$

from Eq. (2.4), where we assume that α' does not change appreciatively with neither time nor baseline and that $\alpha \approx \pi/2$ so that α' is a small number, but not negligible compared to the apparent angular diameter θ.

The relative correlation for Lorentzian distributed light is

$$\begin{aligned}
\mathcal{C}(d) &= \frac{\langle \bar{I}_P \rangle}{\langle \bar{I}_1 \rangle + \langle \bar{I}_2 \rangle} \\
&= 1 + \frac{\langle \bar{I}_a \rangle e^{-|\tau_a|/\tau_c} \cos(\omega\tau_a) + \langle \bar{I}_b \rangle e^{-|\tau_a - d\theta/c|/\tau_c} \cos(\omega\tau_a - kd\theta)}{\langle \bar{I}_a \rangle + \langle \bar{I}_b \rangle},
\end{aligned}$$
$$(2.46)$$

and for Gaussian distributed light

$$\mathcal{C}(d) = 1 + \frac{\langle \bar{I}_a \rangle e^{-\tau_a^2/\tau_c^2} \cos(\omega\tau_a) + \langle \bar{I}_b \rangle e^{-(\tau_a - d\theta/c)^2/\tau_c^2} \cos(\omega\tau_a - kd\theta)}{\langle \bar{I}_a \rangle + \langle \bar{I}_b \rangle}. \quad (2.47)$$

In the same way the relative correlation function for the intensity interferometer is

found from

$$
\mathcal{C}(d) = \frac{\langle I_1 I_2 \rangle}{\langle I_1 \rangle \langle I_2 \rangle} = 1 + \frac{\langle \bar{I}_a \rangle^2 |g_a^{(1)}(\tau_a)|^2 + \langle \bar{I}_b \rangle^2 |g_b^{(1)}(\tau_b)|^2}{\left[\langle \bar{I}_a \rangle + \langle \bar{I}_b \rangle\right]^2}
$$
$$
+ \frac{2\langle \bar{I}_a \rangle \langle \bar{I}_b \rangle |g_a^{(1)}(\tau_a) g_b^{(1)}(\tau_b)| \cos[\omega(\tau_a - \tau_b)]}{\left[\langle \bar{I}_a \rangle + \langle \bar{I}_b \rangle\right]^2}. \quad (2.41)
$$

So, for a Lorentzian distribution we have

$$
\mathcal{C}(d) = 1 + \frac{\langle \bar{I}_a \rangle^2 e^{-2|\tau_a|/\tau_c} + \langle \bar{I}_b \rangle^2 e^{-2|\tau_a - d\theta/c|/\tau_c}}{\left[\langle \bar{I}_a \rangle + \langle \bar{I}_b \rangle\right]^2}
$$
$$
+ \frac{2\langle \bar{I}_a \rangle \langle \bar{I}_b \rangle e^{-|\tau_a|/\tau_c} e^{-|\tau_a - d\theta/c|/\tau_c} \cos(kd\theta)}{\left[\langle \bar{I}_a \rangle + \langle \bar{I}_b \rangle\right]^2}, \quad (2.48)
$$

and for a Gaussian distribution

$$
\mathcal{C}(d) = 1 + \frac{\langle \bar{I}_a \rangle^2 e^{-\pi \tau_a^2/\tau_c^2} + \langle \bar{I}_b \rangle^2 e^{-\pi(\tau_a - d\theta/c)^2/\tau_c^2}}{\left[\langle \bar{I}_a \rangle + \langle \bar{I}_b \rangle\right]^2}
$$
$$
+ \frac{2\langle \bar{I}_a \rangle \langle \bar{I}_b \rangle e^{-\pi/2\tau_a^2/\tau_c^2} e^{-\pi/2(\tau_a - d\theta/c)^2/\tau_c^2} \cos(kd\theta)}{\left[\langle \bar{I}_a \rangle + \langle \bar{I}_b \rangle\right]^2}. \quad (2.49)
$$

The four correlation equations above are computed by the MATLAB script listed in Appendix C.1 and the results are plotted in Figures 2.7 and 2.9 with the parameters defined in Table 2.1. A rudimentary analysis of the orders of magnitude of the parameters can be done to determine how important e.g., the angle α between the incoming light rays and the baseline is compared to the apparent angular diameter θ of the binary star. Before doing any calculations we need to estimate a few of the parameters involved in the equations. For starters, for thermal light the coherence length for thermal radiation is given as [14]

$$
l_c = c\tau_c \approx \frac{hc}{4k_B T} \quad (2.50)
$$

where h is the Planck constant, k_B is Boltzmann's constant and T is the absolute temperature of the light source[13]. The surface of a typical everyday star (this would be the sun) is $T \cong 6000\,\text{K}$, yielding a coherence length of $0.6\,\mu\text{m}$. A reasonable wavelength of the measured light is $540\,\text{nm}$, and in the simulation we let the baseline d vary from 0 to $30\,\text{m}$ (But for aesthetic reasons d takes on negative values in the figures).

From Table 2.1 we see that the arguments of the exponentials in Eqs. (2.46), (2.47),

---

[13]The Boltzmann constant is $k_B = 1.38 \cdot 10^{-23}$ J/K.

Table 2.1: A list of the parameters used in Fig. 2.7 and Fig. 2.9

$$
\begin{aligned}
c \quad &= 3 \cdot 10^8 \text{ m/s} \\
k \quad &= \tfrac{2\pi}{\lambda} = \tfrac{2\pi}{540} \cdot 10^{-9} \text{ m} \\
\theta \quad &= 0.047 \text{ arcsec} = 0.047 \cdot 4.85 \cdot 10^{-6} \text{ rad} = 2.28 \cdot 10^{-7} \text{ rad} \\
d \quad &\propto 10 \text{ m} \\
r_c \quad &= c\tau_c = 10^{-6} \text{ m} \Rightarrow \quad \tau_c = \tfrac{1}{3} \cdot 10^{-14} \text{ s} \\
r_a \quad &= c\tau_a = d\cos\alpha \approx d \cdot 10^{-7} = 10^{-6} \text{ m} \Rightarrow \quad \tau_c = \tfrac{1}{3} \cdot 10^{-14} \text{ s} \\
\langle I_a \rangle \quad &= \langle I_b \rangle = 1
\end{aligned}
$$

(2.48) and (2.49) are on the order of

$$
\begin{aligned}
\tau_a/\tau_c &\propto 1 \\
d\theta/c\tau_c &\propto 2.3 \\
(\tau_a - d\theta/c)/\tau_c &\propto -1.3 \\
2\tau_a d\theta/c\tau_c^2 &\propto 4.6
\end{aligned}
$$

i.e., they are all on the order of 1. Hence there are no obvious means of simplifying the equations by neglecting some terms much smaller than others, however we can still draw relatively simple conclusions from them to use in the interpretation of Figs. 2.7 and 2.9. The easiest case is the correlation function for the intensity interferometer. In Eqs. (2.48) and (2.49) there is only one oscillating factor, namely $\cos(kd\theta)$. So a smaller apparent angle θ gives a longer period and fewer visible oscillations, which is readily seen in Figure 2.7.

In an ideal experiment the minimal values in the correlator output can determine the apparent angular diameter of the binary star in the following way. The minima of $\mathcal{C}(d)$ appear when the cosine term is negative, since all the other terms are always positive and larger than zero:

$$
\cos(kd\theta) = -1 \quad \Rightarrow \quad kd\theta = n\pi, \quad (n = 1, 3, 5, \ldots). \tag{2.51}
$$

So by counting the number of minima outwards from $d = 0$ it is found that

$$
\theta = \frac{n\pi}{kd} = \frac{n\lambda}{2d}. \tag{2.52}
$$

But as seen from Fig. 2.7 there must be a balance between the dampening factor and the oscillating factor, i.e., the difference between α' and θ. As the order of magnitude of θ increases one needs to zoom in to a finer baseline-resolution in order for the rapid oscillations to be discernible.
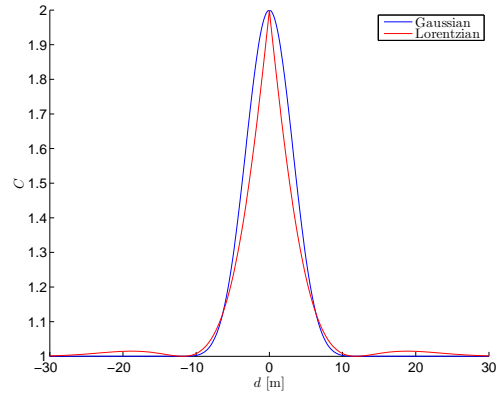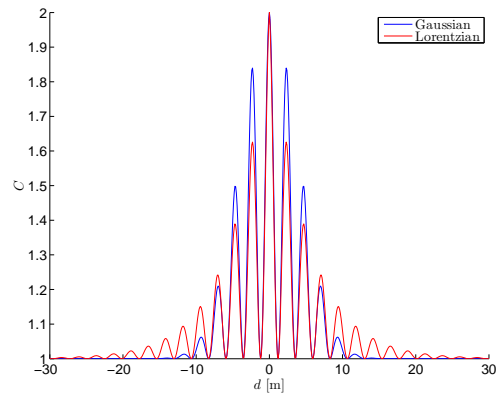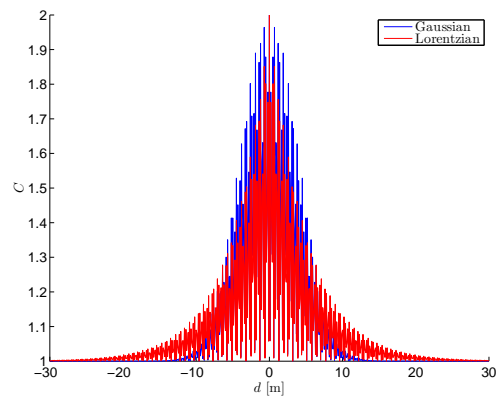
Figure 2.7: The relative intensity correlation as a function of the baseline length for the intensity interferometer. The values of the parameters used are listed in Table 2.1. (a) $\theta = 0.0047$ arcsec, (b) $\theta = 0.047$ arcsec, (c) $\theta = 0.47$ arcsec.

Figure 2.8: Theoretical correlation values were calculated in order to determine the best fit with the experimental data. The difference of just a few thousandths of a second of arc is plainly visible. In this case the angular diameters of $\theta = 0.0052, 0.0047$ and 0.0042 arcsec are assumed for a source radiating light with a Gaussian frequency distribution.

Of course, in real life the correlator will not give pretty readings like those in Fig. 2.7. In the very first measurements on Sirius by Hanbury Brown and Twiss in 1956 they first calculate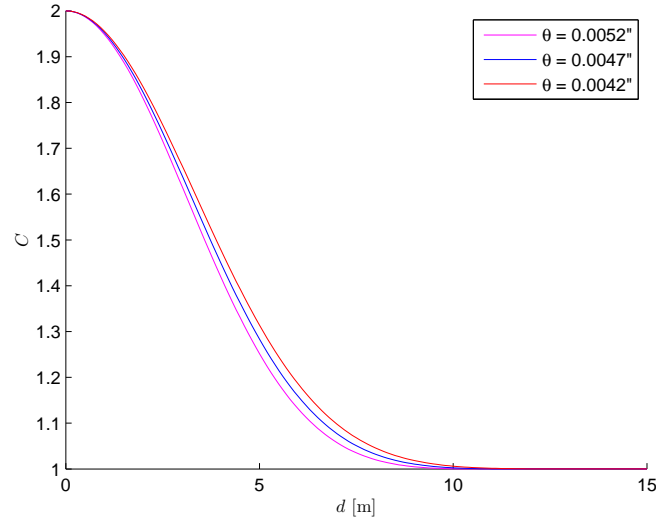d the theoretical correlation values for a star radiating like a black body uniform disk at a typical temperature of its spectral type [12]. The angular diameter which gave the best fit with the measurements was then equal to the true angular diameter to within an acceptable uncertainty. As one can see from Fig. 2.8 it is fairly easy to discern the difference in the correlation between different angular diameters down to a few milliseconds of arc.

On the other hand, with the Michelson interferometer it is not as simple as just counting the minima (which is a point in itself), chiefly due to the presence of two cosine terms with different periods of oscillation, in Eqs. (2.46) and (2.47),

$$\cos(\omega\tau_a - kd\theta) \qquad \text{and} \qquad \cos(\omega\tau_a). \tag{2.53}$$

Rewriting using $c\tau_a \approx d\alpha'$ gives

$$\cos[kd(\alpha' - \theta)] \qquad \text{and} \qquad \cos(kd\alpha'). \tag{2.54}$$

It seems that as long as θ is comparable to or smaller than α', it will not be a very easy task to find θ at all. Looking at Figure 2.9 we see that from (a) to (b) the graph has a gentle oscillation that does not change much when going from $\theta = 0.0047$ arcsec to $\theta = 0.047$ arcsec, while in (c), with another increase by a factor of 10 to $\theta = 0.47$ arcsec, the graph still has its smooth curve, but now with heavy fluctuations. For θ larger

than α', it should be possible to use the period of the fast oscillation to find the value of θ. However, already at this preliminary stage we can easily conclude that the intensity interferometer will more readily allow measurements of much smaller apparent angles than the Michelson interferometer will. In all fairness, the value assumed for α' in Table 2.1 is a ludicrously small number. An angle giving $\cos \alpha \approx 10^{-7}$ means that the interferometer is almost precisely normal to the distance vector $\mathbf{L}$ of the binary star. Better be careful not to sneeze!

It is time for a recapitulation. The degree of second-order coherence is a measure of the coherence of fluctuations of the intensity of an electric field. Similarly the degree of first-order coherence is a measure of the coherence of fluctuations of the electric field amplitude. From Eqs. (2.48) and (2.49) we can glean that it is not actually the degree of second-order coherence itself which is the important ingredient in the correlation function of the intensity interferometer, but rather the real-valued product of the degree of first-order coherences from each source. This is a bit contrary to what most textbooks (seemingly) will have one believe, since they more often than not lead up to the intensity interferometer by first introducing $g^{(2)}(\tau)$. We also know the relation $g^{(2)}(\tau) \sim |g^{(1)}(\tau)|^2$. In a way this is similar to the Poynting vector in that $I \sim |E|^2$. Following this train of thought, if we take the absolute square of the product of $g^{(1)}(\tau)$ from two sources, then another kind of degree of second-order coherence is found, that quantifies the correlation of the intensities from both sources, i.e.,

$$\langle E_a(t)E_a(t+\tau_a)E_b(t)E_b(t+\tau_b)\rangle \neq \langle E_a(t)E_a(t+\tau_a)\rangle\langle E_b(t)E_b(t+\tau_b)\rangle. \quad (2.55)$$

The field amplitude correlations are packaged in the intensity correlations, getting rid of the troublesome $\cos \omega(\tau_a + \tau_b)$ term. It is this that makes the intensity interferometer a lot less of a hassle to work with than the Michelson interferometer.
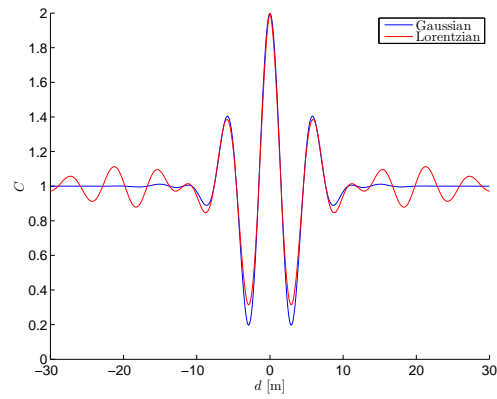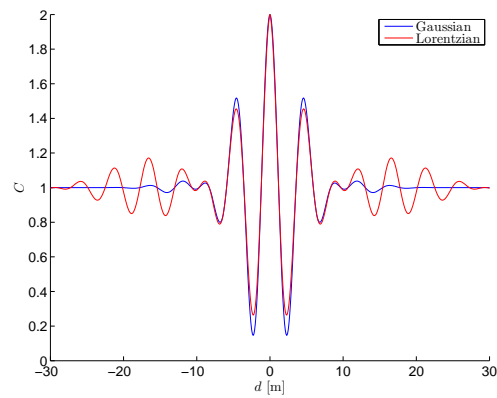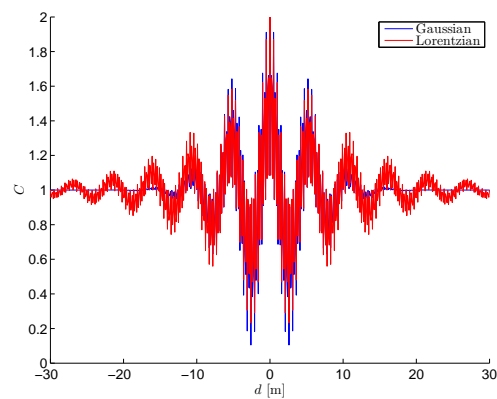
Figure 2.9: The relative field correlation as a function of the baseline length for the Michelson interferometer. The values of the parameters used are listed in Table 2.1. (a) $\theta = 0.0047$ arcsec, (b) $\theta = 0.047$ arcsec, (c) $\theta = 0.47$ arcsec.

Part II

Coherence in quantum optics

Chapter 3

The quantised electric field and quantum coherence

In the previous part the electromagnetic field was treated as a classical field. The classical theory is a successful one in the sense that it accounts for a variety of optical phenomena, especially those dealing with wave propagation, interference and diffraction. But a semiclassical theory, in which the field is treated classically while the particles are treated by quantum theory, is also able to describe what one could think of as purely quantum effects and proof of the existence of photons, such as the photoelectric effect, Compton-scattering and spontaneous emission [15]. However, there are some effects that can only be accounted for by quantum mechanics, one of which is known as photon anti-bunching. This discussion is saved for the end of chapter 4.

The classical degrees of first- and second-order coherence from sections 1.3 and 1.4 can be translated to a quantum mechanical coherence theory. But first the free electromagnetic field must be quantised using field operators. The density operator will also be introduced. This is an essential tool in developing the framework to study the quantum correlations of light. Then in section 3.2 the degrees of first- and second-order coherence functions will be rewritten in terms of field operators. It will be seen that the degree of second-order coherence in fact turns out to be a measure of the "classicalness" of light.

Section 3.3 briefly discusses the quantum Hanbury Brown-Twiss effect and how the intensity interferometer can be interpreted in quantum mechanics. This is followed by section 3.4 where the coherent state is introduced. There it will be concluded that light in a coherent state is the closest the quantum mechanical approach can come to a classical, ideal electric wave.

3.1 Quantisation of the electromagnetic field

Hardly any work on a topic in quantum mechanics can forego mention of the harmonic oscillator, because it is one of few quantum mechanical systems with a simple ex-

act solution, and any potential can be approximated as a harmonic potential near an equilibrium point. The one-dimensional harmonic oscillator Hamiltonian is

$$\hat{H} = \frac{\hat{p}^2}{2m} + \frac{1}{2}m\omega^2\hat{q}^2 \tag{3.1}$$

where m is the mass of a particle subject to a potential V with angular frequency ω, q is the position operator and p is the momentum operator satisfying the canonical commutation relation $[q, p] = i\hbar$.

3.1.1 The ladder-operators of the harmonic oscillator

The reason for bringing up the harmonic oscillator is the very elegant ladder method, due to Paul Dirac, which can be used to solve the eigenvalue problem. This method is also readily generalized to more complicated problems in quantum field theory. Without further ado, we introduce the ladder-operators

$$\begin{aligned}
\hat{a} &= (2\hbar m\omega)^{-1/2}(m\omega\hat{q} + i\hat{p}) \\
\hat{a}^\dagger &= (2\hbar m\omega)^{-1/2}(m\omega\hat{q} - i\hat{p})
\end{aligned} \tag{3.2}$$

which are also known as the annihilation and creation operators, respectively. These satisfy the commutation relation

$$[\hat{a}, \hat{a}^\dagger] = 1, \tag{3.3}$$

and the Hamiltonian expressed in terms of $\hat{a}$ and $\hat{a}^\dagger$ is

$$\hat{H} = \frac{1}{2}\hbar\omega(\hat{a}^\dagger\hat{a} + \hat{a}\hat{a}^\dagger) = \hbar\omega(\hat{a}^\dagger\hat{a} + \frac{1}{2}). \tag{3.4}$$

It is common to define the number operator

$$\hat{N} \equiv \hat{a}^\dagger\hat{a} \tag{3.5}$$

such that the eigenvalue of N is the number of photons in the energy eigenstate $|n\rangle$

$$\hat{N}|n\rangle = n|n\rangle. \tag{3.6}$$

The annihilation operator, $\hat{a}$, decreases the number of particles in $|n\rangle$ by one, while the creation operator, $\hat{a}^\dagger$, increases the number by one,

$$a|n\rangle = n^{1/2}|n-1\rangle, \qquad \hat{a}^\dagger|n\rangle = (n+1)^{1/2}|n+1\rangle. \tag{3.7}$$

The eigenenergy E_n of state $|n\rangle$ is found by applying the Hamilton operator from the left,

$$\hat{H}|n\rangle = \hbar\omega(\hat{N} + 1/2)|n\rangle = E_n|n\rangle \tag{3.8}$$

The vacuum state is the energy state containing zero particles, $|0\rangle$, and can be reached by applying $\hat{a}$ from the left. However, there must be a lower limit since the harmonic oscillator should have positive kinetic and potential energies. Thus

$$\hat{a}|0\rangle = 0. \tag{3.9}$$

From Eq. (3.8) the lowest allowed energy E_0 is found to be

$$\hat{H}\left|0\right\rangle = \frac{1}{2}\hbar\omega\left|0\right\rangle \qquad \Rightarrow \qquad E_0 = \frac{1}{2}\hbar\omega. \tag{3.10}$$

In general the n-photon eigenenergy is

$$E_n = \left(n + \frac{1}{2}\right)\hbar\omega \tag{3.11}$$

It is useful and quite intuitive to think of the energy eigenvalues as the n *photons* of energy-quanta $\hbar\omega$. The eigenstates $\left|n\right\rangle$ are called Fock states or photon number states, and they form a complete set,

$$\sum_{n=0}^{\infty}\left|n\right\rangle\left\langle n\right| = 1. \tag{3.12}$$

From Eq. (3.11) we see that the eigenenergy is discreet and this is the famous contrast to the continuous energy allowed in classical electromagnetism. The state vector is, in general, a superposition of arbitrary Fock states, i.e.,

$$\left|\psi\right\rangle = \sum_{n} c_n \left|n\right\rangle \tag{3.13}$$

where c_n are complex coefficients. A special property worth mentioning is that an electric field in a Fock state contains a precisely determined number of photons, n. There is no uncertainty in this number and so its variation vanishes: $(\Delta n)^2 = 0$.

3.1.2   The quantised free electric field

When quantizing the electromagnetic field it is customary to work with the vector potential $\mathbf{A}$. But the goal here is to rewrite the degrees of first and second-order coherence (Eqs. (1.29) and (1.56)), both of which are functions of the electric field. In section 1.1.2 the electric field $\mathbf{E}(\mathbf{r}, t)$ was prepared as a Fourier expansion with a countable, but infinite number of Fourier coefficients, i.e., the field amplitudes. The total energy of the radiative field was also found and a comparison of Eq. (1.21) to Eq. (3.4) suggests the conversion from the classical electric field amplitudes to the quantum mechanical ladder-operators

$$a_{\mathbf{k}\lambda} \rightarrow \hat{a}_{\mathbf{k}\lambda} \qquad \text{and} \qquad a_{\mathbf{k}\lambda}^{*} \rightarrow \hat{a}_{\mathbf{k}\lambda}^{\dagger} \tag{3.14}$$

The eigenvector $\left|n_{\mathbf{k}}\right\rangle$ represents the number of photons in mode $\mathbf{k}$. The commutation relations for the ladder-operators of independent harmonic oscillators $\mathbf{k}, \mathbf{k}'$ are [16]

$$[\hat{a}_{\mathbf{k}\lambda}, \hat{a}_{\mathbf{k}'\lambda'}] = [\hat{a}_{\mathbf{k}\lambda}^{\dagger}, \hat{a}_{\mathbf{k}'\lambda'}^{\dagger}] = 0,$$
$$[\hat{a}_{\mathbf{k}\lambda}, \hat{a}_{\mathbf{k}'\lambda'}^{\dagger}] = \delta_{\mathbf{k}\mathbf{k}'}. \tag{3.15}$$

The quantized electric field operator then takes the form

$$\hat{\mathbf{E}}(\mathbf{r}, t) = \sum_{\mathbf{k}}\sum_{\lambda}\left(\frac{\hbar\omega_k}{2\epsilon_0 L^3}\right)^{1/2}\hat{\epsilon}_{\mathbf{k}\lambda}\left[\hat{a}_{\mathbf{k}\lambda}e^{i(\mathbf{k}\cdot\mathbf{r}-\omega_k t)} + \hat{a}_{\mathbf{k}\lambda}^{\dagger}e^{-i(\mathbf{k}\cdot\mathbf{r}-\omega_k t)}\right]. \tag{3.16}$$

It is common to write the positive and negative frequency parts of the electric field operator separately

$$\hat{\mathbf{E}}(\mathbf{r}, t) = \hat{\mathbf{E}}^{(+)}(\mathbf{r}, t) + \hat{\mathbf{E}}^{(-)}(\mathbf{r}, t) \tag{3.17}$$

where

$$
\begin{aligned}
\hat{\mathbf{E}}^{(+)}(\mathbf{r}, t) &= \sum_{\mathbf{k}} \sum_{\lambda} \left(\frac{\hbar \omega_k}{2\epsilon_0 L^3} \right)^{1/2} \hat{\epsilon}_{\mathbf{k}\lambda} \hat{a}_{\mathbf{k}\lambda} e^{i(\mathbf{k}\cdot\mathbf{r} - \omega_k t)}, \\
\hat{\mathbf{E}}^{(-)}(\mathbf{r}, t) &= \sum_{\mathbf{k}} \sum_{\lambda} \left(\frac{\hbar \omega_k}{2\epsilon_0 L^3} \right)^{1/2} \hat{\epsilon}_{\mathbf{k}\lambda} \hat{a}_{\mathbf{k}\lambda}^{\dagger} e^{-i(\mathbf{k}\cdot\mathbf{r} - \omega_k t)}.
\end{aligned}
\tag{3.18}
$$

So $\hat{\mathbf{E}}^{(+)}(\mathbf{r}, t)$ contains only the annihilation operators and its adjoint, $\hat{\mathbf{E}}^{(-)}(\mathbf{r}, t)$, contains only the creation operators.

3.1.3 The density operator

We are now almost ready to rewrite the degree of first and second-order coherence of sections 1.3 and 1.4, but first a very important tool must be introduced, namely the density operator. The approach taken is largely based on that taken in [9], but an even more thorough and detailed derivation can be found in [17].

In the optical frequency region, local field measurements can be done by detectors based on the photoelectric effect. To put it simply, an atom in its ground state is placed in a radiation field. The electrons kicked out from the atom, often called photoelectrons, are then observed. This measurement is destructive in the sense that the photon is annihilated in the process of producing a photoelectron. Therefore only the annihilation operator $\hat{\mathbf{E}}^{(+)}(\mathbf{r}, t)$ contributes in this process. To simplify things a bit we assume that the field is linearly polarized along one direction parallel to the unit vector $\hat{\epsilon}$ so that we can deal with the scalar quantity $\hat{E}(\mathbf{r}, t) = \hat{\epsilon} \cdot \hat{\mathbf{E}}(\mathbf{r}, t)$. In practice this would mean fitting the detector with a polarization filter and only recording the photons parallel to $\hat{\epsilon}$. The transition probability of the detector atom at position $\mathbf{r}$ for absorbing a photon from the field is

$$w(\mathbf{r}, t) = |\langle f| \hat{E}^{(+)}(\mathbf{r}, t) |i\rangle|^2 \tag{3.19}$$

where $|i\rangle$ is the initial state before the annihilation, i.e., before the detection, and $|f\rangle$ is the final state after annihilation. But the final state is not measured and so we have to sum over all possible final states,

$$
\begin{aligned}
w(\mathbf{r}, t) &= \sum_{f} |\langle f| \hat{E}^{(+)}(\mathbf{r}, t) |i\rangle|^2 \\
&= \sum_{f} \langle i| \hat{E}^{(-)}(\mathbf{r}, t) |f\rangle \langle f| \hat{E}^{(+)}(\mathbf{r}, t) |i\rangle \\
&= \langle i| \hat{E}^{(-)}(\mathbf{r}, t) \hat{E}^{(+)}(\mathbf{r}, t) |i\rangle,
\end{aligned}
$$

where the last step is accomplished by using the completeness relation

$$\sum_f |f\rangle \langle f| = 1. \tag{3.20}$$

Of course, nature being fickle, it is very rare that there is precise knowledge of the initial state $|i\rangle$ of the field; we may know only the probability for the system to be in $|i\rangle$. In such a situation one can resort to a statistical description by averaging over all the possible initial states weighted by their respective probabilities p_i

$$\hat{\rho} = \sum_i p_i |i\rangle \langle i|. \tag{3.21}$$

This is the *density operator* and it is a valuable tool when a system is not described by a single state vector, but an *ensemble* of state vectors $\{|\psi\rangle_1, |\psi\rangle_2, \ldots, |\psi\rangle_n\}$ with a probability distribution $\{p_1, p_2, \ldots, p_n\}$ defined over the ensemble. While it is tempting to consider this ensemble to contain both *quantum probabilities* carried by the state vectors $|\psi_k\rangle$ and *classical probabilities* carried by the distribution p_k, such a sharp division may not always be so clear [18].

The density operator satisfies certain properties which are straight forward to show,

hermiticity : $\hat{\rho}^\dagger = \hat{\rho} \Rightarrow p_k = p_k^*$.

positivity : $p_k \geq 0$ since $\langle \chi| \hat{\rho} |\chi\rangle \geq 0 \; \forall \; |\chi\rangle$.

normalization : $\text{tr}(\hat{\rho}) = 1 \Rightarrow \sum_k p_k = 1$.

where tr is short for the trace of an operator, which is the invariant sum of its diagonal matrix elements for any complete set of states. What is important to note is that *all measurable information* is contained in the density operator, since the expectation value of *any* observable can be expressed in terms of $\hat{\rho}$,

$$\begin{aligned}
\langle A \rangle &= \sum_k p_k \langle \psi_k| \hat{A} |\psi_k\rangle \\
&= \sum_k p_k \sum_{i,j} \langle \psi_k |\phi_i\rangle \langle \phi_i| \hat{A} |\phi_j\rangle \langle \phi_j |\psi_k\rangle \\
&= \sum_k p_k \sum_{i,j} \langle \phi_j |\psi_k\rangle \langle \psi_k |\phi_i\rangle \, A_{ij} \\
&= \sum_{i,j} \rho_{ij} A_{ij} \\
&= \text{tr}(\hat{\rho}\hat{A}),
\end{aligned} \tag{3.22}$$

where the definition of the *density matrix* has been used:

$$\rho_{ij} = \sum_k p_k \langle \phi_j |\psi_k\rangle \langle \psi_k |\phi_i\rangle. \tag{3.23}$$

So the transition probability can be written as

$$\begin{aligned}
w(\mathbf{r}, t) &= \sum_i p_i \langle i| \hat{E}^{(-)}(\mathbf{r}, t)\hat{E}^{(+)}(\mathbf{r}, t) |i\rangle \\
&= \text{tr}[\hat{\rho}\hat{E}^{(-)}(\mathbf{r}, t)\hat{E}^{(+)}(\mathbf{r}, t)]
\end{aligned} \tag{3.24}$$

3.2 The quantum mechanical degrees of first- and second-order coherence

In section 1.3 the classical first-order correlation function was defined as the long-time[1] average of the electric wave radiated from a single source. Then the ergodic nature of chaotic light was used to equal the time-average to the statistical average of an ensemble of identical atoms. If the radiation fields are wide-sense stationary, (i.e., the correlation functions are independent of time), then the correlation only depends on the time difference $\tau = t_2 - t_1$ between two measurements of the field at the same point $\mathbf{r}$ in space. This leads to the definition of the quantum mechanical first-order correlation function of the electric field

$$\langle \hat{E}^{(-)}(\mathbf{r}, t)\hat{E}^{(+)}(\mathbf{r}, t+\tau)\rangle = \operatorname{tr}\left[\hat{\rho}\hat{E}^{(-)}(\mathbf{r}, t)\hat{E}^{(+)}(\mathbf{r}, t+\tau)\right]. \tag{3.25}$$

Note that the field operators are in *normal order*; The annihilation operators are to the right of all the creation operators in each product of operators. The advantage of normal ordering is that the expectation value of any normal product vanishes. We are free to write any observable in normal order since this merely corresponds to changing the particular order of factors (which are c-numbers) *before* quantization of the field [19]. For example, the average intensity at point $\mathbf{r}$ at time t is

$$\langle I(\mathbf{r}, t)\rangle = \langle \hat{E}^{(-)}(\mathbf{r}, t)\hat{E}^{(+)}(\mathbf{r}, t)\rangle, \tag{3.26}$$

and the observable intensity-intensity correlation function is not $\langle I(\mathbf{r}, t)I(\mathbf{r}, t)\rangle$, but rather the normally ordered product

$$\langle N\{I(\mathbf{r}, t)I(\mathbf{r}, t)\}\rangle = \langle \hat{E}^{(-)}(\mathbf{r}, t)\hat{E}^{(-)}(\mathbf{r}, t)\hat{E}^{(+)}(\mathbf{r}, t)\hat{E}^{(+)}(\mathbf{r}, t)\rangle, \tag{3.27}$$

where $N\{\}$ denotes the normal product.

In a similar way as for Eq. (3.25) we define the quantum mechanical second-order correlation function of the electric field

$$\langle \hat{E}^{(-)}(\mathbf{r}, t)\hat{E}^{(-)}(\mathbf{r}, t+\tau)\hat{E}^{(+)}(\mathbf{r}, t+\tau)\hat{E}^{(+)}(\mathbf{r}, t)\rangle$$
$$= \operatorname{tr}\left[\hat{\rho}\hat{E}^{(-)}(\mathbf{r}, t)\hat{E}^{(-)}(\mathbf{r}, t+\tau)\hat{E}^{(+)}(\mathbf{r}, t+\tau)\hat{E}^{(+)}(\mathbf{r}, t)\right]. \tag{3.28}$$

Thus the normalised quantum mechanical degree of first-order coherence for a wide-sense stationary field is

$$g^{(1)}(\tau) = \frac{\langle \hat{E}^{(-)}(t)\hat{E}^{(+)}(t+\tau)\rangle}{\langle \hat{E}^{(-)}(t)\hat{E}^{(+)}(t)\rangle} \tag{3.29}$$

and the normalised quantum mechanical degree of second-order coherence

$$g^{(2)}(\tau) = \frac{\langle \hat{E}^{(-)}(t)\hat{E}^{(-)}(t+\tau)\hat{E}^{(+)}(t+\tau)\hat{E}^{(+)}(t)\rangle}{\langle \hat{E}^{(-)}(t)\hat{E}^{(+)}(t)\rangle^2} \tag{3.30}$$

---

[1]Long-time as in much longer than the coherence time of the light.

Note that in the definition of $g^{(2)}(\tau)$ the operators have also been *time ordered*. Time ordering is defined as

$$\mathcal{T}\{\phi(x)\phi(x')\} = \begin{cases} \phi(x)\phi(x'), & t > t' \\ \phi(x')\phi(x), & t' > t \end{cases} \tag{3.31}$$

where $t = x/c$ etc. The effect is that the *earliest* operator acts on the state *first*. Specifically the creation operator in $\hat{E}^{(-)}(t)$ will act leftwards on the bra first, followed by $\hat{E}^{(-)}(t+\tau)$, while the annihilation operator in $\hat{E}^{(+)}(t)$ acts to the right on the ket, before $\hat{E}^{(+)}(t+\tau)$.

Remember that we are still dealing with the scalar frequency parts of the electric fields and do not have to worry about the polarisation. Also keep in mind that since we are focussing only on temporal coherence, it is purposeful to keep the notation as simple as possible by only explicitly writing the time dependence of the degrees of coherence. The spatial dependence can always be reintroduced via

$$\tau = t_2 - t_1 - (|\mathbf{r}_2| - |\mathbf{r}_1|)/c. \tag{3.32}$$

3.2.1   In the limits of quantum coherence

The quantum degree of first-order coherence does not lead to any conflict with the classical limits defined in Eq. (1.32), which is equivalent to saying that it does not exhibit any signature of field quantisation. For a single-mode electric field, $g^{(1)}(\tau)$ is greatly simplified as most of the factors cancel out and we are left with simply

$$g^{(1)}(\tau) = \frac{\langle \hat{a}^\dagger \hat{a} \rangle e^{i\omega\tau}}{\langle \hat{a}^\dagger \hat{a} \rangle} = e^{i\omega\tau}. \tag{3.33}$$

This is in accordance with the classical result in Eq. (1.34) and shows that any plane parallel single-mode light beam is first-order coherent for all pairs of space-time points.

Since the numerator in Eq. (3.30) is the expectation value of an operator multiplied with its Hermitian conjugate, it must be positive [1] and it follows that

$$0 \leq g^{(2)}(\tau) \leq \infty, \tag{3.34}$$

which is similar to the range of the classical degree of second-order coherence. However it is not possible to show that the quantum $g^{(2)}(\tau)$ satisfies either of the inequalities Eq. (1.63) or Eq. (1.67).

The degree of second-order coherence also simplifies for a single-mode field to

$$\begin{aligned} g^{(2)}(\tau) &= \frac{\langle \hat{a}^\dagger \hat{a}^\dagger \hat{a} \hat{a} \rangle}{\langle \hat{a}^\dagger \hat{a} \rangle^2} = \frac{\langle (\hat{a}^\dagger \hat{a})^2 \rangle - \langle \hat{a}^\dagger \hat{a} \rangle}{\langle \hat{a}^\dagger \hat{a} \rangle^2} \\ &= \frac{\langle N^2 \rangle - \langle N \rangle}{\langle N \rangle^2} = 1 + \frac{(\Delta N)^2 - \langle N \rangle}{\langle N \rangle^2} \end{aligned} \tag{3.35}$$

where we use the definition of the number operator and the commutator of the ladder-operators. The variance in the photon number cannot be negative, so

$$(\Delta N)^2 \equiv \langle N^2 \rangle - \langle N \rangle^2 \geq 0. \tag{3.36}$$

Inserting this into $g^{(2)}(\tau)$ we see that any single-mode field must satisfy the inequality

$$g^{(2)}(\tau) \geq \begin{cases} 1 - \frac{1}{\langle N \rangle} & \text{for } \langle N \rangle \geq 1 \\ 0 & \text{for } \langle N \rangle < 1. \end{cases} \tag{3.37}$$

This limit is independent of space and time, but it does depend on the nature of the light, since the variance in photon number $(\Delta N)^2$ is not the same for the different types of light. Clearly $g^{(2)}(0)$ violates the classical lower limit Eq. (1.63). Light with degree of second-order coherence outside of the classical range ($\in [1, \infty]$) must then be considered to be *non-classical*. This topic is discussed in more detail in section 4.5.1.

3.3   The Quantum Hanbury Brown-Twiss effect

In section 2.3 we used classical electric fields to demonstrate that the intensity interferometer measures the degree of second-order coherence, $g^{(2)}(\tau)$. We then saw that the Hanbury Brown-Twiss effect gives an enhanced relative intensity correlation between chaotic light beams incident on two photodetectors, an effect not seen for coherent sources.

Hanbury Brown and Twiss originally proposed a radio intensity interferometer to measure the angular diameter of radio stars. This was widely accepted by both radio engineers and physicists since at the wavelengths where radio astronomy is applied, classical electromagnetism is considered to give a sufficient description of the interference effect. However, when they ventured to apply the intensity interferometer to optical wavelengths they were met with outright scepticism and charges of it being a patently absurd idea.

Since the classical derivation has been given much attention it adds a certain completeness to devote a few paragraphs to the quantum approach. We will not go into a detailed derivation but will briefly mention the criticism of the intensity interferometer and how coincidence counting of photons led to the discovery of photon bunching and its relation to the degree of second-order coherence.

3.3.1   Trouble in Hilbert space

The problem with applying the intensity interferometer on light, it was thought, was that at optical wavelengths the energies would require the light to be quantised in a relatively small number of photons. It would then not be correct to use Maxwell's equations on light waves and only introduce quantisation through the discrete energy levels in the photodetectors. What was more, if one instead thought of the light in terms

of photons, the enhanced intensity correlation would imply that the photon's arrival at the two separated detectors would be correlated. Somehow, the photons from two incoherent sources would then "know" that they should arrive at a detector at the same time, in "clumps".

Obviously, in order for the interference to take place there has to be several *different* photons incident on the detectors at the same time. A quite worrisome requirement since P. Dirac stated that [2]

"[A] photon [...] interferes only with itself. Interference between two different photons never occurs."

In order to avoid violation of this dictum one needs to do some mental gymnastics. There are at the least two possible ways to think about this. For example, one can evade the dictum by saying that in a *two-photon* state there is no way to determine which atom emitted or absorbed which photon [20]. Or, one can think of each emitting atom to be coupled to a mode in a universal radiation field, so that a photon is simply a particular energy eigenstate of one such radiation mode [21].

This was not the only objection raised. Hanbury Brown and Twiss also had to fend off complaints of violation of the uncertainty relation[3] and of the laws of thermodynamics[4]. Lastly there were performed a few laboratory experiments that claimed to disprove the correlation of photons at two separate detectors, most notably the experiment by Brannen and Ferguson[5] which concluded that

"[No] correlation [...] exists between photons in coherent light rays",
and that
"[If] such a correlation did exist, it would call for a major revision of some fundamental concepts in quantum mechanics".

These conclusions were quickly shot down as it turned out that the sensitivity of the equipment being used was so low that an observation period of a 1000 years would be necessary in order to see any correlations [22].

In Hanbury Browns own words the remonstrations against the intensity interferometer originated from "*[Troubled] physicists who had been brought up on particles and had not fully appreciated that the concept of a photon is not a complete picture of light*" [7]. In the end Hanbury Brown and Twiss were vindicated, and have since been granted the honour of laying the experimental foundation for contemporary quantum optics and for providing new methods for fundamental tests of quantum mechanics [20].

---

[2] Dirac, P.A.M., *The Principles of Quantum Mechanics*, Oxford Clarendon Press, 4th ed, 1989

[3] A point refuted by the fact that the intensity interferometer measures only the *relative* phase between the two light beams. The total energy and the relative phase can be represented by commuting operators and can incidentally be described by classical theory.

[4] The correction lies in taking into account that the total total fluctuations in the temperature of the body must be treated as due to interaction between incident, emitted and reflected streams of radiation.

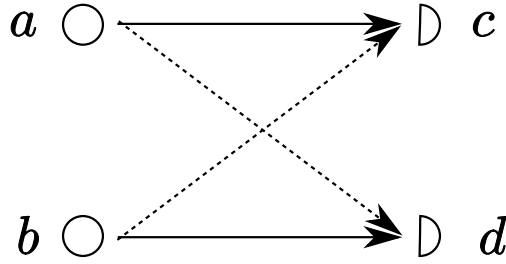[5] Brannen, E. and Ferguson, H.I.S., *Nature*, **178**, 481 (1956).

Figure 3.1: The two indistinguishable events where (solid arrows) a emits a photon detected by c and b emits one detected by d, and (dashed arrows) a emits a photon detected by d and b emits one detected by c.

3.3.2 The essence of the quantum interpretation

Consider two source atoms a and b initially in excited states without any phase correlation. They both emit photons which are absorbed by the "detector" atoms c and d. There are basically four different events that will lead to excitations of c and d if one assumes that each detector can only be excited by one photon at a time [23]: (i) Atom a can emit two photons that are detected at c and d, respectively, and (ii) b can emit two photons that are detected at c and d. These processes are distinguishable and does not lead to any interference. (iii) Atom a can emit a photon detected at c, with b emitting a photon detected in d. (iv) Atom a can emit a photon detected at d, with b emitting a photon detected in c, see Fig. 3.1. It is not possible to tell events (iii) and (iv) apart since photons are *indistinguishable* particles. Thus the system state vector is a superposition of (iii) and (iv)

$$|c,d\rangle = \frac{1}{\sqrt{2}}\big[\,|a \to c, b \to d\rangle + |b \to c, a \to d\rangle\,\big] \qquad (3.38)$$

and this is the origin of the correlation seen in the quantum Hanbury Brown-Twiss effect.

The probability that c is excited when in the presence of sources a and b is the sum of the probabilities that c is excited by a without b present and by b without a present

$$P_c = P(a \to c) + P(b \to c). \qquad (3.39)$$

Likewise the probability that d is excited, P_d. By the argument of Fano [24] the probability of excitation of *both* c and d, $P_{c,d}$, is not just equal to the product $P_c P_d$, nor can it be simply expressed as a function of the probabilities $P(a \to c)$, $P(b \to c)$, $P(a \to d)$ or $P(b \to d)$. Instead $P_{c,d}$ is an oscillatory function of the distance between c and d, provided the two excitations are close enough in time. This result is in complete agreement with what we found from the classical description in section 2.3.

The probability distribution of an excitation over time is equivalent to a counting distribution of n photons detected, so we make a switch in variables. We define a *coincidence* as detections of a photon at c and d simultaneously, where "simultaneous" in practical terms means within some short time τ according to the resolution time of

the setup. If the counter N registers a coincidence when two photons arrive at c, d, the average coincidence rate is

$$\bar{N} = 2\bar{N}_c \bar{N}_d \tau [1 + 1/2|g^{(1)}(0)|^2], \tag{3.40}$$

where $\bar{N}_{c(d)}$ is the average counting rate of photons arriving at $c(d)$ [7]. This result is valid for a resolving time much shorter than the coherence time (which is inversely proportional to the angular frequency). So if the light is not first-order coherent, then the coincidence rate is simply the expected rate for two uncorrelated streams of photons $2\bar{N}_c \bar{N}_d \tau_c$. But if the light is at least partially first-order coherent ($|g^{(1)}(0)| > 0$), there is an excess in the coincidence rate which varies directly with the degree of first-order coherence, i.e., the photons tend to arrive in "clumps". Recall that classical chaotic light is partially first-order coherent for small τ (see Fig. 1.2). This is the quantum Hanbury Brown and Twiss effect. Of course the "clumping" is not unique to photons, but applies generally to bosons. Where bosons are social animals, fermions have antisymmetric wavefunctions which manifests as an "anti-clumping". This "clumping" is discussed more in section 4.5.2 where it will be given a more contemporary name.

As a comment to Eq. (3.38) it does make sense that photons detected within a time interval shorter than their coherence time $\tau_c \sim 1/\Delta\omega$ can be regarded as occupying the same state. Due to the Heisenberg uncertainty principle the uncertainty in energy must be on the order of $\hbar\Delta\omega \sim \hbar/\tau_c$, and the uncertainty in arrival time is similarly $1/\Delta\omega$. These two quantities define a unit cell in phase space, which the resolution time $\tau \ll \tau_c$ is well within [25].

3.4   Coherent states of the electric field

Coherent states were first discovered by E. Schrödinger (1926) as states of the harmonic oscillator with a minimum uncertainty product. These minimum-uncertainty states did not attract much attention until R. J. Glauber (1963) used them to develop a complete quantum mechanical description of the photon statistics of arbitrary radiation fields. The states were renamed coherent states by Glauber, but are also referred to by others as Glauber states. The work was inspired by the then relatively heated debate regarding the results of the optical intensity interferometer and it culminated in a complete quantum mechanical coherence theory to the Nth order.

Up until then nearly all quantum electrodynamical calculations had been carried out through the use of the Fock states, which are purely quantum mechanical states in the sense that they have no equivalence to any known classical fields. In practice this limited the calculations to only dealing with a few photons at a time, while in optics it is often the case that the number of photons is large and not necessarily precisely known. Glauber found that the coherent states, which are closely related to the coherence properties of fields, have the ability to represent the classical limit of a field and still preserve the quantum mechanical aspects of it [16, 26].

The coherent state is the eigenstate of the annihilation operator introduced in section 3.1. As $\hat{a}$ is not Hermitian we must allow for it to have a complex eigenvalue,

$$\hat{a} |\alpha\rangle = \alpha |\alpha\rangle, \tag{3.41}$$

with the corresponding bra-state

$$\langle \alpha | \, \hat{a}^\dagger = \alpha^* \, \langle \alpha | \,. \tag{3.42}$$

The coherent state can be expanded in a linear superposition of the Fock states

$$|\alpha\rangle = e^{-|\alpha|^2/2} \sum_{n=0}^{\infty} \frac{\alpha^n}{\sqrt{n!}} \, |n\rangle \tag{3.43}$$

which is clearly seen to be normalised

$$\langle \alpha \, | \alpha \rangle = e^{-|\alpha|^2} \sum_{n=0}^{\infty} \frac{|\alpha|^{2n}}{n!} \, \langle n \, | n \rangle = 1. \tag{3.44}$$

Furthermore, the coherent-state expectation value for the number operator is

$$\langle n \rangle = \langle \alpha | \, \hat{n} \, | \alpha \rangle = \langle \alpha | \, \hat{a}^\dagger \hat{a} \, | \alpha \rangle = |\alpha|^2 \tag{3.45}$$

and similarly for the second moment

$$\langle n^2 \rangle = \langle \alpha | \, \hat{n}^2 \, | \alpha \rangle = \langle \alpha | \, \hat{a}^\dagger \hat{a}^\dagger \hat{a} \hat{a} \, | \alpha \rangle = \langle \alpha | \, \hat{a}^\dagger \hat{a} \hat{a}^\dagger \hat{a} \, | \alpha \rangle + \langle \alpha | \, \hat{a}^\dagger \hat{a} \, | \alpha \rangle$$
$$= |\alpha|^4 + |\alpha|^2$$

From this we find the variance of the photon number

$$(\Delta n)^2 = \langle n^2 \rangle - \langle n \rangle^2 = |\alpha|^2 \tag{3.46}$$

So the relative variance, or uncertainty, in the number of photons in a coherent state decreases when the amplitude of the coherent state increases,

$$\frac{\Delta n}{\langle n \rangle} = \frac{1}{|\alpha|} = \frac{1}{\sqrt{\langle n \rangle}}. \tag{3.47}$$

The classical analogy of a vanishing variance in photon number is an ideal wave with no intensity fluctuations, which can be called *stable*. So the fact that the variance is non-vanishing can be interpreted as an aspect of the particle nature of light in quantum mechanics. However, the importance of this aspect diminishes with increase in the mean photon number $\langle n \rangle$. This can be viewed as a manifestation of Bohr's correspondence principle; As the number of photons increases, the coherent state becomes more and more classical, with smaller and smaller relative fluctuations in energy.

The quantised electromagnetic field can be in a coherent state, obtainable by specifying a coherent state for each of the modes $\mathbf{k}$ of the field. Each mode of the field corresponds to a single, isolated harmonic oscillator so the multi-mode coherent state vector is the product form

$$|\{\alpha\}\rangle \equiv |\alpha_{\mathbf{k}_1}, \alpha_{\mathbf{k}_2}, \dots, \alpha_{\mathbf{k}_n}\rangle = |\alpha_{\mathbf{k}_1}\rangle \otimes |\alpha_{\mathbf{k}_2}\rangle \otimes \cdots \otimes |\alpha_{\mathbf{k}_n}\rangle \tag{3.48}$$

The electric field operator $\hat{\mathbf{E}}(\mathbf{r}, t)$ has a particularly simple expectation value when the field is in a coherent state,

$$
\begin{aligned}
\langle \mathbf{E}(\mathbf{r}, t) \rangle &= \langle \{\alpha\} | \, \hat{\mathbf{E}}(\mathbf{r}, t) \, | \{\alpha\} \rangle \\
&= \sum_{\mathbf{k}\lambda} \left(\frac{\hbar \omega_k}{2\epsilon_0 L^3} \right)^{1/2} \hat{\epsilon}_{\mathbf{k}\lambda} \left[\alpha_{\mathbf{k}\lambda} e^{i(\mathbf{k}\cdot\mathbf{r} - \omega_k t)} + \alpha_{\mathbf{k}\lambda}^* e^{-i(\mathbf{k}\cdot\mathbf{r} - \omega_k t)} \right]
\end{aligned} \quad (3.49)
$$

This is on the same form as the mode expansion of the corresponding classical field Eq. (1.18), where $\alpha_{\mathbf{k}\lambda}$ represents the well-defined complex amplitude of the classical field mode $\mathbf{k}$. Note, however, that despite this similarity, Eq. (3.49) is merely the *average* field in the coherent state and being a quantised field it also exhibits quantum fluctuations, whereas a coherent classical electric field will not show fluctuations in neither amplitude nor phase. In addition, the variance of the field vector does not vanish event though the expectation values (the first and second moment) resembles that of a classical field of well-defined complex amplitude $\alpha_{\mathbf{k}\lambda}$.

So, quantum fluctuations being a fact of life, the coherent state can be shown to be a quadrature minimum-uncertainty state for all mean photon numbers $\langle n \rangle = |\alpha|^2$. If the annihilation and creation operators are expanded as

$$
\hat{a} = \hat{X}_1 + i\hat{X}_2 \quad \text{and} \quad \hat{a}^\dagger = \hat{X}_1 - i\hat{X}_2 \quad (3.50)
$$

where $\hat{X}_1$ and $\hat{X}_2$ are dimensionless *quadrature operators*[6], a little algebra yields the expectation values of the quadrature operators

$$
\langle \hat{X}_1 \rangle = \frac{1}{2} \langle \alpha | \, \hat{a}^\dagger + \hat{a} \, | \alpha \rangle = \frac{1}{2} (\alpha^* + \alpha) \quad (3.51)
$$

and

$$
\langle \hat{X}_2 \rangle = \frac{i}{2} \langle \alpha | \, \hat{a}^\dagger - \hat{a} \, | \alpha \rangle = \frac{i}{2} (\alpha^* - \alpha). \quad (3.52)
$$

The expectation values of the squares of the quadrature operators are found by employing the commutation identity of the ladder-operators

$$
\hat{X}_1^2 = \frac{1}{4} [\hat{a}^\dagger + \hat{a}]^2 = \frac{1}{4} [\hat{a}^\dagger \hat{a}^\dagger + \hat{a}\hat{a} + 2\hat{a}^\dagger \hat{a} + 1] \quad (3.53)
$$

giving

$$
\langle \hat{X}_1^2 \rangle = \frac{1}{4} [(\alpha^*)^2 + \alpha^2 + 2|\alpha|^2 + 1]. \quad (3.54)
$$

Similarly

$$
\langle \hat{X}_2^2 \rangle = \frac{1}{4} [-(\alpha^*)^2 - \alpha^2 + 2|\alpha|^2 + 1]. \quad (3.55)
$$

---

[6] The quadrature operators can be recognised as dimensionless forms of the quantum mechanical position and momentum operators, $\hat{q}$ and $\hat{p}$ respectively.

The quadrature variances are then[7]

$$(\Delta X_1)^2 = (\Delta X_2)^2 = \frac{1}{4} \qquad\qquad (3.56)$$

which are independent of the photon number. Furthermore, the uncertainty relation is the equality

$$(\Delta X_1)(\Delta X_2) = \frac{1}{4} \qquad\qquad (3.57)$$

Thus for any mean photon number the coherent state is a quadrature minimum-uncertainty state. This also includes the vacuum state where $\alpha = 0$, meaning that all coherent states have the same uncertainty as vacuum. Thus one can interpret the "fuzziness" of the coherent state as being due to vacuum fluctuations. It may be said that the minimum uncertainty represents an incoherent part of the quantised field which is a result of quantum fluctuations. Hence the energy of the total quantised field will be a sum of this vacuum energy and the fields coherent energy [27]. This is in contrast to the classical coherent light which, as mentioned several times now, does not fluctuate and will have no energy addition from the vacuum since the classical vacuum energy is zero. In section 2.3.3 we discussed a phenomena called *shot noise* that is observed in optical detection (specifically in the intensity interferometer) and its origin is thought to be exactly this quantum uncertainty in light, namely the ever present vacuum field modes [3].

A phase diagram for the coherent state $|\alpha\rangle$ can be drawn if α is separated into its amplitude and phase by

$$\alpha = |\alpha|e^{i\phi} \qquad\qquad (3.58)$$

where θ is the mean phase of the coherent-state excitation of the field mode, such that

$$X_1 = |\alpha|\cos\phi, \qquad X_2 = |\alpha|\sin\phi. \qquad\qquad (3.59)$$

$|\alpha\rangle$ can be considered a displaced vacuum state where the uncertainty "cloud" is shifted from the origin by the quadrature vector of length $|\alpha|$ at an angle ϕ to the X_1-axis [3], see Fig. 3.2. The diameter of the shaded circle at the end of $|\alpha|$ is $\Delta X_1 = \Delta X_2 = 1/2$. By geometric means, the variance of the phase, $\Delta\phi$, can be deduced from the diagram,

$$\tan\Delta\phi/2 = \frac{1/2}{2|\alpha|} \qquad\qquad (3.60)$$

The evaluation of the uncertainty in the phase ϕ, however, is not straight forward since a phase eigenstate or a phase operator cannot be represented within the usual infinite Hilbert space [28]. Instead we can derive a number-phase uncertainty relationship based on geometrical arguments rather than commutation relations between number and phase operators. This result will correctly represent a trade-off between the values of the

---

[7] Note that the coherent state is a special case of a *squeezed state* since the quadrature variances are equal, which they need not always be.
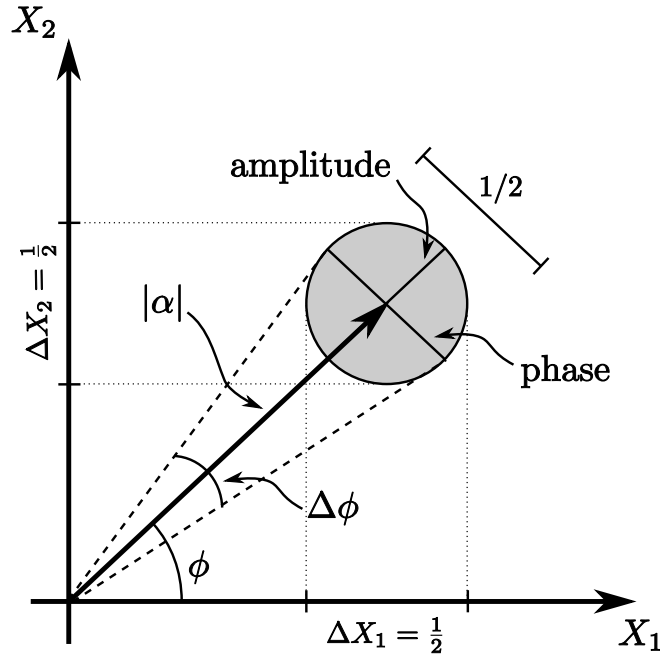
Figure 3.2: Phase diagram for the coherent state $|\alpha\rangle$ with the uncertainty in the quadrature operators X_1 and X_2 shown as a grey circle displaced a distance $|\alpha|$ from the origin. The phase angle ϕ is defined in Eq. (3.58) and by a geometric derivation the uncertainty in the phase, $\Delta\phi$, can be found. Note that this is only well-defined when $\alpha \gg 1$.

amplitude and phase uncertainties of the electric field associated with the coherent state. We therefore assume that the mean photon number is large, $|\alpha| = \sqrt{\langle n \rangle} \gg 1$. From Fig. 3.2 we see that the visual angle $\Delta\phi$ subtended by the diameter of the disk at the origin, provided that $|\alpha| \gg 1$, is

$$\Delta\phi = \frac{1}{2|\alpha|} = \frac{1}{2\Delta n} \tag{3.61}$$

yielding

$$\Delta n \Delta\phi = \frac{1}{2}, \quad |\alpha| \gg 1. \tag{3.62}$$

Thus the uncertainty in both the photon number and in the phase varies like $1/|\alpha|$; As the mean photon number is increased the electric field becomes better defined both in amplitude and phase angle. This point is illustrated by Fig. 3.3 where the mean electric field (solid line) is enveloped by the vacuum noise band (dashed lines). The vertical distance to the dashed lines indicates the uncertainty in the mean number of photons. This separation is constant (according to Eq. (3.56)) as the amplitude of the mean field increases, rendering it insignificant for large enough $|\alpha|$. But if $|\alpha|$ is small, then $\Delta\phi$ becomes large and eventually approaches its maximum value of 2π where the phase is totally undefined.
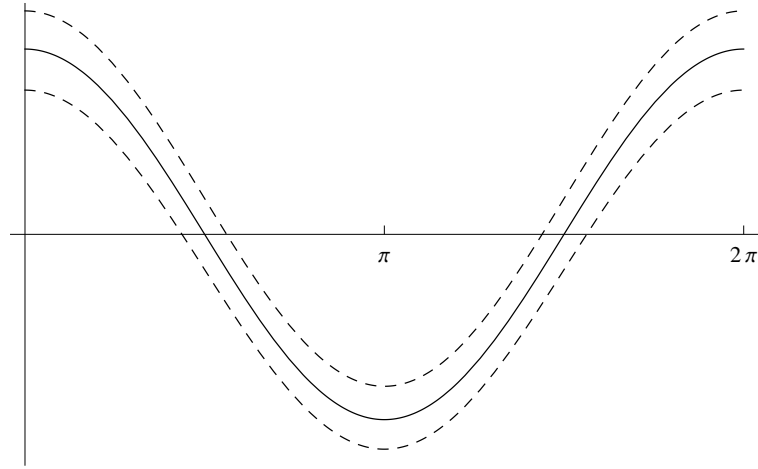
Figure 3.3: One period of the electric field in a single-mode coherent state where the dashed lines indicate the uncertainty in phase and amplitude due to quantum fluctuations. Adapted from [1].

In contrast to the coherent state, the Fock number state has a sharply defined photon number. By the same line of reasoning as above, the Fock state must then have a maximal uncertainty in the phase, that is $\phi \in [0, 2\pi]$. The energy eigenvalue relation can be written in terms of the quadrature operators as

$$\hbar\omega(\hat{a}^\dagger \hat{a} + 1/2) |n\rangle = \hbar\omega(\hat{X}_1^2 + \hat{X}_2^2) |n\rangle = \hbar\omega(n + 1/2) |n\rangle \tag{3.63}$$

resulting in the variances

$$(\Delta X_1)^2 = (\Delta X_2)^2 = \frac{1}{2}(n + 1/2) \tag{3.64}$$

Thus the vacuum state is the quadrature minimum-uncertainty state. Fig. 3.4 illustrates the quadrature properties of the Fock state. The phase of the quadrature operators is maximally uncertain, so the radius of the circle spanned by $\mathbf{X}_1 + \mathbf{X}_2$ is found from Eq. (3.63),

3.5   Summary and discussion

In this chapter we have quantised the electric field and introduced the ladder-operators of the harmonic oscillator. The coherent states are the eigenstates of these operators and they offer very convenient calculations of the electric field near the classical limit. This is seen by both the fact that we can recognize their eigenvalues as the complex amplitude of the classic field, but also because they are *minimum uncertainty states*, which was shown in section 3.4. There we saw that while light in a coherent state *is* by nature quantum mechanical in that it exhibits quantum fluctuations, this aspect grows less and less important for higher eigenvalues (i.e., higher photon number).
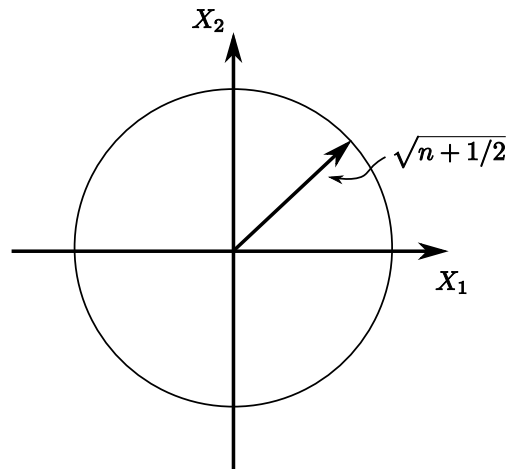
Figure 3.4: Phase-diagram for the Fock state $|n\rangle$, with sharply defined photon number in the quadrature operators, but maximal uncertainty in the phase.

Although the expectation value of the electric field in a coherent state is non-zero with a classical-looking form, as opposed to the vanishing value of a Fock state, this is not *exactly* equal to the classical field. One can instead think of the quantised field as being comprised of two components: the classical field plus a part containing the quantum features, such as the vacuum fluctuation. In conclusion we can declare coherent states to come as close as possible to being classical states of definite complex amplitude. In particular coherent states are especially suited for describing electromagnetic fields generated from so-called coherent sources, lasers being one of them.

The *density operator* was also introduced. This is an invaluable tool when we lack the full information of a quantum system since it provides a statistical description of it instead. The density operator was used in section 3.2 to derive the quantum mechanical degrees of first- and second-order coherence, but the last of $\hat{\rho}$ has not been seen yet: In chapter 5 it is critical in the quantum mechanical description of the laser. But before delving into the properties of the laser the first stop is chapter 4 which investigates how the quantum degrees of first- and second-order coherence differs for light in three different states; the coherent state, the Fock state and the mixed thermal state. The results are used to define some categories pertaining to the statistical properties of the photons. This discussion will show that the mechanism behind the quantum Hanbury Brown-Twiss effect, briefly mentioned in section 3.3, is related to the quantum $g^{(2)}(\tau)$.

Chapter 4

Calculations of the quantum degrees of coherence

The previous chapter introduced the necessary background for investigating the coherence properties of radiation fields. We will now calculate the quantum degrees of first- and second- order coherence for light in three different states, in order of appearance,

- The coherent state
- The Fock state
- The mixed thermal state

For all three, $g^{(1)}(\tau)$ and $g^{(2)}(\tau)$ will be calculated both for single-mode light and for multi-mode light[1].

The quantum Hanbury Brown-Twiss effect was in section 3.3 described as a "clumping" of photons. A more contemporary name is *photon bunching* and a discussion of this and the relation to $g^{(2)}(\tau)$ is covered in section 4.5. There we will also touch upon the photon number statistics of the aforementioned states of light.

4.1   Light in a coherent state

4.1.1   Single-mode photon field

For a single-mode photon field in a coherent state $|\alpha\rangle$ the degree of first-order coherence is

$$g^{(1)}(\tau) = \frac{\langle \hat{a}_{\mathbf{k}}^{\dagger} \hat{a}_{\mathbf{k}} \rangle e^{i\omega_k \tau}}{\langle \hat{a}_{\mathbf{k}}^{\dagger} \hat{a}_{\mathbf{k}} \rangle} = \frac{\langle \alpha | \hat{a}_{\mathbf{k}}^{\dagger} \hat{a}_{\mathbf{k}} | \alpha \rangle \, e^{i\omega_k \tau}}{\langle \alpha | \hat{a}_{\mathbf{k}}^{\dagger} \hat{a}_{\mathbf{k}} | \alpha \rangle} = e^{i\omega_k \tau} \tag{4.1}$$

---

[1] Some textbooks (e.g., [1]) prefer to calculate multi-mode fields as the simpler continuous-mode.

which is a trivial result similar to what was found in the classical case in section 1.3 and it affirms that light in a coherent state is first-degree coherent for all pairs of space-time points.

The degree of second-order coherence is

$$g^{(2)}(\tau) = \frac{\langle \hat{a}_{\mathbf{k}}^\dagger \hat{a}_{\mathbf{k}}^\dagger \hat{a}_{\mathbf{k}} \hat{a}_{\mathbf{k}} \rangle}{\langle \hat{a}_{\mathbf{k}}^\dagger \hat{a}_{\mathbf{k}} \rangle^2} = \frac{\langle \alpha | \hat{a}_{\mathbf{k}}^\dagger \hat{a}_{\mathbf{k}}^\dagger \hat{a}_{\mathbf{k}} \hat{a}_{\mathbf{k}} | \alpha \rangle}{\langle \alpha | \hat{a}_{\mathbf{k}}^\dagger \hat{a}_{\mathbf{k}} | \alpha \rangle^2} = \frac{(\alpha^*)^2 \alpha^2}{(\alpha^* \alpha)^2} = 1. \tag{4.2}$$

Again the result is equal to that for the classical ideal wave Eq. (1.69) and it satisfies the requirement Eq. (1.70) as $|g^{(1)}(\tau)| = g^{(2)}(\tau) = 1$. Thus, single-mode light in a coherent state is second-order coherent. So far we can deduce that in fact the coherent state is the quantum analogue of classical coherent light.

4.1.2   Multi-mode photon field

If the photon field is instead a multi-mode field, the state vector is a product state of the different $\mathbf{k}$ modes

$$|\{\alpha\}\rangle = \prod_{\mathbf{k}} \otimes |\alpha_{\mathbf{k}}\rangle = |\alpha_{\mathbf{k}_1}\rangle \otimes |\alpha_{\mathbf{k}_2}\rangle \otimes \cdots \otimes |n_{\mathbf{k}_\nu}\rangle. \tag{4.3}$$

Here $\{\alpha\}$ denotes the complete set of complex amplitudes that specify the coherent states in each excited mode in the cavity, i.e., each photon present in the radiation field. This gives the degree of first-order coherence as

$$
\begin{aligned}
g^{(1)}(\tau) &= \frac{\sum\limits_{\mathbf{k}_{1,2}} \sqrt{\omega_{k_1}\omega_{k_2}} \langle \hat{a}_{\mathbf{k}_1}^\dagger \hat{a}_{\mathbf{k}_2} \rangle e^{i[(\mathbf{k}_2-\mathbf{k}_1)\cdot\mathbf{r} - (\omega_{k_2}-\omega_{k_1})t]} e^{i\omega_{k_2}\tau}}{\sum\limits_{\mathbf{k}_{1,2}} \sqrt{\omega_{k_1}\omega_{k_2}} \langle \hat{a}_{\mathbf{k}_1}^\dagger \hat{a}_{\mathbf{k}_2} \rangle e^{i[(\mathbf{k}_2-\mathbf{k}_1)\cdot\mathbf{r} - (\omega_{k_2}-\omega_{k_1})t]}} \\[2mm]
&= \frac{\sum\limits_{\mathbf{k}_{1,2}} \sqrt{\omega_{k_1}\omega_{k_2}} \langle \{\alpha\} | \hat{a}_{\mathbf{k}_1}^\dagger \hat{a}_{\mathbf{k}_2} | \{\alpha\} \rangle e^{i[(\mathbf{k}_2-\mathbf{k}_1)\cdot\mathbf{r} - (\omega_{k_2}-\omega_{k_1})t]} e^{i\omega_{k_2}\tau}}{\sum\limits_{\mathbf{k}_{1,2}} \sqrt{\omega_{k_1}\omega_{k_2}} \langle \{\alpha\} | \hat{a}_{\mathbf{k}_1}^\dagger \hat{a}_{\mathbf{k}_2} | \{\alpha\} \rangle e^{i[(\mathbf{k}_2-\mathbf{k}_1)\cdot\mathbf{r} - (\omega_{k_2}-\omega_{k_1})t]}} \\[2mm]
&= \frac{\sum\limits_{\mathbf{k}_{1,2}} \sqrt{\omega_{k_1}\omega_{k_2}} \alpha_{\mathbf{k}_1}^* \alpha_{\mathbf{k}_2} e^{i[(\mathbf{k}_2-\mathbf{k}_1)\cdot\mathbf{r} - (\omega_{k_2}-\omega_{k_1})t]} e^{i\omega_{k_2}\tau}}{\sum\limits_{\mathbf{k}_{1,2}} \sqrt{\omega_{k_1}\omega_{k_2}} \alpha_{\mathbf{k}_1}^* \alpha_{\mathbf{k}_2} e^{i[(\mathbf{k}_2-\mathbf{k}_1)\cdot\mathbf{r} - (\omega_{k_2}-\omega_{k_1})t]}} \\[2mm]
&= \frac{\sum\limits_{\mathbf{k}} \sqrt{\omega_k} \alpha_{\mathbf{k}} e^{i(\mathbf{k}\cdot\mathbf{r}-\omega_k t)} e^{i\omega_k\tau}}{\sum\limits_{\mathbf{k}} \sqrt{\omega_k} \alpha_{\mathbf{k}} e^{i(\mathbf{k}\cdot\mathbf{r}-\omega_k t)}}
\end{aligned} \tag{4.4}
$$

an expression which is identical to the classical $g^{(1)}(\tau)$ for a multi-mode electric field if one identifies the coherent state eigenvalue α with the classical complex field amplitude

a. This is in agreement with the multi-mode coherent state being an eigenstate of the positive frequency part of the electric field operator

$$\hat{E}^{(+)}(\mathbf{r}, t)\,|\{\alpha\}\rangle = \sum_{\mathbf{k}} \left(\frac{\hbar\omega_k}{2\epsilon_0 L^3}\right)^{1/2} \alpha_{\mathbf{k}} e^{i(\mathbf{k}\cdot\mathbf{r}-\omega_k t)}\,|\{\alpha\}\rangle \tag{4.5}$$

The degree of first-order coherence is now a normalised sum of the classical electric field of each mode, modulated by the observation delay τ. Note that $\sum_{\mathbf{k}_{1,2}}$ is a understood to be a multiple sum over different modes, i.e., $\sum_{\mathbf{k}_1\mathbf{k}_2}$. Remember that according to the Wiener-Khinchin theorem $g^{(2)}(\tau)$ is a Fourier pair with the power spectral density of the light (see section 1.3.2). In the case of the single-mode field $S(\omega)$ is the Delta function implying a zero line width of the frequency distribution, as expected. On the other hand, a multi-mode field *should* have a spread in the $\mathbf{k}$-room.

An analogous calculation yields the following expression for $g^{(2)}(\tau)$

$$
\begin{aligned}
g^{(2)}(\tau) &= \frac{\displaystyle\sum_{\mathbf{k}_{1,2,3,4}} \sqrt{\omega_{k_1}\omega_{k_2}\omega_{k_3}\omega_{k_4}} \langle \hat{a}^\dagger_{\mathbf{k}_1} \hat{a}^\dagger_{\mathbf{k}_2} \hat{a}_{\mathbf{k}_3} \hat{a}_{\mathbf{k}_4}\rangle}{\left[\displaystyle\sum_{\mathbf{k}_{1,2}} \sqrt{\omega_{k_1}\omega_{k_2}} \langle \hat{a}^\dagger_{\mathbf{k}_1} \hat{a}_{\mathbf{k}_2}\rangle e^{i[(\mathbf{k}_2-\mathbf{k}_1)\cdot\mathbf{r}-(\omega_{k_2}-\omega_{k_1})t]}\right]^2} \\
&\qquad\times e^{i[(\mathbf{k}_4+\mathbf{k}_3-\mathbf{k}_2-\mathbf{k}_1)\cdot\mathbf{r}-(\omega_{k_4}+\omega_{k_3}-\omega_{k_2}-\omega_{k_1})t]} e^{i(\omega_{k_3}-\omega_{k_2})\tau} \\
&= \frac{\displaystyle\sum_{\mathbf{k}_{1,2,3,4}} \sqrt{\omega_{k_1}\omega_{k_2}\omega_{k_3}\omega_{k_4}}\, \alpha^*_{\mathbf{k}_1} \alpha^*_{\mathbf{k}_2} \alpha_{\mathbf{k}_3} \alpha_{\mathbf{k}_4}}{\left[\displaystyle\sum_{\mathbf{k}_{1,2}} \sqrt{\omega_{k_1}\omega_{k_2}}\, \alpha^*_{\mathbf{k}_1} \alpha_{\mathbf{k}_2} e^{i[(\mathbf{k}_2-\mathbf{k}_1)\cdot\mathbf{r}-(\omega_{k_2}-\omega_{k_1})t]}\right]^2} \\
&\qquad\times e^{i[(\mathbf{k}_4+\mathbf{k}_3-\mathbf{k}_2-\mathbf{k}_1)\cdot\mathbf{r}-(\omega_{k_4}+\omega_{k_3}-\omega_{k_2}-\omega_{k_1})t]} e^{i(\omega_{k_3}-\omega_{k_2})\tau} \\
&= \frac{\displaystyle\sum_{\mathbf{k}_{1,2}} \sqrt{\omega_{k_1}\omega_{k_2}}\, \alpha^*_{\mathbf{k}_1} \alpha_{\mathbf{k}_2} e^{i[(\mathbf{k}_2-\mathbf{k}_1)\cdot\mathbf{r}-(\omega_{k_2}-\omega_{k_1})t]} e^{i(\omega_{k_2}-\omega_{k_1})\tau}}{\displaystyle\sum_{\mathbf{k}_{1,2}} \sqrt{\omega_{k_1}\omega_{k_2}}\, \alpha^*_{\mathbf{k}_1} \alpha_{\mathbf{k}_2} e^{i[(\mathbf{k}_2-\mathbf{k}_1)\cdot\mathbf{r}-(\omega_{k_2}-\omega_{k_1})t]}} \\
&= |g^{(1)}(\tau)|^2 \tag{4.6}
\end{aligned}
$$

Again, this is similar to the classical expression for the degree of second-order coherence of multi-mode light and it is proportional to the degree of first-order coherence. Working with multi-mode light muddies the waters a bit, but we see that this result is on the same form as for single-mode light, since

$$g^{(2)}(\tau)_{\text{single}} = |g^{(1)}(\tau)_{\text{single}}|^2 = 1 \tag{4.7}$$

Without knowing how $|g^{(1)}(\tau)|$ is affected by there being multiple modes, the degree of second-order coherence is still on the same form

$$g^{(2)}(\tau)_{\text{multi}} = |g^{(1)}(\tau)_{\text{multi}}|^2. \tag{4.8}$$

4.2 Light in a Fock state

4.2.1 Single-mode photon field

For a single-mode photon field we find the degree of first-order coherence to be

$$g^{(1)}(\tau) = \frac{\langle \hat{a}_{\mathbf{k}}^\dagger \hat{a}_{\mathbf{k}} \rangle e^{i\omega_k \tau}}{\langle \hat{a}_{\mathbf{k}}^\dagger \hat{a}_{\mathbf{k}} \rangle} = \frac{\langle n | \hat{a}_{\mathbf{k}}^\dagger \hat{a}_{\mathbf{k}} | n \rangle e^{i\omega_k \tau}}{\langle n | \hat{a}_{\mathbf{k}}^\dagger \hat{a}_{\mathbf{k}} | n \rangle} = e^{i\omega_k \tau} \tag{4.9}$$

The above gives the same first-order coherence as for a photon field in a coherent state, leading us to conclude that light in a Fock state is first-order coherent at all pairs of space-time points.

Carrying on, the degree of second-order coherence is

$$g^{(2)}(\tau) = \frac{\langle \hat{a}_{\mathbf{k}}^\dagger \hat{a}_{\mathbf{k}}^\dagger \hat{a}_{\mathbf{k}} \hat{a}_{\mathbf{k}} \rangle}{\langle \hat{a}_{\mathbf{k}}^\dagger \hat{a}_{\mathbf{k}} \rangle^2} = \frac{\langle n_{\mathbf{k}} | \hat{a}_{\mathbf{k}}^\dagger \hat{a}_{\mathbf{k}}^\dagger \hat{a}_{\mathbf{k}} \hat{a}_{\mathbf{k}} | n_{\mathbf{k}} \rangle}{\langle n_{\mathbf{k}} | \hat{a}_{\mathbf{k}}^\dagger \hat{a}_{\mathbf{k}} | n_{\mathbf{k}} \rangle^2} = \frac{\langle n_{\mathbf{k}}^2 \rangle + n_{\mathbf{k}}}{n_{\mathbf{k}}^2} \tag{4.10}$$

where the mean photon number is $\langle n_{\mathbf{k}} \rangle \equiv n_{\mathbf{k}}$. We define the variance in the photon number $n_{\mathbf{k}}$ as

$$(\Delta n_{\mathbf{k}})^2 = \langle n_{\mathbf{k}}^2 \rangle - \langle n_{\mathbf{k}} \rangle^2, \tag{4.11}$$

But the Fock state is the eigenstate of the number operator where the eigenvalue is the mean number of photons in mode $\mathbf{k}$. So the expectation value of the photon number has no uncertainty in it, and therefore there is no variance in the photon number, $\Delta n_{\mathbf{k}} = 0$,

$$g^{(2)}(\tau) = 1 + \frac{(\Delta n_{\mathbf{k}})^2}{n_{\mathbf{k}}^2} - \frac{1}{n_{\mathbf{k}}} = \begin{cases} 1 - \dfrac{1}{n_{\mathbf{k}}} & \text{for} \quad n_{\mathbf{k}} \geq 1 \\ 0 & \text{for} \quad n_{\mathbf{k}} < 1 \end{cases} \tag{4.12}$$

which is in agreement with Eq. (3.34). But, since we cannot show that $g^{(2)}(\tau) > 1$ like we can for the classical degree of second order coherence, so there will be an interval where

$$0 \leq g^{(2)}(\tau) \leq 1 \tag{4.13}$$

which is non-classical in the sense that there are no equivalent classical field with such a value of the second-order coherence. Although $g^{(2)}(\tau)$ does not strictly depend on τ we will stick to this notation for cohesion with the instances where the time-dependency does exist.

Looking back at Eq. (4.9) it could be a little puzzling that what we call the quantum analogue of classical light has the same $g^{(1)}(\tau)$ as the light we just concluded must be entirely non-classical. We will soon see that light in a mixed thermal state also has the same $g^{(1)}(\tau)$ for single-mode light. This is the reason it has been claimed that it is $g^{(2)}(\tau)$ that can distinguish between the nature of different types of light. In fact, any single-mode light will be first-order coherent.

4.2.2 Multi-mode photon field

As with the coherent product state we use a short notation for a multi-mode Fock-state

$$|\{n\}\rangle = \prod_{\mathbf{k}} \otimes |n_{\mathbf{k}}\rangle = |n_{\mathbf{k}_1}\rangle \otimes |n_{\mathbf{k}_2}\rangle \otimes \cdots \otimes |n_{\mathbf{k}_\nu}\rangle . \tag{4.14}$$

where there is no correlation between the different modes $\mathbf{k}_i$, $(i = 1, 2, \ldots, \nu)$. In this setting the meaning of "uncorrelated" relates to the lack of entanglement between photon states of different modes, where entanglement is a purely quantum mechanical phenomenon.

The orthonormality of the number states ensures that the expectation value of an operator consisting of $\hat{a}^\dagger$ and $\hat{a}$ is zero, unless they appear in equal number of the same mode $\mathbf{k}_i$,

$$\sum_{\mathbf{k}_{1,2}} \langle \hat{a}^\dagger_{\mathbf{k}_1} \hat{a}_{\mathbf{k}_2} \rangle = \sum_{\mathbf{k}_{1,2}} \langle n_{\mathbf{k}_1}| \langle n_{\mathbf{k}_2}| \hat{a}^\dagger_{\mathbf{k}_1} \hat{a}_{\mathbf{k}_2} |n_{\mathbf{k}_1}\rangle |n_{\mathbf{k}_2}\rangle$$

$$= \begin{cases} \displaystyle\sum_{\mathbf{k}_{1,2}} \langle \hat{a}^\dagger_{\mathbf{k}_1} \rangle \langle \hat{a}_{\mathbf{k}_2} \rangle = 0 & \text{for uncorrelated modes} \\[2em] \displaystyle\sum_{\mathbf{k}} \langle \hat{a}^\dagger_{\mathbf{k}} \hat{a}_{\mathbf{k}} \rangle = \sum_{\mathbf{k}} n_{\mathbf{k}} & \text{for correlated modes } \mathbf{k}_1 = \mathbf{k}_2 \end{cases} \tag{4.15}$$

Then $g^{(1)}(\tau)$ is

$$g^{(1)}(\tau) = \frac{\displaystyle\sum_{\mathbf{k}_{1,2}} \langle \hat{a}^\dagger_{\mathbf{k}_1} \hat{a}_{\mathbf{k}_2} \rangle \sqrt{\omega_{k_1}\omega_{k_2}} e^{i[(\mathbf{k}_2-\mathbf{k}_1)\cdot\mathbf{r}-(\omega_{k_2}-\omega_{k_1})t]} e^{i\omega_{k_2}\tau}}{\displaystyle\sum_{\mathbf{k}_{1,2}} \langle \hat{a}^\dagger_{\mathbf{k}_1} \hat{a}_{\mathbf{k}_2} \rangle \sqrt{\omega_{k_1}\omega_{k_2}} e^{i[(\mathbf{k}_2-\mathbf{k}_1)\cdot\mathbf{r}-(\omega_{k_2}-\omega_{k_1})t]}}$$

$$= \frac{\displaystyle\sum_{\mathbf{k}_{1,2}} \langle \{n\}| \hat{a}^\dagger_{\mathbf{k}_1} \hat{a}_{\mathbf{k}_2} |\{n\}\rangle \sqrt{\omega_{k_1}\omega_{k_2}} e^{i[(\mathbf{k}_2-\mathbf{k}_1)\cdot\mathbf{r}-(\omega_{k_2}-\omega_{k_1})t]} e^{i\omega_{k_2}\tau}}{\displaystyle\sum_{\mathbf{k}_{1,2}} \langle \{n_{\mathbf{k}}\}| \hat{a}^\dagger_{\mathbf{k}_1} \hat{a}_{\mathbf{k}_2} |\{n_{\mathbf{k}}\}\rangle \sqrt{\omega_{k_1}\omega_{k_2}} e^{i[(\mathbf{k}_2-\mathbf{k}_1)\cdot\mathbf{r}-(\omega_{k_2}-\omega_{k_1})t]}}$$

$$= \frac{\displaystyle\sum_{\mathbf{k}} n_{\mathbf{k}}\omega_k e^{i\omega_k\tau}}{\displaystyle\sum_{\mathbf{k}} n_{\mathbf{k}}\omega_k} \tag{4.16}$$

since $\langle \{n\}| \hat{a}^\dagger_{\mathbf{k}_1} \hat{a}_{\mathbf{k}_2} |\{n\}\rangle = \delta_{\mathbf{k}_1,\mathbf{k}_2}$. As expected the degree of first-order coherence now reflects the presence of many modes in the light[2].

---

[2] A possible way to proceed could be to assume that the light is emitted in wave-packet of a Gaussian form, like in [1]. This would yield a $g^{(2)}(\tau)$ that is identical to that of the single-mode field.

An analogous calculation yields the following expression for the degree of second-order coherence

$$g^{(2)}(\tau) = \frac{\displaystyle\sum_{\mathbf{k}_{1,2,3,4}} \langle \hat{a}_{\mathbf{k}_1}^\dagger \hat{a}_{\mathbf{k}_2}^\dagger \hat{a}_{\mathbf{k}_3} \hat{a}_{\mathbf{k}_4} \rangle \sqrt{\omega_{k_1}\omega_{k_2}\omega_{k_1 3}\omega_{k_4}}}{\left[\displaystyle\sum_{\mathbf{k}_{1,2}} \langle \hat{a}_{\mathbf{k}_1}^\dagger \hat{a}_{\mathbf{k}_2} \rangle e^{i[(\mathbf{k}_2-\mathbf{k}_1)\cdot\mathbf{r}-(\omega_{k_2}-\omega_{k_1})t]} \right]^2}$$
$$\times\, e^{i[(\mathbf{k}_4+\mathbf{k}_3-\mathbf{k}_2-\mathbf{k}_1)\cdot\mathbf{r}-(\omega_{k_4}+\omega_{k_3}-\omega_{k_2}-\omega_{k_1})t]} e^{i(\omega_{k_3}-\omega_{k_2})\tau}$$

Before we proceed we observe that the modes $\mathbf{k}_{1,2,3,4}$ can come in the following combinations

$$1 \neq 2 \neq 3 \neq 4 \;\rightarrow\; \langle \hat{a}_{\mathbf{k}_1}^\dagger \hat{a}_{\mathbf{k}_2}^\dagger \hat{a}_{\mathbf{k}_3} \hat{a}_{\mathbf{k}_4} \rangle e^{i(\omega_{k_3}-\omega_{k_2})\tau} = 0$$
$$1 = 2 \neq 3 = 4 \;\rightarrow\; \langle \hat{a}_{\mathbf{k}_1}^\dagger \hat{a}_{\mathbf{k}_1}^\dagger \hat{a}_{\mathbf{k}_3} \hat{a}_{\mathbf{k}_3} \rangle e^{i(\omega_{k_3}-\omega_{k_1})\tau} = 0$$
$$1 = 3 \neq 2 = 4 \;\rightarrow\; \langle \hat{a}_{\mathbf{k}_1}^\dagger \hat{a}_{\mathbf{k}_2}^\dagger \hat{a}_{\mathbf{k}_1} \hat{a}_{\mathbf{k}_2} \rangle e^{i(\omega_{k_1}-\omega_{k_2})\tau} = n_{\mathbf{k}_1} n_{\mathbf{k}_2} e^{i(\omega_{k_1}-\omega_{k_2})\tau}$$
$$1 = 4 \neq 2 = 3 \;\rightarrow\; \langle \hat{a}_{\mathbf{k}_1}^\dagger \hat{a}_{\mathbf{k}_2}^\dagger \hat{a}_{\mathbf{k}_2} \hat{a}_{\mathbf{k}_1} \rangle e^{i(\omega_{k_2}-\omega_{k_2})\tau} = n_{\mathbf{k}_1} n_{\mathbf{k}_2}$$
$$1 = 2 = 3 = 4 \;\rightarrow\; \langle \hat{a}_{\mathbf{k}}^\dagger \hat{a}_{\mathbf{k}}^\dagger \hat{a}_{\mathbf{k}} \hat{a}_{\mathbf{k}} \rangle e^{i(\omega_k-\omega_k)\tau} = n_{\mathbf{k}}(n_{\mathbf{k}} - 1)$$

Continuing with $g^{(2)}(\tau)$ we have

$$g^{(2)}(\tau) = \frac{\displaystyle\sum_{\mathbf{k}_{1,2}} n_{\mathbf{k}_1} n_{\mathbf{k}_2} \omega_{k_1}\omega_{k_2} e^{i(\omega_{k_1}-\omega_{k_2})\tau} - \sum_{\mathbf{k}} n_{\mathbf{k}} \omega_{k_1}^2}{\displaystyle\sum_{\mathbf{k}_{1,2}} n_{\mathbf{k}_1} n_{\mathbf{k}_2} \omega_{k_1}\omega_{k_2}}$$
$$= |g^{(1)}(\tau)|^2 - \frac{\sum_{\mathbf{k}} n_{\mathbf{k}} \omega_k^2}{\left[\sum_{\mathbf{k}} n_{\mathbf{k}} \omega_k\right]^2} \tag{4.17}$$

This is on a similar form as that for single-mode

$$g^{(2)}(\tau)_{\text{single}} = 1 - \frac{1}{n_{\mathbf{k}}}$$

with

$$g^{(2)}(\tau)_{\text{multi}} = 1 - \frac{1}{n} \tag{4.18}$$

if n is the weighted number of photons of all the populated modes. Consistent with the single-mode result, the degree of second-order coherence is less than the lowest classical limit of $g^{(2)}(\tau)_{\text{cl}} \geq 1$, and thus in the non-classical range $[0,1]$. So even if coherent states and Fock states exhibit the same first-order coherence, they will differ rather dramatically in $g^{(2)}(\tau)$.

4.3 Light in a mixed thermal state

Thermal light is the electromagnetic radiation emitted by a hot body, also called black-body radiation. The properties of thermal light is most often understood by applying the

laws of statistical mechanics to radiation within a cavity at a temperature T. This serves as a heat bath and when the system is in equilibrium, the probability that there will be n photons in some harmonic oscillator mode $\mathbf{k}$ is given by the Boltzmann distribution

$$P(n) = \frac{1}{\mathcal{Z}} e^{-E_n/k_B T} \tag{4.19}$$

where k_B is the Boltzmann constant, $E_n = n\hbar\omega_k$ the energy of the mode and $\mathcal{Z}$ is the partition function

$$\mathcal{Z} = \sum_{n=0}^{\infty} e^{-E_n/k_B T} = \sum_{n=0}^{\infty} e^{-n\hbar\omega_k/k_B T} = \sum_{n=0}^{\infty} \left[e^{-\hbar\omega_k/k_B T} \right]^n$$
$$= \left[1 - e^{-\hbar\omega_k/k_B T} \right]^{-1}.$$

This gives

$$P(n) = \left[1 - e^{-\hbar\omega_k/k_B T} \right] e^{-E_n/k_B T}. \tag{4.20}$$

4.3.1 Single-mode photon field

It is often the case that we do not have enough information to specify completely the state of the system, but can only describe it through the system density operator. A thermal state is such a mixed state, where all we only know is the mean energy of the system in thermodynamic equilibrium with its environment. The density operator for a single-mode field in a mixed thermal state is defined as

$$\hat{\rho} = P(\hat{n}) = \left[1 - e^{-\hbar\omega_k/k_B T} \right] e^{-\hat{H}/k_B T}$$
$$= \left[1 - e^{-\beta_k} \right] e^{-\beta_k \hat{a}_{\mathbf{k}}^\dagger \hat{a}_{\mathbf{k}}}$$
$$= \left[1 - e^{-\beta_k} \right] e^{-\beta_k n_{\mathbf{k}}} |n_{\mathbf{k}}\rangle \langle n_{\mathbf{k}}| \tag{4.21}$$

where $\hat{H} = \hbar\omega_k \hat{a}_{\mathbf{k}}^\dagger \hat{a}_{\mathbf{k}}$ is the Hamiltonian operator for the quantum harmonic oscillator. Only one mode $\mathbf{k}$ is occupied in a single-mode photon field, leaving the other k-rooms with a zero eigenvalue. For brevity in the forthcoming calculations we introduce the dimensionless quantity

$$\beta_k = \frac{\hbar\omega_k}{k_B T}. \tag{4.22}$$

The previous two cases were pure states and so the "squeezing" to find the expectation value was pretty straight forward. Now however it is easier to switch to taking the trace over the density operator $\langle \hat{A} \rangle = \mathrm{tr}(\hat{\rho}\hat{A})$, as derived in Eq. (3.22).

As we might guess by now, the degree of first-order coherence is, as usual,

$$g^{(1)}(\tau) = \frac{\langle \hat{a}_{\mathbf{k}}^\dagger \hat{a}_{\mathbf{k}} \rangle e^{i\omega_k \tau}}{\langle \hat{a}_{\mathbf{k}}^\dagger \hat{a}_{\mathbf{k}} \rangle} = \frac{\mathrm{tr}(\hat{\rho}_{\mathbf{k}} \hat{a}_{\mathbf{k}}^\dagger \hat{a}_{\mathbf{k}}) e^{i\omega_k \tau}}{\mathrm{tr}(\hat{\rho}_{\mathbf{k}} \hat{a}_{\mathbf{k}}^\dagger \hat{a}_{\mathbf{k}})} = e^{i\omega_k \tau} \tag{4.23}$$

in accordance with what we have seen for a classical electric field and light in coherent and Fock-states. The common denominator in these examples is that we consider only single-mode light. Ergo single-mode photon fields are always first-order coherent regardless of its quantum state.

Before we proceed, a trick is used to find the expected photon number of mode $\mathbf{k}$, involving the commutator of the ladder operators, the Lie formula Eq. (B.15) and the cyclic symmetric property of the trace,

$$
\begin{aligned}
\langle n_{\mathbf{k}} \rangle &= \mathrm{tr}\left(e^{-\beta_k \hat{a}_{\mathbf{k}}^\dagger \hat{a}_{\mathbf{k}}} \hat{a}_{\mathbf{k}}^\dagger \hat{a}_{\mathbf{k}} \right) \\
&= \mathrm{tr}\left(e^{-\beta_k \hat{a}_{\mathbf{k}}^\dagger \hat{a}_{\mathbf{k}}} \hat{a}_{\mathbf{k}}^\dagger e^{\beta_k \hat{a}_{\mathbf{k}}^\dagger \hat{a}_{\mathbf{k}}} e^{-\beta_k \hat{a}_{\mathbf{k}}^\dagger \hat{a}_{\mathbf{k}}} \hat{a}_{\mathbf{k}} \right) \\
&= \mathrm{tr}\left([1 - \beta_k - (\beta_k)^2 \frac{1}{2!} - \ldots] \hat{a}_{\mathbf{k}}^\dagger e^{-\beta_k \hat{a}_{\mathbf{k}}^\dagger \hat{a}_{\mathbf{k}}} \hat{a}_{\mathbf{k}} \right) \\
&= e^{-\beta_k} \, \mathrm{tr}\left(e^{-\beta_k \hat{a}_{\mathbf{k}}^\dagger \hat{a}_{\mathbf{k}}} \hat{a}_{\mathbf{k}} \hat{a}_{\mathbf{k}}^\dagger \right) \\
&= e^{-\beta_k} \left[\mathrm{tr}\left(e^{-\beta_k \hat{a}_{\mathbf{k}}^\dagger \hat{a}_{\mathbf{k}}} \hat{a}_{\mathbf{k}}^\dagger \hat{a}_{\mathbf{k}} \right) + \mathrm{tr}\left(e^{-\beta_k \hat{a}_{\mathbf{k}}^\dagger \hat{a}_{\mathbf{k}}} \right) \right] \\
&= e^{-\beta_k} [\langle n_{\mathbf{k}} \rangle + 1]
\end{aligned}
$$

which can be rearranged to give

$$
n_{\mathbf{k}} = \langle n_{\mathbf{k}} \rangle = \frac{1}{e^{\beta_k} - 1}. \tag{4.24}
$$

This is the Bose-Einstein mean photon number and it implies that photons at thermal equilibrium obey Bose-Einstein statistics and that the mean photon number in mode $\mathbf{k}$ is directly dependent on the temperature of the system.

The degree of second-order coherence is

$$
\begin{aligned}
g^{(2)}(\tau) &= \frac{\langle \hat{a}_{\mathbf{k}}^\dagger \hat{a}_{\mathbf{k}}^\dagger \hat{a}_{\mathbf{k}} \hat{a}_{\mathbf{k}} \rangle}{\langle \hat{a}_{\mathbf{k}}^\dagger \hat{a}_{\mathbf{k}} \rangle^2} = \frac{\mathrm{tr}\left(e^{-\beta_k \hat{a}_{\mathbf{k}}^\dagger \hat{a}_{\mathbf{k}}} \hat{a}_{\mathbf{k}}^\dagger \hat{a}_{\mathbf{k}}^\dagger \hat{a}_{\mathbf{k}} \hat{a}_{\mathbf{k}} \right)}{\left[\mathrm{tr}\left(e^{-\beta_k \hat{a}_{\mathbf{k}}^\dagger \hat{a}_{\mathbf{k}}} \hat{a}_{\mathbf{k}}^\dagger \hat{a}_{\mathbf{k}} \right) \right]^2} \\
&= \frac{e^{-\beta \hbar \omega_k} \, \mathrm{tr}\left(e^{-\beta_k \hat{a}_{\mathbf{k}}^\dagger \hat{a}_{\mathbf{k}}} \hat{a}_{\mathbf{k}}^\dagger \hat{a}_{\mathbf{k}} \hat{a}_{\mathbf{k}} \hat{a}_{\mathbf{k}}^\dagger \right)}{n_{\mathbf{k}}^2}
\end{aligned} \tag{4.25}
$$

To calculate the numerator we start by observing that

$$
\hat{a}_{\mathbf{k}}^\dagger \hat{a}_{\mathbf{k}} \hat{a}_{\mathbf{k}} \hat{a}_{\mathbf{k}}^\dagger = 2\hat{a}_{\mathbf{k}}^\dagger \hat{a}_{\mathbf{k}} + \hat{a}_{\mathbf{k}}^\dagger \hat{a}_{\mathbf{k}}^\dagger \hat{a}_{\mathbf{k}} \hat{a}_{\mathbf{k}}
$$

which is inserted into $g^{(2)}(\tau)$ to give

$$
g^{(2)}(\tau) = \frac{e^{-\beta_k} \left[2 \, \mathrm{tr}\left(e^{-\beta_k \hat{a}_{\mathbf{k}}^\dagger \hat{a}_{\mathbf{k}}} \hat{a}_{\mathbf{k}}^\dagger \hat{a}_{\mathbf{k}} \right) + \mathrm{tr}\left(e^{-\beta_k \hat{a}_{\mathbf{k}}^\dagger \hat{a}_{\mathbf{k}}} \hat{a}_{\mathbf{k}}^\dagger \hat{a}_{\mathbf{k}}^\dagger \hat{a}_{\mathbf{k}} \hat{a}_{\mathbf{k}} \right) \right]}{n_{\mathbf{k}}^2} \tag{4.26}
$$

By comparing Eq. (4.25) and Eq. (4.26) it is evident that

$$
\begin{aligned}
\text{tr}\,(e^{-\beta_k \hat{a}_\mathbf{k}^\dagger \hat{a}_\mathbf{k}} \hat{a}_\mathbf{k}^\dagger \hat{a}_\mathbf{k}^\dagger \hat{a}_\mathbf{k} \hat{a}_\mathbf{k}) &= e^{-\beta_k} \big[2\,\text{tr}\,(e^{-\beta_k \hat{a}_\mathbf{k}^\dagger \hat{a}_\mathbf{k}} \hat{a}_\mathbf{k}^\dagger \hat{a}_\mathbf{k}) \\
&\qquad + \text{tr}\,(e^{-\beta_k \hat{a}_\mathbf{k}^\dagger \hat{a}_\mathbf{k}} \hat{a}_\mathbf{k}^\dagger \hat{a}_\mathbf{k}^\dagger \hat{a}_\mathbf{k} \hat{a}_\mathbf{k}) \big] \\
&\Downarrow \\
\text{tr}\,(e^{-\beta_k \hat{a}_\mathbf{k}^\dagger \hat{a}_\mathbf{k}} \hat{a}_\mathbf{k}^\dagger \hat{a}_\mathbf{k}^\dagger \hat{a}_\mathbf{k} \hat{a}_\mathbf{k}) &= \frac{2\,\text{tr}\,(e^{-\beta_k \hat{a}_\mathbf{k}^\dagger \hat{a}_\mathbf{k}} \hat{a}_\mathbf{k}^\dagger \hat{a}_\mathbf{k})}{e^{\beta_k} - 1} \\
&= 2 e^{-\beta_k} n_\mathbf{k}{}^2.
\end{aligned}
$$

This can be inserted into Eq. (4.25), yielding

$$
g^{(2)}(\tau) = \frac{2 e^{-\beta_k} n_\mathbf{k}{}^2}{n_\mathbf{k}{}^2} = 2 e^{-\hbar\omega_k/k_B T}. \tag{4.27}
$$

Although $g^{(2)}(\tau)$ is not a function of τ, the classical inequality

$$
g^{(2)}(\tau) \le g^{(2)}(0), \tag{1.67}
$$

is still satisfied. Instead the degree of second-order coherence is a function of the temperature of the radiation source. For a hot source, as $T \to \infty$, source the light is second-order *in*coherent with $g^{(2)}(\tau) \to 2$. Lowering the temperature also lowers $g^{(2)}(\tau)$ until $g^{(2)}(\tau) = 1$ which happens at $\hbar\omega_k/k_B T = \ln 2$. A rough estimate at the visible wavelength $\lambda = 540$ nm puts this limit at

$$
T = \frac{2\pi\hbar c}{k_B \lambda \ln 2} \approx 10^4 K. \tag{4.28}
$$

A very cool source, as $T \to 0$, will exhibit non-classical properties as $g^{(2)}(\tau) \to 0$. At this temperature there are very few photons per mode, $n_\mathbf{k} \to 0$, as can be seen from Eq. (4.24). This is consistent with the thought that the classical limit is where there are *many* photons in each field mode.

4.3.2 Multi-mode photon field

For a multi-mode field the density operator is a product of the reduced density operator of each mode, i.e.,

$$
\begin{aligned}
\hat{\rho} &= \prod_\mathbf{k} \hat{\rho}_\mathbf{k} = \prod_\mathbf{k} \big[1 - e^{-\beta_k} \big] e^{-\beta_k \hat{a}_\mathbf{k}^\dagger \hat{a}_\mathbf{k}} \\
&= \prod_\mathbf{k} \sum_{n_\mathbf{k}} \big[1 - e^{-\beta_k} \big] e^{-\beta_k n_\mathbf{k}} |n_\mathbf{k}\rangle \langle n_\mathbf{k}|
\end{aligned} \tag{4.29}
$$

Then the degree of first-order coherence is

$$
g^{(1)}(\tau) = \frac{\displaystyle\sum_{\mathbf{k}_{1,2}} \langle \hat{a}_{\mathbf{k}_1}^\dagger \hat{a}_{\mathbf{k}_2}\rangle \sqrt{\omega_{k_1}\omega_{k_2}}\, e^{i[(\mathbf{k}_2-\mathbf{k}_1)\cdot\mathbf{r}-(\omega_{k_2}-\omega_{k_1})t]} e^{i\omega_{k_2}\tau}}{\displaystyle\sum_{\mathbf{k}_{1,2}} \langle \hat{a}_{\mathbf{k}_1}^\dagger \hat{a}_{\mathbf{k}_2}\rangle \sqrt{\omega_{k_1}\omega_{k_2}}\, e^{i[(\mathbf{k}_2-\mathbf{k}_1)\cdot\mathbf{r}-(\omega_{k_2}-\omega_{k_1})t]}}
$$

$$
= \frac{\displaystyle\sum_{\mathbf{k}_{1,2}}\prod_{\mathbf{k}}\sum_{n_{\mathbf{k}}} \mathrm{tr}\left(e^{-\beta_k n_{\mathbf{k}}}\,|n_{\mathbf{k}}\rangle\langle n_{\mathbf{k}}|\,\hat{a}_{\mathbf{k}_1}^\dagger \hat{a}_{\mathbf{k}_2}\right)\sqrt{\omega_{k_1}\omega_{k_2}}\, e^{i[(\mathbf{k}_2-\mathbf{k}_1)\cdot\mathbf{r}-(\omega_{k_2}-\omega_{k_1})t]} e^{i\omega_{k_2}\tau}}{\displaystyle\sum_{\mathbf{k}_{1,2}}\prod_{\mathbf{k}}\sum_{n_{\mathbf{k}}} \mathrm{tr}\left(e^{-\beta_k n_{\mathbf{k}}}\,|n_{\mathbf{k}}\rangle\langle n_{\mathbf{k}}|\,\hat{a}_{\mathbf{k}_1}^\dagger \hat{a}_{\mathbf{k}_2}\right)\sqrt{\omega_{k_1}\omega_{k_2}}\, e^{i[(\mathbf{k}_2-\mathbf{k}_1)\cdot\mathbf{r}-(\omega_{k_2}-\omega_{k_1})t]}}
$$

$$
= \frac{\displaystyle\prod_{\mathbf{k}}\sum_{n_{\mathbf{k}}} e^{-\beta_k n_{\mathbf{k}}}\sum_{\mathbf{k}_{1,2}}\sqrt{n_{\mathbf{k}_1} n_{\mathbf{k}_2}}\sqrt{\omega_{k_1}\omega_{k_2}}\,\delta_{\mathbf{k}_1\mathbf{k}_2}\, e^{i[(\mathbf{k}_2-\mathbf{k}_1)\cdot\mathbf{r}-(\omega_{k_2}-\omega_{k_1})t]} e^{i\omega_{k_2}\tau}}{\displaystyle\prod_{\mathbf{k}}\sum_{n_{\mathbf{k}}} e^{-\beta_k n_{\mathbf{k}}}\sum_{\mathbf{k}_{1,2}}\sqrt{n_{\mathbf{k}_1} n_{\mathbf{k}_2}}\sqrt{\omega_{k_1}\omega_{k_2}}\,\delta_{\mathbf{k}_1\mathbf{k}_2}\, e^{i[(\mathbf{k}_2-\mathbf{k}_1)\cdot\mathbf{r}-(\omega_{k_2}-\omega_{k_1})t]}}
$$

$$
= \frac{\displaystyle\sum_{\mathbf{k}} n_{\mathbf{k}}\omega_k e^{i\omega_k\tau}}{\displaystyle\sum_{\mathbf{k}} n_{\mathbf{k}}\omega_k} \tag{4.30}
$$

where we have used the relation $\mathrm{tr}\left(|\{n\}\rangle\langle\{n\}|\right) = \langle\{n\}|\{n\}\rangle = 1$. On the surface this is the same result as for photon field in coherent states and Fock-states. But now the mean photon number $n_{\mathbf{k}}$ is the Bose-Einstein distribution, meaning that it is possible to solve $g^{(1)}(\tau)$ and see the connection between the coherence time of the radiation field and the temperature of the system. The explicit calculation can be performed by inserting Eq. (4.24) into $g^{(1)}(\tau)$ and by converting the discrete photon modes into continuous ones. For starters, the summation over different $\mathbf{k}$ is converted to an integral over the angular frequency, $\omega_k = |\mathbf{k}|c$, by

$$
\sum_{\mathbf{k}} \to 2\frac{V}{(2\pi)^3}\int \mathrm{d}^3\mathbf{k} = \frac{V}{4\pi^3 c^3}\iint \omega_k^2\,\mathrm{d}\omega_k\mathrm{d}\Omega. \tag{4.31}
$$

The extra factor 2 is due to the wave vector being allowed two polarizations per $\mathbf{k}$ and Ω is the solid angle. The angular frequency does not have any directional dependencies, so we get

$$
\sum_{\mathbf{k}} \to \frac{V}{\pi^2 c^3}\int_0^\infty \omega_k^2\mathrm{d}\omega_k. \tag{4.32}
$$

The agenda now is to take a closer look at the degree of first-order coherence and find out how the coherence time τ varies according to the absolute temperature T. Replacing the sums with integrals

$$
g^{(1)}(\tau) \to \frac{\int_0^\infty \omega_k^3 n_{\mathbf{k}} e^{i\omega_k\tau}\mathrm{d}\omega_k}{\int_0^\infty \omega_k^3 n_{\mathbf{k}}\mathrm{d}\omega_k} \quad = \frac{\int_0^\infty \omega_k^3 (e^{\hbar\omega_k/k_B T}-1)^{-1} e^{i\omega_k\tau}\mathrm{d}\omega_k}{\int_0^\infty \omega_k^3 (e^{\hbar\omega_k/k_B T}-1)^{-1}\mathrm{d}\omega_k} \tag{4.33}
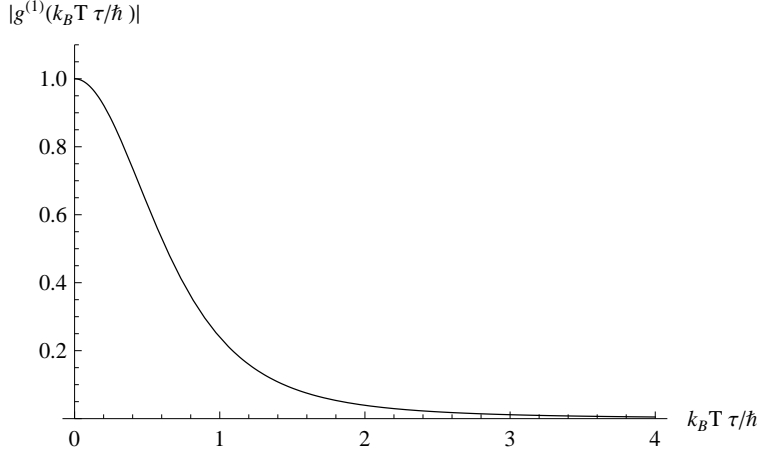$$

Figure 4.1: The coherence as a function of the coherence time and temperature, $\tau_c T$, of multi-mode thermal light.

Wolfram's Mathematica evaluates $g^{(2)}(\tau)$ for us,[3]

$$g^{(1)}(\tau) = \frac{6\zeta(4, 1 - ik_B T\tau/\hbar)}{\pi^4/15} \tag{4.34}$$

With the solution of the degree of the first-order coherence we see light in a multi-mode mixed thermal state is only first-order coherent small temperatures. This is shown in Fig. 4.1 where $|g^{(1)}(\tau)|$ is plotted as a function of $k_B T\tau/\hbar$. It is not surprising that for thermal light the governing variable is the temperature T.

Proceeding with the degree of second-order coherence, which is calculated as follows

$$g^{(2)}(\tau) = \frac{\displaystyle\sum_{\mathbf{k}_{1,2,3,4}} \langle \hat{a}^\dagger_{\mathbf{k}_1} \hat{a}^\dagger_{\mathbf{k}_2} \hat{a}_{\mathbf{k}_3} \hat{a}_{\mathbf{k}_4} \rangle \sqrt{\omega_{k_1}\omega_{k_2}\omega_{k_3}\omega_{k_4}}}{\left[\displaystyle\sum_{\mathbf{k}_{1,2}} \langle \hat{a}^\dagger_{\mathbf{k}_1} \hat{a}_{\mathbf{k}_2} \rangle \sqrt{\omega_{k_1}\omega_{k_2}} e^{i[(\mathbf{k}_2-\mathbf{k}_1)\cdot\mathbf{r} - (\omega_{k_2}-\omega_{k_1})t]} \right]^2}$$
$$\times\, e^{i[(\mathbf{k}_4+\mathbf{k}_3-\mathbf{k}_2-\mathbf{k}_1)\cdot\mathbf{r} - (\omega_{k_4}+\omega_{k_3}-\omega_{k_2}-\omega_{k_1})t]} e^{i(\omega_{k_3}-\omega_{k_2})\tau}$$

$$= \frac{\displaystyle\sum_{\mathbf{k}_{1,2,3,4}} \prod_{\mathbf{k}} \sum_{n_{\mathbf{k}}} \mathrm{tr}\left(e^{-\beta_k n_{\mathbf{k}}} |n_{\mathbf{k}}\rangle \langle n_{\mathbf{k}}| \hat{a}^\dagger_{\mathbf{k}_1} \hat{a}^\dagger_{\mathbf{k}_2} \hat{a}_{\mathbf{k}_3} \hat{a}_{\mathbf{k}_4} \right) \sqrt{\omega_{k_1}\omega_{k_2}\omega_{k_3}\omega_{k_4}}}{\left[\displaystyle\sum_{\mathbf{k}_{1,2}} \prod_{\mathbf{k}} \sum_{n_{\mathbf{k}}} \mathrm{tr}\left(e^{-\beta_k n_{\mathbf{k}}} |n_{\mathbf{k}}\rangle \langle n_{\mathbf{k}}| \hat{a}^\dagger_{\mathbf{k}_1} \hat{a}_{\mathbf{k}_2} \right) \sqrt{\omega_{k_1}\omega_{k_2}} e^{i[(\mathbf{k}_2-\mathbf{k}_1)\cdot\mathbf{r} - (\omega_{k_2}-\omega_{k_1})t]} \right]^2}$$
$$\times\, e^{i[(\mathbf{k}_4+\mathbf{k}_3-\mathbf{k}_2-\mathbf{k}_1)\cdot\mathbf{r} - (\omega_{k_4}+\omega_{k_3}-\omega_{k_2}-\omega_{k_1})t]} e^{i(\omega_{k_3}-\omega_{k_2})\tau}$$

---

[3] where $\zeta()$ is the generalised Riemann zeta function

$$\zeta(a, s) = \sum_{k=0}^{\infty} (k+a)^{-s}.$$

or

$$g^{(2)}(\tau) = \frac{\prod_{\mathbf{k}} \sum_{n_{\mathbf{k}}} e^{-\beta_k n_{\mathbf{k}}} \sum_{\mathbf{k}_{1,2}} n_{\mathbf{k}_1} n_{\mathbf{k}_2} \omega_{k_1} \omega_{k_2} [1 + e^{i(\omega_{k_1} - \omega_{k_2})\tau}]}{\left[\prod_{\mathbf{k}} \sum_{n_{\mathbf{k}}} e^{-\beta_k n_{\mathbf{k}}} \right]^2 \sum_{\mathbf{k}_{1,2}} n_{\mathbf{k}_1} n_{\mathbf{k}_2} \omega_{k_1} \omega_{k_2}}$$

$$= \left[\prod_{\mathbf{k}} \sum_{n_{\mathbf{k}}} e^{-\beta_k n_{\mathbf{k}}} \right]^{-1} \frac{\sum_{\mathbf{k}_{1,2}} n_{\mathbf{k}_1} n_{\mathbf{k}_2} \omega_{k_1} \omega_{k_2} [1 + e^{i(\omega_{k_1} - \omega_{k_2})\tau}]}{\sum_{\mathbf{k}_{1,2}} n_{\mathbf{k}_1} n_{\mathbf{k}_2} \omega_{k_1} \omega_{k_2}}$$

$$= \left[\prod_{\mathbf{k}} \sum_{n_{\mathbf{k}}} e^{-\beta_k n_{\mathbf{k}}} \right]^{-1} \left[1 + |g^{(1)}(\tau)|^2 \right]$$

$$= \prod_{\mathbf{k}} \left[1 - e^{-\beta_k} \right] \left[1 + |g^{(1)}(\tau)|^2 \right] \tag{4.35}$$

This expression agrees with that for classical chaotic light Eq. (1.74), multiplied by a normalisation factor[4]. In Fig. 4.1 we see that $|g^{(1)}(\tau)|$ is a decreasing function of τ, hence $g^{(2)}(\tau)$ also has its maximum for $\tau = 0$, after which a steady decrease is seen. In general $g^{(2)}(\tau)$ is smaller than Eq. (1.74) because of the normalisation factor

$$\prod_{\mathbf{k}} \left[1 - e^{-\beta_k} \right]. \tag{4.36}$$

Remember that the derivation of Eq. (1.74) hinged on the assumption that the radiation sources were (a) many and (b) uncorrelated. In the case of thermal radiation, a high temperature (i.e., larger than Eq. (4.28)) means densely populated photon modes since $n_{\mathbf{k}}$ becomes very large. It is easy to imagine that as the modes are filled, the atoms emitting photons become correlated. So Eq. (4.36) can be interpreted as a correction to the classical $g^{(2)}(\tau)$ for chaotic light in which the sources were assumed to be uncorrelated.

4.4 Discussion

The above calculations shows that for multi-mode coherent and thermal light we find the same expressions for the degrees of first- and second order coherence with the quantum optical approach as we did by using classical electromagnetism (section 1.2), but the latter with a correction for correlated sources. So for chaotic sources these two theories predict identical results for the intensity interferometer, which is good news for those worried scientists who feared a complete revision of contemporary quantum mechanics. But we have also seen demonstrated that the classical limit of the degree of second-order coherence (Eqs. (1.67) and (1.63)) is not always followed. This occurred for light in a Fock state, and as such the light is dubbed non-classical. The next section discusses briefly how one can classify different hallmarks of the mean photon number and $g^{(2)}(\tau)$.

---

[4] The normalisation factor can be interpreted as a kind of time-independent mean photon flux in accordance with the continuous-mode expression found in [1].

4.5 Photon states and their distinctive traits

There are two different phenomena that give rise to bunched or antibunched light. One is related to the statistics of the photon distribution of the light, whether it is super- or sub-Poissonian, respectively. The other kind is time-dependent and related to the degree of second-order coherence. In order to limit the confusion, the former will be referred to as light with super-/sub-Poissonian statistics while the latter is called photon bunching/antibunching. These two effects have been mistaken in literature for being two different manifestations of the same quantum optical phenomenon, however, it has been shown by example that sub-Poissonian photon statistics need not imply photon antibunching, as it can be accompanied by photon bunching. Therefore these are distinct effects and must be dealt with separately [29]. The following discussion of photon statistics and photon bunching is inspired by [1, 3, 17].

4.5.1 Poissonian statistics

Poissonian statistics apply to random processes that can only result in *positive* integer values. The probability $\mathcal{P}(n)$ of detecting n events that are Poisson distributed is given by

$$P(n) = \frac{\mu^n}{n!} e^{-\mu} \tag{4.37}$$

where μ is the mean value. Actually, the mean value of n turns out to equal μ

$$\begin{aligned}
\langle n \rangle &= \sum_{n=0}^{\infty} n P(n) \\
&= e^{-\mu} \sum_{n=0}^{\infty} n \frac{\mu^n}{n!} = \mu e^{-\mu} \left(1 + \mu + \frac{\mu^2}{2!} + \dots \right) \\
&= \mu \sum_{n=0}^{\infty} \frac{\mu^n}{n!} e^{-\mu} = \mu
\end{aligned} \tag{4.38}$$

since $\mathcal{P}(n)$ must be normalised to 1 in order to be a probability function. So the probability of detecting n photons in Poissonian light is

$$P(n) = \frac{\langle n \rangle^n}{n!} e^{-\langle n \rangle}, \quad n = 0, 1, 2, \dots \tag{4.39}$$

where $\langle n \rangle$ is the expected photon number. A similar calculation yields the variance of the photon number

$$(\Delta n)^2 = \sum_{n=0}^{\infty} n^2 P(n) - \langle n \rangle^2 = \langle n \rangle. \tag{4.40}$$

The standard deviation is then

$$\Delta n = \sqrt{\langle n \rangle}. \tag{4.41}$$

This can be used to classify different types of light, and the possibilities are as follows:

Poissonian light: $\Delta n = \sqrt{\langle n \rangle}$.

super-Poissonian light: $\Delta n > \sqrt{\langle n \rangle}$.

sub-Poissonian light: $\Delta n < \sqrt{\langle n \rangle}$.

The previous section explored the coherence properties of the coherent state, the Fock state and the mixed thermal state of light. These three states can be put into one of the categories listed above. For simplicity we focus on single-mode photon fields.

Poissonian light

The probability of finding n photons in a coherent state mode is found by

$$P(n) = |\langle n \,|\, \alpha \rangle|^2 = e^{-|\alpha|^2} \frac{|\alpha|^{2n}}{n!} = e^{-\langle n \rangle} \frac{\langle n \rangle^n}{n!} \tag{4.42}$$

where we have used Eqs. (3.43) and (3.45). This is exactly the Poissonian probability distribution from Eq. (4.39), with the variance equal to the mean photon number $\mu = \langle n \rangle$. This is hardly surprising, in fact we already saw this in section 3.4. Thus light in a coherent state follows Poissonian photon statistics.

Super-Poissonian light

We will now show that the thermal light encountered in the previous section, follows super-Poissonian photon statistics. Predictably, the probability function Eq. (4.20) gave the Bose-Einstein distribution for the mean photon number,

$$\langle n \rangle = \frac{1}{e^{\hbar \omega_k / k_B T} - 1}. \tag{4.24}$$

To find the second moment we define $x = \exp(-\hbar \omega_k / k_B T)$. Then we can write

$$\begin{aligned}
\langle n^2 \rangle &= \sum_{n=0}^{\infty} n^2 P(n) = \sum_{n=0}^{\infty} n x^n (1 - x) \\
&= (1 - x) x^2 \sum_{n=0}^{\infty} n(n-1) x^{n-2} + (1 - x) x \sum_{n=0}^{\infty} n x^{n-1} \\
&= (1 - x) x^2 \frac{\mathrm{d}^2}{\mathrm{d}x^2} \left(\frac{1}{1 - x} \right) + \langle n \rangle \\
&= 2 \langle n \rangle^2 + \langle n \rangle \tag{4.43}
\end{aligned}$$

giving the variance

$$(\Delta n)^2 = \langle n^2 \rangle - \langle n \rangle^2 = \langle n \rangle + \langle n \rangle^2 > \langle n \rangle \tag{4.44}$$

and

$$\Delta n > \sqrt{\langle n \rangle} \tag{4.45}$$

Thus thermal light follows super-Poissonian statistics. But keep in mind that the Bose-Einstein distribution is only valid for single-mode photon fields and therefore our calculation applies only for a single-mode $\mathbf{k}$. But it can be shown that for a multi-mode photon field the photon number variance of ν thermal modes of is given by [17]

$$(\Delta n)^2 = \langle n \rangle + \frac{\langle n \rangle^2}{\nu} \tag{4.46}$$

where $\langle n \rangle = \sum_{\mathbf{k}} \langle n_{\mathbf{k}} \rangle$. In practise it is difficult to produce a single-mode thermal field, so in experiments the thermal light will typically exhibit Poissonian statistics because of the large number of modes ν available [3].

Sub-Poissonian light

An example of sub-Poissonian photon statistics is light in a Fock state, which we discussed in section 4.2. The photon number in the Fock state is sharply defined and the probability for there being n photons is exactly

$$\langle n \rangle = \langle n | \hat{n} | n \rangle = n \tag{4.47}$$

Similarly the second moment is simply

$$\langle n^2 \rangle = \langle n | \hat{n}^2 | n \rangle = n^2 \tag{4.48}$$

The variance is therefore zero

$$(\Delta n)^2 = \langle n^2 \rangle - \langle n \rangle^2 = 0. \tag{4.49}$$

There is no violation of Heisenberg's uncertainty relation if one views the phase of the state as the quantum complementary to the position and momentum. So, when the photon number is exactly known, the phase is completely random. The converse would also be true. Without knowledge of the phase, the Fock state can not be described by classical electromagnetism and we must forget trying to write down a wavefunction for the photon states in terms of a position vector $\mathbf{r}$. Instead we must view the photons as excitations at angular frequency ω of the quantised electromagnetic field.

The most eligible quantum equivalent of classically coherent light is light in a coherent state, which has a Poissonian distribution about $\sqrt{\langle n \rangle}$ and is *near* stable with minimal fluctuations in both amplitude or phase. Thermal light exhibits a wider photon number distribution and it is the quantum candidate for classically chaotic light. It seems then that light with sub-Poissonian statistics must be *more* stable than (quantum) coherent light. Since there are no classical equivalent of sub-Poissonian light this super-stability must be a signature of the quantum nature of light.

Implications of photon statistics

To sum up the three classes of photon statistics we have seen so far

Poissonian light: Coherent light, with minimal intensity fluctuations

super-Poissonian light: Partially coherent thermal light, with intensity fluctuations

sub-Poissonian light: No classical equivalent, with zero intensity fluctuations

In either class the statistics are related to the very particle nature of light and tells us something about the tendency of the particles to arrive completely randomly, closer together in "clumps" or more evenly spaced out in "anti-clumps". To be more precise about what is meant by "arriving"; If one where to send photons around in some sort of loop, and then sample the photon number at a certain position, the counted photon number would be within a variance $(\Delta n)^2$ of the expected mean photon number $\langle n \rangle$. But the size of the variance is dependent of the statistics that the photon field has. If the light is coherent, then the standard deviation in the photon count is $\sqrt{n}$; If the light is thermal, the standard deviation is larger and the photon count would miss the expected mean number by a greater margin; If the light is in a Fock state, with a zero standard deviation, then we would always count the expected mean.

Two of the classes, Poissonian and super-Poissonian light, can be explained by classical wave theory as ideal, monochromatic stable plane wave and thermal light, respectively. But the third, sub-Poissonian light, has no classical wave equivalent and hence can only be understood as a purely quantum mechanical aspect of light. In the next section we will again divide light into three classes, however this time we will use the degree of second-order coherence, $g^{(2)}(\tau)$, to distinguish between them.

4.5.2   Photon bunching and antibunching

In the previous section we classified light beams according to their photon statistics. We now turn to an alternative classification of light which is based on the degree of second-order coherence, $g^{(2)}(\tau)$. The light will be categorised as either *random*, *bunched* or *antibunched*. The intensity interferometer measures $g^{(2)}(\tau)$, the classical limits of which was found in section 1.4. But the quantum theory of light predicts values that are impossible for light waves in classical electromagnetism. By definition the three categories are

Random light: $g^{(2)}(\tau) = 1$ for all $\tau \geq 0$.

Bunched light: $g^{(2)}(0) > 1$ and $g^{(2)}(0) > g^{(2)}(\tau)$.

Antibunched light: $g^{(2)}(0) < 1$ and $g^{(2)}(0) < g^{(2)}(\tau)$.

In short, what this means is that if in an experimental setup a stream of photons is sent at a detector, there will be different probabilities of detecting a photon at a time τ when a photon was detected earlier, at $t = 0$. This section takes a closer look at what this entails.

Random light

Single-mode light in a coherent state has as seen earlier in the present chapter[5]

$$g^{(2)}(\tau) = |g^{(1)}(\tau)|^2 = 1 \quad \text{for all} \quad \tau \tag{4.50}$$

This means that if a photon is detected at time $t = 0$ there is an equal probability that another photon is detected at any time τ. This can be also seen as a manifestation of the Poissonian photon statistics that govern perfectly coherent light. In other words the spacing between the photons in the photon stream is entirely random.

Bunched light

Light is said to be bunched when

$$g^{(2)}(0) > 1 \quad \text{and} \quad g^{(2)}(\tau) < g^{(2)}(0) \tag{4.51}$$

meaning that a detection of a second photon is much more likely to occur for shorter time delays τ than for longer ones. We see from Eq. (1.74) and Eq. (4.35) that classically chaotic light and light in a mixed thermal state falls into this category, respectively. As the intensity interferometer measures $g^{(2)}(\tau)$, it provided the first experimental evidence for photon bunching in thermal light. Thus photon bunching is also known as the Hanbury Brown-Twiss effect. In chapter 3.3 it was claimed that quantum theory could indeed explain the arrival of photons in "clumps", which now is backed up by explicit calculations of the quantum degree of second-order coherence.

But Eq. (4.28) estimates that for thermal sources, $g^{(2)}(\tau) \cong 2$ only for very high temperatures, and it drops to unity for temperatures around $T \sim 10^4$ K. At these temperatures there are relatively few photons per mode ($n_{\mathbf{k}} = 1$). In such cases the bunching effect would be negligible and the light would seem completely random. This is worth keeping in mind when for example, using the stellar intensity interferometer.

Antibunched light

As opposed to coherent and bunched light, antibunched light is defined as having

$$g^{(2)}(0) < 1 \quad \text{and} \quad g^{(2)}(\tau) > g^{(2)}(0) \tag{4.52}$$

which can be understood as a detection of a second photon is much more likely to occur for larger values of τ, i.e., the longer one waits. Antibunching has been experimentally verified, but it is more difficult than for example measuring bunched light. For a source consisting of a single atom antibunching is fairly intuitive. After the atoms is de-excited, some time will necessarily pass before another emission can occur as the atom must

---

[5]This is also valid for multi-mode light, but this was not shown. The reader is referred to [1] for a derivation.
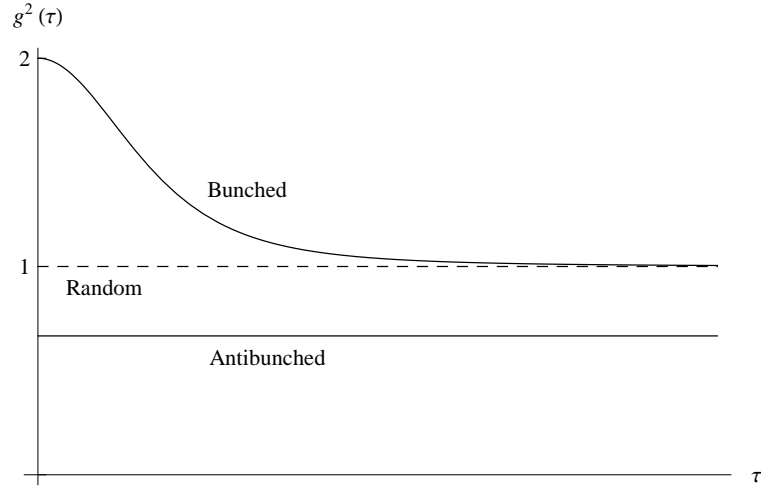
Figure 4.2: Illustration of $g^{(2)}(\tau)$ for bunched light (in the mixed thermal state), random light (in the coherent state) and antibunched light (in the Fock state with a constant photon number).

first be re-excited. But if several atoms radiate at arbitrary times this can effectively obscure the antibunching, hence the experimental difficulties.

The reader may have noticed that the degree of second-order coherence calculated for Fock state light (in section 4.2) was independent of τ, but depended instead on the photon number in mode **k**. So $g^{(2)}(\tau) = $ const. < 1 for all photon numbers $n_{\mathbf{k}}$. However, it is apparent that the more photons present in the photon field, $g^{(2)}(\tau)$ approaches that of the coherent state, i.e., the light has a random photon distribution.

Implications of bunching and antibunching

Summing up the classification of our three photon states

Random light : Coherent state with $g^{(2)}(\tau) = 1$

Bunched light : Thermal state with $g^{(2)}(0) > 1, g^{(2)}(\tau) < g^{(2)}(0)$

Antibunched light : Fock state with $g^{(2)}(0) < 1, g_>^{(2)}(\tau_>)g^{(2)}(0)$

Fig.4.2 illustrates how $g^{(2)}(\tau)$ evolves with τ for bunched light (in the mixed thermal state), random light (in the coherent state) and antibunched light (in the Fock state). The plotted lines are based on the expressions calculated in sections 4.1,4.2 and 4.3, where $g^{(2)}(\tau)$ of the coherent and Fock states were found to be independent of τ. As mentioned, having sub-Poissonian statistics does not preclude the light from also being bunched. For example, if $g^{(2)}(0) < 1$, but $g^{(2)}(0) = g^{(2)}(\tau)$ for all τ, then the light is not antibunched, even though is is a quantum state with no classical analogy [29].

Chapter 5

Coherence in the laser

So far we have seen that the classical coherent light is stable in the sense that it has no fluctuations in neither amplitude nor phase and that the coherent state is the closest quantum equivalent to it, with a minimal variance in amplitude and phase. We have also seen that the the photon statistics of the coherent state is Poissonian with a variance equal to the mean photon number. The goal of the present chapter is to show that laser light is very nearly in a coherent state. In section 5.2 it will be shown that the laser photon statistics, when operating under certain conditions, becomes equal to that of the coherent state. Under the same conditions the laser light is shown to also be both first- and second-order coherent. Then there is the matter of the fluctuations in the phase, which will be dealt with in section 5.4.

The main difference between chaotic (e.g., thermal light) and laser light lies in the fact that laser light is produced mainly by stimulated emission rather than by spontaneous emission and that there is a very strong coupling between a certain transition in the laser medium (i.e., the atoms) and the radiation field mode. The electromagnetic energy is generally concentrated in one mode (or very few modes), so the number of photons in the mode can become very large. This results in the laser radiation being mainly produced by stimulated emission (i.e., is highly coherent) and thus comes very close to a classically coherent source. Nearly all lasers consists of the following four components [17]

1. a cavity, often consisting of two or more mirrors (also called a resonator)

2. a gain medium (e.g., an atomic gas) with population inversion between the two laser energy levels

3. an energy source (e.g., an optical pump) to excite the atoms to the upper laser level

4. a mechanism for light to escape the cavity, (e.g., a semi-transparent mirror)

A complete investigation of the statistical and coherence properties of the laser requires solving the equations of motion where several effects are taken into account, like
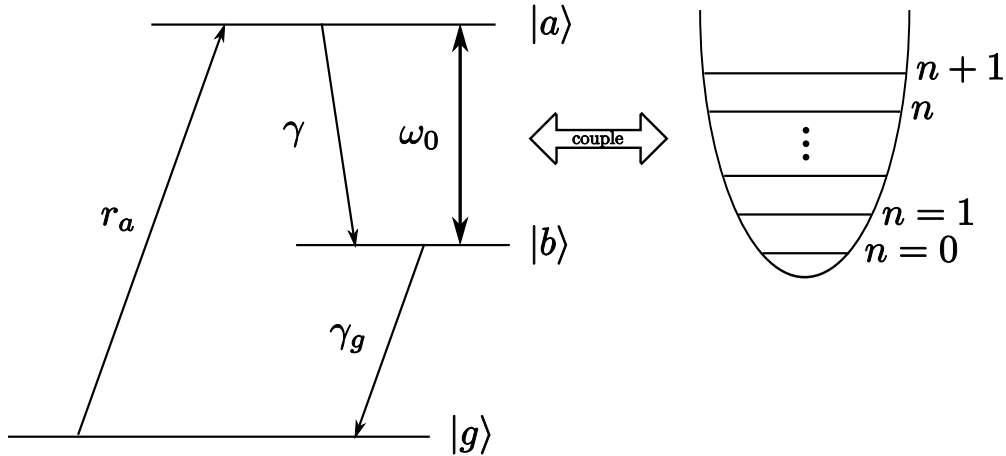
Figure 5.1: The three level model where atoms are pumped from the ground-state $|g\rangle$ into the lasing level $|a\rangle$ at a rate r_a, from which they can undergo spontaneous and stimulated decay to the lower lasing level $|b\rangle$. The lasing transition $|a\rangle \leftrightarrow |b\rangle$, with a frequency difference ω_0, is strongly coupled to the radiation field of frequency Ω. Resonance is assumed so that $\omega_0 = \Omega$. From $|b\rangle$ there is a fast decay to $|g\rangle$, where $\gamma_g \gg r_a$.

the interaction between radiation-atom and radiation-reservoir, including the excitation mechanism, cavity losses, transmission losses, internal vibrations, and so forth. We will limit ourselves to deriving the equation of motion for the simple three-level model, starting right away with section 5.1.

5.1   The equation of motion for the three-level model

A system of atoms are inside a cavity, where each atom has the level structure shown in Fig 5.1. The atoms are pumped up to the excited level $|a\rangle$ from the ground-state $|g\rangle$ at a rate r_a. Laser action takes place between the two excited energy levels $|a\rangle$ and $|b\rangle$, of the energies $\hbar\omega_a$ and $\hbar\omega_b$, respectively. The three-level model provides a credible setting where *population inversion* is readily achieved. The point of population inversion is that the number of atoms in the upper lasing level is much larger than the number in the lower lasing level. Then the rate of emission of photons dominates the rate of absorption, so that the number of photons increases, i.e., the intensity *grows*.

As a matter of convenience in the subsequent calculations, the "mean" frequency is defined

$$\omega_0 = 1/2(\omega_a - \omega_b), \tag{5.1}$$

so that the energy of an atom in $|a\rangle$ is $E_a = \hbar\omega_0/2$, while an atom in $|b\rangle$ has the energy $E_b = -\hbar\omega_0/2$. The decay from $|a\rangle$ to $|b\rangle$ can be *stimulated* by the electromagnetic field in the cavity, or it can be *spontaneous*. When the decay is stimulated the excited atom is perturbed by the field such that it decays, emitting a photon with the same phase

and frequency as the incident photon. The atom in $|b\rangle$ can also absorb photons from the field, moving it back up to $|a\rangle$, where the photon is subsequently re-radiated.

This oscillation between the lasing levels will continue until the atom decays to the ground-state $|g\rangle$ from $|b\rangle$ (at a rate γ_g slower than the oscillation, but faster than r_a), or until spontaneous decay from $|a\rangle$ occurs (at a rate $\gamma \ll \gamma_g$). Spontaneous decay results in a photon with a completely random phase and direction. While the cavity mirrors feeds the photons in the laser mode back into the laser cavity, most photons due to spontaneous decay are lost, except those that are randomly emitted into the laser mode at the rate γ.

We assume a strong coupling of the two levels $|a\rangle$ and $|b\rangle$ with a single mode of the electromagnetic field and *resonance* between the field and the lasing transition

$$\omega_a - \omega_b = \omega_0 = \Omega \tag{5.2}$$

where Ω is the frequency of the field mode. The dynamics of the three-level model is described by the equation of motion of the density operator, $\dot{\rho}(t)$. However, as the laser action occurs between $|a\rangle$ and $|b\rangle$, a two-level model is sufficient since the pumping from, and decay to, the ground state does not affect the lasing process except as to allow for population inversion. The rates r_a and γ_g are then thought of as the rates of available two-level atoms: Freshly excited atoms are pumped in at a rate r_a, while de-excited atoms "vanish" at a rate γ_g. Also, if the ground-state is heavily populated, having $\gamma_g \gg r_a$ ensures that the population-change is negligible. The approach follows that of [17, 9, 21].

5.1.1 The Jaynes-Cummings model

The Jaynes-Cummings model predicts the evolution of the two-level atom when interacting with an electromagnetic field. We will use it to model the oscillations between the lasing levels

$$|a\rangle = \begin{bmatrix} 1 \\ 0 \end{bmatrix} \quad \text{and} \quad |b\rangle = \begin{bmatrix} 0 \\ 1 \end{bmatrix} \tag{5.3}$$

The field is in a Fock number state and thus the atom-field system state is the product state

$$|\psi_{a+f}\rangle = |i\rangle_{\text{atom}} \otimes |n\rangle_{\text{field}} = |i, n\rangle \quad (i = a, b). \tag{5.4}$$

The goal of this section is to find the coefficients of the time-dependent system state

$$|\psi(t)\rangle = C_{an}(t) |a, n\rangle + C_{bn+1}(t) |b, n+1\rangle. \tag{5.5}$$

In order to find $C_{an}(t)$ and $C_{bn+1}(t)$, we have to solve the eigenvalue problem.

The effective Hamiltonian for the two laser levels is

$$\hat{H} = \hat{H}_{\text{atom}} + \hat{H}_{\text{field}} + \hat{H}_{\text{JC}}, \tag{5.6}$$

where

$$\hat{H}_{\text{atom}} = \frac{1}{2}\hbar\omega_0\sigma_z$$
$$\hat{H}_{\text{field}} = \hbar\Omega\hat{a}^\dagger\hat{a} \tag{5.7}$$
$$\hat{H}_{\text{JC}} = -\mathcal{P}E_x(z,t)(\hat{\sigma} + \hat{\sigma}^\dagger)$$

with the subscript indicating the Hamiltonian for the, respectively; two-level atom; single-mode electromagnetic field; interaction between the atom and the field. In the latter, $\mathcal{P}$ is the electric-dipole transition factor, which is not of interest in this work; suffice to say that the dipole approximation is assumed. From the Pauli matrices we have

$$\hat{\sigma_z} = \begin{pmatrix} 1 & 0 \\ 0 & -1 \end{pmatrix}, \qquad \hat{\sigma} = \begin{pmatrix} 0 & 0 \\ 1 & 0 \end{pmatrix}, \qquad \hat{\sigma}^\dagger = \begin{pmatrix} 0 & 1 \\ 0 & 0 \end{pmatrix}. \tag{5.8}$$

where the latter two operators have the effect that they flip the atom from state $|a\rangle$ to $|b\rangle$ and $|b\rangle$ to $|a\rangle$), respectively.

In the Interaction picture the electric field is given as[1]

$$E_x(z) = \mathcal{E}(\hat{a} + \hat{a}^\dagger)\sin kz \tag{5.9}$$

where $\mathcal{E} = \sqrt{\hbar\Omega/2\epsilon_0 L^3}$ and the subscript indicates a chosen polarisation direction. The coupling constant is defined as

$$g \equiv -\frac{\mathcal{P}}{\hbar}\mathcal{E}\sin kz \tag{5.10}$$

and it characterises the strength of the interaction between an atom and the radiation field. Thus $(-\mathcal{P}E_x(z,t)) = \hbar g(\hat{a} + \hat{a}^\dagger)$ and the effective Hamiltonian becomes

$$\hat{H} = \frac{1}{2}\hbar\omega_0\sigma_z + \hbar\Omega\hat{a}^\dagger\hat{a} + \hbar g(\hat{a} + \hat{a}^\dagger)(\hat{\sigma} + \hat{\sigma}^\dagger). \tag{5.11}$$

The last term on the right-hand side corresponds to four different scenarios, two of which conserves energy and two that do not.

1. $\hat{a}\hat{\sigma}$: photon annihilation and decay ($|a,n\rangle \rightarrow |b,n-1\rangle$)
2. $\hat{a}\hat{\sigma}^\dagger$: photon annihilation and excitation ($|b,n+1\rangle \rightarrow |a,n\rangle$)
3. $\hat{a}^\dagger\hat{\sigma}$: photon creation and decay ($|a,n\rangle \rightarrow |b,n+1\rangle$)
4. $\hat{a}^\dagger\hat{\sigma}^\dagger$: photon creation and excitation ($|b,n\rangle \rightarrow |a,n+1\rangle$)

Keeping only the energy conserving terms 2 and 3 we have

$$\hat{H} = \frac{1}{2}\hbar\omega_0\sigma_z + \hbar\Omega\hat{a}^\dagger\hat{a} + \hbar g(\hat{a}^\dagger\hat{\sigma} + \hat{a}\hat{\sigma}^\dagger) \tag{5.12}$$

---

[1]The Interaction picture is an intermediate between the Schrödinger and the Heisenberg pictures as the time-dependence is carried in both the state vectors and the operators.

The eigenvalue problem is solved in Appendix B.3 and yields the coefficients in the Interaction picture[2]

$$
\begin{aligned}
C_{an}(t) &= \cos(g\sqrt{n+1}t) \\
C_{bn+1}(t) &= -i\sin(g\sqrt{n+1}t)
\end{aligned}
\tag{5.13}
$$

where resonance is assumed.

5.1.2 The equation of motion for the density matrix

To describe the dynamics of the laser model we will derive the equation of motion for the reduced radiation field-density operator. It includes the oscillation of the lasing transition, spontaneous emissions and the dampening of the field due to losses.

Assume that each atom in a gas laser contributes to the energy of the field independently of the other atoms, that the other atoms are felt only through the collective electric field. Then the change in the reduced field-density operator is caused by the pumping of a single atom to $|a\rangle$ at time t. With n photons in the field and the atom interaction lasting a time τ, this change is

$$
\delta\rho_{nm} = \rho_{nm}(t+\tau) - \rho_{nm}(t).
\tag{5.14}
$$

Here τ is long compared to an atomic lifetime, but short compared to the macroscopic time at which growth or decay of the laser radiation field is felt. Also, if the field is strong, the oscillations in the laser transition happens on much smaller time scales than the spontaneous decay of the atom. The macroscopic change in the density operator is due to N atoms acting on the field over a time Δt,

$$
\Delta\rho_{nm} = N\delta\rho_{nm} = r_a\Delta t\delta\rho_{nm}
\tag{5.15}
$$

where r_a is the pumping rate.

The atom-field density operator is the product of the reduced atom-density operator and the reduced field-density operator. By tracing over the full system the elements of the field-density matrix is found

$$
\rho_{nm}(t) = \operatorname{tr}_j \rho_{jnjm}(t) = \rho_{anam}(t) + \rho_{bnbm}(t) \qquad (j = a, b)
\tag{5.16}
$$

where the subscripts a and b refers to the state of the atom interacting with the field. The coarse-grained derivative of the laser field-density matrix elements is

$$
\dot{\rho}_{nm} = \frac{\Delta\rho_{nm}}{\Delta t} = r_a[\rho_{an,am}(t+\tau) - \rho_{an,am}(t) + \rho_{bn,bm}(t+\tau) - \rho_{bn,bm}(t)]
\tag{5.17}
$$

---

[2] Where the state vector is

$$
|\Psi_I(t)\rangle = e^{-iE_0 t/\hbar} |\Psi_S(t)\rangle .
$$

Resonance in the present case gives $E_0 = \hbar\Omega(n+1/2)$.

To justify this approximate differential consider that a real laser has many atoms distributed throughout the gain medium, with the pumping mechanism continuously replenishing excited atoms. The single-atom contribution to $\Delta\rho_{nm}$ must therefore be small and if the field evolves slowly, the change $\dot{\rho}_{nm}$ is due to the the single-atom change of N atoms interacting a time Δt.

In Eq. (5.17) $\rho_{bn,bm}(t) = 0$, since the atoms are pumped to level $|a\rangle$ initially at time t. The atom-field density matrix elements are determined by the amplitudes calculated in the previous section,

$$\rho_{an,am}(t) = \sum_{\psi} P_{\psi}\,|\psi\rangle\,\langle\psi| = \sum_{\psi} P_{\psi}C_n(t)C_m^*(t)\,|n\rangle\,\langle m|$$

$$= \rho_{nm}(t) \tag{5.18a}$$

$$\rho_{an,am}(t+\tau) = \sum_{\psi} P_{\psi}C_{an}(t)C_{am}^*(t)\cos(g\sqrt{n+1}\tau)\cos(g\sqrt{m+1}\tau)$$

$$= \rho_{n,m}(t)\cos(g\sqrt{n+1}\tau)\cos(g\sqrt{m+1}\tau) \tag{5.18b}$$

$$\rho_{bn,bm}(t+\tau) = \sum_{\psi} P_{\psi}C_{bn-1}(t)C_{bm-1}^*(t)\cos(g\sqrt{n}\tau)\cos(g\sqrt{m}\tau)$$

$$= \rho_{n-1m-1}(t)\cos(g\sqrt{n}\tau)\cos(g\sqrt{m}\tau) \tag{5.18c}$$

where P_{ψ} is the probability for the system being in state $|\psi\rangle$.

On a larger time scale than τ, but shorter than Δt, the spontaneous decay from level $|a\rangle$ into the laser mode is modelled as an exponential decay at the rate γ. This is a convenient approximation which is not necessarily physically correct. It says that the probability that an atom will stay in state $|a\rangle$ for a time τ is

$$P(\tau)\mathrm{d}\tau = \gamma e^{-\gamma\tau}\mathrm{d}\tau. \tag{5.19}$$

However, the atom is constantly perturbed by the strong radiation field and it is thus not "left in peace" in $|a\rangle$, but rather oscillates rapidly between the laser levels during this time. It might not be very straight forward to predict the behaviour of the atom when in presence of both a strong field (the laser field) and a weak field (from spontaneous decay). Nevertheless, the assumption of exponential decay is adequate in this context, so we proceed to finding the average coarse-grained time rate of change

$$\dot{\rho}_{nm} = -r_a\rho_{n,m}(t)\Big[1 - \gamma\int_0^{\infty}\cos(g\sqrt{n+1}\tau)\cos(g\sqrt{m+1}\tau)e^{-\gamma\tau}\mathrm{d}\tau\Big]$$

$$+ r_a\rho_{n-1,m-1}(t)\gamma\int_0^{\infty}\sin(g\sqrt{n}\tau)\sin(g\sqrt{m}\tau)e^{-\gamma\tau}\mathrm{d}\tau \tag{5.20}$$

The solutions to the integrals can be found in mathematical formularies, giving

$$\dot{\rho}_{nm} = -r_a\rho_{n,m}(t)\left[1 - \frac{1 + \alpha(n+1+m+1)}{1 + 2\alpha(n+1+m+1) + \alpha^2(n-m)^2}\right]$$

$$+ r_a\rho_{n-1,m-1}(t)\frac{2\alpha\sqrt{nm}}{1 + 2\alpha(n+m) + \alpha^2(n-m)^2} \tag{5.21}$$

where $\alpha \equiv (g/\gamma)^2$. These expressions can be simplified by defining

$$\mathcal{A} \equiv 2\alpha r_a \tag{5.22a}$$

$$\mathcal{B} \equiv 4\alpha\mathcal{A} = 8\alpha^2 r_a \tag{5.22b}$$

$$\mathcal{N}'_{nm} \equiv \frac{1}{2}(n+1+m+1) + \frac{1}{8\mathcal{A}}(n-m)^2\mathcal{B} \tag{5.22c}$$

$$\mathcal{N}_{nm} \equiv \frac{1}{2}(n+1+m+1) + \frac{1}{16\mathcal{A}}(n-m)^2\mathcal{B} \tag{5.22d}$$

$\mathcal{A}$ and $\mathcal{B}$ are called the *linear gain* and *saturation* coefficients, respectively [9]. The changes in the field-density matrix due to the gain medium (e.g., the atomic gas) is

$$(\dot{\rho}_{nm})^{\text{gain}} = -\frac{\mathcal{N}'_{nm}\mathcal{A}}{1+\mathcal{N}_{nm}\mathcal{B}/\mathcal{A}}\rho_{n,m}(t) + \frac{\sqrt{nm}\mathcal{A}}{1+\mathcal{N}_{n-1m-1}\mathcal{B}/\mathcal{A}}\rho_{n-1,m-1}(t) \tag{5.23}$$

We also need to include a mechanism to account for the cavity losses, e.g., absorption by imperfect walls or losses to the outside (obviously is an important function of the laser). In a fully quantized theory, photons can only be lost through their coupling to another quantum system, e.g., a reservoir [17]. The changes in the field-density matrix that are due to damping of the field mode can be thought of as the result of photon absorption by atoms with the same level structure as the lasing transition shown in Fig. 5.1. For transmission losses, the reservoir can be atoms outside the cavity, or for losses in general, it can be atoms dispersed throughout the medium. The reservoir atoms are assumed to be initially in the lower laser level $|b, n+1\rangle$. Their purpose is to absorb photons of the laser field at a rate proportional to field intensity, but without re-radiation. The same procedure that led to Eq. (5.23) can be used, but now we must find the atom-field density matrix for atoms initially in the lower laser level. This corresponds to exchanging the state vector amplitudes like

$$\begin{aligned} C_{an}(t+\tau) &\rightarrow -i\sin(g\sqrt{n+1}t)C_{n+1}(t) \\ C_{bn+1}(t+\tau) &\rightarrow \cos(g\sqrt{n+1}t)C_{n+1}(t) \end{aligned} \tag{5.24}$$

Then, to the first order in the coupling constant g, the reservoir atom-field density matrices becomes (analoguous to Eq. (5.18c))

$$\begin{aligned} \rho_{anam}(t+\tau) &\approx g^2\tau^2\sqrt{n+1}\sqrt{m+1}\rho_{n+1m+1}(t) \\ \rho_{bnbm}(t+\tau) &\approx [1 - g^2\tau^2(n+m)]\rho_{nm}(t) \end{aligned} \tag{5.25}$$

yielding

$$\begin{aligned} \rho_{nm}(t+\tau) &= \rho_{anam}(t+\tau) + \rho_{bnbm}(t+\tau) \\ &= g^2\tau^2\sqrt{n+1}\sqrt{m+1}\rho_{n+1,m+1}(t) + [1 - g^2\tau^2(n+m)]\rho_{nm}(t) \end{aligned} \tag{5.26}$$

Then the change in the radiation field-density matrix due to reservoir atoms injected in state $|b, n+1\rangle$, at a rate r_b, is

$$\begin{aligned} (\dot{\rho}_{nm})^{\text{loss}} &= r_b[\rho_{nm}(t+\tau) - \rho_{nm}(t)] \\ &= -\frac{r_b g^2\tau^2}{2}(n+m)\rho_{nm}(t) + r_b g^2\tau^2\sqrt{n+1}\sqrt{m+1}\rho_{n+1,m+1}(t) \end{aligned} \tag{5.27}$$

or

$$(\dot{\rho}_{nm})^{\text{loss}} = -\frac{\mathcal{C}}{2}(n+m)\rho_{nm}(t) + \mathcal{C}\sqrt{n+1}\sqrt{m+1}\rho_{n+1,m+1}(t) \tag{5.28}$$

where the loss rate is

$$\mathcal{C} \equiv r_b g^2 \tau^2. \tag{5.29}$$

This is also related to the quality factor of the cavity Q as $\mathcal{C} = \Omega/Q$ [21].

By adding Eq. (5.23) to Eq. (5.28), the complete equation of motion for the density matrix is found to be

$$\begin{aligned}
\dot{\rho}_{nm} &= -\frac{\mathcal{N}'_{nm}\mathcal{A}}{1+\mathcal{N}_{nm}\mathcal{B}/\mathcal{A}}\rho_{n,m}(t) + \frac{\sqrt{nm}\mathcal{A}}{1+\mathcal{N}_{n-1,m-1}\mathcal{B}/\mathcal{A}}\rho_{n-1,m-1}(t) \\
&\quad - \mathcal{C}/2(n+m)\rho_{nm}(t) + \mathcal{C}\sqrt{n+1}\sqrt{m+1}\rho_{n+1,m+1}(t)
\end{aligned} \tag{5.30}$$

In particular the diagonal elements of the density matrix are

$$\begin{aligned}
\dot{\rho}_{nn} &= -\frac{(n+1)\mathcal{A}}{1+(n+1)\mathcal{B}/\mathcal{A}}\rho_{n,n}(t) + \frac{n\mathcal{A}}{1+n\mathcal{B}/\mathcal{A}}\rho_{n-1,n-1}(t) \\
&\quad - \mathcal{C}n\rho_{nn}(t) + \mathcal{C}(n+1)\rho_{n+1,n+1}(t)
\end{aligned} \tag{5.31}$$

5.2   The diagonal elements and laser photon statistics

The diagonal elements Eq. (5.31) has a simple interpretation as the probability of n photons in the field: $\rho_{nn} \equiv p(n)$. The denominators in Eq. (5.31) can be expanded to the first order as

$$[1 + \mathcal{N}_{nm}\mathcal{B}/\mathcal{A}]^{-1} \approx 1 - \mathcal{N}_{nm}\mathcal{B}/\mathcal{A} \tag{5.32}$$

and since $\mathcal{N}_{nn} = \mathcal{N}'_{nn} = (n+1)$, we get

$$\begin{aligned}
\dot{\rho}_{nn} &= -(n+1)\mathcal{A}[1-(n+1)\mathcal{B}/\mathcal{A}]p(n) + n\mathcal{A}[1-n\mathcal{B}/\mathcal{A}]p(n-1) \\
&\quad - \mathcal{C}np(n) + \mathcal{C}(n+1)p(n+1) \\
&= -\mathcal{A}(n+1)p(n) + \mathcal{B}(n+1)^2 p(n) + \mathcal{A}np(n-1) - \mathcal{B}n^2 p(n-1) \\
&\quad - \mathcal{C}np(n) + \mathcal{C}(n+1)p(n+1)
\end{aligned} \tag{5.33}$$

Each of the terms represents a flow of the probability in and out of state $|n\rangle$ from the adjacent states $|n+1\rangle$ and $|n-1\rangle$. Flow into $|n\rangle$ has a positive sign and flow out is negative. This is illustrated in the probability flow-diagram in Fig 5.2. $\mathcal{A}n$ is the stimulated emission rate and $\mathcal{A}$ is the rate of spontaneous emission into the laser mode. $\mathcal{C}$ represents cavity losses and the two terms multiplied by $\mathcal{B}$,

$$\begin{aligned}
(n+1)^2\mathcal{B} &= \mathcal{A}(n+1) \cdot \mathcal{B}(n+1)/\mathcal{A} \\
n^2\mathcal{B} &= \mathcal{A}n \cdot \mathcal{B}n/\mathcal{A}
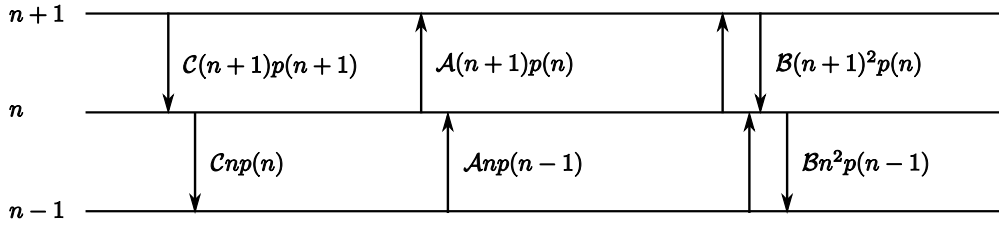\end{aligned}$$

Figure 5.2: The probability flow diagram for Eq. (5.33).

is understood as photon emission at the rate of $\mathcal{A}(n+1)$ (or $\mathcal{A}n$) and re-absorption at $\mathcal{B}(n+1)/\mathcal{A}$ (or $\mathcal{B}n/\mathcal{A}$).

It is also possible to derive an expression for the change in the mean photon number of the field. As usual, the mean number is found by

$$\langle n \rangle = \sum_{n=0}^{\infty} n\rho_{nn} \tag{5.34}$$

Taking the time derivative of $\langle n \rangle$ and inserting Eq. (5.33) gives

$$
\begin{aligned}
\frac{\mathrm{d}\langle n \rangle}{\mathrm{d}t} &= -\mathcal{A}\sum_{n=0}^{\infty} n(n+1)p(n) + \mathcal{B}\sum_{n=0}^{\infty} n(n+1)^2 p(n) + \mathcal{A}\sum_{n=0}^{\infty} n^2 p(n-1) \\
&\quad - \mathcal{B}\sum_{n=0}^{\infty} n^3 p(n-1) - \mathcal{C}\sum_{n=0}^{\infty} n^2 p(n) + \mathcal{C}\sum_{n=0}^{\infty} n(n+1)p(n+1) \\
&= -\mathcal{A}[\langle n^2 \rangle + \langle n \rangle] + \mathcal{B}[\langle n^3 \rangle + 2\langle n^2 \rangle + \langle n \rangle] + \mathcal{A}\sum_{m=-1}^{\infty} (m+1)^2 p(m) \\
&\quad - \mathcal{B}\sum_{m=-1}^{\infty} (m+1)^3 p(m) - \mathcal{C}\langle n^2 \rangle + \mathcal{C}\sum_{m=1}^{\infty} m(m-1)p(m) \\
&= [\mathcal{A} - \mathcal{C}]\langle n \rangle - \mathcal{B}[\langle n^2 \rangle + 2\langle n \rangle + 1] + \mathcal{A} \tag{5.35}
\end{aligned}
$$

If there are no photons present in the laser mode initially, there will be no increase in n due to stimulated emission. However, there can still be a build-up of photons in the laser mode because of spontaneous emission, which is seen from the last term on the right-hand side, $\mathcal{A}$, representing spontaneous emission into the laser mode. This is in stark contrast to a semi-classical treatment of the laser, since a vanishing classical intensity will remain zero for all time [21]. The difference is of course that spontaneous emission is not described by classical electromagnetism. There is also a negative change in $\langle \dot{n} \rangle$ coming from the factor $\mathcal{B}$ so the rate of growth in $\langle n \rangle$ without an external pumping mechanism, is dependent on the ratio $\mathcal{A}/\mathcal{B}$.

5.2.1 The steady-state solution and the threshold $\mathcal{A} = \mathcal{C}$

Before we attempt to solve the general equation of motion of the density matrix (Eq. (5.30)) we will first find the steady-state solution for the diagonal elements $\dot{\rho}_{nn}(t)$.

This will give a clue as to what kind of photon statistics the laser radiation follows. From the discussion in section 4.5 we know that coherent light follows Poissonian statistics, so a similar finding would substantiate the claim that a laser beam is a good approximation to coherent light.

The system is in steady-state if the flow of probabilities *into* a state with n photons is the same as the flow *out* of it, i.e., $\dot{\rho}_{nn} = 0$. According to the principle of *detailed balance*, the steady-state solution of Eq. (5.33) is given by the following equations (recall that $\rho_{nn} \equiv p(n)$)

$$\mathcal{C}(n+1)\rho_{n+1,n+1} - \big[\mathcal{A} - (n+1)\mathcal{B}\big](n+1)\rho_{n,n} = 0$$
$$\mathcal{C}n\rho_{nn} - \big[\mathcal{A} - n\mathcal{B}\big]n\rho_{n-1,n-1} = 0 \tag{5.36}$$

If we assume the linear approximation $\mathcal{B} = 0$ it is readily seen that

$$\rho_{nn} = \frac{\mathcal{A}}{\mathcal{C}}\rho_{n-1,n-1} = \left(\frac{\mathcal{A}}{\mathcal{C}}\right)^n \rho_{00} \tag{5.37}$$

ρ_{00} can be determined by the requirement that the total probability must sum to unity,

$$\sum_{n=0}^{\infty} \rho_{nn} = \sum_{n=0}^{\infty} \left(\frac{\mathcal{A}}{\mathcal{C}}\right)^n \rho_{00} = 1 \tag{5.38}$$

The sum converges only if $\mathcal{A} < \mathcal{C}$, so that this becomes the geometric series, giving

$$\rho_{00} = 1 - \frac{\mathcal{A}}{\mathcal{C}}. \tag{5.39}$$

Hence

$$\rho_{nn} = \left(1 - \frac{\mathcal{A}}{\mathcal{C}}\right)\left(\frac{\mathcal{A}}{\mathcal{C}}\right)^n. \tag{5.40}$$

In the linear approximation, the convergent solution for ρ_{nn} exists only for $\mathcal{A} < \mathcal{C}$. Thus $\mathcal{A} = \mathcal{C}$ can be taken as the *lasing threshold*.

The lasing threshold is a well-known construct in laser physics. From the definitions Eqs. (5.22a) and (5.29), we see that at threshold

$$r_a = \frac{1}{2}r_b\gamma^2\tau^2 \tag{5.41}$$

that is, the pumping of atoms into the upper lasing level balances the cavity loss and the rate of spontaneous emission. The photon statistics of the laser is inherently dependent on whether the laser is operating below, above or far above threshold. Below the threshold, the steady-state solution becomes that of a black-body cavity [9], like for thermal light (see Eq. (4.21)). But far above threshold, $\mathcal{A} \gg \mathcal{C}$, the photon statistics become Poissonian. The linear approximation $\mathcal{B} = 0$ breaks down here, meaning that we must first find the exact steady-state solution of the diagonal density matrix.

5.2.2 The exact steady-state solution of ρ_{nn}

The exact steady-state solution of Eq. (5.31) is found by using the principle of detailed balance in a similar manner as in the linear approximation. For example, for the levels $|n-1\rangle$ and $|n\rangle$,

$$\frac{n\mathcal{A}}{1+n\mathcal{B}/\mathcal{A}}\rho_{n-1,n-1} - \mathcal{C}n\rho_{nn} = 0. \tag{5.42}$$

The solution of ρ_{nn} is the recursive expression

$$\rho_{nn} = \frac{\mathcal{A}/\mathcal{C}}{1+n\mathcal{B}/\mathcal{A}}\rho_{n-1,n-1} = \rho_{00}\prod_{k=1}^{n}\frac{\mathcal{A}^2/\mathcal{B}\mathcal{C}}{\mathcal{A}/\mathcal{B}+k}$$

$$= \rho_{00}\frac{(\mathcal{A}/\mathcal{B})!\left(\mathcal{A}^2/\mathcal{B}\mathcal{C}\right)^n}{(n+\mathcal{A}/\mathcal{B})!} \tag{5.43}$$

where ρ_{00} is determined by the normalisation requirement $\sum_{n=0}^{\infty}\rho_{nn}=1$, giving

$$\rho_{00} = \left[\sum_{n=0}^{\infty}\frac{(\mathcal{A}/\mathcal{B})!\left(\mathcal{A}^2/\mathcal{B}\mathcal{C}\right)^n}{(n+\mathcal{A}/\mathcal{B})!}\right]^{-1}. \tag{5.44}$$

The mean steady-state value of n is found by

$$\langle n\rangle = \sum_{n=0}^{\infty}n\rho_{nn}$$

$$= \rho_{00}\sum_{n=0}^{\infty}\left(n+\frac{\mathcal{A}}{\mathcal{B}}-\frac{\mathcal{A}}{\mathcal{B}}\right)\frac{(\mathcal{A}/\mathcal{B})!\left(\mathcal{A}^2/\mathcal{B}\mathcal{C}\right)^n}{(n+\mathcal{A}/\mathcal{B})!}$$

$$= \rho_{00}\sum_{n=0}^{\infty}\frac{(\mathcal{A}/\mathcal{B})!\left(\mathcal{A}^2/\mathcal{B}\mathcal{C}\right)^n}{(n+\mathcal{A}/\mathcal{B}-1)!} - \rho_{00}\frac{\mathcal{A}}{\mathcal{B}}\sum_{n=0}^{\infty}\frac{(\mathcal{A}/\mathcal{B})!\left(\mathcal{A}^2/\mathcal{B}\mathcal{C}\right)^n}{(n+\mathcal{A}/\mathcal{B})!}$$

$$= \rho_{00}\frac{\mathcal{A}}{\mathcal{B}} + \rho_{00}\frac{\mathcal{A}^2}{\mathcal{B}\mathcal{C}}\sum_{n=1}^{\infty}\frac{(\mathcal{A}/\mathcal{B})!\left(\mathcal{A}^2/\mathcal{B}\mathcal{C}\right)^{n-1}}{(n+\mathcal{A}/\mathcal{B}-1)!} - \frac{\mathcal{A}}{\mathcal{B}}$$

$$= \frac{\mathcal{A}(\mathcal{A}-\mathcal{C})}{\mathcal{B}\mathcal{C}} + \frac{\mathcal{A}}{\mathcal{B}}\rho_{00}$$

If the laser is operating appreciably above threshold, $\mathcal{A}>\mathcal{C}$, the dampening of the laser mode due to losses is much smaller than the gain from the medium. Then ρ_{00} is comparatively small and the mean number of photons in the laser mode at steady-state becomes

$$\langle n\rangle = \frac{\mathcal{A}(\mathcal{A}-\mathcal{C})}{\mathcal{B}\mathcal{C}}. \tag{5.45}$$

5.2.3 Photon statistics above threshold

We insert the mean photon number at steady-state Eq. (5.45) into the normalisation constant ρ_{00}

$$
\begin{aligned}
\rho_{00} &= \left[(\mathcal{A}/\mathcal{B})! \sum_{n=0}^{\infty} \frac{(\langle n \rangle + \mathcal{A}/\mathcal{B})^n}{(n + \mathcal{A}/\mathcal{B})!} \right]^{-1} \\
&= \left[(\mathcal{A}/\mathcal{B})! \sum_{n=0}^{\infty} \frac{(\langle n \rangle + \mathcal{A}/\mathcal{B})^{n+\mathcal{A}/\mathcal{B}}}{(n + \mathcal{A}/\mathcal{B})!} \right]^{-1} (\langle n \rangle + \mathcal{A}/\mathcal{B})^{\mathcal{A}/\mathcal{B}} \\
&= (\mathcal{B}/\mathcal{A})! e^{-(\langle n \rangle + \mathcal{A}/\mathcal{B})}.
\end{aligned}
\tag{5.46}
$$

Using this in Eq. (5.43) gives the diagonal density elements

$$
\begin{aligned}
\rho_{nn} &= \rho_{00}(\mathcal{A}/\mathcal{B})! \frac{(\langle n \rangle + \mathcal{A}/\mathcal{B})^{n+\mathcal{A}/\mathcal{B}}}{(n + \mathcal{A}/\mathcal{B})!} \\
&= \frac{(\langle n \rangle + \mathcal{A}/\mathcal{B})^{n+\mathcal{A}/\mathcal{B}}}{(n + \mathcal{A}/\mathcal{B})!} e^{-(\langle n \rangle + \mathcal{A}/\mathcal{B})}
\end{aligned}
\tag{5.47}
$$

This is a Poissonian distribution with the mean $(\langle n \rangle + \mathcal{A}/\mathcal{B})$, which is broader than the distribution for the coherent state (equal to $\langle n \rangle$)[3].

But far above threshold, where $\mathcal{A} \gg \mathcal{C}$, the mean photon number at steady-state becomes

$$
\langle n \rangle \approx \frac{\mathcal{A}^2}{\mathcal{B}\mathcal{C}}
\tag{5.48}
$$

and we also see that

$$
\frac{\mathcal{B}\langle n \rangle}{\mathcal{A}} = \frac{\mathcal{A}}{\mathcal{C}} \gg 1 \quad \Rightarrow \quad \langle n \rangle \gg \frac{\mathcal{A}}{\mathcal{B}}
\tag{5.49}
$$

The diagonal density matrix is then

$$
\rho_{nn} \equiv p(n) = \frac{\langle n \rangle^n}{n!} e^{-\langle n \rangle}.
\tag{5.50}
$$

This is what we wanted to show, namely that far above threshold, the probability distribution of n photons is Poissonian with a variance equal to the expected photon number, exactly like that for the coherent state, Eq. (4.42). Recall the discussion in section 3.4 where it was found that the coherent state is afflicted by quantum vacuum fluctuations. But as the photon number grows (i.e., as the amplitude increases) the vacuum fluctuations in the photon number becomes less and less important. At a sufficiently large amplitude, light in a quantum coherent state can be considered a very good approximation to classical coherent light. This must be valid for the laser radiation as well, since it obeys the same photon statistics. For the coherent state there was also the issue with the uncertainty in the phase. An investigation into the phase of the laser is done in section 5.4.

---

[3] For the reader interested in cross-referencing with the alternative approach in [1], we make a note that the quantity $\mathcal{A}/\mathcal{B}$ is the *saturation photon number* n_s.

5.3 The degrees of first- and second-order coherence

The calculations in chapter 4 showed that the degree of first-order coherence for single-mode light was identical in both the coherent state, the Fock state and the mixed thermal state. Since we are assuming a single-mode laser field we expect that the degree of first-order coherence for the laser beam is still simply

$$g^{(1)}(\tau) = e^{i\Omega\tau} \tag{5.51}$$

i.e., that the laser also is first-order coherent for all pairs of space-time points. However, the degree of second-order coherence is a more mercurial, and hence intriguing, quantity.

Below threshold $\mathcal{A} < \mathcal{C}$

We first calculate $g^{(2)}(\tau)$ for the linear approximation $\mathcal{B} = 0$, i.e., below threshold. Recall that

$$g^{(2)}(\tau) = \frac{\operatorname{tr}\left(\rho \hat{a}^\dagger \hat{a}^\dagger \hat{a}\hat{a}\right)}{\left[\operatorname{tr}\left(\rho \hat{a}^\dagger \hat{a}\right)\right]^2} \tag{5.52}$$

Inserting Eq. (5.40) into this gives

$$g^{(2)}(\tau) = \frac{\displaystyle\sum_{n=0}^{\infty}(\mathcal{A}/\mathcal{C})^n(1 - \mathcal{A}/\mathcal{C}) \langle n| \hat{a}^\dagger \hat{a}^\dagger \hat{a}\hat{a} |n\rangle}{\left[\displaystyle\sum_{n=0}^{\infty}(\mathcal{A}/\mathcal{C})^n(1 - \mathcal{A}/\mathcal{C}) \langle n| \hat{a}^\dagger \hat{a} |n\rangle\right]^2}$$

$$= \frac{\displaystyle\sum_{n=0}^{\infty}(\mathcal{A}/\mathcal{C})^n n(n-1)}{\left[\displaystyle\sum_{n=0}^{\infty}(\mathcal{A}/\mathcal{C})^n n\right]^2}(1 - \mathcal{A}/\mathcal{C})^{-1} \tag{5.53}$$

The denominator is calculated first

$$\sum_{n=0}^{\infty}(\mathcal{A}/\mathcal{C})^n n = x\sum_{n=0}^{\infty} n x^{n-1} = x\frac{\mathrm{d}}{\mathrm{d}x}(1-x)^{-1}$$

$$= (\mathcal{A}/\mathcal{C})(1 - \mathcal{A}/\mathcal{C})^{-2} \tag{5.54}$$

and a similar approach for the numerator gives

$$\sum_{n=0}^{\infty}(\mathcal{A}/\mathcal{C})^n n(n-1) = 2(\mathcal{A}/\mathcal{C})^2(1 - \mathcal{A}/\mathcal{C})^{-3} \tag{5.55}$$

Thus the degree of second-order coherence becomes

$$g^{(2)}(\tau) = \frac{2(\mathcal{A}/\mathcal{C})^2(1 - \mathcal{A}/\mathcal{C})^{-4}}{\left[(\mathcal{A}/\mathcal{C})(1 - \mathcal{A}/\mathcal{C})^{-2}\right]^2} = 2 \qquad (\mathcal{A} < \mathcal{C}) \tag{5.56}$$

This is in agreement with the statement that below threshold, the laser radiation is like black-body thermal radiation. We have previously shown that $g^{(2)}(0) = 2$ for classical chaotic light and light in a thermal state. Below threshold then, according to the criterion Eq. (1.70), the laser beam is second-order *incoherent* and it will display photon bunching (according to the discussion in section 4.5.2).

Above threshold $\mathcal{A} > \mathcal{C}$

We repeat the procedure for finding the degree of second-order coherence, now above threshold. The density operator from Eq. (5.47) is inserted into Eq. (5.52)

$$g^{(2)}(\tau) = \frac{\displaystyle\sum_{n=0}^{\infty}(\langle n \rangle + \mathcal{A}/\mathcal{B})^{n+\mathcal{A}/\mathcal{B}}/(n + \mathcal{A}/\mathcal{B})!\, e^{-(\langle n \rangle + \mathcal{A}/\mathcal{B})} \langle n| \hat{a}^{\dagger}\hat{a}^{\dagger}\hat{a}\hat{a} |n\rangle}{\left[\displaystyle\sum_{n=0}^{\infty}(\langle n \rangle + \mathcal{A}/\mathcal{B})^{n+\mathcal{A}/\mathcal{B}}/(n + \mathcal{A}/\mathcal{B})!\, e^{-(\langle n \rangle + \mathcal{A}/\mathcal{B})} \langle n| \hat{a}^{\dagger}\hat{a} |n\rangle\right]^{2}}$$

$$= \frac{\displaystyle\sum_{n=0}^{\infty}n(n-1)(\langle n \rangle + \mathcal{A}/\mathcal{B})^{n+\mathcal{A}/\mathcal{B}}/(n + \mathcal{A}/\mathcal{B})!}{\left[\displaystyle\sum_{n=0}^{\infty}n(\langle n \rangle + \mathcal{A}/\mathcal{B})^{n+\mathcal{A}/\mathcal{B}}/(n + \mathcal{A}/\mathcal{B})!\right]^{2}}\, e^{\langle n \rangle + \mathcal{A}/\mathcal{B}} \qquad (5.57)$$

yielding

$$g^{(2)}(\tau) = \frac{(\langle n \rangle + \mathcal{A}/\mathcal{B})e^{2(\langle n \rangle + \mathcal{A}/\mathcal{B})}}{\left[\langle n \rangle e^{2(\langle n \rangle + \mathcal{A}/\mathcal{B})}\right]^{2}} = 1 + \frac{\mathcal{A}}{\langle n \rangle^{2}\mathcal{B}} \qquad (\mathcal{A} > \mathcal{C}) \qquad (5.58)$$

Then from Eq. (5.49) we see that above threshold, as the mean photon number increases, $g^{(2)}(\tau) \to 1$. Thus

$$g^{(2)}(\tau) = |g^{(1)}(\tau)| = 1$$

and laser light far above threshold is first- and second-order *coherent*.

5.4 Phase drift

In the previous sections we have seen that far above threshold, the photons statistics of the laser radiation is equal to that of the coherent state and that the laser beam is *coherent* with $g^{(2)}(\tau) = |g^{(1)}(\tau)| = 1$. This is the basis of the claim that a laser beam is the best candidate for coherent light. However, laser light has one very distinct trait that is not found in coherent light, namely *phase drift*. Recall the phase diagram for the coherent state, Fig. 3.2, which showed the minimum uncertainty in both the photon number (i.e., the amplitude) and the phase. The same applies for the laser, but one has to take into account that spontaneous emission into the laser mode is a random contribution to the field state.
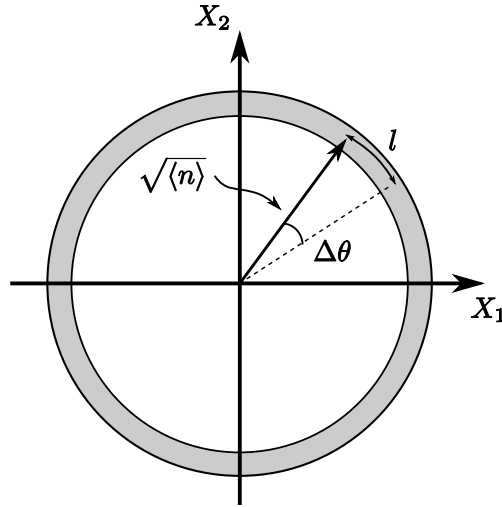
Figure 5.3: The uncertainty in both the amplitude and phase can be viewed as a "noise cloud" on the tip of the quadrature vector. Spontaneous emissions to the laser mode give random perturbations to the phase so that quadrature vector with the "noise cloud" at the tip will random-walk a length l in $\mathcal{A}\tau$-steps, and eventually drift over the entire 2π-annulus.

Above threshold, the spontaneous emission of photons into the lasing mode can be seen as noise in the laser field. The spontaneous emission of a single photon corresponds to the addition of an arrow of unit length and random orientation at the end of the quadrature vector in the phase-diagram of the coherent state, see Fig. 3.2. Repeated emissions causes the tip of the total field vector to move like a random walker and eventually diffuse the phase until it is equally distributed over 2π. This can be seen as a *noise annulus* in Fig. 5.3.

In section 1.3.2 we saw that the degree of first-order coherence is a Fourier pair with the power spectral density. Single-mode coherent light has $g^{(1)}(\tau) = e^{i\omega\tau}$, with the result that the spectral power density becomes the Delta function, which is interpreted as zero spread in the frequency distribution. It will be shown that the laser beam will in fact have a non-vanishing linewidth, although this is not associated with there being a spread in the angular frequency per se (we assume a single-mode laser field), but rather it is the consequence of the random phase drift due to spontaneous emissions.

The linewidth due to phase fluctuations will be investigated in two ways. First we present the phase diffusion model and second we calculate the off-diagonal elements of the equation of motion for the density matrix. They both give the same result, but the former gives a more intuitive explanation, as the physics are more convoluted in the latter.

5.4.1   The phase diffusion model

Far above threshold, we have seen that the laser radiation follows Poissonian statistics. From Eq. (3.61) we know that the standard deviation in the phase of a coherent state is

$$\Delta \theta = \frac{1}{2\Delta n} = \frac{1}{2\sqrt{\langle n \rangle}} \tag{5.59}$$

and from Eq. (3.45) the amplitude is $|\alpha| = \sqrt{\langle n \rangle}$. The positive frequency part of the electric field is then

$$E^{(+)}(t) = \mathcal{E}\sqrt{\langle n \rangle}e^{i(\theta(t)-\Omega t)} \tag{5.60}$$

and $\mathcal{E} \equiv \sqrt{\hbar\Omega/2\epsilon_0 L^3}$. It is assumed that the laser is operating sufficiently above threshold that the amplitude fluctuations are negligible. $\theta(t)$ is the angular displacement of the vector and $\langle n \rangle$ is the steady-state mean photon number from Eq. (5.48).

The effect of the spontaneous emission on the phase of the laser field is that the change in the phase $\Delta\theta$ after a time duration τ is related to the distance l which the vector has travelled along the noise annulus. If each spontaneous emission event is associated with a randomly oriented unit vector the change becomes

$$\Delta\theta = \frac{l}{\sqrt{\langle n \rangle}}. \tag{5.61}$$

as seen in Fig. 5.3, with the mean-square value

$$\bar{l}^2 = 1/2. \tag{5.62}$$

The one-dimensional random-walk theory says that the normalised probability that the distance l travelled after $\mathcal{A}\tau$ steps is [1]

$$p(l) = \frac{1}{\sqrt{2\pi\bar{l}^2\mathcal{A}\tau}}e^{-l^2/2\bar{l}^2\mathcal{A}\tau} \tag{5.63}$$

With a change of variables as prescribed in Eq. (5.61) this becomes the normalised probability of the angular displacement $\Delta\theta$

$$p(\theta) = \left(\frac{\langle n \rangle}{\pi\mathcal{A}\tau}\right)^{1/2} e^{-\langle n \rangle(\Delta\theta)^2/\mathcal{A}\tau} \tag{5.64}$$

The next step is to calculate the electric first-order correlation function, that is

$$\langle E^-(t)E^+(t+\tau)\rangle \equiv \langle E^-(0)E^+(\tau)\rangle \tag{5.65}$$

where we assume that $t = 0$, $\theta(0) = 0$ and $\Delta\theta = \theta(\tau) - \theta(0) \equiv \theta$. This gives the negative and positive frequency electric field parts

$$\begin{aligned} E^-(0) &= \mathcal{E}\sqrt{\langle n \rangle} \\ E^+(\tau) &= \mathcal{E}\sqrt{\langle n \rangle}e^{i(\theta-\Omega\tau)} \end{aligned} \tag{5.66}$$

and

$$\langle E^-(0)E^+(\tau)\rangle = \mathcal{E}^2\langle n\rangle e^{-i\Omega\tau}\langle e^{i\theta}\rangle \tag{5.67}$$

Then standard mathematical formularies gives the mean

$$\langle e^{i\theta}\rangle = \int_{-\infty}^{\infty} p(\theta)e^{i\theta}\mathrm{d}\theta = \left(\frac{\langle n\rangle}{\pi\mathcal{A}\tau}\right)^{1/2}\int_{-\infty}^{\infty} e^{-\langle n\rangle\theta^2/\mathcal{A}\tau}e^{i\theta}\mathrm{d}\theta$$
$$= e^{-\mathcal{A}\tau/4\langle n\rangle} \equiv e^{-\mathcal{D}\tau} \tag{5.68}$$

The degree of first-order coherence is thus

$$g^{(1)}(\tau) = e^{-i\Omega\tau-D\tau}. \tag{5.69}$$

Here $D \equiv \mathcal{A}/4\langle n\rangle$ is the diffusion coefficient[4]. We recognise the form of the Lorentzian distributed $g^{(1)}(\tau)$ in section 1.3.1. The power spectral density is then found by taking the Fourier transform of Eq. (5.69)

$$S(\Omega) = \frac{1}{\pi}\,\mathrm{Re}\int_0^{\infty} g^{(1)}(\tau)e^{i\Omega'\tau}\mathrm{d}\tau. \tag{1.49}$$

so that

$$S(\Omega) = \frac{1}{\pi}\,\mathrm{Re}\int_0^{\infty} e^{-[i(\Omega-\Omega')+D]\tau}\mathrm{d}\tau$$
$$= \frac{1}{\pi}\,\mathrm{Re}\int_0^{\infty} 2e^{-[i(\Omega-\Omega')+D]x^2}x\mathrm{d}x$$
$$= \frac{1}{\pi}\,\mathrm{Re}\,\frac{1}{i(\Omega-\Omega')+D}$$
$$= \frac{1}{2\pi}\frac{1}{(\Omega-\Omega')^2+D^2} \tag{5.71}$$

This is the Lorentzian frequency distribution centred at $\Omega' = \Omega$ with a linewidth (FWHM) of

$$\Delta\Omega = 2D = \frac{\mathcal{A}}{2\langle n\rangle}. \tag{5.72}$$

5.4.2   The off-diagonal elements of $\dot{\rho}_{nm}$

An alternative approach to determining the laser linewidth is to evaluate the off-diagonal elements of the field-density matrix. The electric field operator includes a linear combination of the photon creation and annihilation operators, so the off-diagonal elements

---

[4] We could also have noted that Eq. (5.64) obeys the standard diffusion equation

$$\dot{p}(\theta,t) = D\partial_\theta^2 p(\theta,t) \tag{5.70}$$

where $D = \mathcal{A}/4\langle n\rangle$.

of ρ_{nm} are essential for a complete description of the electric field. The diagonal elements ρ_{nn} of Eq. (5.30) approaches the non-zero steady-state values Eq. (5.43), but the off-diagonal elements decay to zero. The rate of decay of the off-diagonal elements implies a decay of the field, giving rise to the linewidth.

The electric field operator is, as usual,

$$\hat{E}(\mathbf{r}, t) = \left(\frac{\hbar \Omega_k}{2 \epsilon_0 L^3} \right)^{1/2} \left[\hat{a}_{\mathbf{k}} e^{i(\mathbf{k} \cdot \mathbf{r} - \Omega_k t)} + \hat{a}_{\mathbf{k}}^\dagger e^{-i(\mathbf{k} \cdot \mathbf{r} - \Omega_k t)} \right] \tag{5.73}$$

As the radiation field is assumed to be single-mode we drop the subscript $\mathbf{k}$ for notational relief. The expectation value (or statistical ensemble average) is

$$
\begin{aligned}
\langle \hat{E}(\mathbf{r}, t) \rangle &= \mathcal{E} \big[\operatorname{tr}\left(\rho(t) \hat{a} \right) e^{i(\mathbf{k} \cdot \mathbf{r} - \Omega t)} + \operatorname{tr}\left(\rho(t) \hat{a}^\dagger \right) e^{-i(\mathbf{k} \cdot \mathbf{r} - \Omega t)} \big] \\
&= \mathcal{E} \big[\operatorname{tr}\left(\rho(t) \hat{a} \right) e^{i(\mathbf{k} \cdot \mathbf{r} - \Omega t)} + \operatorname{tr}\left(\rho(t) \hat{a}^\dagger \right) e^{-i(\mathbf{k} \cdot \mathbf{r} - \Omega t)} \big] \\
&= \mathcal{E} \sum_{n=0}^{\infty} \big[\langle n | \rho(t) \hat{a} | n \rangle\, e^{i(\mathbf{k} \cdot \mathbf{r} - \Omega t)} + \langle n | \rho(t) \hat{a}^\dagger | n \rangle\, e^{-i(\mathbf{k} \cdot \mathbf{r} - \Omega t)} \big]
\end{aligned}
\tag{5.74}
$$

and $\mathcal{E} \equiv \sqrt{\hbar \Omega / 2 \epsilon_0 L^3}$. Then the mean positive and negative frequency parts are proportional to

$$\langle \hat{E}^{(+)}(t) \rangle \sim \sum_{n=0}^{\infty} \sqrt{n}\, \rho_{n,n-1}(t)$$

$$\langle \hat{E}^{(-)}(t) \rangle \sim \sum_{n=0}^{\infty} \sqrt{n+1}\, \rho_{n,n+1}(t)$$

that is, they are functions of the off-diagonal elements of the field density matrix. By taking the time derivative of $\langle \hat{E}^{(-)}(t) \rangle$, the relationship to Eq. (5.30) is readily established, where $\dot{\rho}_{n,n+1}$ is found by setting $m = n + 1$.

$$
\begin{aligned}
\dot{\rho}_{n,n+1} = &-\frac{\mathcal{N}'_{n,n+1} \mathcal{A}}{1 + \mathcal{N}_{n,n+1} \mathcal{B}/\mathcal{A}} \rho_{n,,n+1}(t) + \frac{\sqrt{n}\sqrt{n+1}\,\mathcal{A}}{1 + \mathcal{N}_{n-1,n} \mathcal{B}/\mathcal{A}} \rho_{n-1,n}(t) \\
&- \mathcal{C}(n + 1/2) \rho_{n,n+1}(t) + \mathcal{C}\sqrt{n+1}\sqrt{n+2}\, \rho_{n+1,n+2}(t)
\end{aligned}
\tag{5.75}
$$

For computational convenience we add some terms to $\dot{\rho}_{n,n+1}$

$$
\begin{aligned}
\dot{\rho}_{n,n+1} = &\dot{\rho}_{n,n+1} + \frac{\sqrt{n+1}\sqrt{n+2}\,\mathcal{A}}{1 + \mathcal{N}_{n,n+1} \mathcal{B}/\mathcal{A}} \rho_{n,n+1}(t) - \frac{\sqrt{n+1}\sqrt{n+2}\,\mathcal{A}}{1 + \mathcal{N}_{n,n+1} \mathcal{B}/\mathcal{A}} \rho_{n,n+1}(t) \\
&+ \mathcal{C}\sqrt{n}\sqrt{n+1}\, \rho_{n,n+1}(t) - \mathcal{C}\sqrt{n}\sqrt{n+1}\, \rho_{n,n+1}(t)
\end{aligned}
\tag{5.76}
$$

and we define

$$\frac{1}{2} \mu_{n,n+1} \equiv \frac{[\mathcal{N}'_{n,n+1} - \sqrt{n+1}\sqrt{n+2}]\mathcal{A}}{1 + \mathcal{N}_{n,n+1} \mathcal{B}/\mathcal{A}} + \mathcal{C}\big[(n + 1/2) - \sqrt{n}\sqrt{n+1} \big]$$

$$c_{n,n+1} \equiv \frac{\sqrt{n+1}\sqrt{n+2}\,\mathcal{A}}{1 + \mathcal{N}_{n,n+1} \mathcal{B}/\mathcal{A}} \tag{5.77}$$

$$d_{n,n+1} \equiv \mathcal{C}\sqrt{n}\sqrt{n+1}$$

Inserting these into Eq. (5.76) gives

$$
\begin{aligned}
\dot{\rho}_{n,n+1} = {} &-\frac{1}{2}\mu_{n,n+1}\rho_{n,n+1} - (c_{n,n+1} - d_{n,n+1})\rho_{n,n+1} \\
&+ c_{n-1,n}\rho_{n-1,n} + d_{n+1,n+2}\rho_{n+1,n+2}
\end{aligned}
\tag{5.78}
$$

where the explicit time-dependence of ρ has been suppressed for notational relief. Detailed balance when $\dot{\rho}_{n,n+1} = 0$ gives the recursive relation

$$
\rho_{n,n+1} = \frac{c_{n-1,n}}{d_{n,n+1}}\rho_{n-1,n} = \rho_{01}\prod_{j=1}^{n}\frac{c_{j-1,j}}{d_{j,j+1}}
\tag{5.79}
$$

which suggests a possible solution for $\rho_{n,n+1}(t)$

$$
\begin{aligned}
\rho_{n,n+1}(t) &= e^{-D_{n,n+1}(t)}\rho_{n,n+1}(0) \\
&= e^{-D_{n,n+1}(t)}\rho_{01}\prod_{j=1}^{n}\frac{c_{j-1,j}}{d_{j,j+1}}
\end{aligned}
\tag{5.80}
$$

where the off-diagonal elements are exponentially dampened by the factor $D_{n,n+1}$. We will show that this dampening factor is equal to that which was derived in the previous section.

Eq. (5.80) is used to express $\rho_{n+1,n+2}$ and $\rho_{n-1,n}$ in Eq. (5.78) in terms of $\rho_{n,n+1}$,

$$
\begin{aligned}
\rho_{n-1,n}(t) &= e^{-D_{n-1,n}}\rho_{0,1}\prod_{j=1}^{n-1}\frac{c_{j-2,j-1}}{d_{j-1,j}} \cdot e^{-(D_{n,n+1}-D_{n,n+1})} \cdot \frac{c_{n-1,n}}{d_{n,n+1}} \cdot \frac{d_{n,n+1}}{c_{n-1,n}} \\
&= e^{-(D_{n-1,n}-D_{n,n+1})}\frac{d_{n,n+1}}{c_{n-1,n}}\rho_{n,n+1}(t)
\end{aligned}
\tag{5.81}
$$

and

$$
\begin{aligned}
\rho_{n+1,n+2}(t) &= e^{-D_{n+1,n+2}}\rho_{0,1}\prod_{j=1}^{n+1}\frac{c_{j,j+1}}{d_{j+1,j+2}} \cdot e^{-(D_{n,n+1}-D_{n,n+1})} \\
&= e^{-(D_{n+1,n+2}-D_{n,n+1})}\frac{c_{n,n+1}}{d_{n+1,n+2}}\rho_{n,n+1}(t)
\end{aligned}
\tag{5.82}
$$

This gives

$$
\begin{aligned}
\dot{\rho}_{n,n+1}(t) = \bigg\{ &-\frac{1}{2}\mu_{n,n+1} - c_{n,n+1}\left[1 - e^{-(D_{n+1,n+2}-D_{n,n+1})}\right] \\
&- d_{n,n+1}\left[1 - e^{-(D_{n-1,n}-D_{n,n+1})}\right]\bigg\}\rho_{n,n+1}(t)
\end{aligned}
\tag{5.83}
$$

It is seen from Eq. (5.80) that

$$
\dot{\rho}_{n,n+1}(t) = -\dot{D}_{n,n+1}(t)\rho_{n,n+1}(0)
\tag{5.84}
$$

implying

$$
\dot{D}_{n,n+1}(t) \equiv \frac{1}{2}\mu_{n,n+1} + c_{n,n+1}\left[1 - e^{-(D_{n+1,n+2}-D_{n,n+1})}\right]
$$
$$
+ d_{n,n+1}\left[1 - e^{-(D_{n-1,n}-D_{n,n+1})}\right] \tag{5.85}
$$

Before proceeding, some simplifying assumptions must be made. If $D_{n,n+1}$ varies very little with n, so that $|D_{n-1,n} - D_{n,n+1}| \approx 0$ (and also $|D_{n+1,n+2} - D_{n,n+1}| \approx 0$), then the exponentials in Eq. (5.85) can be expanded to the lowest order, yielding

$$
\dot{D}_{n,n+1}(t) \cong \frac{1}{2}\mu_{n,n+1} \tag{5.86}
$$

or

$$
\mathrm{d}D_{n,n+1} = |D_{n-1,n} - D_{n,n+1}| \cong \frac{1}{2}\mu_{n,n+1}\mathrm{d}t
$$
$$
\Rightarrow \quad \left|\frac{\partial D}{\partial n}\right| \cong \frac{1}{2}\left|\frac{\partial \mu}{\partial n}\right| t \approx 0 \tag{5.87}
$$

meaning that $\mu_{n,n+1}$ is also a slowly varying function of n. We can then replace n with $\langle n \rangle$ so that

$$
\rho_{n,n+1}(t) \cong e^{-\frac{1}{2}\mu_{\langle n\rangle,\langle n\rangle+1}t}\rho_{n,n+1}(0) \tag{5.88}
$$

Thus the negative frequency part of the electric field operator becomes proportional to

$$
\langle E^{(-)}(t)\rangle \sim e^{-Dt}\sum_{n=0}^{\infty}\sqrt{n+1}\rho_{n,n+1}(0) \tag{5.89}
$$

where

$$
2D \equiv \mu_{\langle n\rangle,\langle n\rangle+1}. \tag{5.90}
$$

The linewidth of the laser operating above threshold, with $\langle n \rangle \gg 1$ is then found by solving Eq. (5.77),

$$
2D \cong \left\{\frac{\langle n\rangle + 3/2 + \mathcal{B}/8\mathcal{A} - (\langle n\rangle + 3/2 - 1/8(\langle n\rangle + 1)^{-1})}{1 + (\langle n\rangle + 3/2 + \mathcal{B}/16\mathcal{A})\mathcal{B}/\mathcal{A}}\right\}\mathcal{A}
$$
$$
+ \mathcal{C}\left[(\langle n\rangle + 1/2) - (\langle n\rangle + 1/2 - 1/8\langle n\rangle)\right]
$$
$$
\cong \frac{\mathcal{A} + \mathcal{C}}{4\langle n\rangle} \tag{5.91}
$$

Near threshold, where $\mathcal{A} \cong \mathcal{C}$, this is in full agreement with Eq. (5.72), namely

$$
2D \cong \frac{\mathcal{A}}{2\langle n\rangle}. \tag{5.92}
$$

5.4.3   Phase drift above threshold

The linewidth in the laser frequency distribution becomes narrower the farther above threshold the laser operation is, as seen from

$$2D = \frac{\mathcal{A} + \mathcal{C}}{4\langle n \rangle} \tag{5.93}$$

When $\mathcal{A} \gg \mathcal{C}$ this becomes

$$2D \cong \frac{\mathcal{A}}{4\langle n \rangle} \cong \frac{\mathcal{B}\mathcal{C}}{4\mathcal{A}} \ll \mathcal{B}/4 \tag{5.94}$$

The high monochromaticity and directionality of the contemporary laser is due to its narrow linewidth.

5.5   Summary and discussion

This chapter gave an introduction to the basic theory of the laser. The three-level model was used to demonstrate the underlying principles where population inversion and resonance with the laser radiation was assumed. However, to describe the lasing process it was sufficient to derive the equation of motion of the density operator for a two-level atom, which was the result of section 5.1.

In section 5.2 we saw that when the field gain is much larger than the losses from the laser mode, the laser field has the same photon statistics as that of light in a coherent state, namely Poissonian with a variance equal to the mean photon number in steady-state. We have also shown by calculating the degree of second-order coherence that the laser light is coherent.

Then, if the laser light is in a coherent state, with the minimal vacuum fluctuations in phase and amplitude (as shown in section 3.4), how long will the light stay coherent? The "problem" with the laser is that spontaneous emission into the laser mode disturbs both the amplitude and the phase of the light, i.e., there is a *random* addition to the system state in the form of a complex unit vector of random phase. While the random addition to the amplitude can be ignored since it is both small compared to the mean amplitude, but also as it is constrained to oscillate about $\sqrt{\langle n \rangle}$, the phase can change freely around the noise annulus shown in Fig. 5.3.

The random phase drift leads to a finite linewidth of the laser's power spectral density and the full-width at half maximum (FWHM) was determined by two different approaches in section 5.4. First by the phase diffusion model, where the physics of the problem is fairly intuitive and second, by finding the linewidth through dampening of the off-diagonal elements of the field-density operator. For laser operation far above threshold the dampening factor was shown to become very small, resulting in a narrow linewidth.

But, what does having phase drift mean in practice? Modern advances in laser technology has shown that the phase drift can be a slow process, and that it may take

on the order of minutes before the phase becomes uncorrelated [30]. Comparing to the time scales often used in experiments in quantum optics, this is a "small eternity", meaning that, yes, the laser operating far above threshold produces a light beam that is in a coherent state; with such a large amplitude that it is a very good approximation to classical coherent light and with a very narrow linewidth, so as to be nearly monochromatic.

However, that being said, the next and final chapter in this work will raise the question if the whole idea of the coherent state is even *necessary* for describing phenomena in quantum optics and if light in a coherent state has ever been produced, let alone measured.

Chapter 6

Unexpected coherence

So far in this work we have talked about coherent light and how it is modelled in both electromagnetism and quantum optics. The coherent state was introduced by Glauber as a more convenient set of basis states for calculations in quantum optics. We have seen in the previous chapters that light in the coherent state is indeed a good approximation to classical ideal wave, albeit with the unavoidable quantum vacuum fluctuations. But a question yet to be raised is; Are the coherent states *necessary* for describing phenomena in quantum optics, and have they ever really been observed in quantum optics? To conclude this work we will demonstrate that the concept of coherent light is indeed convenient, but not a requisite to explaining phenomena in quantum optics.

The Mølmer-model is investigated and numerically simulated, with the results demonstrating that two uncorrelated light beams illuminating two photodetectors will develop entanglement as a result of the measuring process. The behaviour of the state during photodetection is shown to be identical to that of a system in a product coherent state, even though initially the state is incoherent with a vanishing field expectation value.

6.1   The Mølmer-model

Klaus Mølmer proposes [31] an optical experiment where it is shown that observed interference can be explained without requiring the field modes to initially be coherent. The model is fairly simple, with two single-mode cavities, a and b, which are assumed to each be populated by n photons in the Fock producct state

$$|n, n\rangle = |n\rangle \otimes |n\rangle , \quad t = 0. \tag{6.1}$$

See Fig. 6.1 for an illustration. Partially transparent mirrors in front of the cavities emit photons at the rate of Γ, in modes of different angular frequencies ω_a and ω_b. The field from cavity a has a positive frequency part containing the annihilation operator $\hat{a}$, while the field from cavity b has a positive frequency part containing the annihilation operator
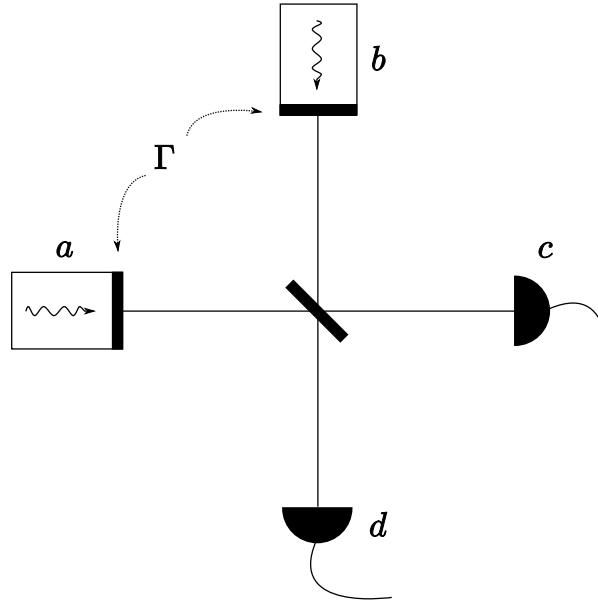
Figure 6.1: Setup of the optical experiment. The two cavities a and b are populated by n photons each and have partially transparent mirrors in the front, allowing photons to escape at the same rate Γ. The output beams are mixed in the lossless beam splitter, after which the resulting state is measured by either photodetector c or d depending on its linear combination.

$\hat{b}$. After escaping the cavities, the fields are combined in a lossless beam splitter such that the resulting linear superposition is

$$\hat{c} = (\hat{a} + \hat{b})/\sqrt{2} \quad \text{and} \quad \hat{d} = (\hat{a} - \hat{b})/\sqrt{2} \tag{6.2}$$

which are measured by the detectors c and d, respectively.

Mølmer points out that according to the density matrix method one would not expect any interference, i.e., no contribution to the field from terms containing creation and annihilation from each cavity $\sim \hat{a}^\dagger \hat{b}$. This is true if one initially defines the reduced density matrix of the *subsystems* (which is the cavities) ρ^a and ρ^b such that

$$\rho = \rho^a \otimes \rho^b. \tag{6.3}$$

This product state is a *pure state* with no correlations between the subsystems. For an observable $\hat{a}$ acting on a and $\hat{b}$ acting on b, the expectation value of the product operator $\hat{a}\hat{b}$ is then simply the product of the expectation values

$$\langle \hat{a}\hat{b} \rangle = \langle \hat{a} \rangle_a \langle \hat{b} \rangle_b \tag{6.4}$$

The expectation value of a lonesome annihilation operator is always zero when the field is in a Fock state, so any cross terms of the above type will vanish, hence no correlation between the cavities are expected[1].

---

[1] But keep in mind that the *total* system state after a photon emission is no longer pure, but rather a mixed state because of the coupling to an external reservoir. However, the cavities are isolated from each other and the emission by the one is not influenced by the other.

The initial state is not entangled and so there is an equal probability of a photon detection in c or d. Assume that the first detection happens at c. Then the state vector becomes

$$\hat{c}\,|n,n\rangle = \sqrt{\frac{n}{2}}[|n-1,n\rangle + |n,n-1\rangle] \tag{6.5}$$

which is an entangled state since the expectation value of cross terms $\sim \langle \hat{a}^\dagger \hat{b}\rangle$ is now non-zero. The detection rates are no longer equal for the detectors and if the angular frequencies of the two modes differ, the detection probabilities will oscillate at the frequency difference $\Delta\omega = \omega_a - \omega_b$.

One can interpret the entanglement as a direct consequence of measurement on the system. If there were no photodetectors present to measure the state and feed back the new information to the system, we would simply see two cavities ejecting photons randomly, but at equal rates. So without detection and collapsing of the wavefunction there is no coupling between the cavities and thus no entanglement.

The system wave function is propagated with the effective Hamiltonian

$$\begin{aligned}\hat{H}_{\text{eff}} &= \hbar\omega_a(\hat{a}^\dagger\hat{a} + 1/2) + \hbar\omega_b(\hat{b}^\dagger\hat{b} + 1/2) - i\hbar\frac{\Gamma}{2}(\hat{a}^\dagger\hat{a} + \hat{b}^\dagger\hat{b}) \\ &= \hat{H}_0 - \hat{H}_j \end{aligned} \tag{6.6}$$

which is non-Hermitian due to the last term on the right hand side. The time evolution of the system is interrupted at random times τ when a *quantum jump* occurs

$$|\psi\rangle \rightarrow \hat{c}\,|\psi\rangle, \hat{d}\,|\psi\rangle \tag{6.7}$$

which is to say that a photon is detected at either c or d. This reduces the initial total number of photons $2n$ by 1, and increases the overall photon detection counter q by 1. If at time $t = 0$ the field state is such that the total number of photons are

$$N(0) = \langle n,n|\,\hat{a}^\dagger\hat{a} + \hat{b}^\dagger\hat{b}\,|n,n\rangle = 2n \tag{6.8}$$

then the state at a later time T has

$$N(T) = 2n - q \tag{6.9}$$

photons. This implies that the field state can be written as

$$|\psi(t)\rangle = \sum_{k=0}^{q} c_k(t)\,|n-k, n-q+k\rangle. \tag{6.10}$$

The non-Hermitian part of Eq. (6.6), $\hat{H}_j$, acts identically on each state in the product $|\rangle \otimes |\rangle$, so it is sufficient to use only the Hermitian part to determine the time evolution of the amplitudes $c_k(t)$ in between jumps. From the time-dependent Schrödinger equation we have

$$i\hbar\frac{\partial}{\partial t}\,|\psi(t)\rangle = \left[\hbar\omega_a(\hat{a}^\dagger\hat{a} + 1/2) + \hbar\omega_b(\hat{b}^\dagger\hat{b} + 1/2)\right]|\psi(t)\rangle$$

$$i\hbar\sum_{k=0}^{q}\dot{c}_k(t)\,|n-k, n-q+k\rangle = \sum_{k=0}^{q} c_k(t)\big\{\hbar\omega_a[(n-k) + 1/2]$$

$$+ \hbar\omega_b[(n-q+k) + 1/2]\big\}\,|n-k, n-q+k\rangle \tag{6.11}$$

and

$$\begin{aligned}
\dot{c}_k(t) &= -ic_k(t)\big[n(\omega_a + \omega_b) - k(\omega_a - \omega_b) - \omega_b q + (\omega_a + \omega_b)/2\big] \\
&= ik\Delta\omega c_k(t) - ic_k(t)\big[(n + 1/2)(\omega_a + \omega_b) - \omega_b q\big] \\
&= ik\Delta\omega c_k(t)
\end{aligned} \tag{6.12}$$

where the last step is achieved by choosing some fancy rotating frame and setting $\Delta\omega = \omega_a - \omega_b$ [31]. The solution to $\dot{c}_k(t)$ is

$$\int_{c_k(t)}^{c_k(t+\tau)} \frac{\mathrm{d}c_k}{c_k} = \int_t^{t+\tau} ik\Delta\omega \mathrm{d}t'$$
$$\Rightarrow \qquad c_k(t + \tau) = c_k(t)e^{ik\Delta\omega\tau} \tag{6.13}$$

The total jump rate is calculated from the non-Hermitian part of Eq. (6.6),

$$\begin{aligned}
&\langle \hat{H}_j \rangle \\
&= i\hbar\frac{\Gamma}{2} \langle \psi(t)| \hat{a}^\dagger\hat{a} + \hat{b}^\dagger\hat{b} |\psi(t)\rangle \\
&= i\hbar\frac{\Gamma}{2} \sum_{k,k'=0}^{q} c_k^*(t)c_{k'}(t) \langle n - k, n - q + k| \hat{a}^\dagger\hat{a} + \hat{b}^\dagger\hat{b} |n - k', n - q + k'\rangle \\
&= i\hbar\frac{\Gamma}{2} \sum_{k,k'=0}^{q} c_k^*(t)c_{k'}(t) \left[\sqrt{(n - k)(n - k')} + \sqrt{(n - q + k)(n - q + k')} \right]\delta_{kk'} \\
&= i\hbar\frac{\Gamma}{2} \sum_k |c_k(t)|^2(2n - q) \\
&= i\hbar\frac{\Gamma}{2}(2n - q)
\end{aligned} \tag{6.14}$$

i.e., independent of the amplitudes c_k. Since we can write

$$\hat{a}^\dagger\hat{a} + \hat{b}^\dagger\hat{b} = \hat{c}^\dagger\hat{c} + \hat{d}^\dagger\hat{d} \tag{6.15}$$

the frequencies with which a quantum jump is performed to either c or d can be identified as

$$\begin{aligned}
\gamma_c &= \Gamma \langle \psi(t)| \hat{c}^\dagger\hat{c} |\psi(t)\rangle \\
\gamma_d &= \Gamma \langle \psi(t)| \hat{d}^\dagger\hat{d} |\psi(t)\rangle
\end{aligned} \tag{6.16}$$

In other words

$$\Gamma(2n - q) = \gamma_c + \gamma_d. \tag{6.17}$$

This means that the time between jumps is exponentially distributed since the change in the photon number goes as the rate

$$\frac{\mathrm{d}N}{\mathrm{d}t} = -(\gamma_c + \gamma_d)N = -\Gamma(2n - q)N$$
$$\Rightarrow \qquad \frac{N(t + \tau)}{N(t)} = e^{-\Gamma(2n-q)\tau} \equiv \epsilon \tag{6.18}$$

where ϵ is in effect a random, dimensionless number between 0 and 1.

We also know that

$$\hat{c}^\dagger\hat{c} = \hat{a}^\dagger\hat{a} + \hat{b}^\dagger\hat{b} + \hat{a}^\dagger\hat{b} + \hat{b}^\dagger\hat{a} = \hat{a}^\dagger\hat{a} + \hat{b}^\dagger\hat{b} + 2\,\mathrm{Re}\,\{\hat{a}^\dagger\hat{b}\} \tag{6.19}$$

giving the rate of photon detection at detector c

$$\gamma_c = \Gamma\langle\hat{a}^\dagger\hat{a} + \hat{b}^\dagger\hat{b} + 2\,\mathrm{Re}\,\{\hat{a}^\dagger\hat{b}\}\rangle = \Gamma[2n - q + 2\,\mathrm{Re}\,Q] \tag{6.20}$$

and similarly the rate at detector d

$$\gamma_d = \Gamma\langle\hat{a}^\dagger\hat{a} + \hat{b}^\dagger\hat{b} - 2\,\mathrm{Re}\,\{\hat{a}^\dagger\hat{b}\}\rangle = \Gamma[2n - q - 2\,\mathrm{Re}\,Q] \tag{6.21}$$

where Q is non-zero for an entangled state

$$
\begin{aligned}
Q &= \langle\hat{a}^\dagger\hat{b}\rangle = \langle\psi(t)|\,\hat{a}^\dagger\hat{b}\,|\psi(t)\rangle \\
&= \sum_{k,k'=0}^{q-1} c_{k'}^*(t)c_k(t)\,\langle n-k', n-q+k'|\,\hat{a}^\dagger\hat{b}\,|n-k, n-q+k\rangle \\
&= \sum_{k,k'=0}^{q-1} c_{k'}^*(t)c_k(t)\sqrt{n-k'}\sqrt{n-q+k} \\
&\qquad\qquad \times \langle n-k'-1, n-q+k'\,|n-k, n-q+k-1\rangle \\
&= \sum_{k,k'=0}^{q-1} c_{k'}(t)^*c_k(t)\sqrt{n-k'}\sqrt{n-q+k}\,\delta_{k,(k'+1)} \\
&= \sum_{k=0}^{q-1} c_k(t)^*c_{k+1}(t)\sqrt{n-k}\sqrt{n-(q-1)+k} \tag{6.22}
\end{aligned}
$$

When the $\hat{c}$ or $\hat{d}$ annihilation operator acts on the field state, q is increased by unity,

$$
\begin{aligned}
(\hat{a}\pm\hat{b})\,|\psi(t)\rangle &= (\hat{a}\pm\hat{b})\sum_{k=0}^{q} c_k(t)\,|n-k, n-q+k\rangle \\
&= \sum_{k=0}^{q+1} c_k(t)\big[\sqrt{n-k}\,|n-k-1, n-q+k\rangle \\
&\qquad\qquad \pm \sqrt{n-q+k}\,|n-k, n-(q+1)+k\rangle\big] \\
&= \sum_{k'=0}^{q+1} c_{k'-1}(t)\sqrt{n-k'+1}\,|n-k', n-(q+1)+k'\rangle \\
&\qquad\qquad \pm \sum_{k=0}^{q+1} c_k(t)\sqrt{n-q+k}\,|n-k, n-(q+1)+k\rangle \\
&= \sum_{k=0}^{q+1} c_k(t)'\,|n-k, n-(q+1)+k\rangle \tag{6.23}
\end{aligned}
$$

where

$$c_k(t)' = c_{k-1}(t)\sqrt{n-(k-1)} \pm c_k(t)\sqrt{n-q+k}. \tag{6.24}$$

After each photon detection Eq. (6.10) is updated with the new amplitude $c_k(t)'$, with a suitable normalisation such that $\sum_k |c_k(t)'|^2 = 1$.

6.2 The numerical recipe

We now have all the ingredients needed to run a Monte Carlo simulation of the optical experiment. A (semi-) random number generator provides the value of ϵ uniformly distributed $\in [0,1]$, which determines the time τ from Eq. (6.18) at which the next quantum jump will take place (i.e., a photon detection)

$$\tau = -\frac{\ln(\epsilon)}{\Gamma(2n-q)} \tag{6.25}$$

Exactly which detector does the detecting depends on the ratio of γ_c and γ_d. In practise this comes down to whether Q is positive or negative. If Q is positive then detector c is more likely to detect a photon than d is, and vice versa for a negative value of Q. For example, the rate of jumps to $c(d)$ is given by

$$\gamma'_{c(d)} \equiv \frac{\gamma_{c(d)}}{\Gamma(2n-q)} = 1 \pm \frac{2\,\mathrm{Re}\,Q}{\Gamma(2n-q)} = 1 \pm x \tag{6.26}$$

So the corresponding probability is just the normalised rate

$$p_{c(d)} = (1 \pm x)N. \tag{6.27}$$

The normalisation N factor is readily found to be

$$p_{\text{total}} = p_c + p_d = 2N \equiv 1 \quad \Rightarrow \quad N = \frac{1}{2}. \tag{6.28}$$

The probability that a photon is detected at c or d is thus

$$p_{c(d)} = \frac{1}{2}(1 \pm x). \tag{6.29}$$

A second random number ϵ' is drawn, and if $\epsilon' \in [0, p_c]$, then a jump to c has occurred. On the other hand, if $\epsilon' \in (p_c, 1]$, the photon is detected at d. The scheme is described in pseudo-code in Algorithm 1 and the Matlab script is found in Appendix C.2.

6.3 The results of the simulation

Staying true to the original article [31] we have chosen identical parameters where given. The initial number of photons in each cavity is $n = 10^5$, the frequency difference

---

Algorithm 1 Quantum jump

---

procedure MOLMER(n,q_{max},$\Delta\omega$, Γ)
   $q \leftarrow 0$ ▷ Initially no detected photons
   $c_k \leftarrow 1$ ▷ Initial state is $|n, n\rangle$

   while detected photons $q < q_{max}$ **do**
      $\tau \leftarrow -\ln(\text{random})/\Gamma(2n - q)$ ▷ Next jump occurs at τ
      $c_k \leftarrow c_k e^{ik\tau\Delta\omega}$ ▷ Time evolve according to Hamiltonian

      for $k \leftarrow 1, q - 1$ **do**
         $Q \leftarrow Q + \sqrt{n - k}\sqrt{n - q + k + 1}c_k^* c_{k+1}$ ▷ Calculate Q
      end for
      $x \leftarrow 2\,\mathrm{Re}\,Q/\Gamma(2n - q)$
      $\epsilon' \leftarrow$ random number $\in [0, 1]$

      if $\epsilon' < (1 + x)/2$ **then**
         $|\psi\rangle \leftarrow \hat{c}\,|\psi\rangle$ ▷ Jump to c
      else
         $|\psi\rangle \leftarrow \hat{d}\,|\psi\rangle$ ▷ Jump to d
      end if

      for $k \leftarrow 1, q + 1$ **do**
         $c_k \leftarrow \sqrt{n - k + 1}c_{k-1} \pm \sqrt{n - q + k}c_k$ ▷ Jump to c/d
      end for
      $q \leftarrow q + 1$ ▷ increase photon count
   end while
end procedure

$\Delta\omega = 1000\Gamma$ and the simulation is stopped when a total of $q = 3000$ photons has been detected. The field dampening rate Γ is the only parameter not explicitly defined, but the simulation behaved quite nicely for Γ equal to unity.

In Fig 6.2 we see that the rates of photon detection in either detector varies sinusoidally. Initially the probability for a photon to make a quantum jump to c or d is equal, however, after only a few detections a trend is established where photons are exclusively detected at c and no photons are found by d, and vice versa. This is closely related to the sinusoidal evolution of the "entanglement" factor Q. After a short time initially where the physical quantities are smothered by randomness, Q undergoes a smooth harmonic evolution during the jumps which is seen in Fig. 6.3. The maxima and minima of Q can be identified with detection of solely c-mode or d-mode photons, respectively.
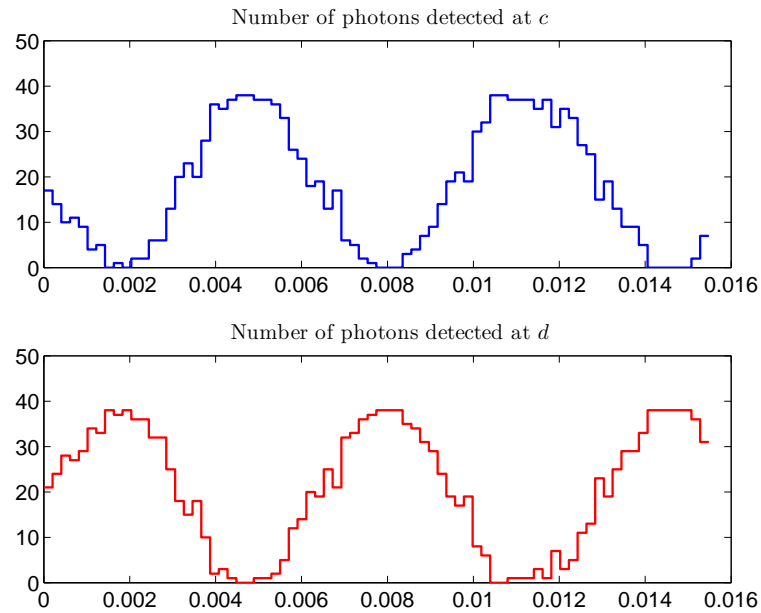
Figure 6.2: The number of photons detected at (upper) detector c and (lower) at detector d. The duration of each "bin" in the stair-diagram is $\Delta t = 0.0002\Gamma^{-1}$.
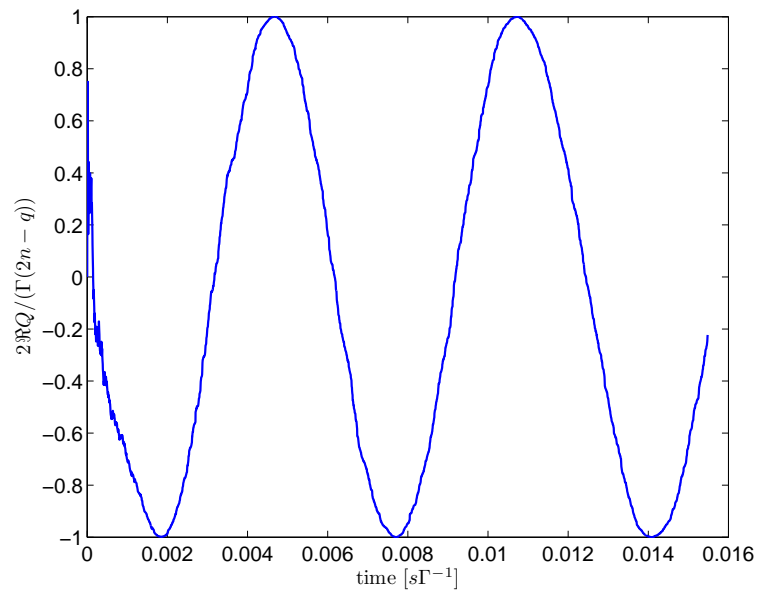

Figure 6.3: The time evolution of the "entanglement" variable Q during quantum jumps represented as the normalised quantity $2\operatorname{Re}Q/(\Gamma(2n-q))$ for $q = [0, 3000]$. We clearly see the transition from initial randomness to steady harmonic variation.

In fact, the smooth behaviour of Q closely resembles that which one would expect if the cavity modes had been prepared in coherent states instead. If the initial state of the system had been the product coherent state

$$|\psi(0)\rangle = |\alpha, \beta\rangle = |\alpha\rangle \otimes |\beta\rangle \tag{6.30}$$

where $|\alpha\rangle$ is the eigenstate of $\hat{a}$ and $|\beta\rangle$ the eigenstate of $\hat{b}$, then the annihilation operators $\hat{a}$ and $\hat{b}$ would have no effect on the kets, i.e., the state would be unchanged during jumps. However, in-between jumps the state would evolve according to the Hamiltonian. The time evolution of a coherent state can be found by writing it in terms of a Fock-state on which the time evolution operator is be applied:

$$|n(t)\rangle = \hat{\mathcal{U}}(t)|n(0)\rangle = e^{-i\hat{H}t/\hbar}|n(0)\rangle \tag{6.31}$$

For instance, the coherent state $|\alpha\rangle$, in terms of the Fock-state is

$$|\alpha\rangle = e^{-|\alpha|^2/2} \sum_{n=0}^{\infty} \frac{\alpha^n}{\sqrt{n!}} |n\rangle \tag{3.43}$$

and the effective Hamiltonian gives the eigenenergy

$$E_a = \langle \hat{H}_{eff,a} \rangle = \hbar[\omega_a - i\Gamma/2]\langle \hat{a}^\dagger \hat{a} \rangle = \hbar[\omega_a - i\Gamma/2]n \tag{6.32}$$

where we have redefined the energy-origin to get rid of the zero-energy term in $\hat{H}$. This gives

$$\begin{aligned}
|\alpha(t)\rangle &= e^{-|\alpha|^2/2} \sum_{n=0}^{\infty} \frac{\alpha^n}{\sqrt{n!}} |n(t)\rangle \\
&= e^{-|\alpha|^2/2} \sum_{n=0}^{\infty} \frac{\alpha^n}{\sqrt{n!}} e^{-iE_a t/\hbar} |n(0)\rangle \\
&= e^{-|\alpha|^2/2} \sum_{n=0}^{\infty} \frac{1}{\sqrt{n!}} \left(\alpha e^{-i\omega_a t - \Gamma t/2}\right)^n |n(0)\rangle \\
&= \left|\alpha e^{-i\omega_a t - \Gamma t/2}\right\rangle
\end{aligned} \tag{6.33}$$

The same argument is valid for $|\beta\rangle$, thus the evolution of the two-mode product state is

$$|\alpha, \beta\rangle \rightarrow \left|\alpha e^{-i\omega_a t - \Gamma t/2}, \beta e^{-i\omega_b t - \Gamma t/2}\right\rangle. \tag{6.34}$$

The rates of the detection events in this case is

$$\gamma_{c(d)} = \Gamma\left[|\alpha|^2 + |\beta|^2 \pm 2|\alpha||\beta|\cos(\Delta\omega t + \phi)\right] e^{-\Gamma t} \tag{6.35}$$

where the c-numbers α, β are defined as

$$\alpha = |\alpha|e^{i\phi_a} \quad \text{and} \quad \beta = |\beta|e^{i\phi_b} \tag{6.36}$$

and $\phi = \phi_a - \phi_b$ is some random relative phase. Then the coherent state-equivalent to the "entanglement" factor Q is here the term
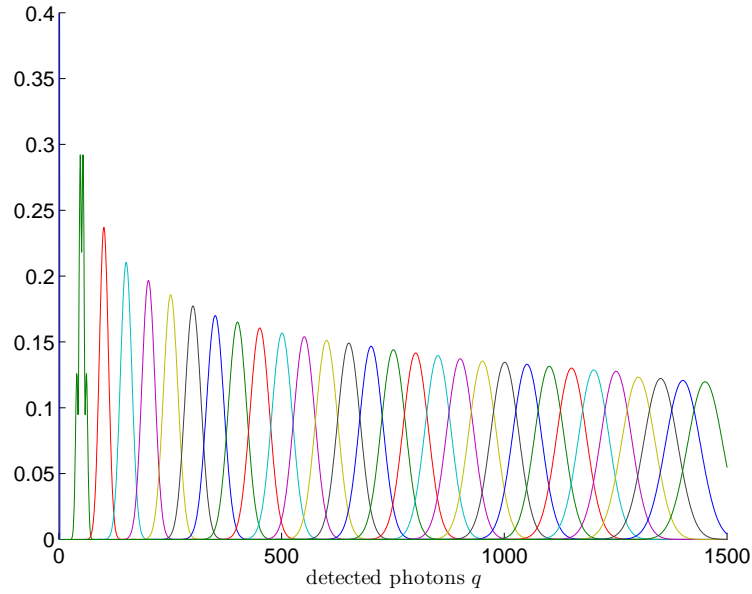
$$|\alpha||\beta|\cos(\Delta\omega t + \phi).$$

Figure 6.4: The time evolution of the c_k amplitudes, here calculated numerically as $|c_k|^2$. The x-axis shows k, where $k \in [0, q]$, which increases by unity for every time step in the simulation, i.e., for every new photon detected. In this plot only the probabilities at every 100 detection is shown, with increasing k from left to right. As expected, the most likely state of the system is that the $2n - q$ photons left are equally distributed in the cavities a and b.

It exhibits the same sinusoidal behaviour as Q for the product number state-case, with a period equal to the frequency difference of the two cavity modes.[2] In the simulation there are no mean fields (i.e., $Q = 0$) neither initially nor during the jumps. But during the jumps (or detections if you will), mean fields are measured and the resulting entangled state behaves similarly to a product coherent state.

We can also numerically verify that the amplitudes c_k evolve smoothly during jumps, see Fig. 6.4. The figure shows $|c_k|^2$ for the kth photon detected, where $k \in [0, q]$ increases by unity for every time step in the simulation, i.e., for every new photon detected. In this plot only the probabilities at every 100 detection is shown, with increasing k from left to right. As expected, the most likely state of the system is that the $2n - k$ photons left are equally distributed in the cavities a and b. That is, $|c_k|^2$ is strongly peaked at $k/2$.

---

[2] It is quite mind boggling and unintuitive that the amplitude of the coherent state is not reduced by the detection of photons leaving the cavities, but rather by *no* photon emission at all! This can be explained by Bayesian probability theory where for each time step of no-detection it is more likely that the system (i.e., source atom) already has emitted the photon and is in the ground state [32].

6.4   Summary and discussion

The conclusion to be drawn from the Mølmer-model is that it is not necessary to require the cavity modes to be coherent initially. The apparent coherent behaviour is a consequence of measurement on the state and thereby collapse of the wave function. Feeding the information of which state the system is in, back to the system, will induce entanglement between the cavity modes, thus introducing a coherent behaviour. Another thing is that it does not in particular matter what the frequency difference $\Delta\omega$ is, only that it is non-zero. The entanglement will still occur as Q will still be sinusoidal; only the period of the oscillations will be affected.

Some of the points Mølmer makes in [31] follows. The physical difference between an ensemble of number states and an ensemble of coherent states lies in the ensemble averaged density matrix. If this is the same for both ensembles, then even if we have precise knowledge that there is no mean electric field (i.e., $\langle E^{(+)} \rangle = 0$), we may still utilize coherent states in the calculations.

Also, formally the one- and two-time expectation values (i.e., $\langle \hat{a}(t) \rangle$ and $\langle \hat{a}^\dagger(t)\hat{a}(t+\tau) \rangle \sim g^{(1)}(\tau)$) obey the same set of equations (through the quantum regression theorem, which we won't go into). So the application of non-vanishing means produces correct quantitative results, not for one-time means and products like $\langle \hat{a}(t) \rangle$, but for expectation values like $\langle \hat{a}^\dagger(t)\hat{a}(t+\tau) \rangle$. In the typical photodetection experiment it is the degree of second-order coherence that is measured. If it uses two single-mode sources that are uncorrelated, like in the Mølmer model, there is no contribution from terms involving $\hat{a}^\dagger\hat{b}$, $\hat{b}^\dagger\hat{a}$. However, the relative intensity correlation function will contain a term proportional to $\langle \hat{a}^\dagger(t)\hat{a}(t+\tau)\hat{b}^\dagger(t+\tau)\hat{b}(t) \rangle$ which is non-vanishing and proportional to the product of $\langle \hat{a}^\dagger(t)\hat{a}(t+\tau) \rangle$ and $\langle \hat{b}^\dagger(t)\hat{b}(t+\tau) \rangle$ (similar to what we saw for the intensity interferometer in section 2.3). This contribution can be mistaken for an interference peak due to a non-vanishing mean field, i.e., that the light beam impinging on the detectors is in a coherent state, when in fact this is not the case.

Mølmer also puts forward that a closer scrutiny of the mechanism behind many quantum optical experiments will reveal that it is not necessary to use light beams initially prepared in coherent states, as it is the backaction of the information gained in measuring the system that is the true source of entanglement. In addition it is likely that *no* coherent electric fields in the optical regime has been observed yet, or even created, as that would require classical oscillators (i.e., a moving charge distribution) and not quantum systems with a vanishing dipole moment. However, for low non-optical frequencies, classically moving charged objects do exist and they do emit coherent radiation.

Another interesting point is that in the simulations of the Mølmer model, the entanglement is not so fragile as to be destroyed by the influence of the environment, in this case by physical observation. Coherent states are usually considered to be more robust in this sense as the act of observation of the field leaves the state unaltered (which we have discussed in both the previous section and in section 3.4).

Chapter 7

Concluding remarks

For brevity the reader is referred to the end-section of each chapter for a detailed summary of our investigation. Here we will simply try to answer the questions posed in the Introduction.

What is coherence and how is it quantified, calculated, measured? In this work both the classical and the quantum mechanical side of *coherence* has been looked into. A collective term may be optical coherence theory, including the degrees of Nth-order coherence, of which only the first two has been studied here. So we know the *mathematics* of coherence; in the classical sense it is the time average of two functions multiplied together and whenever these behave "similarly" there is a positive, or constructive, addition to the average, and a negative, destructive, addition when they behave "dissimilarly". In the quantum mechanical sense coherence is calculated as the expectation value of the field operators. Nevertheless, the term coherence in itself is a concept that is somewhat hard to quantify the precise meaning of. To speak in the broadest sense, optical coherence theory is a statistical description of fluctuations that can be found in any optical field in nature [33]. Coherence can be said to be the manifestation of correlations between such fluctuations.

In section 2.2 we saw that the degree of first-order coherence can be measured by finding the visibility of the interference fringes that arise from superposing two electric fields. $g^{(1)}(\tau)$ can also be found by measuring the power spectral density of the field. The intensity interferometer measures the degree of second-order coherence, as seen in section 2.3.

What is the difference between coherent light and incoherent light? Coherent light in this work is regarded as having degrees of first- and second-order coherence equal to unity

$$|g^{(1)}(\tau)| = 1 \quad \text{and} \quad g^{(2)}(\tau) = 1. \tag{1.70}$$

It was found in sections 1.4 and 4.1 that only the classical ideal wave and single-mode light in a coherent state is coherent (but this can also be shown for multi-mode light). Far above threshold, laser light is approximately coherent as well (section 5.3).

Can light be something in-between? By referring to the degree of first-order coherence, light can be coherent, incoherent or *partially* coherent, as seen from the derivation of the limits in sections 1.3 and 3.2. But from the definitions and the criterion Eq. (1.70) it is seen that light is either second-order coherent or second-order incoherent.

Can coherence be explained by both classical theory and quantum mechanics? Are the explanations equivalent? The full theory of coherence covers both the classical electromagnetic theory and the quantum optical theory. In our calculations of $g^{(1)}(\tau)$ and $g^{(2)}(\tau)$ for light in the coherent state and in the mixed thermal state (section 4), the results were analogous to their classical counterparts, the stable, ideal wave and chaotic light. However, one must keep in mind that the quantum theory carries with it inevitable vacuum fluctuations that are not present in classical theory. For the thermal state an additional factor representing a source-correlation correction turned up.

Does it matter which statistical properties the light has? We saw in section 4.2 that for light in a Fock state, which does not have a classical equivalent, its photon statistics led to classically illegal values of $g^{(2)}(\tau)$. This gives rise to photon antibunching, a purely quantum mechanical characteristic.

The unasked questions

Along the way we also stumbled upon other key points of interest, like the Hanbury Brown-Twiss effect, which was shown in section 2.3 to be an excess in the intensity correlation due to classical chaotic light having $g^{(2)}(0) = 2$. In the quantum picture this was seen to manifest as photon bunching. Coherent light did not exhibit neither.

How similar is laser radiation really to classical coherent light? The route to the answer goes first through the coherent state. Far above threshold the laser beam has the same photon statistics and degrees of first- and second-order coherence as the coherent state, albeit with random perturbations due to spontaneous emission. The laser is a good approximation to classical coherent light if one accepts the minimal uncertainty in amplitude and phase as negligible, and the phase drift due to spontaneous emission as slow enough to be disregarded.

Do we really need the coherent states to describe the coherence properties in light? In section 6 we investigated the Mølmer-model in which coherence is shown to be induced by the process of updating the system state with information regarding its photon emission. I.e., entanglement is created, where initially the two subsystems were uncorrelated. The induced coherence was shown to be identical to the coherence which the system would exhibit if it was initially in a coherent state. So, at least in this example the coherent state was not necessary, but it did provide a shorter and more convenient path to measuring the coherence.

The unanswered questions

Is there merit to Mølmer's claim that coherent light has never been observed?

Are there other models where one can test the hypothesis that coherent states are not necessary for finding coherence?

Is there a better way to derive the properties of the laser without resorting to the complex and convoluted machinery of the density operator method?

Is it justifiable to assume no interactions between the atoms in the laser gain medium at shorter times $\sim \tau$?

Will not the rate of spontaneous emission by the laser gain medium be affected by the presence of the strong laser field so that an exponential decay (Eq. (5.19)) is inadequate?

The author leaves these questions, and others, in the hands of future students of quantum optics.

Appendix A

Determining the statistical properties of chaotic light

The following are the derivation of the Lorentzian and the Gaussian frequency distributions used for the degree of first-order coherence in section 1.3.1.

A.1   Collision (pressure) broadening

Again consider a gas of atoms interacting with a radiation field. If there are other mechanisms in addition to spontaneous and stimulated transitions that depletes the excited state, the spectral lines will be *broadened*, i.e. the allowed frequency range increases, $\omega_k' = \omega_k + \Delta\omega$. One such broadening mechanism is collisions between the atoms. *Inelastic* collisions can have quite a complicated effect on the energy levels and wavefunctions on the atom, so we will only consider *elastic* collisions that leaves the atom in the same energy level as before and only changes the phase of the atomic wavefunction.

So, picture a particular excited atom radiating light at frequency ω_0. In between each collision the frequency will stay the same, but the phase of the radiated wave is now unrelated to the phase before the collision. The occurrence of collisions between the atoms in a gas is a random process and the probability that an atom has a period τ of free flight between collisions is given by the kinetic theory of gases

$$p(\tau)\mathrm{d}\tau = \frac{1}{\tau_0}e^{-\tau/\tau_0}\mathrm{d}\tau. \tag{A.1}$$

The mean time τ_0 of free flight is a function of the number density of the atoms and of the relative velocity of between pairs of atoms, both of which also depend on the temperature and pressure of the gas, and as such are a major source of information about physical conditions in stellar atmospheres.

The point of using a model of collision broadened light is that the line intensity is proportional to a Lorentzian frequency distribution. To be specific, assume that the

129

wave train radiated by an atom has a complex amplitude of the form

$$E(t) = E_0 e^{-i(\omega_0 t + \phi(t))} \tag{A.2}$$

where the phase $\phi(t)$ is constant in the periods of free flight, but changes abruptly each time a collision occurs. The total electric field amplitude produced by a large number ν of atoms, all radiating with the same amplitude E_0 and frequency ω_0, is then

$$\begin{aligned} E(t) &= E_1(t) + E_2(t) + \ldots + E_\nu(t) \\ &= E_0 e^{-i\omega_0 t} \left[e^{i\phi_1(t)} + e^{i\phi_2(t)} + \ldots + e^{i\phi_\nu(t)} \right] \end{aligned} \tag{1.58}$$

where all the ν atoms are equivalent. The real electric field described by Eq. (1.58) consists of a carrier wave of frequency ω_0 which is modulated by the sum of the random phases of each atom.

Because of the ergodic nature of light we can then view the first-order correlation function of the light, which is a time average of the field emitted by an atom, as a statistical average over each ν atom,

$$\begin{aligned} \langle E^*(t) E(t+\tau) \rangle = E_0^2 e^{-i\omega_0 \tau} \Big\langle &\left[e^{-i\phi_1(t)} + e^{-i\phi_2(t)} + \ldots + e^{-i\phi_\nu(t)} \right] \\ &\times \left[e^{i\phi_1(t+\tau)} + e^{i\phi_2(t+\tau)} + \ldots + e^{i\phi_\nu(t+\tau)} \right] \Big\rangle. \end{aligned} \tag{A.3}$$

The angle-bracket notation will now be used for both the time average and the statistical average. In multiplying out the contents of the brackets the cross terms of different atoms will average to zero, since they are independent and are not correlated. Provided that τ is less than the mean period of free flight between each collision, only cross terms containing the phases $\phi_i(t)$ and $\phi_i(t + \tau)$ from the same atom i will contribute to the average

$$\langle E^*(t) E(t+\tau) \rangle = E_0^2 e^{-i\omega_0 \tau} \sum_{i=1}^{\nu} \langle e^{i(\phi_i(t+\tau) - \phi_i(t))} \rangle = \nu \langle E_i^*(t) E_i(t+\tau) \rangle. \tag{A.4}$$

In other words the correlation function of the entire beam of light is determined by the single-atom contribution. To proceed we need to find an expression for the single-atom correlation function. This term is zero if a collision occurs within the delay time τ, since the wave train then has a phase unrelated to that before. The only contribution is when the atom has a period of free flight longer than τ, and the probability for this is given by Eq. (A.1). So the correlation function can be written as

$$\langle E^*(t) E(t+\tau) \rangle = \nu E_0^2 e^{-i\omega_0 \tau} \int_\tau^\infty d\tau' p(\tau') = \nu E_0^2 e^{-i\omega_0 \tau - \tau/\tau_c} \tag{A.5}$$

where we have renamed the mean period of free flight τ_0 of the atom to the coherence time τ_c since these are for all intents and purposes equivalent.

The degree of first-order correlation is the normalised correlation function

$$g^{(1)}(\tau) = e^{-i\omega_0 \tau - |\tau|/\tau_c}. \tag{1.40}$$

In the last step here the correlation function has been generalised for both positive and negative τ according to the symmetry relation Eq. (1.31).

A.2 Doppler broadening

If Doppler broadening is the main mechanism of spread in the frequency spectrum of chaotic light, the calculation is slightly different from the above. Consider again a gas of atoms interacting with photons. A stationary atom will absorb a photon that carries the appropriate momentum $\hbar\mathbf{k}_0$, where $k_0 = \omega_0/c$. If the atom is moving at a non-relativistic velocity and v is the component of the velocity along the line of sight, the frequency of the emitted light is, to first order in v/c,

$$\omega = \omega_0\left(1 + \frac{v}{c}\right) \tag{A.6}$$

where v is negative if the atom is receding from the observer. This is known as the *first-order* Doppler effect. Another way to view this effect is that light is absorbed only when its frequency ω differs from ω_0 by the Doppler shift appropriate to the initial atomic velocity. So a spread in the atomic velocity of the gas will result in a spread of the absorbed frequencies.

To sum it up, the effect of collision broadening is to alter the phase angle ϕ to some random value completely unrelated to the previous, while the frequency ω_0 stays the same. In contrast, Doppler broadening results in a shift from ω_0 by amounts determined by the atomic velocities, while the phase angles have fixed, but randomly distributed, values.

If the gas has the absolute temperature T, the number of atoms, $\mathrm{d}N$, with velocities between v and $v + \mathrm{d}v$ is given by Maxwell's velocity distribution

$$\mathrm{d}N = N_0 e^{-Mv^2/(2k_BT)}\mathrm{d}v \tag{A.7}$$

where k_B is Boltzmann's constant, M is the atomic mass and N_0 is a constant. It is convenient to normalise this to the total number of atoms ν, for reasons that will soon be apparent,

$$\nu = \int_0^\nu \mathrm{d}N = N_0\int_{-\infty}^\infty e^{-Mv^2/(2k_BT)}\mathrm{d}v = N_0\sqrt{\frac{2\pi k_BT}{M}} \tag{A.8}$$

which gives

$$N_0 = 2\nu\sqrt{\frac{M}{2\pi k_BT}} \tag{A.9}$$

Inserting $\mathrm{d}v = (c/\omega_0)\,\mathrm{d}\omega$ (from Eq. (A.6)) into Eq. (A.7) we find

$$\mathrm{d}N = N_0\frac{c}{\omega_0}e^{-Mc^2(\omega-\omega_0)^2/(2k_BT\omega_0^2)}\mathrm{d}\omega. \tag{A.10}$$

If we define

$$\Delta = \omega_0\sqrt{\frac{k_BT}{Mc^2}} \tag{A.11}$$

Maxwell's velocity distribution as a function of the angular frequency takes on the form

$$\mathrm{d}N = \nu(2\pi\Delta^2)^{-1/2}e^{-(\omega-\omega_0)^2/(2\Delta^2)}\mathrm{d}\omega \tag{A.12}$$

In keeping with Eq. (1.58), the total electric field of a linearly polarised light beam can be written as

$$E(t) = E_0 \sum_{i=1}^{\nu} e^{-i(\omega_i t + \phi_i)} \tag{A.13}$$

where E_0 and ϕ_i are the fixed amplitude and phase angle of the wave radiated by the ith atom, and the angular frequency ω_i is Doppler shifted from ω_0. The first-order correlation function is thus

$$\langle E^*(t)E(t+\tau)\rangle = E_0^2 \sum_{i,j=1}^{\nu} \langle e^{i(\omega_i t - \phi_i - \omega_j(t+\tau)+\phi_j)}\rangle = E_0^2 \sum_{i=1}^{\nu} e^{-i\omega_i\tau}, \quad \text{(A.14)}$$

where the terms for $i \neq j$ average to zero since the phase angles are randomly distributed. The sum can be approximated to an integral by assuming that $\exp(-i\omega_i\tau)$ will vary so little as to be almost constant in an interval of frequencies $\Delta\omega$ emitted by ΔN sources,

$$\sum_i f_i \approx \sum_i f_i \cdot \Delta N$$

And if this interval approaches infinitesimal, we get

$$\sum_i f_i \cdot \frac{\Delta N}{\Delta\omega}\Delta\omega \to \int f(\omega)\frac{\mathrm{d}N}{\mathrm{d}\omega}\mathrm{d}\omega.$$

Then we insert Eq. (A.12), which gives

$$\langle E^*(t)E(t+\tau)\rangle = \nu E_0^2(2\pi\Delta^2)^{-1/2}\int_0^\infty e^{-i\omega\tau}e^{-(\omega_0-\omega)^2/(2\Delta^2)}\mathrm{d}\omega$$
$$= \nu E_0^2 e^{-i\omega_0\tau - \frac{1}{2}\Delta^2\tau^2}, \tag{A.15}$$

where the last step is achieved by completing the square in the exponential function and solving the Gaussian integral with the substitution

$$\omega \to \omega' = (2\Delta^2)^{-1/2}(\omega - \omega_0), \qquad \mathrm{d}\omega' = (2\Delta^2)^{-1/2}\mathrm{d}\omega.$$

This change of variables will give the lower integration limit

$$\omega = 0 \Rightarrow \omega' = -(2\Delta^2)^{-1/2}\omega_0,$$

which according to basic dimension analysis is around -10^6. This allows us to approximate the integral over the entire real line,

$$\int_0^\infty \mathrm{d}\omega \to \int_{-\infty}^\infty \mathrm{d}\omega'.$$

Noting that Δ has units $[rad/s]$ a convenient definition of the coherence time [1] is

$$\tau_c = \frac{\sqrt{\pi}}{\Delta}. \tag{A.16}$$

In a similar form of Eq. (1.40), we have found the degree of first-order coherence for Doppler broadened light

$$g^{(1)}(\tau) = e^{-i\omega_0\tau - \frac{\pi}{2}(\tau/\tau_c)^2}. \tag{1.41}$$

Appendix B

Selected tedious calculations

B.1 The energy of the classic radiation field

The total energy of the radiation field in the cavity with volume $V = L^3$ from section 1.1.2, is

$$H_R = \frac{1}{2}\epsilon_0 \int_V (\mathbf{E}^2 + c^2\mathbf{B}^2)\mathrm{d}\mathbf{r}. \tag{1.20}$$

Before starting this potentially unpleasant integration, we take a moment to consider the type of integral we will end up with. If the scalar products are between different modes $\mathbf{k}, \mathbf{k}'$, there will be terms of the form

$$\frac{1}{V} \int_V e^{\pm i(\mathbf{k}+\mathbf{k}')\mathbf{r}}\mathrm{d}\mathbf{r} = \delta_{\mathbf{k}(-\mathbf{k}')} \tag{B.1}$$

for cross terms of $a_{\mathbf{k}\lambda}a_{\mathbf{k}'\lambda'}$ or c.c.[1], and

$$\frac{1}{V} \int_V e^{\pm i(\mathbf{k}-\mathbf{k}')\mathbf{r}}\mathrm{d}\mathbf{r} = \delta_{\mathbf{k}\mathbf{k}'} \tag{B.2}$$

for cross terms of $a_{\mathbf{k}\lambda}a_{\mathbf{k}'\lambda'}^*$ or c.c., These are identities of the Dirac delta function and give no contribution unless $\mathbf{k}'$ is either $-\mathbf{k}$ or $\mathbf{k}$, respectively. The frequency ω_k is the same in either case. We will also get the scalar product of the unit polarisation vectors which will further simplify the matters since the two different directions λ, λ' are perpendicular, and in addition

$$(\mathbf{k} \times \boldsymbol{\epsilon}_{\mathbf{k}\lambda}) \cdot (\mathbf{k} \times \boldsymbol{\epsilon}_{\pm\mathbf{k}\lambda'}) = (\mathbf{k} \cdot \mathbf{k})(\boldsymbol{\epsilon}_{\mathbf{k}\lambda} \cdot \boldsymbol{\epsilon}_{\pm\mathbf{k}\lambda'}) = \pm k^2 \delta_{\lambda\lambda'}. \tag{B.3}$$

The calculation goes as follows, where we denote the primed indices by priming the variable itself and $\chi = \mathbf{k} \cdot \mathbf{r} - \omega_k t$ etc,

$$|\mathbf{E}|^2 \sim \sum_{\mathbf{k}\mathbf{k}'} \sum_{\lambda\lambda'} \boldsymbol{\epsilon} \cdot \boldsymbol{\epsilon}' \big[aa' e^{i(\chi+\chi')} + aa'^* e^{i(\chi-\chi')}$$
$$+ a^*a' e^{-i(\chi-\chi')} + a^*a'^* e^{-i(\chi+\chi')} \big], \quad \text{(B.4)}$$

---

[1]The abbreviation c.c. stands for complex conjugated.

and integrating gives

$$\frac{1}{V}\int_V |\mathbf{E}|^2 \mathrm{d}\mathbf{r}$$

$$\sim \sum_{\mathbf{k}\mathbf{k}'}\sum_{\lambda\lambda'}\delta_{\lambda\lambda'}\left[aa'\delta_{\mathbf{k},-\mathbf{k}'}e^{-2i\omega_k t} + aa'^*\delta_{\mathbf{k},\mathbf{k}'} + a^*a'\delta_{\mathbf{k},\mathbf{k}'} + a^*a'^*\delta_{\mathbf{k},-\mathbf{k}'}e^{-i\omega_k t}\right]$$

$$= \sum_{\mathbf{k}}\sum_{\lambda}[a_{\mathbf{k}\lambda}a_{-\mathbf{k}\lambda}e^{-2i\omega_k t} + a_{\mathbf{k}\lambda}a_{\mathbf{k}\lambda}^* + a_{\mathbf{k}\lambda}^*a_{\mathbf{k}\lambda} + a_{\mathbf{k}\lambda}^*a_{-\mathbf{k}\lambda}^* e^{2i\omega_k t}] \quad \text{(B.5)}$$

The same procedure gives for the magnetic field

$$|\mathbf{B}|^2 \sim \sum_{\mathbf{k}\mathbf{k}'}\sum_{\lambda\lambda'}\frac{(\mathbf{k}\times\boldsymbol{\epsilon})\cdot(\mathbf{k}'\times\boldsymbol{\epsilon}')}{\omega_k\omega_{k'}}\left[aa'e^{i(\chi+\chi')} + aa'^*e^{i(\chi-\chi')}\right.$$

$$\left. + a^*a'e^{-i(\chi-\chi')} + a^*a'^*e^{-i(\chi+\chi')}\right], \quad \text{(B.6)}$$

and after integrating

$$\frac{1}{V}\int_V c^2|\mathbf{B}|^2\mathrm{d}\mathbf{r}$$

$$\sim \sum_{\mathbf{k}\mathbf{k}'}\sum_{\lambda\lambda'}\frac{c^2}{\omega_k\omega_{k'}}\delta_{\lambda\lambda'}\left[aa'k(-k')\delta_{\mathbf{k},-\mathbf{k}'}e^{-2i\omega_k t} + aa'^*kk'\delta_{\mathbf{k},\mathbf{k}'}\right.$$

$$\left. + a^*a'kk'\delta_{\mathbf{k},\mathbf{k}'} + a^*a'^*k(-k')\delta_{\mathbf{k},-\mathbf{k}'}e^{2i\omega_k t}\right]$$

$$= \sum_{\mathbf{k}}\sum_{\lambda}[-a_{\mathbf{k}\lambda}a_{-\mathbf{k}\lambda}e^{-2i\omega_k t} + a_{\mathbf{k}\lambda}a_{\mathbf{k}\lambda}^* + a_{\mathbf{k}\lambda}^*a_{\mathbf{k}\lambda} - a_{\mathbf{k}\lambda}^*a_{-\mathbf{k}\lambda}^*e^{2i\omega_k t}] \quad \text{(B.7)}$$

The resulting total radiative energy is then simply

$$H_R = \sum_{\mathbf{k}}\sum_{\lambda}\frac{1}{2}\hbar\omega_k(a_{\mathbf{k}\lambda}a_{\mathbf{k}\lambda}^* + a_{\mathbf{k}\lambda}^*a_{\mathbf{k}\lambda}) = \sum_{\mathbf{k}}\sum_{\lambda}\hbar\omega_k a_{\mathbf{k}\lambda}a_{\mathbf{k}\lambda}^* \quad \text{(B.8)}$$

B.2 The Lie formula

Every now and then in quantum mechanics we will need to evaluate expressions on the form

$$e^{\hat{X}}\hat{Y}e^{-\hat{X}} \quad \text{(B.9)}$$

It is fairly easy to show that the solution is

$$e^{\hat{X}}\hat{Y}e^{-\hat{X}} = \hat{Y} + [\hat{X}, \hat{Y}] + \frac{1}{2!}[\hat{X}, [\hat{X}, \hat{Y}]] + \frac{1}{3!}[\hat{X}, [\hat{X}, [\hat{X}, \hat{Y}]]] + \dots \quad \text{(B.10)}$$

Proof is found by considering the operator

$$\hat{F}(\lambda) = e^{\lambda\hat{X}}\hat{Y}e^{-\lambda\hat{X}}. \quad \text{(B.11)}$$

The trick is to do a Taylor expansion, so we need the derivative

$$\frac{\mathrm{d}\hat{F}}{\mathrm{d}\lambda} = e^{\lambda\hat{X}}\hat{X}\hat{Y}e^{-\lambda\hat{X}} - e^{\lambda\hat{X}}\hat{Y}\hat{X}e^{-\lambda\hat{X}} = \hat{X}\hat{F} - \hat{F}\hat{X} = [\hat{X},\hat{F}], \tag{B.12}$$

and the second derivative is found to be

$$\frac{\mathrm{d}^2\hat{F}}{\mathrm{d}\lambda^2} = \frac{\mathrm{d}}{\mathrm{d}\lambda}[\hat{X},\hat{F}] = [\hat{X},[\hat{X},\hat{F}]]. \tag{B.13}$$

This pattern is repeated and we find that the Taylor expansion is

$$\hat{F}(\lambda) = \hat{F}(0) + \lambda\hat{F}'(0) + \frac{\lambda^2}{2!}\hat{F}''(0) + \frac{\lambda^3}{3!}\hat{F}'''(0)\ldots \tag{B.14}$$

Finally this gives the Lie formula

$$e^{\lambda\hat{X}}\hat{Y}e^{-\lambda\hat{X}} = \hat{Y} + [\hat{X},\hat{Y}] + \frac{\lambda}{2!}[\hat{X},[\hat{X},\hat{Y}]] + \frac{\lambda}{3!}[\hat{X},[\hat{X},[\hat{X},\hat{Y}]]] + \ldots \tag{B.15}$$

B.3 Solving the eigenvalue problem

We now solve the eigenvalue problem of section 5.1.1 to find the system state amplitudes $C_{an}(t)$ and $C_{bn+1}(t)$ from Eq. (5.5).

The effective Hamiltonian is defined as

$$\hat{H} = \frac{1}{2}\hbar\omega_0\sigma_z + \hbar\Omega\hat{a}^\dagger\hat{a} + \hbar g(\hat{a}^\dagger\hat{\sigma} + \hat{a}\hat{\sigma}^\dagger) \tag{B.16}$$

or

$$\begin{aligned}
\hat{H} &= \hbar\begin{pmatrix} \frac{1}{2}\omega_0 + \Omega n & g\sqrt{n+1} \\ g\sqrt{n+1} & -\frac{1}{2}\omega_0 + \Omega(n+1) \end{pmatrix} \\
&= \hbar\begin{pmatrix} \frac{1}{2}(\omega_0 - \Omega) + \Omega(n+1/2) & g\sqrt{n+1} \\ g\sqrt{n+1} & \frac{1}{2}(\omega_0 - \Omega) + \Omega(n+1/2) \end{pmatrix} \\
&= \hbar\begin{pmatrix} \Omega(n+1/2) & g\sqrt{n+1} \\ g\sqrt{n+1} & \Omega(n+1/2) \end{pmatrix} \tag{B.17}
\end{aligned}$$

where the last step is due to assumed resonance.

The next move is to find the eigenvalues $\hbar\lambda$ of the Hamiltonian,

$$\begin{aligned}
\det(\hat{H} - \hbar\lambda) &= \det\hbar\begin{pmatrix} \Omega(n+1/2) - \lambda & g\sqrt{n+1} \\ g\sqrt{n+1} & \Omega(n+1/2) - \lambda \end{pmatrix} \\
&= \hbar(\Omega(n+1/2) - \lambda)^2 - \hbar(g\sqrt{n+1})^2 \\
&\equiv 0 \tag{B.18}
\end{aligned}$$

This gives the two eigenvalues

$$\begin{aligned}
\lambda_1 &= \Omega(n+1/2) + g\sqrt{n+1}, \\
\lambda_2 &= \Omega(n+1/2) - g\sqrt{n+1} \tag{B.19}
\end{aligned}$$

For each eigenvalue there is an eigenvector that can be found from

$$(\hat{H} - \hbar\lambda_i)\mathbf{v}_i = \mathbf{0} \quad (i = 1, 2) \tag{B.20}$$

The straight forward calculation yields

$$\begin{aligned}
\mathbf{v}_1 &= \begin{bmatrix} 1 \\ 1 \end{bmatrix} && \text{for } \lambda_1 = \Omega(n + 1/2) + g\sqrt{n+1} \\
\mathbf{v}_2 &= \begin{bmatrix} 1 \\ -1 \end{bmatrix} && \text{for } \lambda_2 = \Omega(n + 1/2) - g\sqrt{n+1}
\end{aligned} \tag{B.21}$$

Then the time-dependent state can be written in terms of the eigenvalues and eigenvectors as

$$|\psi(t)\rangle = c_1 \mathbf{v}_1 e^{-i\lambda_1 t} + c_2 \mathbf{v}_2 e^{-i\lambda_2 t} \tag{B.22}$$

and with the initial condition that the atoms are in the upper laser level at $t = 0$, we have

$$|\psi(0)\rangle = c_1 \mathbf{v}_1 + c_2 \mathbf{v}_2 = \begin{bmatrix} 1 \\ 0 \end{bmatrix} = |a\rangle. \tag{B.23}$$

This gives

$$c_1 \begin{bmatrix} 1 \\ 1 \end{bmatrix} + c_2 \begin{bmatrix} 1 \\ -1 \end{bmatrix} = \begin{bmatrix} 1 \\ 0 \end{bmatrix} \quad \Rightarrow \quad c_1 = 1/2 \quad \text{and} \quad c_2 = 1/2 \tag{B.24}$$

and

$$|\psi(t)\rangle = \frac{1}{2} \begin{bmatrix} 1 \\ 1 \end{bmatrix} e^{-i[\Omega(n+1/2)+g\sqrt{n+1}]t} + \frac{1}{2} \begin{bmatrix} 1 \\ -1 \end{bmatrix} e^{-i[\Omega(n+1/2)-g\sqrt{n+1}]t} \tag{B.25}$$

Finally, the amplitudes for the atom being in state $|a, n\rangle$ or $|b, n+1\rangle$ after time t are, respectively,

$$\begin{aligned}
C_{an}(t) &= \cos(g\sqrt{n+1}t)e^{-i\Omega(n+1/2)t} \\
C_{bn+1}(t) &= -i\sin(g\sqrt{n+1}t)e^{-i\Omega(n+1/2)t}
\end{aligned} \tag{B.26}$$

As a matter of computational simplicity we can change from the Schrödinger picture to the Interaction picture i.e., pulling the exponentials in Eq. (B.26) into the state vector, thus

$$\begin{aligned}
C_{an}(t) &= \cos(g\sqrt{n+1}t) \\
C_{bn+1}(t) &= -i\sin(g\sqrt{n+1}t).
\end{aligned} \tag{B.27}$$

Appendix C

Source code listings

C.1 Script for calculating coherences

The following listing was used to calculate the intensity correlations for the Michelson stellar interferometer and the intensity interferometer. Eqs.(2.46) and (2.48) was used for a Lorentzian frequency distribution, and for a Gaussian frequency distribution the Eqs.(2.47) and (2.49). The results are plotted in Figs. 2.7 and 2.9.

Coherence.m

```matlab
function D = coherence
    close all; clc; clear;

    r = input('Enter \n 1 for intensity int. \n 2 for michelson int.');

    if     r == 1, funk = 'intensity';
    elseif r == 2, funk = 'michelson';
    end

    freq = ['g','l'];
    freq_name = {'Gaussian', 'Lorentzian'};

    % colors for the plot
    clr  = {'-b', '-r', '--g', '-m'};

    angle = [0.0047 0.047 0.47];

    j = 0;
    r = 1;

    for n = 1:length(freq)
        for s = 1:1:length(angle)    % want to compare directly 3 different
            j = j + 1;               % angles of the same order of magnitude

                param         = initialiseParam( 10^(1-r), angle(s) );
                C{j,1}        = { calculation(funk, param, freq(n)) };
                figlapp{j,1}  = strcat(freq_name(n),...
                                ': $\theta=',num2str(angle(s)),'"$' );

        end
    end

    r = 1;
```

138

```
        for t = 1:3:j          %plot 3 angles in the same image
            figure;
            hold on;

            plot(param.d, C{t,1}{:},    clr{1});
            if j > 1, plot(param.d, C{t+1,1}{:}, clr{2});
                        lapp = [figlapp{t,1},figlapp{t+1,1}]; end
41          if j > 2, plot(param.d, C{t+2,1}{:}, clr{3});
                lapp = [figlapp{t,1},figlapp{t+1,1},figlapp{t+2,1}]; end

            legend(lapp, 'Interpreter','latex','FontSize',14);
            xlabel('$d$ [m]', 'Interpreter','latex','FontSize',14);
            ylabel('$C$', 'Interpreter','latex','FontSize',14);
            set(gca, 'FontSize', 14);

            if t <= floor(j/2)
                frekv = freq(1);
51          else
                if length(freq) > 1, frekv = freq(2); end
            end

            th = num2str(angle(r));
            outfile = [funk '_' frekv '_' num2str(param.I_a)...
                'Ia' num2str(param.I_b) 'Ib_' th(3:end) ];
            %saveimages(gcf, outfile);
            r = r + 3;
            if r > length(angle), r = 1; end
61      end
    end

    % Initialise the required parameters for the calculations
    function param = initialiseParam(angle)
        param.c       = 3e8;
        lambda        = 540e-9;          % a guess!
        param.k       = 2*pi/lambda;     % k = w/c = 2pi/L

        arcsecond     = pi/648000;       % radians
71      param.arcsec= arcsecond;
        param.theta = angle*arcsecond;

        d             = -0:0.01:3;       % d theta = r_a - r_b
        param.d       = d*1e0;           % the baseline              10^1
        param.d_c     = 1e-6;            % coherence length of thermal light
        param.r_a     = param.d*1e-7;    % r_a = c*tau_a = d.L/L = d*cos(pi/2)
        % param.r_b    = d;              % r_b = r_a - d theta
        param.I_a     = 1;
        param.I_b     = 1;
81
    end

    % Returns the degree of first-order coherence
    function result = g1(source, distr, j, s)
        d_c = s.d_c;
        r_a = s.r_a;
        d   = s.d;
        c   = s.c;
        theta = s.theta;
91      k   = s.k;

        switch distr
            case 'g'      %gaussian
                if strcmp(source,'a')  %a
                    result = exp(-i*k*r_a(j) - pi/2*(r_a(j)/d_c)^2);
                elseif strcmp(source,'b')
                    result = exp(-i*k*(r_a(j) - d(j)*theta)...
                        - pi/2*( r_a(j)/d_c - d(j)*theta/d_c/c)^2);
```

```matlab
                end
101     case 'l'     %lorentzian
            if strcmp(source,'a')
                result = exp(-i*k*r_a(j) - abs(r_a(j)/d_c));
            elseif strcmp(source,'b')
                result = exp(-i*k*(r_a(j) - d(j)*theta)...
                             - abs(r_a(j)/d_c - d(j)*theta/d_c/c));
            end
    end
end


% Returns degree of second-order coherence
function result = g2(source, distr, j, s)
    d_c = s.d_c;
    r_a = s.r_a;
    d   = s.d;
    c   = s.c;
    theta = s.theta;

    switch distr
        case 'g'     %gaussian
            if strcmp(source,'a')
                result = 1 + exp(-pi*(r_a(j)/d_c)^2);
            elseif strcmp(source,'b')
                result = 1 + exp(-pi*(r_a(j)/d_c - d(j)*theta/d_c/c)^2);
            end
        case 'l'     %lorentzian
            if strcmp(source,'a')
                result = 1 + exp(-2*abs(r_a(j)/d_c));
            elseif strcmp(source,'b')
                result = 1 + exp(-2*abs(r_a(j)/d_c - d(j)*theta/d_c/c));
            end
    end
end


% Calculate the correlation function for intensity int & Michelson int
function C = calculation(funk, s, freq)

    d   = s.d;
    I_a = s.I_a;
    I_b = s.I_b;
    k   = s.k;
    theta = s.theta;

    switch funk
        case 'intensity'
            for j = 1:length(d)
                C(j) = I_a^2*g2('a', freq, j, s)...
                        + I_b^2*g2('b', freq, j, s)...
                        + I_a*I_b*(2...
                         + g1('a', freq, j, s)*conj(g1('b', freq, j, s))...
                         + conj(g1('a', freq, j, s))* g1('b', freq, j, s) );
                C(j) = C(j)/(I_a + I_b)^2;
            end
        case 'michelson'
            for j = 1:length(d)
                C(j) = I_a*(1 + real(g1('a', freq, j, s)) )...
                        + I_b*(1 + real(g1('b', freq, j, s)) );
                C(j) = C(j)/(I_a + I_b);
            end
    end
end
```

C.2   Script for calculating Monte Carlo quantum jumps

The following Matlab-script was used to compute the Monte Carlo quantum jump described by Algorithm 1 in section 6.2. The results of the simulation is plotted in Figs.6.2, 6.3 and 6.4.

<div align="center">molmer.m</div>

```matlab
clear; clc; close all;

% Initial values, at t = 0
c_0      = 1;
c_1      = 0;
Q_0      = 0;
Gamma    = 1;
delta    = 1000*Gamma;

n        = 1e5;                   % Number of photons in each cavity
q_max    = 3000;                  % When the measurement stops
q        = 0;
t        = 0;

% Initialise vectors for enhanced performance
c_k      = zeros(q_max, 1);       % complex amplitude
Q        = zeros(q_max, 1);       % <\dagger{a}b>
tau      = zeros(q_max, 1);
c_at_t   = zeros(q_max, 1);       % jumps to c at time t
d_at_t   = zeros(q_max, 1);       % jumps to d at time t
ck_all   = zeros(q_max,q_max);    % amplitude evo. for all t

c_k(1,1)= c_0;
Q(1,1)  = Q_0;
tau(1,1)= 0;

jump2c   = 0;
jump2d   = 0;

% Temporary storage
tempQ_c = Q;
temp_c  = c_k;
tempQ   = 0;

idx = 1;

while q < q_max

    ck_all(:,idx) = c_k;

    epsilon  = rand(1);
    tau(idx) = -log(epsilon)/(Gamma*(2*n-q));

    % Time is now: t = tau(q)
    t    = t + tau(idx);

    % Time evolution of the amplitudes by effective Hamiltonian
    c_k = exp(i*(0:q_max-1)*delta*tau(idx))'.*c_k;
    c_k = c_k./norm(c_k);

    % The first jump goes to c, since there is a 50% chance either way:
    % Remember that when Q == 0 the state is not entangled, and it
    % should be equally likely to jump either to c or d!
    if q == 0
        Q(idx)      = 0;
        jumpSign    = +1;
        jump2c      = jump2c + 1;
```

```
              c_at_t(idx) = 1;

59          else
              % Calculate Q to find the direction of the next jump
              for k = 0:q−1
                  tempQ_c(k+1) = sqrt(n−k)*sqrt(n−q+k+1)...
                                     *conj(c_k(k+1))*c_k(k+2);
              end
              tempQ   = sum(tempQ_c);
              Q(idx)  = 2*real(tempQ)/(Gamma*(2*n−q));

69          e = rand(1);

              if e < (1 + Q(idx))/2          % Jump to c
                  jumpSign    = +1;
                  jump2c      = jump2c + 1;
                  c_at_t(idx) = 1;

              else                          % Jump to d
                  jumpSign    = −1;
                  jump2d      = jump2d + 1;
79                d_at_t(idx) = 1;

              end
          end

          % Calculate the amplitudes of the new state after jump
          for k = 0:q+1
              if k == 0
                  temp_c(k+1) = jumpSign*sqrt(n−q+k)*c_k(k+1);
              elseif k == q+1
89                temp_c(k+1) = sqrt(n−k+1)*c_k(k);
              else
                  temp_c(k+1) = sqrt(n−k+1)*c_k(k)...
                                   + jumpSign*sqrt(n−q+k)*c_k(k+1);
              end
          end

          % Update the state amplitudes
          c_k = temp_c./norm(temp_c);

99        idx = idx + 1;
          q   = q + 1;

      end

  % Plot time evolution of 2ReQ/(Gamma(2n−q))
  figure(1);
  time = linspace(0,t,length(Q)−1);
  plot(time,Q(1:end−1));
  xlabel('time $[s\Gamma^{-1}]$',    'Interpreter', 'latex');
109 ylabel('$2\Re Q/(\Gamma(2n-q))$', 'Interpreter', 'latex');

  outfile = 'molmer_timeEvolQ';
  saveimages(1, outfile);

  % Plot time evolution of |c_k|^2
  figure(2); hold all; for j = 1:100:q_max, plot(abs(ck_all(:,j))); end
  xlim([0 q_max/2]); ylim([0 0.4]);
  xlabel('detected photons $q$',                  'Interpreter', 'latex');
  ylabel('probability ${\lvert c_k \rvert}^2$', 'Interpreter', 'latex');
119
  outfile = 'molmer_timeEvolck2';
  saveimages(2, outfile);

  dt          = 0.0002*Gamma^−1;
```

```
    nbins     = floor(sum(tau)/dt);
    intervall = floor(length(c_at_t)/nbins);

    c_photon = zeros(nbins,1);
    d_photon = zeros(nbins,1);
129
    for j = 1:nbins
        c_photon(j) = sum( c_at_t( (j-1)*intervall+1:j*intervall ) );
        d_photon(j) = sum( d_at_t( (j-1)*intervall+1:j*intervall ) );
    end

    figure(3);
    time = linspace(0,t, nbins);
    subplot(2,1,1), stairs(time, c_photon, 'b');
    title('Number of photons detected at $c$', 'Interpreter', 'latex');
139 ylim([0 50]);
    subplot(2,1,2), stairs(time, d_photon, 'r');
    title('Number of photons detected at $d$', 'Interpreter', 'latex');
    ylim([0 50]);

    outfile = 'molmer_photonDetec';
    saveimages(3, outfile);
```

References

[1] Loudon R.. *The quantum theory of light*. Oxford Univ. Press3rd ed. 2003.

[2] Goodman J.W.. *Statistical optics*. Wiley New York 1985.

[3] Fox M.. *Quantum Optics: An Introduction*. Oxford Univ. Press, USA 2006.

[4] Mitchell ACG, Zemansky MW. *Resonance Radiation and Excited Atoms*. Cambridge Univ. Press, London 1934.

[5] Hanbury Brown R., Davis J., Allen LR, Rome JM. The stellar interferometer at Narrabri Observatory-II. The angular diameters of 15 stars *Mon. Not. R. Astron. Soc..* 1967;137.

[6] Richichi A., Percheron I.. CHARM: A Catalog of High Angular Resolution Measurements *A&A.* 2002;386:492–503.

[7] Hanbury Brown R.. *The intensity interferometer. Its applications to astronomy*. Taylor & Francis, London 1974.

[8] Paganin D.M.. *Coherent x-ray optics*. Oxford University Press, USA 2006.

[9] Scully M.O., Zubairy M.S.. *Quantum Optics*. Cambridge Univ. Press 1997.

[10] Michelson AA. An Interferometer for Measuring Stellar Diameter *Astrophys. J..* 1920;51:257.

[11] Michelson AA. On the application of interference methods to astronomical measures *Am. J. Sci..* 1890;39:579–590.

[12] Hanbury Brown R., Twiss RQ. A Test of a New Type of Stellar Interferometer on Sirius *Nature.* 1956;178:1046–1048.

[13] Hanbury Brown R., Twiss RQ. Interferometry of the Intensity Fluctuations in Light II. An Experimental Test of the Theory for Partially Coherent Light *Proc. R. Soc. Lon. SER-A.* 1958;243:291–319.

[14] Donges A.. The coherence length of black-body radiation *Eur. J. Phys..* 1998;19:245–250.

[15] Garrison J., Chiao R.. *Quantum Optics*. Oxford Univ. Press 2008.

[16] Glauber R.J.. Coherent and Incoherent States of the Radiation Field *Phys. Rev.*. 1963;131:2766–2788.

[17] Mandel L., Wolf E.. *Optical Coherence and Quantum Optics*. Cambridge Univ. Press 1995.

[18] Leinaas J.M.. Non-Relativistic Quantum Mechanics Lecture notes in FYS4110, Department of Physics, University of Oslo 2004.

[19] Mandl F., Shaw G.. *Quantum Field Theory*. Wiley 2003.

[20] Silverman M.P.. *Quantum Superposition Counterintuitive Consequences of Coherence, Entanglement, and Interference*. Springer 2008.

[21] Sargent M., Scully M.O., Lamb W.E.. *Laser physics*. Westview Press 1978.

[22] Hanbury Brown R., Twiss RQ. The question of correlation between photons in coherent light rays *Nature*. 1956;178:1447.

[23] Baym G.. The Physics of Hanbury Brown-Twiss Intensity Interferometry: from Stars to Nuclear Collisions *Acta Phys. Pol. B*. 1998;29:1839–1884.

[24] Fano U.. Quantum theory of interference effects in the mixing of light from phase-independent sources *American Journal of Physics*. 1961;29:539.

[25] Mandel L.. Fluctuations of light beams *Progress in Optics*. 1993;31:181–245.

[26] Glauber R.J.. The Quantum Theory of Optical Coherence *Phys. Rev.*. 1963;130:2529–2539.

[27] Peřina J.. *Quantum Statistics of Linear and Nonlinear Optical Phenomena*. Kluwer Academic Pub.2nd completely rev. ed. 1991.

[28] Pegg D.T., Barnett S.M.. Tutorial review Quantum optical phase *J. Mod. Optics*. 1997;44:225–264.

[29] Zou XT, Mandel L.. Photon-antibunching and sub-Poissonian photon statistics *Phys. Rev. A*. 1990;41:475–476.

[30] Hanamura E., Kawabe Y., Yamanaka A.. *Quantum nonlinear optics*. Springer1st ed. 2007.

[31] Mølmer Klaus. Optical coherence: A convenient fiction *Phys. Rev. A*. 1997;55:3195–3203.

[32] Haroche S., Raimond J.M.. *Exploring the quantum: atoms, cavities and photons*. Oxford Univ. Press, USA 2006.

[33] Mandel L., Wolf E.. Coherence Properties of Optical Fields *Reviews of Modern Physics*. 1965;37:231–287.